Abstract

This thesis deals with the channel access problem in a wireless network using analytical approaches based on game theory and Markov chain theory. The goal is to improve the performance of the network. Particular emphasis is placed on channel access for unicast traffic and multicast traffic. Two random access mechanisms are studied in this thesis, namely, “Slotted ALOHA Enhanced by ZigZag Decoding (SAZD)” and “Multicast Collision Prevention (MCP)”. SAZD is an enhancement of the Slotted ALOHA random access mechanism by ZigZag decoding technique, while MCP is a multicast mechanism designed for high-performance video communications. MCP belongs to the same family of random access mechanisms as SAZD, and it is characterized by the functionality of channel sensing, implemented by the CSMA (Carrier-Sense Multiple Access) mechanism. Moreover, it is based on the DCF (Distributed Coordination Function) mechanism, which exploits the BEB (Binary Exponential Backoff) scheme to access the wireless channel.

The thesis is composed of two parts. The first part is devoted to our contributions to the SAZD mechanism, and the second is devoted to our contributions to the MCP mechanism.

For the SAZD mechanism, we initially proposed a cooperative game model to model a wireless network scenario where users (i.e., players) transmit data according to this mechanism. The proposed model takes into consideration the following constraints: maximizing throughput, minimizing delay, and optimizing the throughput-delay trade-off. Next, we introduce two cooperative game pricing strategies to control user behavior and further optimize the trade-off between throughput and delay. Then, we study the previous scenario using this time a non-cooperative game. Thus, we consider selfish users who share the same transmission channel. Our analysis shows that users, in this case, transmit using a very high probability. This aggressive behavior leads to a dramatic situation where the wireless network fails. To address this issue, we propose introducing a transmission cost to mitigate the aggressive behavior of users. Thus, we can decrease the level of the selfishness of users without adding a central coordination unit, which allows us to have a significant improvement in network performance. Afterward, we propose to look for the optimal cost which allows for transforming the non-cooperative game into a cooperative game like the one studied in the first chapter. We then extend the two previous models into a general game model in which cooperative and non-cooperative users coexist. This model generalizes several models that consider either the concept of cooperation or non-cooperation to model a wireless network system.

For the MCP mechanism, we first propose a Markov model that models its operation in the case of saturated traffic. This model takes into account the existence of other types of traffic, such as unicast traffic, and it takes into account the backoff freezing if the channel is busy. Our goal is to achieve reliability of over 99.999% for multicast traffic. All the results found are validated by extensive simulations. We also study this model in the case of unsaturated traffic, and we evaluate different parameters of the Quality of Service (QoS) and the Quality of Experience (QoE) of the network based on the MCP mechanism. Finally, we propose a new approach to evaluate the energy consumption in the network. We estimate the energy consumed between two successive transmissions for unicast traffic and multicast traffic.

Keywords:
Game Theory, Stochastic Games, Nash Equilibrium, Cooperation, Selfishness, Markov Process, ALOHA, ZigZag, Multicast, Unicast.

N° d’ordre

Ahmed Boujnoui

Stochastic Game Analysis and Probabilistic Approach towards the Design of Random Access Mechanisms

2021/2022, Mathématiques, Informatique et Applications

Université Hassan 1er
Centre d’Études Doctorales en Sciences et Techniques & Sciences Médicales

Faculté des Sciences et Techniques Settat

THÈSE DE DOCTORAT

Pour l’obtention de grade de Docteur en Sciences et Techniques

Formation Doctorale : Mathématiques, Informatique et Applications

Spécialité : Mathématiques Appliquées

Sous le thème

Stochastic Game Analysis and Probabilistic Approach towards the Design of Random Access Mechanisms

Présentée par :

Ahmed BOUJNOUI

Soutenue le 20 Octobre 2022 à 14h30 à la Faculté des Sciences et Techniques devant le jury composé de :

Pr. Ahmed Roubi	**PES**	**Faculté des Sciences et Techniques, Settat**	**Président**
Pr. Antonio Javier García Sánchez	**Professeur**	**Université Polytechnique de Cartagena, Espagne**	**Rapporteur**
Pr. Abdelghani Ben Tahar	**PES**	**Faculté des Sciences et Techniques, Settat**	**Rapporteur**
Pr. Mohamed Hanini	**PH**	**Faculté des Sciences et Techniques, Settat**	**Examinateur**
Pr. Said El Kafhali	**PH**	**Faculté des Sciences et Techniques, Settat**	**Examinateur**
Pr. Luis Orozco Barbosa	**Professeur**	**Université de Castilla-La Mancha, Espagne**	**Co-Directeur de thèse**
Pr. Abdelkrim Haqiq	**PES**	**Faculté des Sciences et Techniques, Settat**	**Directeur de thèse**

Année Universitaire : 2021/2022

To my family, professors, and friends
for their help
and unwavering support.

Acknowledgments

First and foremost, praises and thanks to ALLAH, the Almighty, for giving me the strength to successfully complete my thesis. Any elegance in this work stems from him, and any clumsiness is my own.

The research work of this doctoral thesis has been carried out between the IR2M laboratory, Hassan First University of Settat, Morocco, and the Albacete Research Institute of Informatics (I3A), University of Castilla-La Mancha, Spain.

Mostly, I would like to express my profound gratitude and appreciation to my supervisors, Dr. Abdelkrim Haqiq and Dr. Luis Orozco Barbosa for their continuous support and invaluable guidance. I have greatly benefited from their experience and their wisdom. Discussion with them always clarifies my confusions and inspires new ideas. Having two supervisors provided me with a strong foundation in two fundamental fields: mathematics and computer science, which have been both fruitful and valuable to the research presented in this thesis. Their immense knowledge offers me many ideas and suggestions. I extremely appreciate your priceless patience with me, your ideas, and your support during my thesis. Thank you for encouraging my research and for all the time you have always been willing to spend on me when I have needed it.

I would like to express my heartfelt appreciation to Dr. Abdellah Zaaloul, Dr. Javier Gomez, and Dr. J. J. Camacho Escoto who are co-authors of most of the papers presented in this thesis. Sincere acknowledgments also go to Dr. Mohamed Hanini with whom I co-authored some other papers. It has been a pleasure, and an honor, to work together.

I would like to acknowledge the support and friendship provided by all my colleagues in the IR2M laboratory of the Hassan First University, and the colleagues inside and outside of the department of mathematics and computer science. In addition, I would like to thank all the members of the RAAP group for the wonderful moments spent at the I3A institute of the University of Castilla-La Mancha.

I am grateful for the support and kindness of the administration staff of the Hassan First University: Dr. Ahmed Fahli, and Dr. Bouchaib Bencharkib, and the administration staff of the University of Castilla-La Mancha: Ana Raquel Sicilia Fernandez and Julia Corredor Cañadas. Many thanks also go to all the technical staff of I3A. Especially, Raúl Galindo Moreno, and Vicente López Camacho who have always been very helpful.

Sincere gratitude is also due to all the thesis committee members, for their willingness and valuable time to be part of my defense committee. I would like to thank my internal examiner, Dr. Abdelghani Bentahar, and my external examiners Dr. Antonio Javier García Sánchez, and Dr. Sabir Essaid for serving on my examining committee and for the valuable time they dedicated to reviewing my manuscript, and contributed valuable suggestions and comments that helped in the improvement of this thesis's quality. I am pleased and honored to have them on my thesis jury.

I would like to thank my parents, brothers, sisters, and family who have given me unconditional support during my study journey. Many thanks to my friends Boukanjime Brahim, Allal Brahim,

and El Khalifi Mohamed, who helped review the first draft of my thesis manuscript.

Finally, I want to acknowledge the financial support provided by the Erasmus+ KA107. I also appreciate the financial support provided by the Hassan First University of Settat.

Ahmed Boujnoui
Albacete, April 2022

Abstract

This thesis deals with the channel access problem in a wireless network using analytical approaches based on game theory and Markov chain theory. The goal is to improve the performance of the network. Particular emphasis is placed on channel access for unicast traffic and multicast traffic. Two random access mechanisms are studied in this thesis, namely, "Slotted ALOHA Enhanced by ZigZag Decoding (SAZD)" and "Multicast Collision Prevention (MCP)". SAZD is an enhancement of the Slotted ALOHA random access mechanism by ZigZag decoding technique, while MCP is a multicast mechanism designed for high-performance video communications. MCP belongs to the same family of random access mechanisms as SAZD, and it is characterized by the functionality of channel sensing, implemented by the CSMA (Carrier-Sense Multiple Access) mechanism. Moreover, it is based on the DCF (Distributed Coordination Function) mechanism, which exploits the BEB (Binary Exponential Backoff) scheme to access the wireless channel.

The thesis is composed of two parts. The first part is devoted to our contributions to the SAZD mechanism, and the second is devoted to our contributions to the MCP mechanism.

For the SAZD mechanism, we initially proposed a cooperative game model to model a wireless network scenario where users (i.e., players) transmit data according to this mechanism. The proposed model takes into consideration the following constraints: maximizing throughput, minimizing delay, and optimizing the throughput-delay trade-off. Next, we introduce two cooperative game pricing strategies to control user behavior and further optimize the trade-off between throughput and delay. Then, we study the previous scenario using this time a non-cooperative game. Thus, we consider selfish users who share the same transmission channel. Our analysis shows that users, in this case, transmit using a very high probability. This aggressive behavior leads to a dramatic situation where the wireless network fails. To address this issue, we propose introducing a transmission cost to mitigate the aggressive behavior of users. Thus, we can decrease the level of the selfishness of users without adding a central coordination unit, which allows us to have a significant improvement in network performance. Afterward, we propose to look for the optimal cost which allows for transforming the non-cooperative game into a cooperative game like the one studied in the first chapter. We then extend the two previous models into a general game model in which cooperative and non-cooperative users coexist. This model generalizes several models that consider either the concept of cooperation or non-cooperation to model a wireless network system.

For the MCP mechanism, we first propose a Markov model that models its operation in the case of saturated traffic. This model takes into account the existence of other types of traffic, such as unicast traffic, and it takes into account the backoff freezing if the channel is busy. Our goal is to achieve reliability of over 99.999% for multicast traffic. All the results found are validated by extensive simulations. We also study this model in the case of unsaturated traffic, and we evaluate different parameters of the Quality of Service (QoS) and the Quality of Experience (QoE) of the network based on the MCP mechanism. Finally, we propose a new approach to evaluate the energy consumption in the network. We estimate the energy consumed between two successive transmis-

sions for unicast traffic and multicast traffic.

Keywords: Game Theory, Stochastic Games, Nash Equilibrium, Cooperation, Selfishness, Markov Process, ALOHA, ZigZag, Multicast, Unicast.

Résumé

Cette thèse s'intéresse au problème d'accès au canal dans un réseau sans fil en utilisant des approches analytiques basées sur la théorie des jeux et la théorie des chaînes de Markov. L'objectif est d'améliorer les performances du réseau. L'accent est mis particulièrement sur l'accès au canal du trafic unicast et du trafic multicast. Deux mécanismes d'accès aléatoires sont proposés dans cette thèse, à savoir, "Slotted ALOHA ZigZag Decoding (SAZD)" et "Multicast Collision Prevention (MCP)". SAZD est une amélioration du mécanisme d'accès aléatoire Slotted ALOHA par la technique de décodage ZigZag alors que MCP est un mécanisme de multidiffusion conçu pour des communications vidéo très performantes. MCP appartient à la même famille des mécanismes d'accès aléatoire que SAZD, et il est caractérisé par la fonctionnalité de l'écoute du canal, mise en place par le mécanisme CSMA (Carrier-Sense Multiple Access). De plus, il est basé sur le mécanisme DCF (Distributed Coordination Function), qui exploite le schéma BEB (Binary Exponential Backoff) pour accéder au canal sans fil.

La thèse est composée de deux parties. La première partie est consacrée à nos contributions sur le mécanisme SAZD et la deuxième est consacré à nos contributions sur le mécanisme MCP.

Pour le mécanisme SAZD, nous proposions au début un modèle de jeu coopératif pour modéliser un scenario de réseau sans fil où les utilisateurs (les joueurs) transmettent les données suivant ce mécanisme. Le modèle proposé, prend en considération les contraintes suivantes: maximiser le débit, minimiser le délai, et optimiser le compromis débit-retard. Ensuite, nous introduisons deux stratégies de tarification au jeu coopératif afin de contrôler le comportement des utilisateurs et d'optimiser davantage le compromis entre le débit et le retard. Ensuite, nous étudions le scenario précédent en utilisant cette fois-ci un jeu non-coopératif. Ainsi, nous considérons des utilisateurs égoïstes qui partagent le même canal de transmission. Notre analyse montre que les utilisateurs dans ce cas transmettent en utilisant une probabilité très élevée. Ce comportement agressif conduit à une situation dramatique où le réseau sans fil tombe en panne. Pour résoudre ce problème, nous proposons d'introduire un coût de transmission afin d'atténuer le comportement agressif des utilisateurs. Ainsi, nous pouvons diminuer le niveau d'égoïsme des utilisateurs sans ajouter une unité centrale de coordination, ce qui nous permet d'avoir une amélioration importante au niveau des performances du réseau. Après, nous proposons de chercher le coût optimal qui permet de transformer le jeu non-coopératif à un jeu coopératif comme celui étudié en premier lieu. Nous étendons ensuite les deux modèles précédents en un modèle de jeu général dans lequel coexiste des utilisateurs coopératifs et non coopératifs. Ce model généralise plusieurs modèles qui considèrent soit le concept de la coopération ou la non-coopération pour modéliser un system de réseau sans fil.

Pour le mécanisme MCP, nous proposons d'abord un modèle de Markov qui modélise son fonctionnement dans le cas d'un trafic saturé. Ce modèle prend en considération l'existence d'autres types de trafics comme le trafic monodiffusion, et il prend en compte l'arrêt du compteur si le canal est occupé. Notre objectif est d'atteindre une fiabilité de plus de 99.999% pour le trafic multicast.

Tous les résultats trouvés sont validés par plusieurs simulations. Nous étudions aussi ce modèle dans le cas d'un trafic non saturé et nous évaluons différents paramètres de la qualité de service (QoS) et de la qualité d'expérience (QoE) du réseau en se basant sur le mécanisme MCP. Enfin, nous proposons une nouvelle approche pour évaluer la consommation d'énergie dans le réseau. Nous estimons l'énergie consommée entre deux transmissions successives pour le trafic unicast et le trafic multicast.

Mots clés: Théorie des jeux, Jeux stochastiques, Équilibre de Nash, Coopération, Égoïsme, Processus de Markov, ALOHA, ZigZag, Multicast, Unicast.

Resumen

Esta tesis aborda el estudio de mecanismos de acceso al canal en redes inalámbrica haciendo uso de métodos de análisis basados en la teoría de juegos y la teoría de cadenas de Markov. El objetivo es mejorar el rendimiento de las redes inalámbricas. Se pone especial énfasis en el acceso al canal para el tráfico unicast y el tráfico multicast. Se estudian dos mecanismos de acceso aleatorio, a saber, "Slotted ALOHA Enhanced by ZigZag Decoding (SAZD)" y "Multicast Collision Prevention (MCP)". SAZD es una mejora del mecanismo de acceso aleatorio Slotted ALOHA mediante la técnica de decodificación ZigZag, mientras que MCP es un mecanismo multicast diseñado para comunicaciones de video. MCP pertenece a la misma familia de mecanismos de acceso aleatorio que SAZD, y se caracteriza por la funcionalidad de detección de la actividad en el cana de comunicación, implementada por el mecanismo CSMA (Carrier-Sense Multiple Access). Además, se basa en el mecanismo DCF (Función de Coordinación Distribuida), que explota el esquema BEB (Binary Exponential Backoff) para acceder al canal inalámbrico.

La tesis se compone de dos partes. La primera parte está dedicada al estudio del mecanismo SAZD, y la segunda está dedicada a nuestras contribuciones al mecanismo MCP.

Para el mecanismo SAZD, inicialmente se propone un modelo de juego cooperativo para modelar un escenario de red inalámbrica donde los usuarios (es decir, los jugadores) transmiten datos de acuerdo con este mecanismo. El modelo propuesto tiene en cuenta las siguientes restricciones: maximizar el rendimiento, minimizar el retraso y optimizar la compensación rendimiento-retraso. A continuación, se presentan dos estrategias de costes de juegos cooperativos para controlar el comportamiento del usuario y optimizar aún más la compensación entre el rendimiento y la demora. Luego, se estudia el escenario anterior utilizando esta vez un juego no cooperativo. Así, se consideran usuarios egoístas que comparten el mismo canal de transmisión. Nuestro análisis muestra que los usuarios, en este caso, transmiten con una probabilidad muy alta. Este comportamiento agresivo conduce a una pésima situación en la que la operación de la red inalámbrica se pone en riesgo. Para abordar este problema, se propone el uso de un coste de transmisión para mitigar el comportamiento agresivo de los usuarios. Así, se logra mitigar el nivel de egoísmo de los usuarios sin agregar una unidad central de coordinación, lo que permite obtener una mejora significativa en el rendimiento de la red. Posteriormente, se propone buscar el coste óptimo que permita transformar el juego no cooperativo en un juego cooperativo como el estudiado en el primer capítulo. Luego, se propone una mejora a los dos modelos anteriores a un modelo de juego general en el que coexisten usuarios cooperativos y no cooperativos. Este modelo generaliza varios modelos que consideran el concepto de cooperación o no cooperación para modelar un sistema de red inalámbrica.

Para el mecanismo MCP, primero se propoen un modelo de Markov que modela su operación en el caso de tráfico saturado. Este modelo tiene en cuenta la existencia de tráfico unicast, y tiene en cuenta la interrupción del mecanismo de backoff cuando el canal se detecta ocupado. Nuestro objetivo es lograr una fiabilidad de más de 99.999% para el tráfico de multicast. Todos los resultados encontrados son validados por medio de simulaciones. Luego se aborda el estudio del

protocolo MCP en el caso de tráfico no saturado, y se realiza una evaluación del mismo por medio de diferentes parámetros de Calidad de Servicio (QoS) y la Calidad de Experiencia (QoE) de la red basados. Finalmente, proponemos un nuevo enfoque para evaluar el consumo de energía en la red. Estimamos la energía consumida entre dos transmisiones sucesivas para tráfico unicast y tráfico multicast.

Palabras clave: Teoría de Juegos, Juegos Estocásticos, Equilibrio de Nash, Cooperación, Egoísmo, Proceso de Markov, ALOHA, ZigZag, Multicast, Unicast.

Contents

List of Figures

List of Tables

Notations

Symbol	Description
M	Number of cooperative users
N	Number of non-cooperative users
m	Number of cooperative backlogged users
n	Number of non-cooperative backlogged users
p_a^i	Arrival probability to a user i
q_r^i	Retransmission probability of user i
$Q_a(i,n)$	Transmission probability of i unbacklogged users
$Q_r(i,n)$	Retransmission probability of i backlogged users
T_s	Packet transmission time
$\pi(p_a, q_r)$	Steady-state distribution of the Markov chain
$P_(n, n+i)$	Transition probability of the Markov chain from state n to state $n+i$.
D_n	Drift at state n which represents the average state change at the next transition
P_{idle}	The probability that no one is transmitting
S_M	Set of cooperative users
S_N	Set of non-cooperative users
u_i	Utility function of a user i
$\left([\mathbf{q_r}]^{-i}, q_r^i\right)$	Vector of the retransmission probabilities of all users, where q_r^i is the retransmission probability of user i, and $[\mathbf{q_r}]^{-i}$ is the vector of the retransmission probability of users in $S_N \setminus \{i\}$.
$\mathcal{R}_i$	Set of the best response strategies of a user i
q_c	Retransmission probability of a cooperative user
q_{nc}	Retransmission probability of a non-cooperative user
Ψ_c	Strategy profile of cooperative users
Ψ_{nc}	Strategy profile of non-cooperative users
A_i	Set of pure strategies
σ	Duration of empty time slot
τ	Transmission probability of unicast senders
Λ	Average system slot time

List of Abbreviations

Abbreviation	Meaning
KPIs	Key Performance Indicators
MOS	Mean Opinion Score
DCF	Distributed Coordination Function
ESS	Evolutionary Stable Strategies
NE	Nash Equilibrium
MAC	Medium Access Control
SAZD	Slotted ALOHA mechanism enhanced by ZigZag Decoding
SA	Slotted ALOHA
CSMA	Carrier Sense Multiple Access
CSMA/CA	Carrier Sense Multiple Access with Collision Avoidance
MCP	Multicast Collision Prevention
AP	Access Point
VQM	Video Quality Metric
US	Unicast Sender
IoT	Internet-of-Things
QoS	Quality-of-Service
QoE	Quality-of-Experience
MPR	Multiple Packet Reception
SNR	Signal-to-Noise Ratio
DRL	Deep Reinforcement Learning
ALOHA-Q	ALOHA with Q learning
ALOHA-QT	ALOHA with Quantitative Tree algorithm
MPL-BEB	multiple power level Binary Exponential Backoff
RA	Random Access
ZD	ZigZag Decoding
CSA	Coded Slotted ALOHA
SIC	Successive Interference Cancellation
CE	Capture Effect
NOMA	Non-Orthogonal Multiple Access
SINR	Signal-to-Interference-plus-Noise Ratio
AoI	Age of Information
WLANs	Wireless Local Area Networks
PCF	Point Coordination Function
DIFS	Distributed Inter-Frame Space

ACK	Acknowledgment
SIFS	Short Inter-Frame Space
DMS	Directed Multicast Service
GCR-U	Groupcast with Unsolicited Retries
GCR-BA	Groupcast with Block ACK
RIFS	Reduced Inter-Frame Space
PIFS	Point Inter- Frame Space
DTMC	Discrete-Time Markov Chain
RTS/CTS	Request-to-Send/Clear-to-Send
MRs	Multicast Receivers
EDCA	Enhanced Distributed Channel Access
NDN	Named Data Networking
IP	Internet Protocol
VOD	Video-on-Demand
HD	High Definition
UHD	Ultra-High Definition
ARQ	Automatic Repeat Request
LBP	Leader Based Protocol
NACK	Negative Acknowledgment
LAA	Licensed Assisted Access
LBT	Listen Before Talk
BEB	Binary Exponential Backoff
PGP	Parallel Gated Poll
PSM	Power Saving Mode
HCCA	Controlled Channel Access

Research Activities

List of publications

- **Boujnoui, A.**, Zaaloul, A., Orozco-Barbosa, L., Haqiq, A. "Stochastic Game Analysis of Cooperation and Selfishness in a Random Access Mechanism". Mathematics 2022, 10, 694. https://doi.org/10.3390/math10050694.
- **Boujnoui A.**, Zaaloul A., Haqiq A. "Enhanced Pricing Strategy for Slotted ALOHA with ZigZag Decoding: A Stochastic Game Approach". International Journal of Computer Information Systems and Industrial Management Applications (IJCISIM). ISSN 2150-7988, Volume 13 (2021) pp. 160-171. MIR Labs, https://www.mirlabs.net/ijcisim/regular_papers_2021/IJCISIM_15.pdf.
- **Boujnoui A.**, Zaaloul A., Haqiq A. "Cooperative Slotted ALOHA with ZigZag Decoding and a Pricing Mechanism". In: Abraham A., Sasaki H., Rios R., Gandhi N., Singh U., Ma K. (eds) Innovations in Bio-Inspired Computing and Applications. IBICA 2020. Advances in Intelligent Systems and Computing, vol 1372. Springer, Cham. https://doi.org/10.1007/978-3-030-73603-3_10.
- **Boujnoui, A.**, Barbosa, L.O. & Haqiq, A. "Performance evaluation and tuning of an IEEE 802.11 audio video multicast collision prevention mechanism". Wireless Networks (2020). https://doi.org/10.1007/s11276-020-02364-6.
- **Boujnoui, A.**, Zaaloul, A. & Haqiq A. "Mathematical Model based on Game Theory and Markov Chains for Analysing the Transmission Cost in SA-ZD Mechanism". International Journal of Computer Information Systems and Industrial Management Applications. ISSN 2150-7988 Volume 10 pp. 197–207 (2018). https://www.mirlabs.net/ijcisim/regular_papers_2018/IJCISIM_20.pdf.
- **Boujnoui, A.**, Zaaloul, A. & Haqiq A. "A Stochastic Game Analysis of the Slotted ALOHA Mechanism Combined with ZigZag Decoding and Transmission Cost". International Conference on Innovations in Bio-Inspired Computing and Applications. Springer, Cham, (2017). https://doi.org/10.1007/978-3-319-76354-5_10.

Oral communications

- The 2nd Technical Meeting organized by the COST Action CA20120, "Intelligence-Enabling Radio Communications for Seamless Inclusive Interactions". June 13-15 2022, LYON, FRANCE.
- The 1st Technical Meeting, University of Bologna, Department of Electrical, Electronic, and Information Engineering "Guglielmo Marconi"- DEI, Bologna, Italy, February 8 - 11, 2022.
- The 11th International Conference on Innovations in Bio-Inspired Computing and Applications, December 16 - 18, 2020.
- JP2019: Journées de Probabilités 2019, Dourdan, France, Jun 24 - 28, 2019.
- The 8th International Conference on Innovations in Bio-Inspired Computing and Applications, Marrakesh, Morocco, December 11 - 13, 2017.

Posters

- École d'automne 2019 UM6P/ENPC, Benguerir, Morocco, Novembre 13 - 14 - 15, 2019.
- Doctoral Day of Hassan First University of Settat, (First award of communication poster), Settat, Morocco, April 5, 2018.

Training schools and workshops

- Game Theory and Applications for Big Data, Cloud computing and Cybernetics, University Mohammed 1er E.N.S.A., OUJDA, Morroco, December 19 to December 21, 2018.
- CIMPA school, Algebraic, combinatorial and analytical aspects of free probabilities, the school of Centre International de Mathématiques Pures et Appliquées at FST of Settat, Morroco, April 17 to April 28, 2017.
- Machine Learning and Distributional Data, faculty of sciences and techniques of Marrakesh, University Cadi Ayyad, Marrakesh, Morocco, February 13 to February 16, 2017.
- Summer school, Smart, Secure, Embedded and Mobile, e-Next Generation Networks, Marrakesh, Morocco, July 15 to July 17, 2016.

Research internships

- Research Internship, Albacete research institute of informatics (I3A), University of Castilla–La Mancha, Spain, partially supported by an Erasmus+ KA107 grant, June 11, 2021 to June 30, 2022.

- Research Internship, Albacete research institute of informatics (I3A), University of Castilla–La Mancha, Spain, supported by a mobility grant from Hassan First University of Settat, Albacete, Spain, April 22 to June 21, 2019.
- Research Internship, Albacete research institute of informatics (I3A), University of Castilla–La Mancha, Spain, supported by a mobility grant from Hassan First University of Settat, Albacete, Spain, May 16 to July 09, 2018.

General Introduction

Introduction

Since the introduction of the first generation (1G) wireless technologies in 1979, we have been witnessing a tremendous increase in the number of wireless technologies, the number of wireless-connected devices, as well as the development of a wide number of applications and services.

Nowadays, numerous services are being deployed not only to better support human-operated applications, but an increasing number of device-based or the so-called Internet-of-Things (IoT) applications. However, the massive deployment of connected devices requires efficient wireless channel management. Thus, reliable channel access mechanisms are required due to the significant demand experienced by wireless systems and the increasing demand for video services. The increase in the number of users and the ever-increasing variety of novel applications characterized by different traffic patterns and Quality-of-Service (QoS) and Quality-of-Experience (QoE) are making necessary the introduction of novel control mechanisms. Such mechanisms should not only be able to provide the required key performance indicators (KPIs), such as throughput, delays, and loss rates, but equally, important the perceived QoE by the end users, such as the Mean Opinion Score (MOS) used to evaluate subjective video quality. However, the main challenges facing the design and the enhancement protocols do not only be centered on showing the effectiveness of novel mechanisms, but they should also be able to consider the inter-operation with legacy technologies. This inter-operation should even consider the co-existence of new mechanisms and the legacy ones.

Random access mechanisms have been widely employed in wireless telecommunications to manage channel access and mitigate multiple-access contention. Regardless of the channel state, users can transmit their data without any prior coordination. As a result, different users may interfere with each other, which may cause data loss and network performance degradation. Dealing with channel contention and data loss is one of the main challenges addressed in this thesis. ALOHA is the most random access mechanism studied in the literature. It simply specifies that the data packet should be transmitted immediately after it is generated. Thus, simultaneous transmission from different users may collide, which may lead to partial or complete data loss. Then, Slotted ALOHA was proposed to increase the maximum throughput to up to 36.8% compared with only 18.4% for ALOHA. Nowadays, Slotted ALOHA is adopted in many modern technologies, such as, satellite networks [1], LoRaWAN networks [2, 3, 4], IoT applications [5], Machine-to-Machine (M2M) communications [6], and NOMA (Non-Orthogonal Multiple Access) for the Next Generation IoT [7].

When packets collide, the data packet is considered lost, and retransmission is scheduled according to the same access mechanism. However, collisions may occur even during retransmissions,

causing more collisions and system stability issues. To mitigate this problem, many collision resolution schemes have been proposed, such as Successive Interference Cancellation (SIC) [8], Capture Effect [9], and ZigZag Decoding (ZD) [10, 11, 12]. In this thesis, we consider ZigZag Decoding as a collision resolution scheme to improve the performance of Slotted ALOHA. The receiver equipped with ZigZag can decode two packets sent at the same time slot. As a result, collisions in the enhanced mechanism occur only when three or more users transmit at the same time slot.

Research has lately started to focus on mathematical models explaining channel access mechanisms such as ALOHA and its enhanced variants. In [13], the authors provide an analytical model of the pure and Slotted ALOHA with Multiple Packet Reception (MPR). They found that time slotting has positive and negative consequences. On the one hand, it prevents the ongoing transmission from colliding with another potential transmission. The authors in [14] proposed to enhance the Slotted ALOHA using the Capture Effect (CE) mechanism. With the CE, the receiver can decode the packet sent at high power among simultaneous transmissions as long as the tagged packet is the only one sent with the highest power. The authors also proposed combining ZD and CE mechanisms to enhance further the Slotted ALOHA mechanism [15]. The extended mechanism showed very efficient in terms of all performance metrics. The authors showed that it outperforms the standard Slotted ALOHA [16] as well as the enhanced versions, i.e., with ZD [17], and with CE [14].

Another enhancement mechanism to the Slotted ALOHA is the Successive Interference Cancellation: a collision resolution approach based on the received Signal-to-Noise Ratio (SNR). SIC refers to the ability of the receiver to decode packets that are transmitted with an SNR higher than a given threshold. In [18], it was assumed that users select a transmission power level based on a given distribution. In [19], the receiver adopts a set of power levels, and each user adapts the transmission power based on the channel state. In [20], the authors analyzed the maximum sum rates of Slotted ALOHA with ordered SIC and unordered SIC. They also studied the effect of MPR on system performance.The authors in [21] presented a model analysis of an extension of the Slotted ALOHA named threshold-ALOHA. In this mechanism, the users implement the Slotted ALOHA mechanism only when their age reaches a certain threshold. Otherwise, they have to stay silent in order not to disturb the users who have larger ages. Thus, if the age is below a certain threshold, the user should stay silent, and if not, it will transmit with a fixed probability using the Slotted ALOHA mechanism.

In [22], the authors proposed a novel approach based on the policy trees to improve the Slotted ALOHA mechanism. The proposed approach makes a balance between the ALOHA-Q and DRL-based (Deep Reinforcement Learning) approaches. They introduced two ALOHA variants. The first one, ALOHA-QT, uses the Quantitative Tree (QT) algorithm, which varies the transmission rate of the user and adapts to the number of active nodes. In contrast, the ALOHA-QTF variant achieves fairness in short periods.

The transmission cost is another approach that was proposed in the literature to enhance the performance of the Slotted ALOHA and mitigate contention between users. In [16], they proposed a new pricing mechanism for the standard Slotted ALOHA using a cooperative and non-cooperative

game framework. For every transmission and retransmission, they associated a cost denoted by c. Although the idea seems interesting, it yields the same trade-off addressed in this paper for the improved version SAZD. A similar strategy was adopted in [23], where they investigated the Binary Exponential Backoff Algorithm with Multi-Power Diversity (MPL-BEB). The proposed game model shows that the improved MPL-BEB outperforms the standard MPL-BEB and BEB.

On the other hand, significant works have been proposed to model the Carrier Sense Multiple Access (CSMA) [24] for IEEE 802.11 networks. Most previous research efforts focus on modeling the Distributed Coordination Function (DCF) access mechanisms implemented by the CSMA. Among them is the work of Bianchi [25], in which a bi-dimensional Markov chain was proposed with infinite retransmission attempts. The study of Bianchi provides the saturated throughput of the basic access mechanism as well as the Request-to-Send/Clear-to-Send (RTS/CTS) mechanism. This model has been reviewed and improved in the literature to better capture the performance of the access mechanisms.

Besides the works reported on the evaluation of IEEE 802.11 models [26, 27], most works deals with the unicast service provided by the IEEE 802.11 networks. However, not many works considered the presence of multicast traffic. The evaluation of the multicast service is of great interest since it has a significant impact on the unicast service. In [28], the authors proposed to analytically model the legacy multicast mechanism of IEEE 802.11 in the presence of both unicast and multicast traffic. They further extended their work to the case of unsaturated traffic conditions [29, 30], where packets may not always be ready for transmission at the stations' buffer. In [31], the authors introduced a simple multicast mechanism. They showed that their proposal could properly coexist with the legacy DCF mechanism. The authors have further conducted a simulation-based performance study [32]. Despite confirming that their proposal is able to properly interoperate with legacy IEEE 802.11 mechanisms, they have not provided the configuration guidelines for guaranteeing the QoS requirements of audio/video services.

The optimization of most multicast mechanisms introduced in the literature, including the IEEE 802.11aa amendments, is still an open issue [27, 33]. The debate is still open within the standards community, actively seeking simple multicast mechanisms developed on top of the legacy DCF mechanism [34]. In order to validate the effectiveness of the amendments and numerous proposals, researchers have focused their efforts on developing accurate mathematical models.

Regarding the methods and tools used in the evaluation of communications, the probabilistic approaches and game theory are widely used by the research community and the industry. As the level of complexity and details characterizing the use of simulation tools makes possible not only the validation of the probabilistic models, but also the evaluation of the proposed solutions taking into account a wider spectrum of variables.

This thesis is organized into two main parts. Part 1 focuses on the study of the ALOHA mechanism, including the ZigZag decoding. This study is based on game analysis of the aforementioned protocol and decoding scheme. These sections include a cooperative, a non-cooperative, and a general analysis of the slotted ALOHA mechanism while implementing the ZigZag decoding scheme. Part 2 deals with a multicast mechanism. A performance model of the mechanism and its evalua-

tion is first carried out under saturated traffic conditions. Thereafter, a study under non-saturated conditions is introduced. Finally, an energy-consumption study was undertaken to evaluate the energy efficiency of the multicast mechanism.

Research Objectives and Challenges

The works of this thesis have two main objectives.

- Study of the wireless medium access control mechanisms. This part includes the study of the well established ALOHA protocol supplemented by the ZigZag decoding scheme. Despite some of the major drawbacks exhibited by the ALOHA protocol, this access mechanism is being used by the latest IoT network technologies, such as LoRA. This objective also includes the study of a multicast wireless access mechanism for the IEEE 802.11 standard.
- The modelling, evaluation and simulation based on mathematical principles, probabilistic approaches to evaluate the performance of the access mechanisms. Furthermore, the game theory is used to evaluate the impact of the behavior of selfish users over the performance of a network implementing the ALOHA protocol and using the ZigZag decoding scheme. As for the study of the multicast mechanism, a probabilistic model has been developed and validated via simulation. The performance metrics for this multicast mechanism include four QoS metrics, namely throughput, delay, jitter and packet loss probability as well as QoE metrics.

Research Contributions

The main contributions of this thesis are listed as follows:

1. A cooperative game model was proposed to evaluate the performance of the SAZD mechanism. Furthermore, different pricing mechanisms have been proposed to efficiently optimize the trade-off between newly arrived packets and backlogged ones.
2. A non-cooperative game model was proposed to evaluate the performance of the SAZD mechanism. Moreover, a pricing mechanism was proposed to stimulate users' cooperation without central coordination unity.
3. This contribution proposes and develops a general stochastic game model that incorporates the cooperative and non-cooperative game theories. The model extends the models proposed in the two first contributions.
4. A bi-dimensional Markov model of an opportunistic multicast access mechanism for video communications under saturated conditions was proposed, in which, unicast and multicast data traffic are considered. Furthermore, an optimization approach was adopted to derive the optimal MCP parameter L^*, which yields a loss rate of less than 10^{-5}.

5. Considering unsaturated conditions, the MCP mechanism was modeled using a bi-dimensional Markov chain. Besides, a QoS/QoE study was undertaken in order to show the effectiveness of MCP.

6. The last contribution aims to evaluate the energy consumption of the MCP mechanism. The energy was evaluated between two successful transmissions. Moreover, an energy comparative study was made between the energy-consumption of the AP operating the MCP mechanism and the energy-consumption of unicast senders operating DCF mechanism.

To tackle these contributions, we are based mainly on the mathematical tools introduced in the next section.

Mathematical Tools

Among the methods and tools used on the evaluation of communications, the probabilistic approaches and game theory are widely used by the research community and the industry. As the level of complexity and details characterizing the use of simulation tools makes possible not only the validation of the probabilistic models, but also the evaluation of the proposed solutions taking into account a wider spectrum of variables.

Probabilistic Approaches

The goal of probability theory is to create a mathematical model that may be used to describe and interpret a specific set of observed phenomena [35]. The phrases "probability" and "probable" are frequently used in regular conversation. In practice, we would like to assign probabilities to occurrences in such a way that the probability assignment accurately reflects the event's likelihood of occurring.

We come across examples in many different sectors of practical and scientific endeavors where specific tests or observations can be performed several times under uniform conditions, each time yielding a certain definite results.

If the outcome cannot be predicted, the experiment can be described as a stochastic one by using the concept of probability. The mathematical model of probability is represented by the triplet $(\Omega, \mathcal{E}, P)$, where Ω is the set of stochastic experiment outcomes, $\mathcal{E}$ is a set of events, and P is a probability measure, i.e., a map that assigns uniquely real numbers to events.

Any probability measure is acceptable in the axiomatic theory of probability if it satisfies the following axioms:

i) The occurrence probability of any event $\mathcal{A}$ is a real number lying in the interval $[0, 1]$. i.e., $0 \leq P(\mathcal{A}) \leq 1$.

ii) The universal or certain event is assigned probability 1. i.e., $P(\Omega) = 1$.

iii) For any countable collection of events $\{\mathcal{A}_i\}_{i\geq 1}$ that are mutually exclusive (i.e., $\mathcal{A}_j \cap \mathcal{A}_k = \varnothing, \forall j \neq k$), we have $P(\bigcup_{i\geq 1} \mathcal{A}_i) = \sum_{i\geq 1} P(\mathcal{A}_i)$.

There are no specific difficulties as long as the sample space is finite or denumerable, and it is always possible to specify a probability value for any event, i.e., $\mathcal{E}$ can coincide with the power set of Ω. When Ω is infinite and nondenumerable, this is no longer true in general (e.g., the points belonging to a segment of the real line). In that situation, Ω must be limited to events for which probability meeting all three above axioms can be assigned, i.e., events must be sets to which a "measure" can be assigned. The mathematical theory of probability is, in fact, inextricably linked to the theory of measurement.

Since the last century, there has been a growing recognition that stochastic or non-deterministic models are suitable and more realistic than deterministic models in many situations. The stochastic process is the mathematical description of a random phenomenon that changes over time. Any attempt at mathematically describing observed phenomena must involve some idealization of genuinely observed facts. The mathematician's formulae can only provide a simplified mathematical model of reality, a kind of idealized picture of the characteristics of the phenomenon under investigation. Many phenomena in the physical and life sciences are evaluated not only as random events, but also as ones that change through time and space. Similar considerations are made in other fields, such as social sciences, economics, and management sciences. The applications of stochastic processes that are functions of time, space, or both began to draw the attention of many scientists.

In the context of the computer communications, and in particular medium access protocols, probabilistic models have been widely used over the past 50 years. Throughout this thesis, we make extensive use of the probabilistic approach to model the operation of the two main protocols under study.

Markov Processes

Modern probability theory investigates chance processes in which previous results influence the predictions of future experiments. In general, when we observe a series of random experiments, all of the previous outcomes can influence our predictions for the next experiments. This should be the case, for example, when predicting a student's grades on a series of exams in a course. However, allowing this much generality would make it extremely difficult to prove general results. A. A. Markov began researching a significant new type of chance process in 1907. In this process, the result of a given experiment can influence the result of the next one. This type of process is called a Markov chain.

Consider a stochastic process $(X_t)_{t\in I}$ representing a certain random phenomena, where t refers to time. We say that the process $(X_t)_{t\in I}$ satisfies the Markov property, or that $(X_t)_{t\in I}$ is a Markov process, if the transition probabilities $\mathbb{P}(X_{t_{n+1}} = x_{n+1}|X_{t_n} = x_n, ..., X_{t_1} = x_1)$ are a function of x_n only, and do not depend on $x_1, ..., x_{n-1}$, i.e., if

$$\mathbb{P}\left(X_{t_{n+1}} = x_{n+1}|X_{t_n} = x_n, ..., X_{t_1} = x_1\right) = \mathbb{P}\left(X_{t_{n+1}} = x_{n+1}|X_{t_n} = x_n\right)$$

holds for all time points $0 \leq t_1 < ... < t_{n-1} < t_{n+1}$. To understand this definition, we consider t_n as the present time so that t_{n+1} represents some point in the future and $t_1, t_2, ..., t_{n-1}$ represent different points in the past. The Markovian property then states that the future is independent of the past given the present. In other words, the future of the random process depends only on where it is now and not on how it got there. A picturesque description of the Markov chain is given in [36], where it is described as a frog jumping on a set of lily pads. The frog starts on one of the pads and then jumps from lily pad to lily pad with the appropriate transition probabilities.

A Markov process's distribution is completely specified by two pieces of information, namely

- The initial distribution of the process $\mathbb{P}(X_{t_0})$.
- The transition probabilities

$$P_{i,j} = \mathbb{P}(X_t = j | X_s = i), \quad i, j \in E, \quad s, t \in I,$$

  where E is the state space of the Markov chain.

Markov processes are perhaps the simplest model of a random evolution without long-term memory. R. A. Howard [36] provides us with a picturesque description of a Markov chain as a frog jumping on a set of lily pads. The frog starts on one of the pads and then jumps from lily pad to lily pad with the appropriate transition probabilities.

In practice, we are interested in characterizing the statistics of the Markov chain as t tends to infinity. Many problems modeled by Markov chains address issues that live theoretically on the whole time axis, i.e., those are steady-state issues. Hence, it is essential to understand if and how the transient dies out and to what limit the probability distribution tends eventually.

Markov chains have been used in modeling physical, biological, social, and engineering systems such as population dynamics, queueing networks, and manufacturing systems. The advances in technology have opened up new domains and provided greater opportunities for further exploration. Applications of Markovian models have emerged from wireless communications, internet traffic modeling, and financial engineering in recent years. One of the main advantages of using Markovian models is that it is general enough to capture the dominant factors of system uncertainty. In the meantime, it is mathematically tractable.

Most dynamic systems in the real world are inevitably large and complex, mainly due to their interactions with the numerous subsystems. Moreover, rapid progress in technology has also made modeling more challenging. An example is the design of random access mechanisms for wireless networks.

In the second part of this thesis, we develop a Markov chain to model and evaluate the performance of a multicast mechanism under various scenarios. We start by considering a traffic saturation scenario in the presence of unicast and multicast traffic. Our model better captures the operation details of the random access mechanism, the so-called Distributed Coordination Function (DCF) of the IEEE 802.11 standard when compared to the widely cited model developed by Bianchi [25]. Furthermore, we derive the expression allowing us to evaluate four metrics of particular interest in the area of wireless multicast video communications.

Stochastic Games

Game theory is a field of applied mathematics for analyzing complex interactions among entities. It is basically a study of strategic decision-making, usually referred to as "players" or "agents". In a more formal sense, it is the study of mathematical models of cooperation and conflict between intelligent, rational decision-makers [37]. Game theory has found its widespread application in mathematical economics and business for modeling competing behaviors of interacting agents. Application of game theory includes various economic and engineering phenomena such as auctions, bargaining, duopolies, oligopolies, and mechanism design.

One of the most useful applications of game theory is the evolutionary game theory which was originally developed in biological sciences for studying the evolution and equilibrium behavior, called Evolutionary Stable Strategies (ESS), of evolving populations. It was defined by J. M. Smith and G. R. Price in 1973 as strategies and the mathematical criteria that can be used to predict the results of competing strategies [38]. While rich theoretical foundations of evolutionary games allow biologist to explain past and present evolution and predict future evolution [39], it can be further used for protocol design and architect evolution [40] [41].

Stochastic games were first introduced by Shapley in 1953. In his seminal paper, Shapley [42] demonstrated the existence of value and optimal stationary strategies for zero-sum discounted stochastic games. His proof naturally provided a recipe for the iterative computation of the value of the game. Gillette [43] then studied zero-sum undiscounted stochastic games and showed that, in general, they might not possess optimal stationary strategies. The existence of Nash Equilibrium (NE) in stationary strategies for discounted nonzero-sum stochastic games was independently established by Fink [44], Takahashi [45] and Rogers [46]. Hoffman [47] studied nonterminating stochastic games with an average payoff and gave a policy-iteration algorithm for solving such games. Ligget [48] demonstrated the existence of pure stationary strategy equilibrium in such games under perfect information.

Recently, computer science and engineering have been added to the list of scientific areas applying game theory. For example, it can be applied to communication networks from several aspects: the physical layer, link layer, and network layer. However, there are certain challenges when applying game theory principles to wireless networks. For example, it assumes that players act rationally, which does not precisely reflect real systems. Furthermore, realistic scenarios necessitate complex models, yet the main challenge is to select the appropriate utility function due to a lack of analytical models that would map each node's available actions to higher layer metrics.

The basic entity in all game-theoretic models is a player. A player can be interpreted as either an individual or a group of individuals making decisions. Once the set of players has been defined, we can distinguish between two types of models: those in which all players attempt to optimize the overall payoff, and those in which each individual player seeks to optimize its own payoff. Models of the first type are referred to as "cooperative," while models of the second type are referred to as "non-cooperative."

Cooperative game theory studies the situation of collaboration between players through binding agreements. In cooperative games, players work together by forming groups, also called coalitions,

and take joint actions so as to realize their goals. However, players are not assumed to be altruistic, i.e., they only join a coalition if this helps them increase their individual profit. Indeed, competition plays an important role in cooperative games, as the agents have to divide the fruits of their collective labor. For example, in political games, parties or individuals can form coalitions to improve their voting power.

Non-cooperative game theory provides the theoretical framework for studying the interaction between selfish players. In general, a non-cooperative game consists of a set of players, while each player has its strategy, whereby utility (payoff) for each player measures its level of satisfaction. Each player's objective is to maximize the expected value of its own payoff [37]. In non-cooperative games, a crucial concept is called Nash Equilibrium (NE) [49]. NE is a set of strategies in which each strategy is the best response to other strategies. If all players are playing the strategies in a NE, nobody has a unilateral incentive to deviate.

An essential notion in game theory models is the information provided to players. A game has perfect information, if all players are fully informed about each other's moves, i.e., each player is aware of or can see the moves of the other players. Chess is a good example because each player can see the other player's pieces on the board. On the other hand, a game has imperfect information when decisions must be made concurrently and when players cannot be sure exactly what has taken place so far in the game and what their position is. The card game in which each player's card is hidden from the other players is an example of an imperfect information game. The notion of information set was introduced by John von Neumann, motivated by studying the game of Poker.

One of the most interesting situations in game theory is the prisoner's dilemma. A prisoner's dilemma is a situation in which players or decision-makers are always interested in a strategy profile that yields an outcome that is less than the optimal outcome for the individuals as a group. In other words, a player would gain more if he cooperated. However, if one defects, the other will be heavily penalized. The classic illustration of the prisoner's dilemma [50] goes like this: Two members of a criminal organization have been apprehended and incarcerated. Each prisoner is in solitary confinement and is unable to communicate with the other. Prosecutors do not have enough evidence to convict them together on the main charge, but they do have enough to convict both on a lesser charge. Therefore, the prosecutors make a deal with each prisoner. Each prisoner is given the option of betraying the other by testifying that the other committed the crime or cooperating with the other by remaining silent. The typical prisoner's dilemma is set up in such a way that both parties choose to protect themselves at the expense of the other participant. As a result, both participants find themselves in a worse state than if they had cooperated with each other in the decision-making process. The prisoner's dilemma is one of the most well-known concepts in modern game theory, and it occurs in many aspects of the economy and networking. Some of the scenarios introduced in this thesis are described as the prisoner's dilemma situation.

In this thesis, we applied the principle of game theory a cooperative, a non-cooperative and a general game model of the slotted ALOHA protocol enhanced using a ZigZag decoding scheme. The results of this study are highly relevant to the analysis of MAC mechanisms in the current context of wireless communications. As mentioned in the introduction, the ever-increasing use of

wireless facilities requires an analysis of the protocols under various scenarios. Our study shows the impact of the user behavior over the overall network performance and the individual users.

Discrete Event Simulations

With the increasing computational power of low-cost computers, simulation of various systems is becoming extremely prevalent. Even when a problem is analytically tractable, writing a program to simulate the desired results is of great interest. The purpose of the simulation is to validate the results obtained through analytical study and provide simple guidelines on tuning up the main system parameters. It is also used in the concept of learning from using simulation models.

Computer simulation for random access mechanisms in the MAC layer entails creating a detailed operational model of the access mechanism and then reproducing all of the processes and events involved in that detailed model using a computer program. This is obviously not a real-life system; rather, it is a virtual representation of how a simplified version of the real-life system would operate. The only limitations of this approach are the limitations of the coding language and the available computational resources. In fact, setting up a simulation program requires specialized equipment and a high software coding skill level or sometimes extensive training on specific packages. Another drawback of simulation models is their flexibility limitations. Indeed, making minor modifications to the simulation model requires a lot of effort and time.

The simulation results presented in this thesis are obtained using the discrete event simulation approach, which simulates the evolution of a complex system over time. This approach is used for modeling real-world systems that can be decomposed into a series of sequential events or processes that autonomously progress over time. One might wonder why we didn't perform real-life experiments instead of focusing on the simulation. Well, real-life implementation of the access mechanism introduced in this thesis requires a change on the MAC layer, which is not possible unless we make hardware modifications, i.e., create a piece that does the job. As this is a costly and high-level operation, simulation remains the best choice.

In this thesis, we develop a custom-made Matlab simulator using the discrete event simulation approach. To make sure that the stationary regime (analytically referred to as steady-state) is reached, we run every single simulation for $10^9\,\mu s \approx 16$ minutes.

To better understand the stationary regime, we plot in Figure 1 the evolution over time of the unicast throughput. The figure shows that the steady-state is reached after only $7.4s$ from the start of the simulation. We emphasize that this transition period before reaching the steady-state represents only 0.08% of the simulation time. To get accurate results, we run each simulation 100 times. Of course, it is possible to run the simulations as many times as possible. However, this will requires more time and much more computational resources. According to our tests, 100 simulations are more than enough to get very accurate results.

All the simulations and analytical results have been obtained using MATLAB, under the academic license provided by the University of Castilla-La Mancha (UCLM). The simulations were performed in Galgo, the supercomputer installed in the Albacete Research Institute of Informatics,

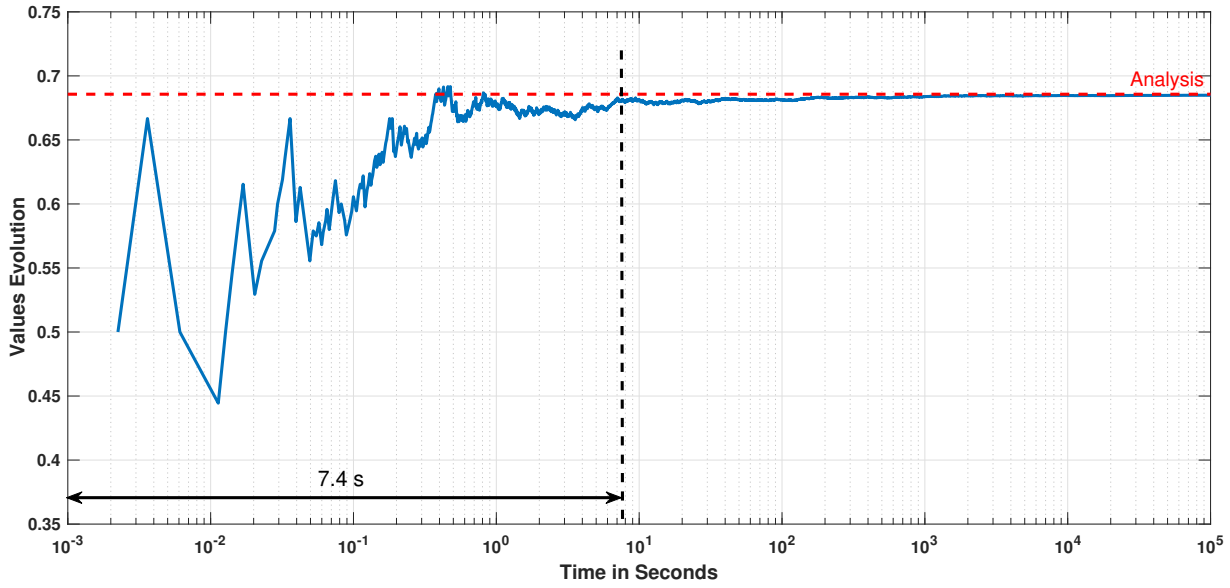

Figure 1: Simulation of the evolution of unicast throughput in the presence of unicast and multicast traffic.

University of Castilla-La Mancha.

Thesis Structure

In the following, we present a preliminary survey of the contents of each chapter, introducing the main results that we achieved in more detail.

Chapter 1: Cooperative Game Analysis of the Slotted ALOHA Mechanism Enhanced by ZigZag Decoding

This chapter considers a cooperative game framework to analyze a network scenario where M bufferless users share a common wireless channel for data transmission. The random access mechanism under study is the Slotted ALOHA mechanism enhanced by ZigZag Decoding (SAZD). However, a comparative study with the regular Slotted ALOHA (SA) is also provided. The cooperative game model takes into account different cooperation scenarios, such as maximizing the network throughput or minimizing the access delay. The results showed that SAZD outperforms SA in terms of all performance metrics of interest. Furthermore, we showed the existence of a trade-off between the throughput and the backlogged packets. In the second part of this chapter, we introduce a pricing mechanism to the game using two different strategies. The goal is to efficiently optimize the game and get rid of the inherent trade-off.

Chapter 2: Non-cooperative Game Analysis of the Slotted ALOHA Mechanism Enhanced by ZigZag Decoding

In this chapter, we investigate the case where users act selfishly by attempting to optimize their own benefits irrespective of the impact of this behavior on other users and on the overall network. To model such a situation, we propose a mathematical model based on the non-cooperative game theory. We consider a network scenario consisting of N selfish users competing to access a shared wireless channel using the SAZD mechanism. The network system state is obtained using a bi-dimensional Markov chain, from which we derive all the performance metrics.

We then investigate the impact of introducing a pricing mechanism on the behavior of selfish users. At first, we introduced a fixed cost for every transmission attempt. The results of this approach show that we are able to reduce the selfishness level of users. Then, we conducted an optimization study of the transmission cost that allowed us to convert the non-cooperative game into a cooperative game similar to the one studied in Chapter 1. The proposed optimization study takes into account the existing trade-off between the throughput and the backlogged delay. We propose different optimal costs to address this problem: the first one provides the best throughput, the second one guarantees a minimal delay for backlogged packets, and the last one compromises the existing throughput-delay trade-off. The originality here is that we are able to force the cooperation between selfish users. This way, we get the same performance as if all users are cooperating with each other.

Chapter 3: General Game Model for Slotted ALOHA and Slotted ALOHA Enhanced by ZigZag Decoding

This chapter provides an extension model that generalizes the two previous chapters. We propose a stochastic game analysis of a network scenario consisting of M cooperative and N non-cooperative users that access a shared wireless channel using the SAZD access mechanism. We assume that cooperative users access the channel with the intention that everyone is cooperating for the overall benefit. However, each non-cooperative user, on the other hand, seeks to optimize its own utility regardless of the impact of this behavior on the other users.

To get the system state in the stationary regime, we construct and develop a bi-dimensional Markov chain. We derive all the performance metrics of interest such as the throughput, the delay, and the number of backlogged packets for both cooperative and non-cooperative users. The equilibrium of the proposed game combines the social optimality concept of the cooperative game and the Nash equilibrium of the non-cooperative game. We prove the existence of such an equilibrium. Interestingly, the results of this work show that in some cases, non-cooperating users get better performance compared to the cooperating users. Furthermore, we showed that the network could practically benefit from the existence of non-cooperative users. However, as their number gets larger, their selfish behavior might ruin the game, which results in the collapse of the entire network performance. In game theory, this situation is known as the prisoner's dilemma, where players know that non-cooperating is not efficient; however, it is the rational choice since deviating from it might lead to the worst individual performance. The results also show that the network

could tolerate the existence of up to two selfish users thanks to the ZigZag scheme.

ALOHA [51] and CSMA (Carrier Sense Multiple Access) [24] belong to the same family of random access mechanisms. These mechanisms and their variants have been widely studied and enhanced over the past few years. In the next part of the manuscript, we study a variant of the CSMA mechanism named Multicast Collision Prevention mechanism (MCP), that is originally introduced to enhance the reliability of video communications [32].

Chapter 4: Performance evaluation and tuning of an IEEE 802.11 audio video multicast collision prevention mechanism: Saturated conditions

In this chapter, we study the MCP random access mechanism that was proposed in [32]. We consider the scenario of multiple users that share the same wireless channel for data transmission to a single Access Point (AP). Users transmit uplink unicast data to the AP using the CSMA/CA (Carrier Sense Multiple Access with Collision Avoidance) mechanism which is based on the Distributed Coordination Function (DCF) mechanism. On the other hand, the AP that is in charge of transmitting multicast packets implements the MCP mechanism. However, the AP can also transmit regular unicast packets as any other station using the CSMA/CA mechanism. The novelty of this chapter is to mathematically model such a complex scenario where different mechanisms are implemented. We focus in this chapter on the case of saturated traffic conditions, i.e., a packet is always available at the buffer whenever the current one is transmitted.

Using two bi-dimensional Markov chains, we model the operation of the AP as well as other unicast users, and we derive all their performance metrics. One of the interesting features of the MCP mechanism is the use of a second timer after the expiration of the original timer introduced by the DCF access mechanism. The second novelty of this work is to appropriately set the length of this timer using a mathematical optimization approach.

We show that in the legacy IEEE 802.11 multicast mechanism, the loss rate increases with the number of unicast stations. In contrast, the MCP mechanism with the optimal timer's length L^* guarantees a loss rate below 10^{-5} for any number of contending unicast stations. These results are very interesting for video applications where the video content is streamed to a group of users. The results of this chapter are validated through a costume-made MATLAB simulator.

Chapter 5: Opportunistic Multicast Access Mechanism for Video Communications over IEEE 802.11 with QoS/QoE Guarantees: Unsaturated Conditions

In this chapter, we undertake the study of the MCP mechanism under unsaturated conditions, i.e., packets are not always available at the station's queue. The scenario proposed in this chapter considers that the AP holds a queue for unicast packets and another separate queue for multicast packets. Thus, we distinguish between three kinds of packet traffic: 1) unicast packets that are sent by the AP, 2) unicast packets that are sent by the unicast users that are connected to the AP, and 3) multicast packets that are transmitted only by the AP. This scenario extends the originally proposed scenario [32], where the AP can only transmit multicast packets.

We propose to model the backoff operation of each packet traffic using three different Markov

chains and by considering the unsaturated conditions. For every traffic, we derive all the performance metrics, such as throughput, delay, and loss probability. With this new scenario, we consider a novel optimization study that takes into account the QoS requirements of the most robust video communications. Furthermore, we provide a QoE-aware study of the MCP mechanism in terms of the Mean Opinion Score (MOS) and Video Quality Metric (VQM) using the three most known video codecs H.265, VP9, and Xvid. The results of this chapter are validated with a costume-made MATLAB simulator.

Chapter 6: Energy Analysis of a Multicast Access Mechanism for Video Communications over IEEE 802.11

This chapter evaluates the energy consumed for transmitting unicast and multicast packets. We define the energy cycle as the energy wasted by a station (i.e., AP or Unicast Sender (US)) between two successive successful transmissions. The proposed model takes into account all the station's states, i.e., transmitting, listening, receiving, and idling. To show the energy efficiency of the MCP mechanism, we compare its energy consumption with the energy consumption of the legacy multicast mechanism defined by the standard IEEE 802.11. The results show that the MCP mechanism attains an energy gain of up to 70% compared with the legacy multicast mechanism. Furthermore, we compare the energy consumption of the AP when transmitting multicast packets using MCP and the energy consumption of USs when transmitting unicast packets using DCF. The results show that besides being very reliable, the MCP mechanism is also an energy-efficient mechanism that would be a great candidate to be integrated into the reliable and efficient multicast MAC mechanisms for future amendments of IEEE 802.11. Finally, the results of this chapter are validated with a costume-made MATLAB simulator.

Part I

Game Theory Analysis of Slotted ALOHA Enhanced by ZigZag Decoding

Chapter 1

Cooperative Game Analysis of the Slotted ALOHA Mechanism Enhanced by ZigZag Decoding

Contents

1.1 Introduction

In this chapter, we undertake a stochastic-game study of the random access mechanisms SAZD and SA. We propose a Markov chain model to derive the system state in the stationary regime, which allows us to derive all the performance metrics of interest. Then, we construct a cooperative game where players (i.e., users) cooperate to optimize a common objective function. We propose different game scenarios with various objective functions. By analyzing a game scenario where

players attempt to maximize the system throughput, we showed the existence of an inherent trade-off between the system throughput and the delay of backlogged packets. To optimize this trade-off, we proposed a second game scenario with an objective function that takes into account the system throughput and the backlogged delay.

The second part of this chapter studies the cooperative game model with a pricing mechanism. In the first approach, we consider that each user pays a cost $C \in [0, 1]$ for every transmission and retransmission attempt. The results of this approach show that the behavior of users is strongly affected by the transmission cost C. Thus, users lower their retransmission rate as the cost increases, which affects the network performance. In this approach, users prefer not to transmit their packets due to the cost introduced, which wastes the channel resources. To efficiently optimize the network resources, we propose an enhanced pricing mechanism that takes into account different channel states. This approach efficiently controls the users' behavior and also optimizes the network resources. Moreover, we propose three various pricing schemes that allow a more efficient optimization of the throughput-delay trade-off found in the first part.

1.2 Analytical Model

1.2.1 Markov Model

In this section, we describe the cooperative Slotted ALOHA enhanced by ZigZag Decoding scheme and we construct a Markov model based on [52], from which the performance parameters are measured.

We consider a cellular system where M bufferless users transmit over a shared channel to a base station. It is assumed that time is divided into fixed-length slots, and transmission of one packet takes a single slot. The arrival flow of packets to each source follows a Bernoulli process with parameter p_a (i.e., at each time slot, there is a probability p_a of a new arrival at a source, and all arrivals are independent). For simplicity purposes, we restrict to the case where p_a is the same for all users.

Let us denote by $Q_a(i, m)$ the probability that i unbacklogged users transmit packets in a given slot.

$$Q_a(i,m) = \binom{M-m}{i} (1-p_a)^{(M-m-i)} p_a^i, \tag{1.1}$$

and let $Q_r(i, m)$ be the probability that i out of backlogged users retransmit packets in a given slot.

$$Q_r(i,m) = \binom{m}{i} (1-q_r)^{(m-i)} q_r^i. \tag{1.2}$$

Let M_k denote the number of backlogged packets at the beginning of time slot k. To simplify the description of the system state, we assume that the buffer of each station can hold at most one packet. This assumption is not far from real implementations. In fact, many wireless technologies operate in a bufferless mode, such as the IEEE 802.16 Standard.

To simplify the description of the state of the network, we assume that a station can hold at most one frame waiting for transmission. Hence, we can identify the number of backlogged stations M_k with the number of frames contending to access the channel.

Theorem 1.2.1 *For all $q_r \in (0, 1]$ the stochastic process $(M_k)_{k\in\mathbb{N}}$ is a time-homogeneous Markov chain with unique stationary distribution.*

Proof Let us consider the stochastic process taking the values from the state space $S = \{0, ..., M\}$. Let A_k be the number of new packets that arrive during slot $k-1$. These packets should be transmitted in the next slot according to the SAZD specifications. Besides those new packets, there will be retransmissions of backlogged packets. Let B_k be the random variable representing the number of backlogged packets transmitted at a given slot k. Thus the random variables A_k and B_k are defined as:

$$P(A_k = i/M_k = m) = Q_a(i, m), \qquad i = 0, 1, ..., M, \tag{1.3}$$

$$P(B_k = i/M_k = m) = Q_r(i, m), \qquad i = 0, 1, ..., M. \tag{1.4}$$

Therefore, the number of transmission attempts occurring in the time slot k can be obtained as follows:

$$Y_k = A_k + B_k. \tag{1.5}$$

The outcome of the channel contention can be expressed using the process Y_k as follows:

- $Y_k = 0$, no station attempts transmission.
- $Y_k = 1$, one station successfully transmit a valid packet.
- $Y_k = 2$, two stations attempt transmission. Hence the two packets will be successfully decoded thanks to the ZigZag decoding scheme.
- $Y_k \geq 3$, more than two stations attempt transmission, and thus a collision occurs.

Now, we can express the evolution of the number of backlogged frames M_k as follows:

$$M_{k+1} = M_k + A_k - \mathbb{1}_{\{Y_k=1\}} - 2 \cdot \mathbb{1}_{\{Y_k=2\}}, \qquad k \in \mathbb{N}, \tag{1.6}$$

where $\mathbb{1}$ is the indicator function.

The number of backlogged users at the beginning of a given time slot $k+1$ depends not only on the number of arrivals and departures in the previous slot k but also on the system state M_k (i.e., the current number of backlogged users). Thus, for all $m_0 \in S$ and $k \in \mathbb{N}$, we have

$$P\{M_{k+1} = m_{k+1}|M_k = m_k, M_{k-1} = m_{k-1}, ..., M_0 = m_0\} \tag{1.7}$$

$$= P\{M_k + A_k - \mathbb{1}_{\{Y_k=1\}} - 2 \cdot \mathbb{1}_{\{Y_k=2\}} = m_{k+1}|M_k = m_k, M_{k-1} = m_{k-1}, ..., M_0 = m_0\} \tag{1.8}$$

$$= P\{A_k = m_{k+1} - M_k + \mathbb{1}_{\{Y_k=1\}} + 2 \cdot \mathbb{1}_{\{Y_k=2\}}|M_k = m_k, M_{k-1} = m_{k-1}, ..., M_0 = m_0\} \tag{1.9}$$

$$= P\{A_k = m_{k+1} - M_k + \mathbb{1}_{\{Y_k=1\}} + 2 \cdot \mathbb{1}_{\{Y_k=2\}}|M_k = m_k\} \tag{1.10}$$

$$= P\{M_{k+1} = m_{k+1}|M_k = m_k\}. \tag{1.11}$$

Thus, we have proved that the stochastic process M_k is a Markov chain where m_0 is its initial state. The Markov property states that the future states of the stochastic process are independent of the past states.

Now, let us assume that $q_r = 0$. Thus, the Markov chain has three absorbing states, namely M, $M-1$, and $M-2$. For $p_a > 0$ all other states are transient. The three absorbing states can be reached with a positive probability p_a from any non-absorbing state. Therefore, we should exclude the case of $q_r = 0$.

The stochastic process $\{M_k, k \in \mathbb{N}\}$ can now be described as time-homogeneous Markov process with a space state $S = \{0, ..., M\}$. The transition diagram is given in Figure 1.1 and the transition probabilities are given as follows:

$$P_{(m,m+i)} = \begin{cases} Q_a(i,m), & 3 \leq i \leq M-m, \\ Q_a(1,m)\left(1 - Q_r(0,m) - Q_r(1,m)\right), & i = 1, \quad 2 \leq m \leq M-1, \\ Q_a(2,m)\left(1 - Q_r(0,m)\right), & i = 2, \quad 1 \leq m \leq M-2, \\ Q_a(0,m)\left[1 - Q_r(1,m) - Q_r(2,m)\right] + Q_a(1,m)Q_r(0,m) & \\ \quad + Q_a(2,m)Q_r(0,m), & i = 0, \\ Q_a(0,m)Q_r(1,m) + Q_a(1,m)Q_r(1,m) & i = -1, \quad 1 \leq m \leq M, \\ Q_a(0,m)Q_r(2,m), & i = -2, \quad 2 \leq m \leq M, \\ 0, \quad \text{otherwise.} & \end{cases} \tag{1.12}$$

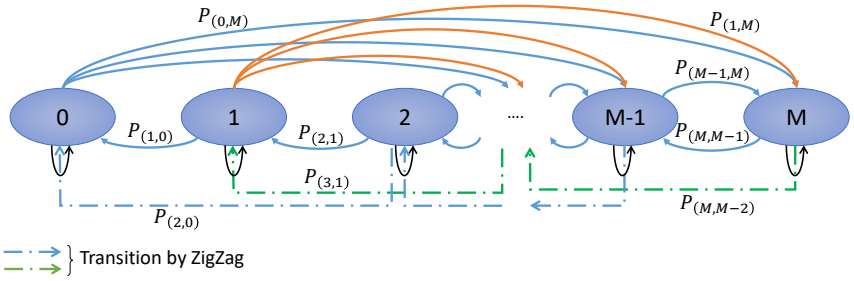

Figure 1.1: Markov chain of the cooperative game problem

Since all the states of the Markov chain communicate with each other and the state space is finite, the Markov chain is ergodic [53]. Therefore, the steady-state distribution exists, and it is unique. Let $\pi(p_a, q_r)$ denotes the vector of the steady-state distribution where its n^{th} entry $\pi_m(p_a, q_r)$ is the probability that the system contains m backlogged users. The steady-state distribution can be derived by solving the problem 1.13 by using a simple iterative method.

$$\begin{cases} \pi(p_a, q_r) = \pi(p_a, q_r)P(p_a, q_r), & \\ \pi_m(p_a, q_r) \geq 0, & m = 0, ..., M, \\ \sum_{m=0}^{M} \pi_m(p_a, q_r) = 1. & \end{cases} \tag{1.13}$$

□

Note that the only absorbing state with a null throughput is the state M. Therefore, we consider that $q_r \in [\varepsilon, 1]$, where $\varepsilon = 10^{-4}$.

1.2.2 Stability

According to Theorem 1.2.1, the Markov chain M_k attains a statistical equilibrium regime for all $q_r \in (0, 1]$. In terms of the stability of the random access mechanism SAZD, the stability result can be obtained by examining the drift D_m at state m, which denotes the average state change at the next transition, given the current state m. It can be expressed as follows:

$$D_m = p_a\,(M - m) - P_{succ}(m), \tag{1.14}$$

where $P_{succ}(m)$ is the average number of transmitted frames at state m, and it is defined by

$$P_{succ}(m) = \big[Q_a(1,m) + Q_a(1,m)\big]Q_r(0,m) + Q_a(1,m)\big[Q_r(1,m) + Q_r(2,m)\big] + Q_a(1,m)Q_r(1,m). \tag{1.15}$$

If $D_m \geq 0$, offered traffic flow becomes greater than the traffic flow leaving the system. As a result, the system state tends to increase. However, if $D_m \leq 0$, the system state tends to decrease since the actual flow leaving the system at a given state m is more significant than the traffic flow entering the system.

The drift can also be expressed by considering the evolution of the Markov chain M_k.

$$\begin{aligned} D_m &= E[M_{k+1} - M_k / M_k = m] && (1.16)\\ &= E[A_k - \mathbb{1}_{\{Y_k=1\}} - 2 \cdot \mathbb{1}_{\{Y_k=2\}} / M_k = m] && (1.17)\\ &= E[A_k] - E[\mathbb{1}_{\{Y_k=1\}} / M_k = m] - 2 \cdot E[\mathbb{1}_{\{Y_k=2\}} / M_k = m] && (1.18)\\ &= a - P(Y_k = 1 / M_k = m) - 2 \cdot P(Y_k = 2 / M_k = m), && (1.19) \end{aligned}$$

where $a = \sum_{i=0}^{\infty} i \cdot P(A_k = i)$.

Intuitively, the Markov chain attains the statistical equilibrium regime if and only if the drift becomes negative as m grows. From the system point of view, this means that the multi-access channel equipped with the SAZD MAC mechanism can carry the offered traffic without getting overloaded. If the drift is negative, the mean rate at which the backlog is cleared is bigger than the average arrival rate of new frames. We say that the random access mechanism SAZD is stable.

1.2.3 Performance Evaluation

Proposition 1.2.2 *The average throughput of transmitted packets is given as follows*

$$TH(p_a, q_r) = \frac{p_a}{T_s(p_a, q_r)} \sum_{m=0}^{M} (M - m)\pi_m(p_a, q_r). \tag{1.20}$$

Proof To get the throughput expression, we first need to define the packet transmission time $T_s(p_a, q_r)$, which is equal to

$$T_s(p_a, q_r) = 1 \cdot (1 - P_{zigzag}) + 2 \cdot P_{zigzag}, \tag{1.21}$$

$$= 1 + P_{zigzag}, \tag{1.22}$$

where P_{zigzag} is the probability of the event ZigZag, and it is defined by

$$P_{zigzag} = \sum_{m=0}^{M} \left[Q_a(0,m)Q_r(2,m) + Q_a(2,m)Q_r(0,m) + Q_a(1,m)Q_r(1,m) \right] \pi_m(p_a, q_r). \tag{1.23}$$

The throughput can now be defined as the average number of successfully transmitted packets in a time $T_s(p_a, q_r)$. At the stationary regime, it is equal to the average number of arrivals. Thus, the number of unbacklogged users at state m is $M - m$, and their total arrival rate is $p_a(M - m)/T_s(p_a, q_r)$. The throughput expression can then be derived by taking all the possible states of m as in equation (1.20). □

Remark 1.2.3 *The throughput can also be expressed as the average number of departures at the stationary regime.*

$$TH(p_a, q_r) = \frac{1}{T_s(p_a, q_r)} \sum_{m=1}^{M} \left[P_{succ}^{m} \pi_m(p_a, q_r) \right] + \left(Q_a(1,0) + 2Q_a(2,0) \right) \pi_0(p_a, q_r), \tag{1.24}$$

where

$$\begin{aligned} P_{succ}^{m} = & Q_a(0,m)Q_r(1,m) + Q_a(1,m)Q_r(0,m) + 2Q_a(0,m)Q_r(2,m) + 2Q_a(2,m)Q_r(0,m) \\ & + 2Q_a(1,m)Q_r(1,m). \end{aligned} \tag{1.25}$$

Proposition 1.2.4 *The average number of backlogged users, or equivalently backlogged packets, is given by*

$$S_B(p_a, q_r) = \sum_{m=0}^{M} m \cdot \pi_m(p_a, q_r). \tag{1.26}$$

Proof Users get backlogged when they collide, and therefore they should retransmit the collided packet using a probability q_r. Using the proposed Markov chain, we can derive it by considering the current number of backlogged users m and taking the sum over all its possible states {0,...,M} as in equation (1.26). □

Corollary 1.2.4.1 *Using equation (1.20) and equation (1.26), we can derive the following formula of the throughput.*

$$TH(p_a, q_r) = \frac{p_a}{T_s(p_a, q_r)} \cdot \left(M - S_B(p_a, q_r) \right). \tag{1.27}$$

Proof We can get this result by developing equation (1.20) as follows

$$TH(p_a, q_r) = \frac{p_a}{T_s(p_a, q_r)} \sum_{m=0}^{M} (M - m) \cdot \pi_m(p_a, q_r), \tag{1.28}$$

$$= \frac{p_a}{T_s(p_a, q_r)} \big[M \cdot \sum_{m=0}^{M} \pi_m(p_a, q_r) - m \cdot \sum_{m=0}^{M} \pi_m(p_a, q_r) \big], \tag{1.29}$$

$$= \frac{p_a}{T_s(p_a, q_r)} \left(M - S_B(p_a, q_r) \right). \tag{1.30}$$

□

Proposition 1.2.5 *The access delay of transmitted packets is given by*

$$D(p_a, q_r) = 1 + \frac{S_B(p_a, q_r)}{TH(p_a, q_r)}. \tag{1.31}$$

Proof We define the delay as the average time a user requires to transmit a data packet from the source to the destination. According to Little's result, [53], the average number of packets in a stationary system is equal to the average effective throughput multiplied by the average time that a packet spends in the system. Using the Little's result, the packet access delay is obtained as follows:

$$D(p_a, q_r) = 1 + \frac{S_B(p_a, q_r)}{TH(p_a, q_r)}. \tag{1.32}$$

□

In order to undertake an exhaustive performance evaluation study, we should explore the performance metrics of backlogged packets. The following proposition provides the average throughput of backlogged users. The throughput of backlogged packets is defined as the number of backlogged packets that have been transmitted at the stationary regime. The ability to transmit the awaiting packets is very interesting for real-time applications.

Proposition 1.2.6 *The throughput of backlogged packets is given as follows:*

$$BTH(p_a, q_r) = TH(p_a, q_r) - TH_{succ}(p_a, q_r), \tag{1.33}$$

where

$$TH_{succ}(p_a, q_r) = \frac{1}{T_s(p_a, q_r)} \sum_{m=0}^{M-1} \Big[Q_a(1, m) Q_r(0, m) + Q_a(1, m) Q_r(1, m) + 2 Q_a(2, m) Q_r(0, m) \Big] \pi_m(p_a, q_r). \tag{1.34}$$

Proof The total throughput comprises the throughput of newly arrived packets and backlogged packets. Thus, to derive the throughput of backlogged packets, we first need to compute the average throughput of newly arrived packets. At the stationary regime, a newly arrived packet can be successfully transmitted if, at most, two stations transmit at the same time slot, which can be expressed as follows:

$$TH_{succ}(p_a, q_r) = \frac{1}{T_s(p_a, q_r)} \sum_{m=0}^{M-1} \Big[Q_a(1,m)Q_r(0,m) + Q_a(1,m)Q_r(1,m) + 2Q_a(2,m)Q_r(0,m) \Big] \pi_m(p_a, q_r). \tag{1.35}$$

Therefore, the backlogged throughput expression (1.33) can be derived by subtracting (1.35) from (1.20). □

Proposition 1.2.7 *The access delay of backlogged packets is given by*

$$BD(p_a, q_r) = 1 + \frac{S_B(p_a, q_r)}{BTH(p_a, q_r)}. \tag{1.36}$$

Proof The access delay is defined as the time elapsed from the moment of the transmission until the reception of the packet. According to the Little result [53], the expression access delay of backlogged packets can be obtained as follows:

$$BD(p_a, q_r) = \frac{BTH(p_a, q_r) + S_B(p_a, q_r)}{BTH(p_a, q_r)}, \tag{1.37}$$

$$= 1 + \frac{S_B(p_a, q_r)}{BTH(p_a, q_r)}. \tag{1.38}$$

□

Remark 1.2.8 *To better estimate the overall system performance, we define the backlog level as the percentage of backlogged users among the total number of users. The backlog level is an important metric that highlights the fairness between newly arrived packets and backlogged packets, and it is defined as follows*

$$Backlog = \left(\frac{S_B(p_a, q_r)}{M} \times 100 \right) \%. \tag{1.39}$$

1.3 Cooperative Game Formulation

In a cooperative game, players seek to optimize the common utility function (denoted by $objective\,(p_a, q_r)$). We propose herein four approaches to optimize the performance of the system. First, we assume that all users maximize the global throughput 1.3.1. Then, we take as the objective function the delay of transmitted packets 1.3.2. Next, we consider that users minimize the delay of backlogged

packets 1.3.3. Finally, we propose to compromise between the throughput and the delay of backlogged packets 1.3.4.

$$\max_{q_r \in [\varepsilon,1]} \textit{objective}\,(p_a, q_r) \text{ subject to:}$$
$$\begin{cases} \pi(p_a, q_r) = \pi(p_a, q_r).P(p_a, q_r), \\ \pi_m(p_a, q_r) \geq 0, \quad m = 0, ..., M, \\ \sum_{m=0}^{M} \pi_m(p_a, q_r) = 1. \end{cases} \tag{1.40}$$

Singularity at $q_r = 0$: The only point where the Markov chain does not have a single stationary distribution is at $q_r = 0$, where it has three absorbing states: $m = M$, $m = M-1$ and $m = M-2$. All remaining states are transient (for any $p_a > 0$), and the probability to end at one of the absorbing states depend on the initial distribution of the Markov chain. We note that if the state $M-1$ is reached then the throughput is p_a, otherwise if the state M is reached then the throughput equals 0, which means that it is a deadlock state. For $p_a > 0$ and $q_r = 0$, the deadlock state is reached with positive probability from any initial state other than absorbing states $M-1$ and $M-2$. We shall therefore exclude the case of $q_r = 0$ and optimize only on the range $\varepsilon \leq q \leq 1$. We chose throughout this chapter $\varepsilon = 10^{-4}$.

Existence of a solution: The steady state probabilities $\pi(p_a, q_r)$ are continuous over $0 < q_r \leq 1$ which is not a close interval, therefore a solution may not exist. However, as we restrict to the closed interval $[\varepsilon, 1]$ where $\varepsilon > 0$, an optimal solution indeed exists. Therefore for any $\gamma > 0$, there exists some $q_r^* > 0$ which is γ-optimal. ($q_r^* > 0$ is said to be γ-optimal if it satisfies $\textit{objective}(p_a, q_r^*) \geq \textit{objective}(p_a, q_r) - \gamma$ for all $q_r \in [\varepsilon, 1]$.)

Game information: We consider that all players share a common knowledge, which is: the total number of players in the game, the strategy space, and the common utility function. Since we considered a cooperative game, we assume that all players cooperate with each other.

1.3.1 Throughput Maximization

We consider in this part the case where all users maximize the system throughput. Thus, users face the Problem (1.40) where

$$\textit{objective}\,(p_a, q_r) = TH(p_a, q_r). \tag{1.41}$$

The maximization of the system throughput results in a very high delay for backlogged packets as in [54]. Therefore, by maximizing the throughput, the system prioritizes newly arrived packets over backlogged ones.

1.3.2 Access Delay Minimization

Minimizing the average access delay is done by considering $objective\,(p_a, q_r) = -D(p_a, q_r)$. However, according to the delay formula (1.31), minimization of the access delay is equivalent to maximizing the system throughput.

1.3.3 Backlogged Delay Minimization

Since the last two parts result in a very high backlogged-packets delay, we may think of minimizing the delay of backlogged packets. Thus, we here consider that users attempt to optimize the delay of backlogged packets. The objective function is then $objective\,(p_a, q_r) = -BD(p_a, q_r)$.

1.3.4 Throughput-Delay trade-off Optimization

Taking the system throughput as the objective function, as proposed in 1.3.1, yields the best throughput. However, in heavy traffic conditions, the delay of backlogged packets increases by several orders of magnitude. On the other hand, minimizing the delay of backlogged packets yields low throughput. This trade-off exists in both mechanisms, SA and SAZD. To manage and optimize this trade-off, we propose an objective function that combines the system throughput and packets backlogged delay.

$$objective(p_a, q_r) = \frac{TH(p_a, q_r)}{BD(p_a, q_r)}. \tag{1.42}$$

1.4 Numerical Results

In this section, we present the results of the cooperative game model for $M = 10$ as a function of the arrival probability p_a. We compare two game-scenarios: 1) a game with the objective function 1.3.1, and 2) the game with the objective function 1.3.4. In order to show the efficiency of SAZD mechanism, we compare its performance with SA in terms of all performance metrics of interest.

Tables 1.1 and 1.2 show respectively the results obtained from the first and second game scenario 1.3.1, 1.3.4. In each game scenario, we compare the performance of both random access mechanisms SAZD and SA.

Since players are cooperating, the optimal retransmission probability q_r^* decreases as the load increases (i.e., $p_a \to 1$). Players decrease their retransmission probabilities to allow everyone to use the channel and to reduce the number of collisions as much as possible. However, the optimal retransmission probability in the second game scenario is slightly higher than in the first game scenario. In very heavy load conditions (i.e., $p_a \geq 0.9$), players in the first game scenario use the lowest retransmission probability $q_r^* = 10^{-3}$. The reason behind this behavior is that the random access mechanisms SAZD and SA specify that packets that arrive during a slot should be transmitted at the next slot. Thus, when the arrival rate is very high, players in the first game scenario reduce their retransmission rate to allow the newly arrived packets to be transmitted. However, this behavior causes system resources to be used only by newly arrived packets. As a

Table 1.1: First game scenario 1.3.1, objective $(p_a, q_r) = TH(p_a, q_r)$.

RA Mechanism	p_a	q_r^*	TH	S	D	BD
SAZD	0.0001	0.447 29	0.001	9.0209×10^{-10}	1	3.5065
	0.100 59	0.236 26	0.6791	1.6744	3.4656	9.4693
	0.201 08	0.115 67	0.702 99	5.5295	8.8656	19.6247
	0.301 58	0.085 519	0.701 29	7.0392	11.0376	25.5788
	0.402 07	0.075 469	0.701 58	7.7796	12.0886	28.749
	0.502 56	0.070 445	0.702 47	8.2194	12.7007	30.8141
	0.603 05	0.065 42	0.703 83	8.5113	13.0928	33.0202
	0.703 55	0.055 371	0.707 11	8.7172	13.3279	37.8526
	0.804 04	0.035 272	0.716 34	8.8601	13.3686	55.5272
	0.904 53	0.0001	0.745 08	8.9256	12.9794	17 942.379
	1	0.0001	0.783 05	8.9258	12.3988	20 585.2006
SA	0.0001	0.582 96	0.001	2.6326×10^{-6}	1.0026	3.923
	0.100 59	0.100 59	0.387 41	6.1487	16.8711	26.8122
	0.201 08	0.075 469	0.387 58	8.0725	21.8279	35.1307
	0.301 58	0.070 445	0.389 13	8.7097	23.3821	38.0175
	0.402 07	0.065 42	0.391 94	9.0252	24.0268	40.378
	0.502 56	0.060 395	0.396 27	9.2115	24.2456	42.8475
	0.603 05	0.050 346	0.403 13	9.3315	24.1478	48.1499
	0.703 55	0.040 297	0.4144	9.411	23.71	56.7668
	0.804 04	0.025 223	0.434 59	9.4595	22.7664	83.1838
	0.904 53	0.0001	0.476 04	9.4737	20.901	18 271.797
	1	0.0001	0.526 19	9.4738	19.0045	20 014.0052

result, the performance of backlogged packets is heavily penalized. To overcome this issue, the second game scenario proposes an optimal retransmission probability that considers the system throughput but does not penalize the backlogged packets.

By comparing the two random access mechanisms in terms of normalized throughput, we show that SAZD is up to 42% better than SA. The first game scenario provides the best throughput for both mechanisms. However, it yields a huge delay for backlogged packets. In contrast, the second game scenario guarantees a fair delay for backlogged packets with a slight drop in the system throughput.

1.5 Pricing Mechanism

In this section, we provide two pricing strategies that allow us to control the utility function of users. In the first pricing strategy, we propose associating a cost C to every transmission and

Table 1.2: Second game scenario 1.3.4, objective $(p_a, q_r) = TH(p_a, q_r)/BD(p_a, q_r)$.

RA Mechanism	$\mathbf{p_a}$	$\mathbf{q_r^*}$	TH	S	D	BD
SAZD	0.0001	0.6332	0.001	7.7634×10^{-10}	1	3.1569
	0.100 59	0.291 53	0.675 21	1.6769	3.4836	8.9746
	0.201 08	0.191 04	0.675 72	5.6256	9.3253	16.0974
	0.301 58	0.165 91	0.662 35	7.1442	11.7862	19.2993
	0.402 07	0.155 86	0.656 39	7.8796	13.0045	20.9367
	0.502 56	0.150 84	0.652 35	8.3154	13.7468	21.9144
	0.603 05	0.145 81	0.651 16	8.5993	14.2061	22.6462
	0.703 55	0.145 81	0.645 66	8.8104	14.6456	23.0485
	0.804 04	0.145 81	0.640 43	8.9682	15.0034	23.3937
	0.904 53	0.150 84	0.629 17	9.1002	15.4639	23.5271
	1	0.155 86	0.617 67	9.202	15.8979	23.713
SA	0.0001	0.582 96	0.001	2.6326×10^{-6}	1.0026	3.923
	0.100 59	0.130 74	0.380 09	6.2215	17.3687	25.1278
	0.201 08	0.105 62	0.377 01	8.1251	22.5516	31.991
	0.301 58	0.095 568	0.379 28	8.7424	24.0502	34.7124
	0.402 07	0.095 568	0.378 01	9.0599	24.9675	35.9376
	0.502 56	0.090 543	0.382 13	9.2396	25.1796	37.2421
	0.603 05	0.090 543	0.383 57	9.364	25.4127	38.0746
	0.703 55	0.090 543	0.386 09	9.4512	25.4794	38.9451
	0.804 04	0.090 543	0.389 86	9.5151	25.4066	39.9465
	0.904 53	0.090 543	0.395 08	9.5632	25.2059	41.1664
	1	0.090 543	0.401 55	9.5985	24.9036	42.6176

retransmission attempt. Then, we propose a second pricing strategy as an enhancement of the first one, which considers different medium states.

1.5.1 Pricing strategy 1

As discussed above each transmission and retransmission is related to a cost expressed in terms of the battery energy consumed, which is denoted by C. We consider a normalized cost $C \in [0, 1]$ where 1 represents the maximum energy consumption and 0 represents no consumption. Now, we can express the utility function of the team as

$$objective(p_a, q_r) = (1 - C)TH(p_a, q_r) - Cq_r \sum_{m=1}^{M} m\pi_m(p_a, q_r). \tag{1.43}$$

1.5.2 Pricing strategy 2

In this section, we provide an enhancement of the pricing mechanism proposed in section 1.5.1. We associate a cost to each event respectively as follows:

- C_s: Price for a new arrived packet crowned with success.
- C_b: Price for successful transmission of backlogged packet.
- C_{idle}: Price for idling.
- C_c: Price for collision.

where all the prices are normalized in the range $[0, 1]$.

The utility function of the new proposed game is given by:

$$objective(p_a, q_r) = C_s P_{succN} + C_b P_{succB} + C_{\text{idle}} P_{\text{idle}} + C_c P_c. \tag{1.44}$$

P_{succN} is the probability that a newly arrived packet will be transmitted successfully at the first attempt, and it is given by:

$$P_{succN} = \sum_{m=0}^{M} \left[Q_a(1,m)Q_r(0,m) + Q_a(2,m)Q_r(0,m) + Q_a(1,m)Q_r(1,m) \right] \pi_m(p_a, q_r). \tag{1.45}$$

P_{succB} is the probability that a backlogged packet will be successfully transmitted in a given slot. It is given by:

$$P_{succB} = \sum_{m=0}^{M} \left[Q_a(0,m)Q_r(1,m) + Q_a(0,m)Q_r(2,m) + Q_a(1,m)Q_r(1,m) \right] \pi_m(p_a, q_r). \tag{1.46}$$

P_{idle} is the idle probability, and it is defined as the probability that no one is transmitting or retransmitting over the channel. It is given by:

$$P_{\text{idle}} = \sum_{m=0}^{M} Q_a(0,m)Q_r(0,m)\pi_m(p_a, q_r). \tag{1.47}$$

Finally, P_c is the collision probability, and it is given by:

$$P_c = 1 - P_{succN} - P_{succB} - P_{\text{idle}}. \tag{1.48}$$

Scheme	1	2	3
C_s	0.1	0.3	0.1
C_b	0.1	0.1	0.1
C_{idle}	0.5	0.5	0.3
C_c	0.5	0.5	0.8

Table 1.3: Parameters used in the numerical results of different schemes

1.6 Numerical results and discussion

In this section, we present the numerical results of the cooperative game model with the pricing mechanism. The optimal policy to save energy and avoid collisions is not transmitting at all. However, this is not the optimal policy that we are interested in since we aim to maximize the throughput and minimize the delay. Table 1.3 shows the three pricing schemes used in the numerical results.

The following results plot the performance metrics of different cost configurations. We also compare the two pricing strategies.

In this section, we evaluate the performance of the two pricing strategies under different load conditions. We set the number of users to 10, and we vary the arrival probability p_a from 0 to 1. We set $\varepsilon = 10^{-4}$.

In the first approach, we consider a fixed cost in the set $C = \{0, 0.2, 0.4, 0.6, 0.8, 1\}$ for every transmission and retransmission attempt, and we compare the performance metrics obtained for all arrival probabilities. In the second approach, we adopt a different pricing strategy in order to improve system performance. Therefore, we associate to every newly arrived packet which is crowned with success a cost denoted by C_s; for the successful transmission of a backlogged packet, we associate a cost C_b. In the case of no transmission, we associate a cost C_{idle}, and finally, we associate a cost C_c for the collision. The numerical results are obtained using Matlab, and the parameters used for the second approach are listed in Table 1.3.

Figure 1.2 shows the optimal retransmission probability as a function of the arrival probability for different pricing mechanisms. In the first approach, we notice that the optimal retransmission probability is considerably lower compared to the enhanced pricing strategy. The reason behind this behavior is straightforward: In the first approach, users do not charge any cost when they do not transmit. Therefore, they would rather defer the transmission than attempt to transmit. On the other hand, in the first approach, the optimal retransmission probability goes to 0 in heavy load conditions (i.e., when $p_a \to 0$) regardless of the price used. In fact, this is not efficient because when the retransmission probability $q_r^* = 0$ the backlogged packets will not be transmitted, which yields a huge delay. On the contrary, our enhanced pricing strategy keeps the optimal retransmission probability above 0 for the three different pricing schemes. However, we can see that scheme 2 provides the highest retransmission probability, followed by schemes 1 and 3, respectively.

In Figure 1.3, we show the overall system throughput as a function of arrival rate. The through-

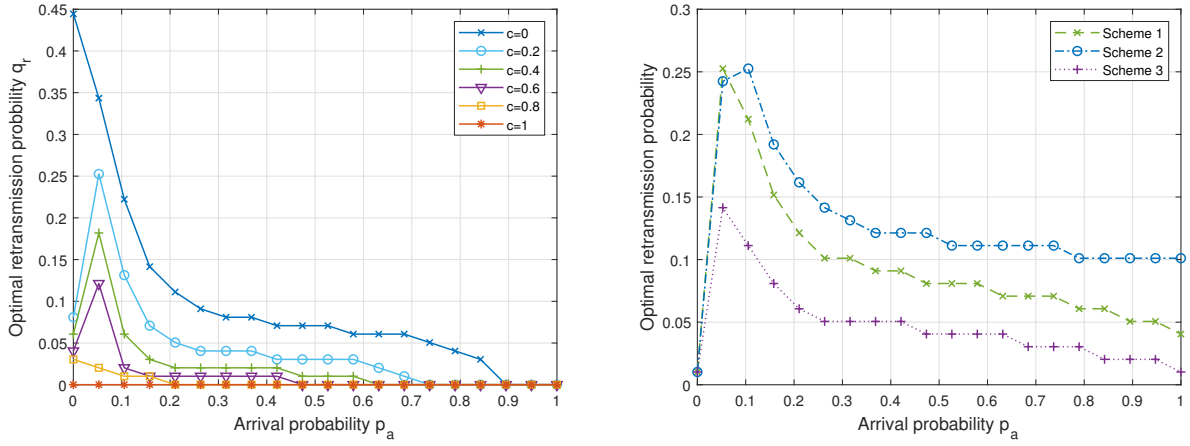

(a) Pricing strategy 1 of Section 1.5.1

(b) Improved pricing strategy 2 of Section 1.5.2

Figure 1.2: Optimal retransmission probability as a function of arrival probability for both pricing mechanisms

put is given in equation (1.24), and it includes the newly arrived packets that are transmitted successfully at the first attempt and also the backlogged packets that are successfully transmitted after a previous collision. We emphasize that the throughput, as well as the other performance metrics, are derived from the optimal retransmission probability depicted in Figure 1.2. In the first pricing strategy, the throughput decreases as the price increases, which is expected since the corresponding retransmission probability shown in Figure 1.2a decreases dramatically as the price increase. This can be explained by the fact that users do not take the risk of transmitting a packet when the price is high. Instead, they prefer not to transmit, which negatively affects the system throughput. However, in the second approach, the system throughput stays at a high value for the tree schemes with a slight difference in heavy load conditions.

We plot in Figure 1.4 the delay of transmitted packets as a function of the arrival probability. The delay represents the number of slots required to send a packet from its source to its destination. As shown in Figure 1.2, implementing a high cost in the first approach yields a delay increase since transmission probability becomes very low. However, the second pricing strategy yields a low delay for the three proposed schemes.

Figure 1.5 shows the throughput of backlogged packets as a function of the arrival probability. In the case of a low price, the backlogged throughput in the first approach increases and then decreases for the arrival probability. When we increase the price, the backlogged throughput decreases dramatically, especially in the higher price case (i.e., $C = 1$), where the backlogged throughput becomes 0, which means no backlogged packet is transmitted over the channel. However, in the improved approach, the backlogged throughput never drops to 0, which is very impressive. The three proposed schemes provide different backlogged throughput values. In particular, the second

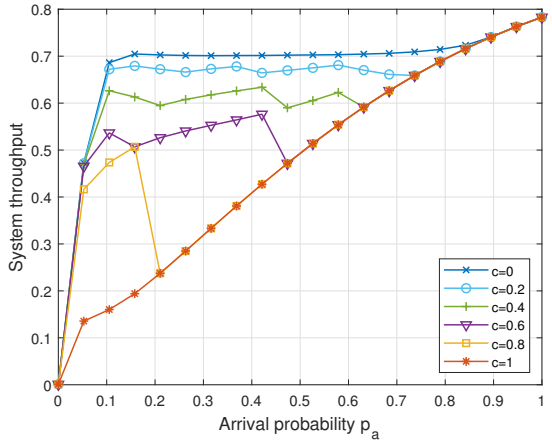

(a) Pricing strategy 1 of Section 1.5.1

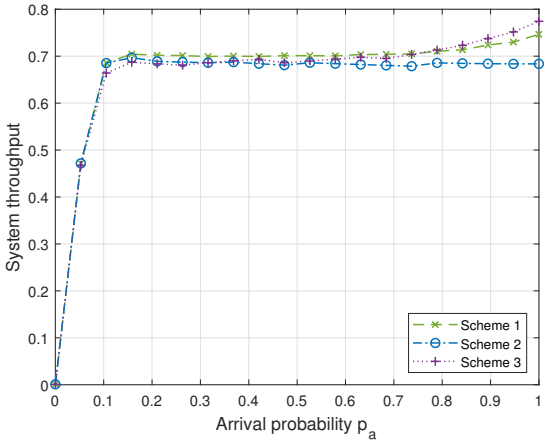

(b) Improved pricing strategy 2 of Section 1.5.2

Figure 1.3: Normalized throughput of the system, which includes the backlogged and newly transmitted packets

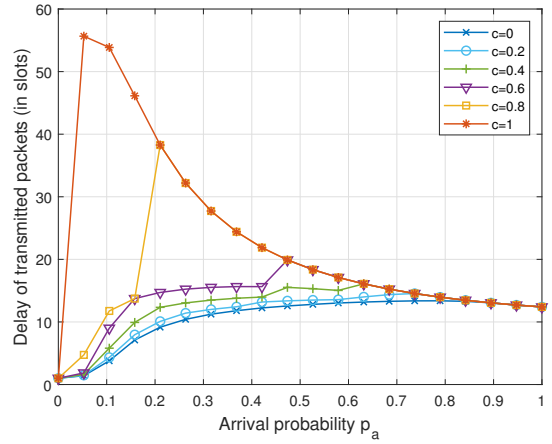

(a) Pricing strategy 1 of Section 1.5.1

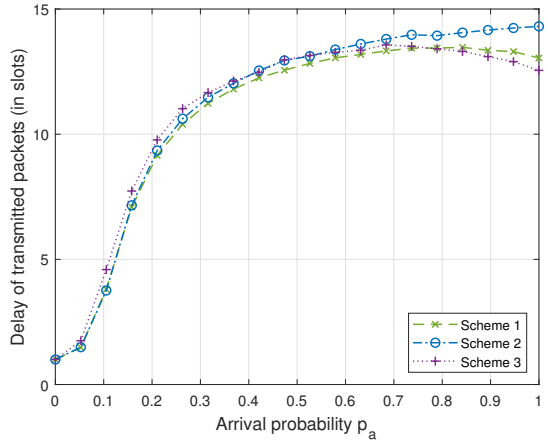

(b) Improved pricing strategy 2 of Section 1.5.2

Figure 1.4: Transmitted packets delay (in slots) as a function of arrival probability

scheme ensures the highest value compared to the first and the third one.

In Figure 1.6, we plot the throughput of packets that arrives and are successfully sent in the first attempt. We notice that different costs provide different throughput values. In light traffic, increasing the cost results in a throughput drop. Whereas, in a high traffic load, increasing the cost improves the throughput but at the expense of the backlogged throughput. On the other hand, the results depicted in Figure 1.6b show a reasonable throughput without sacrificing the

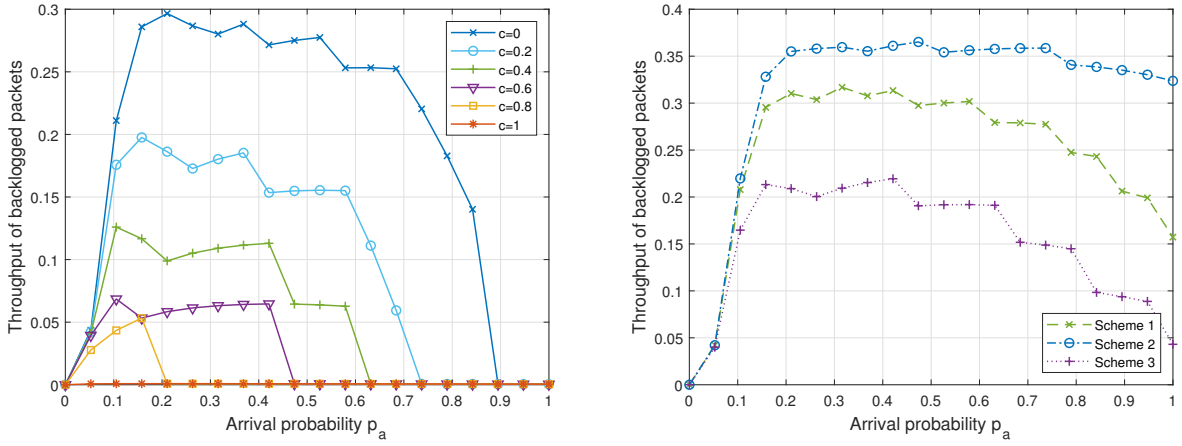

(a) Pricing strategy 1 of Section 1.5.1 (b) Improved pricing strategy 2 of Section 1.5.2

Figure 1.5: Normalized throughout of backlogged packets as a function of arrival probability

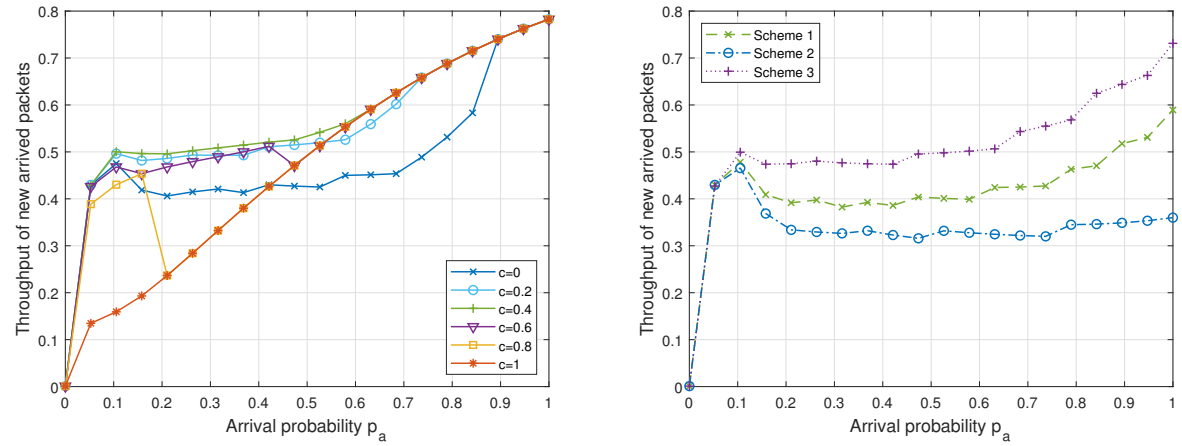

(a) Pricing strategy 1 of Section 1.5.1 (b) Improved pricing strategy 2 of Section 1.5.2

Figure 1.6: Normalized throughput of newly arrived packets

backlogged packets. Unlike the results shown in Figure 1.5, we notice that scheme 2 provides the lowest throughput compared to the third scheme. In fact, scheme 2 prefers the backlogged packets, and scheme 3 prefers newly arrived ones, whereas scheme 1 compromises between the two schemes.

Figure 1.7 shows the delay of backlogged packets as a function of the arrival probability. In the first approach, increasing the price yields a huge delay (10^4 slots). In heavy load conditions, the delay becomes huge even when no cost is included ($C = 0$). However, as seen in Figure 1.3, the corresponding throughput of $C = 0$ is very good. This trade-off between the throughput and

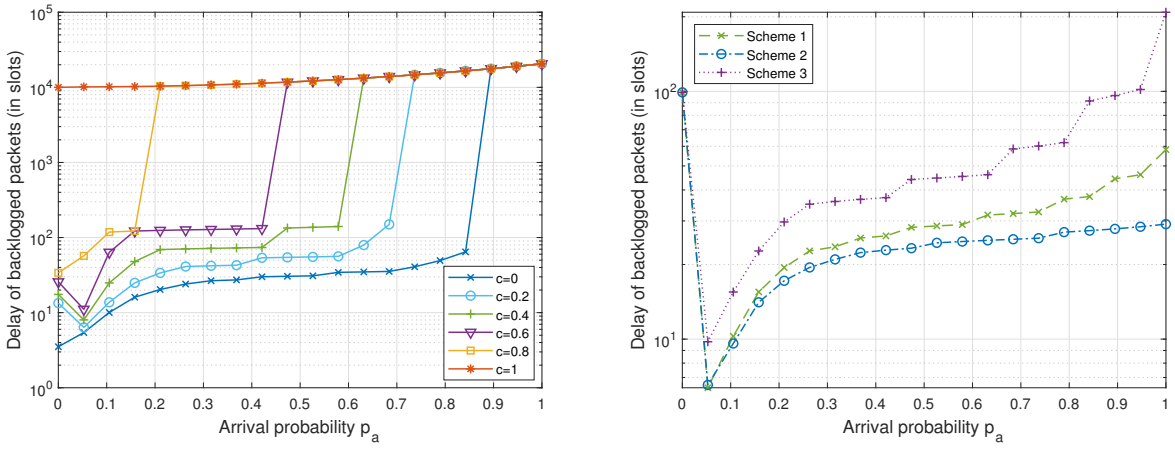

(a) Pricing strategy 1 of Section 1.5.1 (b) Improved pricing strategy 2 of Section 1.5.2

Figure 1.7: Backlogged packets delay (in slots) as a function of arrival probability

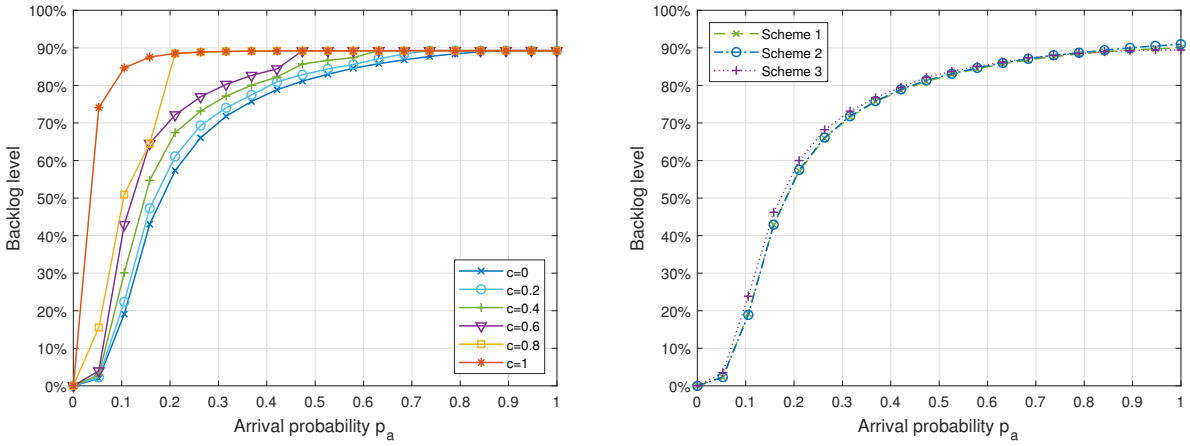

(a) Pricing strategy 1 of Section 1.5.1 (b) Improved pricing strategy 2 of Section 1.5.2

Figure 1.8: Backlog level, defined as the ratio of backlogged users among the total number of users M

backlogged delay is a very challenging task since we are interested in maximizing the throughput and meanwhile minimizing the backlogged delay, which does not seem to be done using the first approach. However, Our approach is very efficient in addressing this trade-off. Figure 1.7b, shows the delay of backlogged packets using the improved pricing mechanism. Compared to the first approach, it provides a backlogged delay of less than 100 slots for the three proposed schemes while maintaining a maximal throughput.

Finally, we plot in Figure 1.8 the backlog level, which is defined as the percentage of backlogged users among all contended users. It also refers to the number of packets that require retransmission over all packets in the system. Figure 1.8a shows that, in the first approach, the backlog level of the system goes up very quickly to 90%. However, the three schemes of the enhanced approach achieve a 90% of the backlog level only in heavy load conditions, which is expected since the collision rate increases due to the increasing number of transmission attempts.

1.7 Conclusion

In this chapter, we have studied two random access mechanisms SAZD and SA using cooperative game theory towards different game scenarios. First, we highlighted the existence of a tread-off between the system throughput and backlogged delay. Then, we have proposed to optimize this tread-off using an alternative objective function. Furthermore, we introduced two pricing mechanisms to the cooperative game model. In the first pricing approach, we have introduced the transmission cost concept to model the battery consumption of users. The results showed that, in some cases, the transmission cost prevents users from transmitting. Therefore, the channel resources are wasted.

This chapter shows that cooperation is encouraged between users since it yields the best performance. However, in many cases, users do not cooperate, and the interaction between them should be then studied using non-cooperative game theory, which is the content of the next chapter.

Chapter 2

Non-cooperative Game Analysis of the Slotted ALOHA Mechanism Enhanced by ZigZag Decoding

Contents

2.1 Introduction

This chapter studies the non-cooperative game model of a network scenario operating under the SAZD mechanism. In a non-cooperative game, each player (i.e., user) seeks to maximize his own gain. Unfortunately, this selfish behavior can sometimes lead to an overall network collapse and inefficient resource management.

To derive the system state, we construct a bi-dimensional Markov chain that allows us to get various performance metrics for a single user. Then, we adjust the game so that each user pays a cost for every transmission and retransmission attempt. This pricing mechanism allows us to control the users' behavior and mitigate competitors' selfishness. Finally, we compare the results of the non-cooperative game using different pricing settings with the results of the cooperative model reported in the previous chapter.

Then, we optimize the transmission cost in order to get the same performance as the cooperative game. This optimization study allows us to convert the non-cooperative game to a cooperative game. Furthermore, we propose different optimization approaches for the transmission cost. In the

first approach, we propose an optimal transmission cost that gives the best system throughput, which is equivalent to the cooperative game in 1.3.1. In the second approach, we seek the optimal transmission cost that minimizes the delay of backlogged packets as in the cooperative game 1.3.3. Finally, we propose an optimal adjustable cost to compromise the trade-off between the system throughput and the delay of backlogged packets.

2.2 Analytical Model

We consider a set $S_N := \{1, ..., N\}$ of N users that compete for accessing a shared channel. Let n be the number of users that hold a pending packet due to a previous collision, which we refer to as backlogged users. Assuming that users are bufferless, i.e., each user can hold at most one packet. Therefore, the number of backlogged users is equivalent to the number of backlogged packets. Let q_r be the retransmission probability of backlogged users. The arrival flow of packets to each source follows a Bernoulli process with parameters p_a.

Let $Q_a(j, n)$ be the probability that j unbacklogged users transmit at a given time slot.

$$Q_a(j, n) = \binom{N-n}{j} (1 - p_a)^{(N-n-j)} p_a^j, \tag{2.1}$$

and let $Q_r(j, n)$ be the probability that j backlogged users retransmit at a given time slot.

$$Q_r(j, n) = \binom{n}{j} (1 - q_r)^{(n-j)} q_r^j. \tag{2.2}$$

Let consider the stochastic process $\{(X_k, Y_k), k \in \mathbb{N}\}$, where X_k denotes the number of backlogged packets holding by $N - 1$ users at time sot k, and Y_k denotes the number of backlogged packets of a tagged user i at time slot k. The process $\{(X_k, Y_k), k \in \mathbb{N}\}$ takes values in the set $\{0, 1, ..., N - 1\} \times \{0, 1\}$. We denote by $\left([\mathbf{q_r}]^{-i}, q_r^i\right)$ the vector of the retransmission probabilities of all users, where $[\mathbf{q_r}]^{-i}$ is the vector of the retransmission probabilities of users in $S_N \setminus \{i\}$, and q_r^i is the retransmission probability of a user i. Furthermore, let p_a^i be the arrival probability of a tagged user i.

Theorem 2.2.1 *For any choice of $q_r \in (0, 1]$ and $q_r^i \in (0, 1]$, the stochastic process $(X_k, Y_k)_{k\in\mathbb{N}}$ is Markovian with a unique stationary distribution.*

Proof Consider the stochastic process $\{(X_k, Y_k), k \in \mathbb{N}\}$ with the state space $\{0, 1, ..., N - 1\} \times \{0, 1\}$. Let A_k be the r.v. representing the number of newly arrived packets during slot $k-1$ which are scheduled for the first transmission attempt in slot k, and let B_k be the r.v. representing the number of new packets that arrive at the user i. Furthermore, let C_k be the r.v. representing the number of backlogged users that transmit in slot k, and let D_k be the r.v. representing the number

of backlogged packet transmitted by the user i. We have

$$P\left(A_k = j | X_k = n\right) = Q_a(j,n), \qquad j = 0, ..., N-1, \tag{2.3}$$
$$P\left(B_k = j | X_k = n\right) = p_a^i, \qquad j = 0, 1, \tag{2.4}$$
$$P\left(C_k = j | X_k = n\right) = Q_r(j,n), \qquad j = 0, ..., N-1, \tag{2.5}$$
$$P\left(D_k = j | X_k = n\right) = q_r^i, \qquad j = 0, 1. \tag{2.6}$$

Then, let consider the r.vs. E_k and F_k that correspond to the number of transmission attempts coming respectively from the $N-1$ users and the user i at slot k. E_k and F_k can be expressed as follows:

$$E_k = A_k + C_k, \tag{2.7}$$
$$F_k = B_k + D_k. \tag{2.8}$$

The number of backlogged users at slot $k+1$ can then be expressed as follows:

$$X_{k+1} = X_k + A_k - \mathbb{1}_{\{E_k=1\}} - 2 \cdot \mathbb{1}_{\{E_k=2\}}, \tag{2.9}$$
$$Y_{k+1} = Y_k + B_k - \mathbb{1}_{\{F_k=1\}}. \tag{2.10}$$

The evolution of stochastic process $\{(X_k, Y_k), k \in \mathbb{N}\}$ shows that the number of backlogged users at the beginning of a slot $k+1$ depends on the system state (X_k, Y_k) at the previous slot k, and also on the number of arrivals and departures at slot k. Thus, the future states of the process are independent of the past states given the present state. Therefore, the following Markov property holds for all $(x_0, y_0), ..., (x_{k+1}, y_{k+1}) \in \{0, 1, ..., N-1\} \times \{0, 1\}$, and $k \in \mathbb{N}$.

$$\begin{aligned} P\{(X_{k+1}, Y_{k+1}) = (x_{k+1}, y_{k+1}) \,|\, (X_k, Y_k) = (x_k, y_k), ..., (X_0, Y_0) = (x_0, y_0)\} \\ = P\left((X_{k+1}, Y_{k+1}) = (x_{k+1}, y_{k+1}) \,|\, (X_k, Y_k) = (x_k, y_k)\right), \end{aligned} \tag{2.11}$$

where (x_0, y_0) denotes the initial state of the Markov chain.

Assume that $q_r = 0$ and $q_r^i = 0$. Then, the Markov chain contains five absorbing states, namely $(N-1, 0)$, $(N-1, 1)$, $(N-2, 0)$, $(N-2, 1)$ and $(N-3, 1)$. The other non-absorbing states are transients for any $p_a > 0$ and $p_a^i > 0$. Since the absorbing states can be reached for any $p_a > 0$ and $p_a^i > 0$, we shall exclude the case of $q_r = 0$ and $q_r^i = 0$. Thus, from now on, we consider $(q_r, q_r^i) \in [\varepsilon, 1]^2$, such that $\varepsilon = 10^{-4}$.

Now, we can describe the stochastic process $\{(X_k, Y_k), k \in \mathbb{N}\}$ as a homogeneous finite Markov process with $2 \times N$ possible states where the transition probabilities are given in (2.12), and the transition diagram is given in Figure 2.1.

$$P_{(n,a)(n+j,b)}\left([\mathbf{q_r}]^{-i}, q_r^i\right) =$$

$$\begin{cases}
\left.\begin{array}{ll} Q_a(j,n), & a=b=1, \\ Q_a(j,n)(1-p_a), & a=b=0, \\ Q_a(j,n)p_a, & a=0,b=1, \end{array}\right\} \text{if } \ 3 \le j \le N-1-n, \\
\left.\begin{array}{ll} Q_a(1,n)\left[1-Q_r(0,n)-Q_r(1,n)\right]+q_r^i Q_a(1,n)Q_r(1,n), & a=b=1, \\ (1-p_a)Q_a(1,n)\left[1-Q_r(0,n)-Q_r(1,n)\right], & a=b=0, \\ p_a Q_a(1,n)\left[1-Q_r(0,n)\right], & a=0,b=1, \end{array}\right\} \text{if } \ j=1, \\
\left.\begin{array}{ll} Q_a(2,n)\left[1-Q_r(0,n)\right]+q_r^i Q_a(2,n)Q_r(0,n), & a=b=1, \\ (1-p_a)Q_a(2,n)\left[1-Q_r(0,n)\right], & a=b=0, \\ p_a Q_a(2,n), & a=0,b=1, \end{array}\right\} \text{if } \ j=2, \\
\left.\begin{array}{ll} (1-q_r^i)Z+q_r^i Q_a(0,n)\left[1-Q_r(0,n)-Q_r(1,n)\right], & a=b=1, \\ (1-p_a)Z+p_a\left[Q_a(0,n)+Q_a(1,n)\right]Q_r(0,n), & a=b=0, \\ p_a Q_a(0,n)\left[1-Q_r(0,n)-Q_r(1,n)\right], & a=0,b=1, \\ q_r^i\left[Q_a(0,n)+Q_a(1,n)\right]Q_r(0,n), & a=1,b=0, \end{array}\right\} \text{if } \ j=0, \\
\left.\begin{array}{ll} (1-q_r^i)Q_r(1,n)\left[Q_a(0,n)+Q_a(1,n)\right], & a=b=1, \\ (1-p_a)Q_r(1,n)\left[Q_a(0,n)+Q_a(1,n)\right]+p_a Q_r(1,n)Q_a(0,n), & a=b=0, \\ q_r^i Q_r(1,n)Q_a(0,n), & a=1,b=0, \end{array}\right\} \text{if } \ j=-1, \\
\left.\begin{array}{ll} (1-q_r^i)Q_r(2,n)Q_a(0,n), & a=b=1, \\ (1-p_a)Q_r(2,n)Q_a(0,n), & a=b=0, \end{array}\right\} \text{if } \ j=-2, \\
0, \qquad \text{otherwise},
\end{cases} \tag{2.12}$$

where $Z = Q_a(0,n)\left[1-Q_r(1,n)-Q_r(2,n)\right]+Q_a(1,n)Q_r(0,n)+Q_a(2,n)Q_r(0,n)$. We consider the same arrival probability for all users, i.e., $\forall i \in S_N$, $p_a^i = p_a$.

Since the space state is finite and all states communicate with each other, the Markov chain $\{(X_k, Y_k), k \in \mathbb{N}\}$ is ergodic [53]. Therefore, the steady-state probability exists, and it is unique. Let denote by $\pi\left([\mathbf{q_r}]^{-i}, q_r^i\right) = \left(\pi_{i,j}\left([\mathbf{q_r}]^{-i}, q_r^i\right)\right)_{i\in\{0,..,N-1\}, j\in\{0,1\}}$ the vector of the of the steady-state probability, where $\pi_{i,j}$ represents the probability that system state is (i,j) in the stationary regime. The steady-state distribution can be obtained by solving the following problem:

$$\begin{cases}
\pi\left([\mathbf{q_r}]^{-i}, q_r^i\right) = \pi\left([\mathbf{q_r}]^{-i}, q_r^i\right) P\left([\mathbf{q_r}]^{-i}, q_r^i\right), \\
\pi_{i,j}\left([\mathbf{q_r}]^{-i}, q_r^i\right) \ge 0, \qquad i = 0, ..., N-1 \ \text{ and } \ j = 0, 1 \\
\displaystyle\sum_{i=0}^{N-1}\sum_{j=0}^{1} \pi_{i,j}\left([\mathbf{q_r}]^{-i}, q_r^i\right) = 1.
\end{cases} \tag{2.13}$$

□

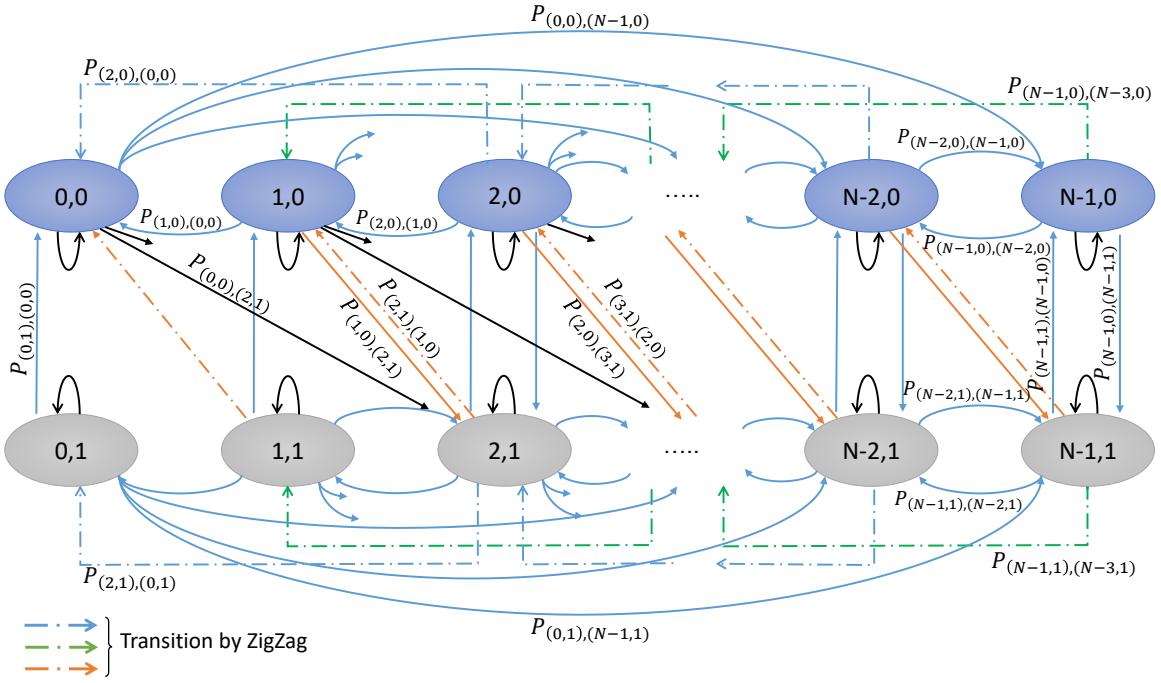

Figure 2.1: Bi-dimensional Markov chain for the non-cooperative game problem

2.3 Performance Evaluation

In this section, we provide the performance metrics of the user i.

Proposition 2.3.1 *The average throughput is defined as follows*

$$TH_i\left([\mathbf{q_r}]^{-i}, q_r^i\right) = \frac{p_a}{T_s\left([\mathbf{q_r}]^{-i}, q_r^i\right)} \sum_{i=0}^{N-1} \pi_{i,0}\left([\mathbf{q_r}]^{-i}, q_r^i\right). \tag{2.14}$$

Proof Let's first define the packet transmission time $T_s\left([\mathbf{q_r}]^{-i}, q_r^i\right)$, which is equal to two slots in the case of a transmission using ZigZag Decoding (ZD). Otherwise, it is equal to one slot. Thus, we have

$$\begin{aligned} T_s\left([\mathbf{q_r}]^{-i}, q_r^i\right) &= 1 \cdot (1 - P_{zigzag}) + 2 \cdot P_{zigzag}, &(2.15)\\ &= 1 + P_{ZigZag}. &(2.16)\end{aligned}$$

P_{ZigZag} is the probability that two packets are transmitted using ZD, and it is given by

$$P_{ZigZag} = \sum_{i=0}^{N-1} P_1 \cdot \pi_{i,0}\left([\mathbf{q_r}]^{-i}, q_r^i\right) + P_2 \cdot \pi_{i,1}\left([\mathbf{q_r}]^{-i}, q_r^i\right), \tag{2.17}$$

where

$$\begin{cases} P_1 = & p_a \left[Q_a(1,N)Q_r(0,N) + Q_a(0,N)Q_r(1,N)\right] \\ & +(1-p_a)\left[Q_a(0,N)Q_r(2,N) + Q_a(2,N)Q_r(0,N) + Q_a(1,N)Q_r(1,N)\right], \\ P_2 = & q_r^i \left[Q_a(1,N)Q_r(0,N) + Q_a(0,N)Q_r(1,N)\right] \\ & +(1-q_r^i)\left[Q_a(0,N)Q_r(2,N) + Q_a(2,N)Q_r(0,N) + Q_a(1,N)Q_r(1,N)\right]. \end{cases} \tag{2.18}$$

The throughput can now be obtained as the average number of packets sent by the user i during a time slot $T_s\left([\mathbf{q_r}]^{-i}, q_r^i\right)$, which equals the average number that arrives during the same period $T_s\left([\mathbf{q_r}]^{-i}, q_r^i\right)$. The user can receive newly arrived packets with a probability p_a only if it does not hold a backlogged packet. Therefore, we shall consider state $j = 0$ and all states $i = 0, ...N-1$. Thus, we have

$$TH_i\left([\mathbf{q_r}]^{-i}, q_r^i\right) = \frac{p_a}{T_s\left([\mathbf{q_r}]^{-i}, q_r^i\right)} \sum_{i=0}^{N-1} \pi_{i,0}\left([\mathbf{q_r}]^{-i}, q_r^i\right). \tag{2.19}$$

□

Proposition 2.3.2 *The average number of backlogged packets held by the user i is given as follows*

$$S_i\left([\mathbf{q_r}]^{-i}, q_r^i\right) = \sum_{i=0}^{N-1} \pi_{i,1}\left([\mathbf{q_r}]^{-i}, q_r^i\right). \tag{2.20}$$

Proof The average number of backlogged packets that the user i is holding in the stationary regime can be derived from the steady-state probability $\pi_{i,1}$, which represents the probability that the user i holds a backlogged packet. Then, we consider all the possible states $i = 0, ..., N-1$. □

Proposition 2.3.3 *The delay of packets transmitted by the user i is given as*

$$D_i\left([\mathbf{q_r}]^{-i}, q_r^i\right) = 1 + \frac{S_i\left([\mathbf{q_r}]^{-i}, q_r^i\right)}{TH_i\left([\mathbf{q_r}]^{-i}, q_r^i\right)}. \tag{2.21}$$

Proof The delay of transmitted packets is computed from the packet's arrival time at the user i until its successful transmission. It can be obtained from the Little's result [53] as follows:

$$D_i\left([\mathbf{q_r}]^{-i}, q_r^i\right) = \frac{TH_i\left([\mathbf{q_r}]^{-i}, q_r^i\right) + S_i\left([\mathbf{q_r}]^{-i}, q_r^i\right)}{TH_i\left([\mathbf{q_r}]^{-i}, q_r^i\right)}, \tag{2.22}$$

$$= 1 + \frac{S_i\left([\mathbf{q_r}]^{-i}, q_r^i\right)}{TH_i\left([\mathbf{q_r}]^{-i}, q_r^i\right)}. \tag{2.23}$$

□

In the following propositions, we provide the performance metrics of backlogged packets.

Proposition 2.3.4 *The throughput of backlogged packets sent by the user i is given as follows*

$$BTH_i\left([\mathbf{q_r}]^{-i}, q_r^i\right) = \frac{1}{T_s\left([\mathbf{q_r}]^{-i}, q_r^i\right)} \sum_{i=0}^{N-1} \sum_{i'=0}^{N-1} P_{(i,0)(i',1)}\left([\mathbf{q_r}]^{-i}, q_r^i\right) \cdot \pi_{i,0}\left([\mathbf{q_r}]^{-i}, q_r^i\right), \tag{2.24}$$

where P is the transition matrix of the Markov chain.

Proof Let us consider the transition matrix P, where $P_{(i,j)(i',j')}$ denotes probability that system state change from (i,j) to (i',j'). The user i will successfully transmit his backlogged packet if the system state change from $(i,1)$ to $(i',0)$, where i and i' corresponds to the change in the number of backlogged packets of other users. Thus, by considering all the possible states of i and i', and by dividing by the transmission time T_s, we get the result of the proposition. □

Proposition 2.3.5 *The delay of backlogged packets sent by the user i is given as follows*

$$BD_i\left([\mathbf{q_r}]^{-i}, q_r^i\right) = 1 + \frac{S_i\left([\mathbf{q_r}]^{-i}, q_r^i\right)}{BTH_i\left([\mathbf{q_r}]^{-i}, q_r^i\right)}. \tag{2.25}$$

Proof The delay of backlogged packets can be derived from the Little's result [53] as follows

$$BD_i\left([\mathbf{q_r}]^{-i}, q_r^i\right) = \frac{BTH_i\left([\mathbf{q_r}]^{-i}, q_r^i\right) + S_i\left([\mathbf{q_r}]^{-i}, q_r^i\right)}{BTH_i\left([\mathbf{q_r}]^{-i}, q_r^i\right)}, \tag{2.26}$$

$$= 1 + \frac{S_i\left([\mathbf{q_r}]^{-i}, q_r^i\right)}{BTH_i\left([\mathbf{q_r}]^{-i}, q_r^i\right)}. \tag{2.27}$$

□

2.4 Non-Cooperative Game Formulation

In this section, we formulate the non-cooperative game model of N players (i.e., users). We consider a wireless network where N bufferless users share a common transmission channel. We assume that all users implement the SAZD access mechanism for channel access.

The non-cooperative game components are listed as follows:

- **Players:** We consider a set $S_N := \{1, 2, ..., N\}$ players that play a non-cooperative game. In what follows, player and user refer to the same thing.
- **Strategy space:** The users' actions form the strategy space. Thus, we define the set of pure strategies $A_i = \{T, W\}$, where T represents the action "Transmit", and W is the action "Wait". Furthermore, we define the mixed strategies as the set of all the distributions over A_i, which is $\psi_i = \{q_r^i, 1 - q_r^i\}$ for a user i.

- **Utility:** Let $u_i : \psi_i \times \psi_{-i} \rightarrow \mathbb{R}$ denote the utility function of user i. u_i could be the average throughput, the access delay, or any other performance metric of interest, and it depends on q_r^i the transmission probability of user i and the vector $q_r^{-i} = [q_r^1, q_r^2, ..., q_r^{i-1}, q_r^{i+1}, ..., q_r^N]$ of others' transmission probabilities.
- **Game information:** We consider that players are aware of the total number of users that compete for channel access. Moreover, every player knows his utility function and strategy space and the others' utility function and their strategy space.

In this non-cooperative game, each player seeks to optimize his utility function regardless of the impact that this behavior on other users. We assume a symmetric strategy profile where all users use the same retransmission probability.

Definition 2.4.1 *A strategy profile* $\mathbf{q_r^*} = (q_r^*, q_r^*, ..., q_r^*)$*, where* $q_r^* \in [\varepsilon, 1]$ *and* $\varepsilon > 0$*, is called a Nash equilibrium if it satisfies*

$$u_i(\mathbf{q_r^*}) \geq u_i(q_r^*, ..., q_r^i, ..., q_r^*), \quad \forall q_r^i \neq q_r^*, \quad \forall i \in S_N. \tag{2.28}$$

The Nash equilibrium corresponds to the situation where no player has the intention unilaterally deviates from his strategic choice. Thanks to symmetry, verifying (2.28) for a single player is a sufficient condition to have $\mathbf{q_r^*} = (q_r^*, q_r^*, ..., q_r^*)$ as an equilibrium.

Let $\mathbf{q_r} = \left([\mathbf{q_r}]^{-i}, q_r^i\right)$ denote a strategy profile, where $[\mathbf{q_r}]^{-i}$ is the retransmission probability of everyone except user i; and q_r^i is the retransmission probability of user i. We define the set of the best response strategies of a user i as follows:

$$\mathcal{R}_i\left(\mathbf{q_r}\right) = \underset{q_r^i \in [\varepsilon,1]}{\operatorname{argmax}} \left\{ u_i\left([\mathbf{q_r}]^{-i}, q_r^i\right) \right\}. \tag{2.29}$$

$\mathbf{q_r^*}$ is a symmetric equilibrium if

$$q_r^* \in \mathcal{R}_i\left(\mathbf{q_r^*}\right), \quad \forall i \in S_N. \tag{2.30}$$

Equation (2.30) provides the existence condition of the Nash equilibrium for the non-cooperative game.

2.4.1 Non-Cooperative Game with a pricing mechanism

In this section, we consider the non-cooperative game model previously introduced. The motivation of this section is that when the arrival-traffic load increases, non-cooperative players tend to be more aggressive at equilibrium [23, 55]. As a result, the system performance gets heavily penalized since users act selfishly by attempting to access the channel with a high retransmission probability q_r, which increases the number of collisions and, therefore, a high energy consumption. To overcome this issue, it is required to control the behavior of users and lower their retransmission rate. The main idea behind this is to reduce the failure probability by limiting the aggressiveness of the

competing users. Towards this end, we propose to associate a transmission cost denoted by C (which can, in particular, represent the battery power consumption) to each transmission attempt.

To illustrate the proposed game, we consider the example shown in Table 2.1, where a player J_1 plays against a couple of players $\{J_2, J_3\}$. The first player can choose between two actions, either transmit or wait. However, players $\{J_2, J_3\}$ can choose between three actions, either they both transmit (TT), they both wait (WW), or one transmits and the other waits (TW). If exactly one player decides to transmit while the others decide to wait, he receives $(1 - C)$, and the others receive 0. Remember that users implement SAZD to access the channel. Thus, two simultaneous transmission can be decoded. Therefore, if two players decide to transmit, each receives $1-C$ thanks to ZD, while the player who decides to wait receives 0. If all three players decide to transmit, a collision occurs, and each receives $-C$, which represents the cost of the transmission.

Table 2.1: Non-cooperative game of 3 players with pure strategies and a pricing mechanism.

Player J_1	Players $\{J_2, J_3\}$		
	TT	TW	WW
Transmit (T)	$(-C, -2C)$	$(1 - C, 1 - C)$	$(1 - C, 0)$
Wait (W)	$(0, 2(1 - C))$	$(0, 1 - C)$	$(0, 0)$

To derive the utility function of a player i, we consider the non-cooperative game model where a player i receives $1 - C$ for every successful transmission; and for a failed transmission, he pays a transmission cost C. Thus, the utility function can be derived as follows:

$$u_i\left([\mathbf{q_r}]^{-i}, q_r^i\right) = (1 - C) \cdot TH_i\left([\mathbf{q_r}]^{-i}, q_r^i\right) - C \cdot q_r^i \sum_{j=0}^{N} \pi_{j,1}\left([\mathbf{q_r}]^{-i}, q_r^i\right). \tag{2.31}$$

In order to maximize his own profit, a user i is faced with the following optimization problem

$$\text{maximize}_{q_r^i \in [\varepsilon, 1]} \left\{u_i\left([\mathbf{q_r}]^{-i}, q_r^i\right)\right\}. \tag{2.32}$$

2.5 Numerical Results

2.5.1 Fixed Transmission Cost

In this section, we compare the performance metrics of the Slotted ALOHA mechanism combined with ZigZag Decoding, on the one hand as a cooperative game problem and on the other hand as a non-cooperative game problem with various transmission costs ($C = 0$, 0.2, 0.5, 0.8). Furthermore, we show how this transmission cost can affect the system's performance metrics.

We depict in Figure 2.2 and Figure 2.3 the global throughput at Nash equilibrium and Nash equilibrium retransmission probability, respectively, as a function of p_a for different values of C.

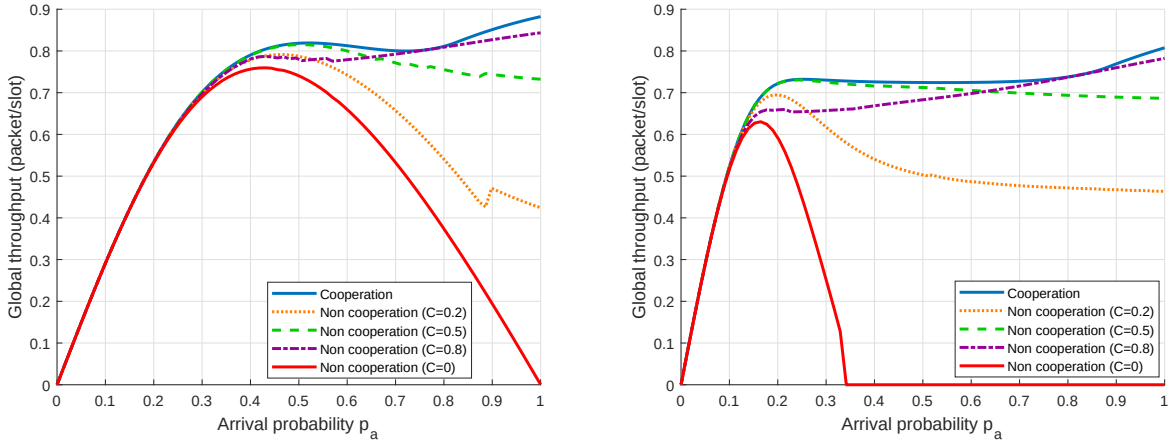

(a) for $N = 3$ (b) for $N = 6$

Figure 2.2: Global throughput versus arrival probability for 3 (a) and 6 (b) users, under different values of $C = [0\ 0.2\ 0.5\ 0.8]$

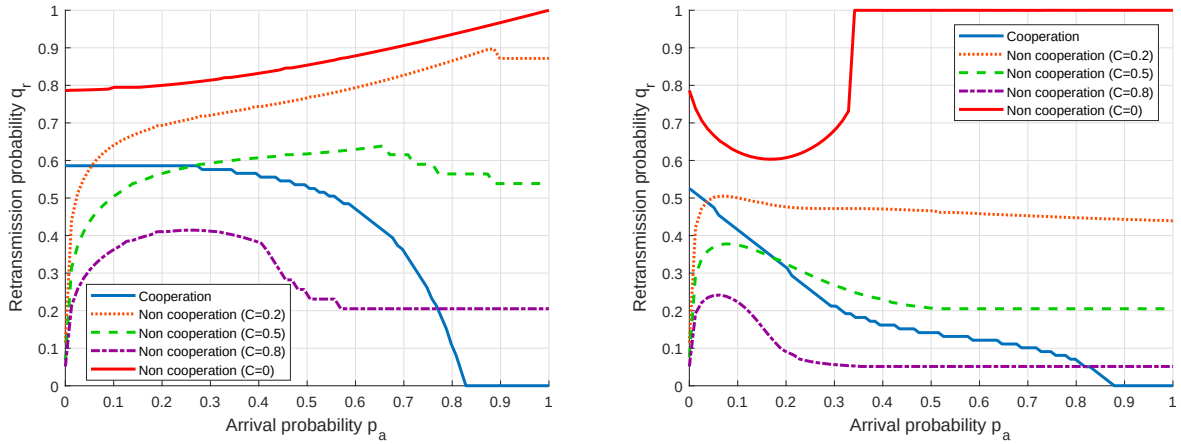

(a) for $N = 3$ (b) for $N = 6$

Figure 2.3: The retransmission probabilities as a function of arrival probability for 3 (a) and 6 (b) users, under different values of $C = [0\ 0.2\ 0.5\ 0.8]$

We compare the non-cooperative case (in which various transmission costs have been added $C = 0, 0.2, 0.5, 0.8$) with the cooperative case. We take the cooperative game (section 1.3.1) as a benchmark to measure the impact of adding a transmission cost on the selfish behavior of competing users. As shown in Figure 2.2 the Slotted ALOHA combined with ZigZag Decoding and

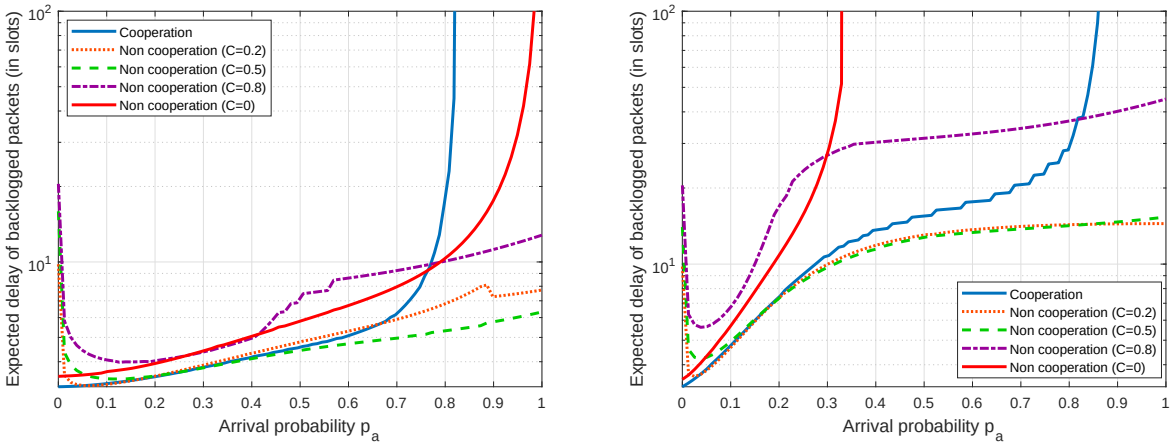

(a) for $N = 3$ (b) for $N = 6$

Figure 2.4: Expected delay of backlogged packets as a function of the arrival probability p_a for 3 (a) and 6 (b) users, under different values of $C = [0\ 0.2\ 0.5\ 0.8]$

transmission cost proves very effective, especially for large arrival probability p_a. In Figure 2.3 we see a decrease in the equilibrium retransmission probability as the cost increases, which means that the pricing mechanism strongly affects the behavior of users.

We plot in Figure 2.4 and Figure 2.5, the expected delay of backlogged and successfully transmitted packets, respectively, as a function of arrival probability p_a for different values of C. We note that transmission cost leads to a bounded delay. However, large pricing could have a negative impact (i.e., huge delay) since users will never transmit when the transmission cost is greater or equal to the gain obtained in a successful transmission. Furthermore, we may wonder here (when p_a is close to 1, see Figure 2.4) why the pricing mechanism could look very effective than the cooperative game. This is mainly because the cooperative system prioritizes the new arrival packets (since p_a is great) in order to maximize the global throughput. This priority mechanism does not appear in the non-cooperative game. Therefore, introducing a transmission cost in the non-cooperative game makes the system more effective.

Note that the equilibrium depends on the transmission cost C. Therefore, we should carefully choose the value of the cost C that gives the best equilibrium results.

2.5.2 Optimization on the Transmission Cost

According to the previous results, we observe that for different values of arrival probability p_a, we obtain different costs C giving the best throughput. Therefore, we seek the cost C that is necessary for the equilibrium retransmission probabilities to coincide with those obtained in the team problem (Chapter 1, Section 1.2). First, we define C_0 (2.33) to be the cost corresponding to

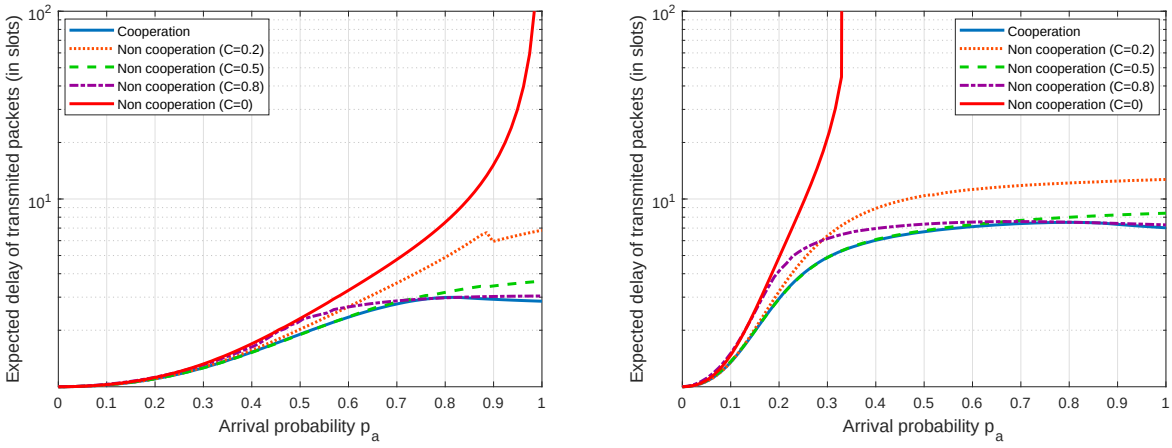

(a) for $N = 3$ (b) for $N = 6$

Figure 2.5: Expected delay of packets that are successfully transmitted as a function of the arrival probability p_a for 3 (a) and 6 (b) users, under different values of $C = [0\ 0.2\ 0.5\ 0.8]$

the best average throughput (i.e., the cost giving the same results as in Section 1.3.1. Then, we define the cost C_1 (2.34) that minimizes the delay of backlogged packets (same performances as the cooperative game of Section 1.3.3). Finally, C_α (2.35) is defined to be an adjustable cost with parameter α that compromises between the throughput and the delay of backlogged packets. The cost C_α generalizes the cost C_3 in [56]. Indeed, it takes all the values between C_0 and C_1. Thus, in the numerical results, we focus on $\alpha = \frac{1}{2}$.

$$\max_{C\in[0,1]} \left\{TH_i\left(p_a, q_r^*(C)\right)\right\} , \tag{2.33}$$

$$\max_{C\in[0,1]} \left\{\frac{1}{BD_i\left(p_a, q_r^*(C)\right)}\right\} , \tag{2.34}$$

where $q_r^*(C)$ is the Nash equilibrium which depends on the transmission cost.

$$C_\alpha = (1-\alpha)C_0 + \alpha C_1 . \tag{2.35}$$

We depict in Figure 2.6a and Figure 2.6b, the optimal transmission cost C_0, C_1 and $C_{\frac{1}{2}}$, as a function of arrival probability, respectively, for 3 and 10 users. In both cases, we note that C_0 reaches the congestion cost (i.e., $C = 1$) when the arrival probability p_a is too large, In fact, the system prioritizes the new arriving packets in order to maximize the global throughput. Whereas C_1 and $C_{\frac{1}{2}}$ never reach 1 so that the backlogged packets are just as privileged as the new arriving packets.

We depict in Figure 2.7 and Figure 2.8, respectively, the aggregate throughput and the retransmission probability, as a function of arrival probability, for 3 and 10 users. We observe that we

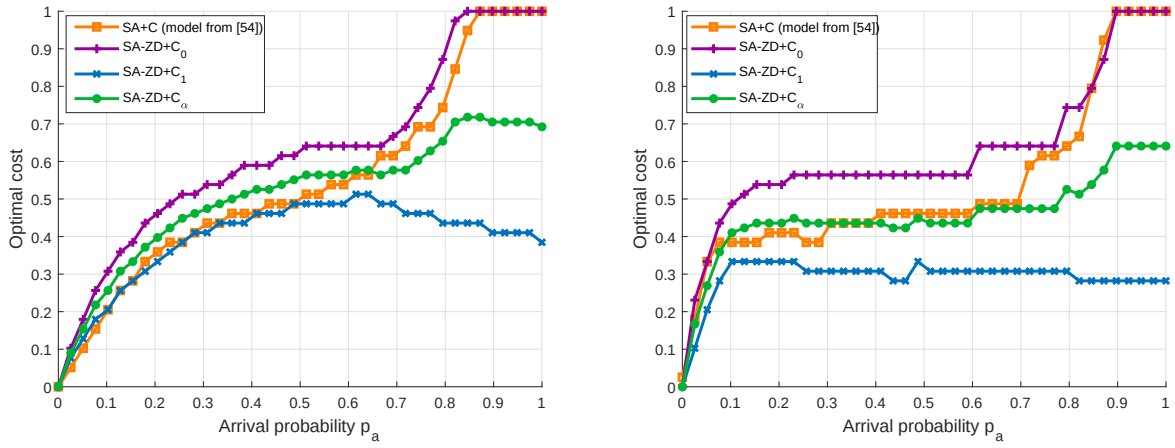

(a) for $N = 3$ (b) for $N = 10$

Figure 2.6: The optimal transmission cost as a function of arrival probability p_a for 3 (a) and 10 (b) users

achieve the maximum global throughput by using the cost C_0. However, when we use the cost C_1, we obtain a minimum delay of backlogged packets. Finally, when the cost $C_{\frac{1}{2}}$ is used, a compromise is achieved. This compromise is compensated with a bounded delay of backlogged packets (see Figure 2.9). In Figure 2.8, we see a visible and significant improvement in the retransmission probability. As a result, we notice a decrease in the selfish behavior of competing users.

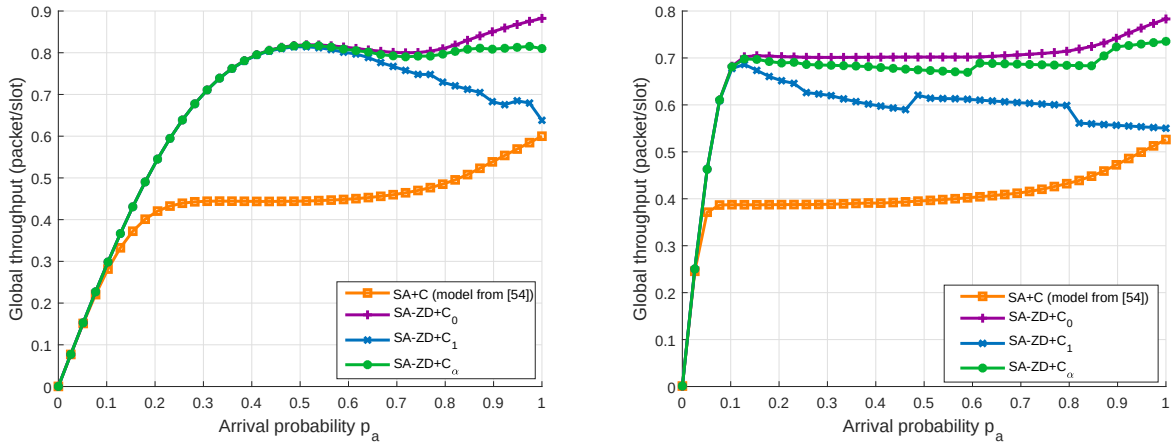

(a) for $N = 3$ (b) for $N = 10$

Figure 2.7: The global throughput in the game case with various optimal transmission cost

In Figure 2.9, we plot the delay of backlogged packets as a function of arrival probability. As we discussed before, we see that the delay of backlogged packets when using C_0 is huge even if the corresponding throughput is maximal. On the other side, Figure 2.10 shows the expected delay of transmitted packets and confirms that the system prioritizes the new arriving packets when using C_0. However, for the case of C_1 and $C_{\frac{1}{2}}$ there is no priority mechanism.

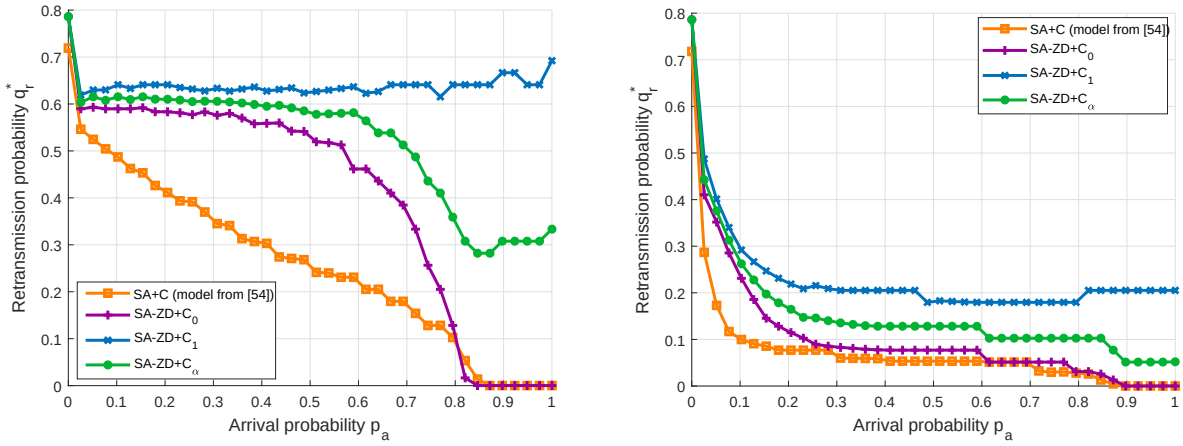

(a) for $N = 3$ (b) for $N = 10$

Figure 2.8: The retransmission probability in the game case with various optimal transmission cost

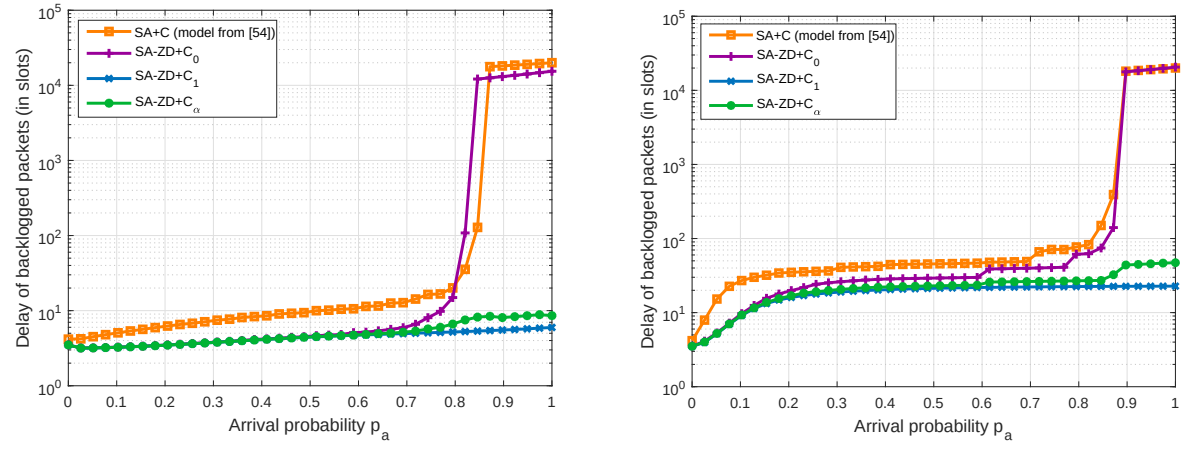

(a) for $N = 3$ (b) for $N = 10$

Figure 2.9: Expected delay of backlogged packets in the game case with various optimal transmission cost

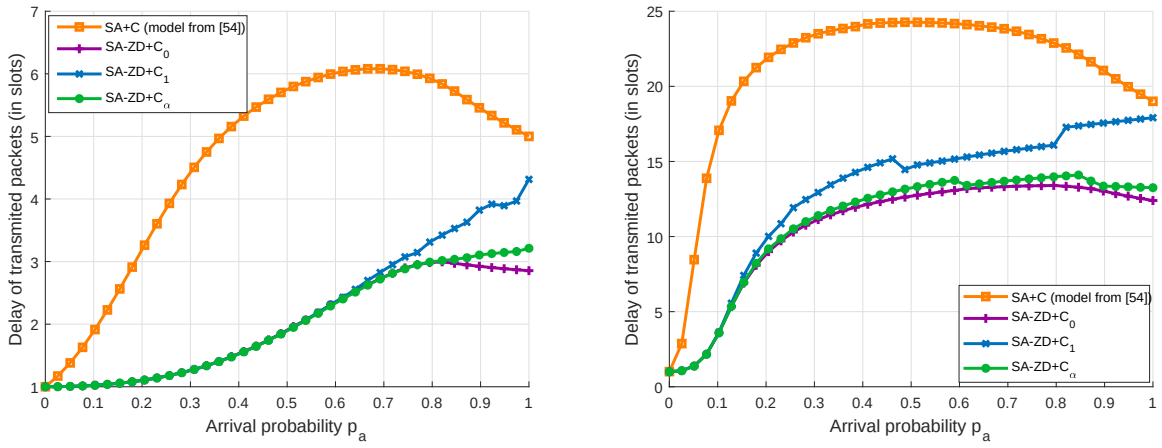

(a) for $N = 3$ (b) for $N = 10$

Figure 2.10: Expected delay of packets that are successfully transmitted in the game case with various optimal transmission cost

2.6 Conclusion

In this chapter, we have constructed and investigated the non-cooperative game model where users act selfishly and seek to optimize their own utility functions. First, we have proposed a bidimensional Markov chain to get the system's state at the stationary regime. Then, we derived all the performance metrics of interest, such as the throughput and the access delay. We showed that selfishness yields the worst network performance compared to the cooperative game model. To overcome this issue, we have proposed a pricing mechanism that implements the energy stored in the user's battery in order to mitigate the users' selfish behavior. Our results show that we were able to convert a non-cooperative game into a cooperative game by using this pricing mechanism. Moreover, we optimized the existing trade-off between the throughput and the delay of backlogged delay.

In the next chapter, we extend the two previous chapters into a general stochastic game model with a mix of cooperative and non-cooperative players. The model provides a general framework of many existing models in the literature [57, 58, 59, 60, 61, 2].

Chapter 3

General Game Model of Cooperation and Selfishness in Slotted ALOHA Enhanced by ZigZag Decoding

Contents

3.1 Introduction

Random access mechanisms are the fundamental schemes for channel access under distributed access systems. These mechanisms can be divided into two categories: ALOHA and its enhanced variants [51, 5, 6, 56, 62]; and Carrier Sense Multiple Access (CSMA)-based schemes [25]. Many approaches have been proposed over recent years to improve the performance of ALOHA, such as Age of Information (AoI) threshold mechanism [63], Coded Slotted ALOHA (CSA) [62], Successive Interference Cancellation (SIC) [8], Capture Effect (CE) [9], ZigZag Decoding [11, 12]. In ALOHA, users transmit whenever they generate a packet. Whereas, in CSMA, users implement carrier sensing before accessing the channel. This chapter focuses on the Slotted ALOHA enhanced by

ZigZag decoding. In slotted ALOHA, users are allowed to transmit only at the beginning of a slot. This feature provides a peak throughput equal to 36.8% compared with only 18.4% for the pure ALOHA.

The game theory framework can be classified into two game categories: cooperative and non-cooperative games. In the cooperative game models, users know their neighbor's action plan, strategy space, and utility functions. Thus, users cooperate to make decisions that lead to an equilibrium solution that makes the group satisfied. The cooperation leads to the best performance, whereas the non-cooperative game model yields the worst system performance [64].

The cooperative game framework provides highly effective approaches for modeling collaborative environments. It has been widely applied to solve various types of interactive situations such as channel access, resource management, and bandwidth allocation. In wireless networks, cooperation is performed by a central entity to optimize the overall system performance. Thus, either maximizing the system throughput, minimizing the access channel delay, or minimizing the backlog level of the network.

In non-cooperative game models [65, 66, 56], each user attempts to maximize their utility without considering the potential impact on other users. Unfortunately, this selfish behavior usually leads to dramatic degradation of the performance of all users. To address this issue, several approaches have been proposed in the literature. For example, in our previous work [64], we proposed to force the cooperation by associating a cost for every transmission attempt.

Most game theory models [67, 1, 68, 69, 70, 65, 66, 66] consider that either all users cooperate or all users do not. However, in this chapter, we propose a game theory model with both user categories. Thus, the proposed network scenario consists of cooperative and selfish users who share the same wireless channel. In this context, cooperative users behave for the benefit of the overall system. Consequently, they attempt to maximize the overall network performance. In contrast, selfish users are self-contained, and they act independently by trying to maximize their own utility instead of the utility of the overall system. This study aims to investigate the interaction between cooperative and non-cooperative users within the same wireless network, and also to evaluate the impact of selfish behavior on the performance of the cooperative users and on the overall system performance.

This chapter presents a novel and general stochastic game model of a network scenario combining cooperative and non-cooperative players (i.e., users). The model considers the principles of both cooperative and non-cooperative game theories and considers incomplete game information. The random access mechanism implemented by all users is the Slotted ALOHA combined with ZigZag Decoding (SAZD). The model assumes that cooperative players seek to optimize the global utility of the system (e.g., throughput, delay, loss rate) regardless of their individual interests. In contrast, non-cooperative players act selfishly and optimize their own benefits irrespective of this behavior's impact on others and the entire network system. The game equilibrium is characterized by the social optimum and the Nash equilibrium, where the former is adopted by cooperative players and the latter is the equilibrium strategy of non-cooperative players. Using a comparative study, where each player type dominates the game differently, we showed that selfishness strongly affects other

players and the entire system.

The main contributions of this chapter are as follows:

- We propose a novel stochastic game model incorporating cooperative and non-cooperative players in the same game.
- We develop a bi-dimensional Markov chain to get the system's state at the stationary regime.
- We show that the game admits an equilibrium solution that integrates the Nash and social optimality concepts.
- We explore different performance metrics, such as throughput, delay, number of backlogged packets, and the equilibrium retransmission policy.
- We undertake a comparative study of two game scenarios with different levels of cooperation and selfishness.

3.2 Prior Related Researches

Slotted ALOHA is one of the most widely used random access schemes. Nowadays, it is implemented in many technologies, e.g, satellite networks [1], LoRaWAN networks [2, 3, 4], IoT applications [5], Machine-to-Machine (M2M) communications [6], and NOMA (Non-Orthogonal Multiple Access) for the Next Generation IoT [7].

3.2.1 Cooperative game models

Cooperative models study the situation of collaboration and coalition between users. In our previous work [71, 64], we proposed a cooperative model of SA and SAZD. Our results showed that cooperation leads to the best results in both mechanisms. We also showed that the SAZD mechanism outperforms the standard SA in terms of all performance metrics. However, in heavy traffic conditions, the cooperation between users leads to unfair resource allocation due to the system specifications that allows newly arrived packets to be transmitted immediately after their arrival. Thus, even if the overall system performance is maximized, it is only used by newly arrived packets, making backlogged packets stay on hold for a very long time. To address this issue, we have proposed in [11] an enhanced pricing mechanism that allows us to guarantee a fairness level between newly arrived and backlogged packets.

The authors in [67] proposed a cooperative scheme for SA with power diversity transmission and interference cancellation technique for multi-satellite networks. Using an optimization approach, they derived the optimal transmission power distribution. Their results show that the cooperative SA with optimized transmission power outperforms the SA with uniform power distribution. Even though their analysis and results focus mainly on the throughput, they investigated the access delay and energy consumption in [1].

The authors in [68] studied a cooperative SA full-duplex wireless network with two users. They found that the cooperation should be done only by the user having a higher successful transmission probability. However, the cooperation concept proposed in their study is a relay-based approach between a source and relay node, which could be extended to multiple user scenarios. The authors also proposed in [69] an optimal cooperation policy that outperforms, in some cases, the full-cooperation and non-cooperation policies.

In [70], the authors proposed a beamforming collision resolution scheme that exploits multiple satellites' cooperation to decode the collided packets. The beamforming algorithm is used when a deadlock state is reached. Otherwise, they use the Successive Interference Cancellation (SIC).

3.2.2 Non-cooperative game models

Non-cooperative game theory provides a framework analysis of the interaction between selfish users. The Slotted ALOHA mechanism and its variants have been widely studied using non-cooperative models. In [64, 56], we have proposed a stochastic game model of Slotted ALOHA combined with ZigZag Decoding. The model assumes that all users are selfish, and therefore they do not cooperate with each other. Compared with the cooperative model, we found that the selfish behavior of users yields the worst system performance, especially in the case of a large number of users.

In [65], the authors provided a non-cooperative game model for Slotted ALOHA. To achieve the desired throughput, they proposed to adjust users' transmission probabilities at each iteration of the game. Then they investigated the equilibrium of the game.

The authors in [66] proposed a non-cooperative game analysis of a network scenario operating using the carrier sense multiple access with collision avoidance (CSMA/CA) mechanism. Each user in the proposed scheme attempts to minimize the age of his information. They studied different profiles of pure and mixed strategies. They found that the collision length affects the dominant strategy of the game.

3.2.3 Mixed game models

The authors in [72] studied the cooperative and non-cooperative game models for Slotted ALOHA with channel capture. The optimal threshold strategy is used to characterize the equilibrium in the case of cooperation, whereas the non-cooperative equilibrium is given as the Bayesian Nash equilibrium. The authors showed that in the non-cooperative game, users transmit with a higher probability than cooperative scenario. This aggressive behavior comes from the fact that in non-cooperative games, users consider only their own payoffs.

In [73], an extensive investigation of cooperation and selfishness was carried out using stochastic games and evolutionary game theory. According to the study, the system resource depends on the strategic choices of the users. Thus, it increases in the case of cooperation and decreases in the case of non-cooperation. The same behavior was found in SA and in SAZD systems [64].

The authors in [74] proposed a game model with a mix of cooperative and non-cooperative users for Wifi networks. They found that the cooperation is beneficial even if some users choose to

deviate. Besides, they claimed that most defected users are penalized by getting the worst Signal-to-Interference-plus-Noise Ratio (SINR). However, the results focus mainly on the SINR; and the impact of the mixed user scenario on other performance metrics, e.g., throughput and delay, is not investigated.

In [75], the authors developed an optimal caching algorithm using the social selfishness concept to achieve the best caching strategy for a mix of cooperative and non-cooperative users. The social selfishness concept adopted takes into account the social relationship between users. Thus, each user cares more about the cooperative users with whom he has a strong social relationship.

3.3 Problem Formulation

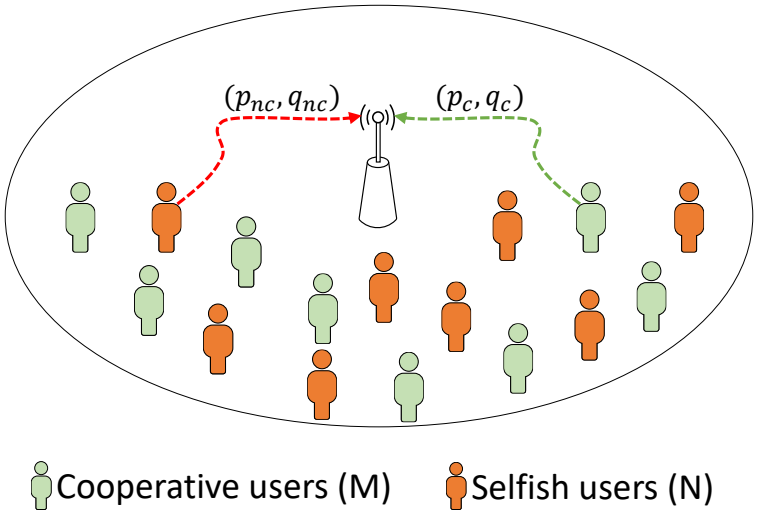

Figure 3.1: A scenario of a wireless network where M cooperative users share the same medium with N selfish users.

3.3.1 Model description

We consider a wireless network consisting of two groups of users sharing a common transmission channel. Let M be the number of users in the first group and N the number of users in the second group, and let m and n be the number of backlogged users in each group. The arrival flow of packets to each source in each group follows a Bernoulli process with parameters p_c and p_{nc} respectively. Similarly, let q_c and q_{nc} be, respectively, the retransmission probability of backlogged users in each group.

We define $Q_c(i, m)$ and $Q_{nc}(i, n)$ as the transmission probability of i unbacklogged nodes in the

first and the second group respectively.

$$Q_c(i,m) = \binom{M-m}{i} p_c^i (1-p_c)^{M-m-i}, \tag{3.1}$$

$$Q_{nc}(i,n) = \binom{N-n}{i} p_{nc}^i (1-p_{nc})^{N-n-i}. \tag{3.2}$$

Similarly, we define $Q_c^r(i,m)$ and $Q_{nc}^r(i,n)$ as the retransmission probability of i backlogged nodes in the first and the second group.

$$Q_c^r(i,m) = \binom{m}{i} q_c^i (1-q_c)^{m-i}, \tag{3.3}$$

$$Q_{nc}^r(i,n) = \binom{n}{i} q_{nc}^i (1-q_{nc})^{n-i}. \tag{3.4}$$

3.3.2 Analytical model

In this section, we provide the theoretical model of the proposed mechanism. Let $\{(X_k, Y_k)\,,\ k \in \mathbb{N}\}$ be the stochastic process representing the number of backlogged users in each group at the beginning of the time slot k. The reason behind using a bi-dimensional stochastic process comes from the subdivision of the users into two groups. In what follows, we consider the first group as the set of cooperative users and the second group as the set of selfish users.

Theorem 3.3.1 *For any choice of values $q_c \in]0,1]$ and $q_{nc} \in]0,1]$, $(X_k, Y_k)_{k\in\mathbb{N}}$ is Markovian with a unique stationary distribution.*

Proof

Consider the process $\{(X_k, Y_k),\ k \in \mathbb{N}\}$ representing the number of backlogged nodes among cooperative and selfish users in a given time slot k. The state space is then

$$S = \{0, 1, ..., M\} \times \{0, 1, ..., N\},$$

where M and N denotes respectively, the total number of cooperative and selfish users.

Let A_k and B_k denote the number of newly arrived packets, respectively, for cooperative and selfish users during slot $k-1$ and are scheduled for the first transmission attempt in slot k. Furthermore, let C_k and D_k be, respectively, the number of cooperative and selfish backlogged users that attempt to transmit in slot k. Thus, we have

$$P\left(A_k = i | X_k = m\right) = Q_c(i,m), \qquad i = 0, ..., M, \tag{3.5}$$

$$P\left(B_k = i | Y_k = n\right) = Q_{nc}(i,n), \qquad i = 0, ..., N, \tag{3.6}$$

$$P\left(C_k = i | X_k = m\right) = Q_c^r(i,m), \qquad i = 0, ..., M, \tag{3.7}$$

$$P\left(D_k = i | Y_k = n\right) = Q_{nc}^r(i,n), \qquad i = 0, ..., N. \tag{3.8}$$

Therefore, the number of transmissions occurring in a given slot k among cooperative and selfish users, denoted respectively by E_k and F_k, can be expressed as follows:

$$E_k = A_k + C_k, \tag{3.9}$$
$$F_k = B_k + D_k. \tag{3.10}$$

The evolution of the number of backlogged nodes found in the system at the beginning of slot $k+1$ can now be expressed by the following equations:

$$X_{k+1} = X_k + A_k - \mathbb{1}_{\{E_k=1\}} - 2 \cdot \mathbb{1}_{\{E_k=2\}}, \tag{3.11}$$
$$Y_{k+1} = Y_k + B_k - \mathbb{1}_{\{F_k=1\}} - 2 \cdot \mathbb{1}_{\{F_k=2\}}, \tag{3.12}$$

where $\mathbb{1}$ is the indicator function.

Thus, the number of backlogged nodes at the beginning of a given time slot $k+1$ depends not only on the number of arrivals and departures in the previous slot k but also on the system state (X_k, Y_k) (i.e., the number of backlogged users). Therefore, the following Markov property holds since the future states of the process are independent of the past states.

For all $(x_0, y_0), ..., (x_{k+1}, y_{k+1}) \in S$ and $k \in \mathbb{N}$ we have:

$$\begin{aligned} P\big\{ (X_{k+1}, Y_{k+1}) = (x_{k+1}, y_{k+1}) \,|\, (X_k, Y_k) = (x_k, y_k), ..., (X_0, Y_0) = (x_0, y_0) \big\} \\ = P\big\{ (X_{k+1}, Y_{k+1}) = (x_{k+1}, y_{k+1}) \,|\, (X_k, Y_k) = (x_k, y_k) \big\}, \end{aligned} \tag{3.13}$$

where (x_0, y_0) denotes the initial state of the Markov chain.

Now, let us assume that $q_c = 0$ and $q_{nc} = 0$, then the Markov chain has six absorbing states, namely (M, N), $(M-1, N)$, $(M, N-1)$, $(M-2, N)$, $(M, N-2)$ and $(M-1, N-1)$. For $p_c > 0$ and $p_{nc} > 0$, all other states are transient. The absorbing states can be reached with positive probabilities $p_c > 0$ and $p_{nc} > 0$ from any initial state, except from another absorbing state. Therefore, we shall exclude the case of $q_c = 0$ and $q_{nc} = 0$.

The stochastic process $\{(X_k, Y_k),\ k \in \mathbb{N}\}$ can now be described as a homogeneous finite Markov process with $(M+1) \times (N+1)$ possible states where the transition probabilities are given in the appendix. The transition diagram is given in Figure 3.2.

Since all states communicate with each other and the state space is finite, the Markov chain is ergodic [53]. Therefore, the steady-state probability exists, and it is unique. We denote by $\Pi = (\Pi_{i,j})_{i \in \{0,..,M\}, j \in \{0,...,N\}}$ the vector of the steady-state probability, where $\Pi_{i,j}$ is the probability that the system contains i backlogged nodes of the cooperative group and j backlogged nodes of the selfish group. This steady-state distribution can be obtained by solving the following problem:

$$\begin{cases} \Pi = \Pi \cdot P, \\ \Pi_{i,j} \geq 0, \quad i = 0, ..., M,\ j = 0, ..., N \\ \sum_{i=0}^{M} \sum_{j=0}^{N} \Pi_{i,j} = 1, \end{cases} \tag{3.14}$$

where P is the transition block matrix which is given as follows:

$$
P_{(m,n)(m+i,n+j)} =
$$

$$
\begin{cases}
Q_c(i,m)\cdot Q_{nc}(j,n), & \text{if } 3\le i\le M-m \text{ and } 0\le j\le N-n,\\
\left.\begin{array}{l} Q_c(i,m)\cdot(1-Q_c^r(0,m)-Q_c^r(1,m))\cdot Q_{nc}(j,n)\\ \quad +Q_c(i,m)\cdot Q_c^r(0,m)\cdot(1-Q_{nc}^r(0,n)-Q_{nc}^r(1,n))\cdot Q_{nc}(j,n)\\ \quad +Q_c(i,m)\cdot Q_c^r(1,m)\cdot(1-Q_{nc}^r(0,n))\cdot Q_{nc}(j,n), \end{array}\right\} & \text{if } i=1 \text{ and } j=0,\\
\left.\begin{array}{l} Q_c(i,m)\cdot(1-Q_c^r(0,m))\cdot Q_{nc}(j,n)\\ \quad +Q_c(i,m)\cdot Q_c^r(0,m)\cdot(1-Q_{nc}^r(0,n))\cdot Q_{nc}(j,n), \end{array}\right\} & \text{if } i=1 \text{ and } j=1,\\
Q_c(i,m)\cdot Q_{nc}(j,n), & \text{if } i=1 \text{ and } 2\le j\le N-n,\\
\left.\begin{array}{l} Q_c(i,m)\cdot(1-Q_c^r(0,m))\cdot Q_{nc}(j,n)\\ \quad +Q_c(i,m)\cdot Q_c^r(0,m)\cdot(1-Q_{nc}^r(0,n))\cdot Q_{nc}(j,n), \end{array}\right\} & \text{if } i=2 \text{ and } j=0,\\
Q_c(i,m)\cdot Q_{nc}(j,n), & \text{if } i=2 \text{ and } 1\le j\le N-n,\\
\left.\begin{array}{l} Q_c(0,m)\cdot(1-Q_c^r(0,m)-Q_c^r(1,m)-Q_c^r(2,m))\cdot Q_{nc}(j,n)\\ \quad +Q_c(0,m)\cdot Q_c^r(0,m)\cdot Q_{nc}(0,n)\cdot(1-Q_{nc}^r(1,n)-Q_{nc}^r(2,n))\\ \quad +Q_c(0,m)\cdot Q_c^r(1,m)\cdot Q_{nc}(0,n)\cdot(1-Q_{nc}^r(0,n)-Q_{nc}^r(1,n))\\ \quad +Q_c(0,m)\cdot Q_c^r(2,m)\cdot Q_{nc}(0,n)\cdot(1-Q_{nc}^r(0,n))\\ \quad +Q_c(1,m)\cdot Q_c^r(0,m)\cdot Q_{nc}(0,n)\cdot Q_{nc}^r(0,n)\\ \quad +Q_c(2,m)\cdot Q_c^r(0,m)\cdot Q_{nc}(0,n)\cdot Q_{nc}^r(0,n)\\ \quad +Q_c(0,m)\cdot Q_c^r(0,m)\cdot Q_{nc}(1,n)\cdot Q_{nc}^r(0,n)\\ \quad +Q_c(0,m)\cdot Q_c^r(0,m)\cdot Q_{nc}(2,n)\cdot Q_{nc}^r(0,n)\\ \quad +Q_c(1,m)\cdot Q_c^r(0,m)\cdot Q_{nc}(1,n)\cdot Q_{nc}^r(0,n), \end{array}\right\} & \text{if } i=0 \text{ and } j=0,\\
\left.\begin{array}{l} Q_c(i,m)\cdot Q_{nc}(j,n)\cdot(1-Q_{nc}^r(0,n)-Q_{nc}^r(1,n))\\ \quad +Q_c(i,m)\cdot(1-Q_c^r(0,m)-Q_c^r(1,m))\cdot Q_{nc}(j,n)\cdot Q_{nc}^r(0,n)\\ \quad +Q_c(i,m)\cdot(1-Q_c^r(0,m))\cdot Q_{nc}(j,n)\cdot Q_{nc}^r(1,n), \end{array}\right\} & \text{if } i=0 \text{ and } j=1,\\
\left.\begin{array}{l} Q_c(i,m)\cdot Q_{nc}(j,n)\cdot(1-Q_{nc}^r(0,n))\\ \quad +Q_c(i,m)\cdot(1-Q_c^r(0,m))\cdot Q_{nc}(j,n)\cdot Q_{nc}^r(0,n), \end{array}\right\} & \text{if } i=0 \text{ and } j=2,\\
Q_c(i,m)\cdot Q_{nc}(j,n), & \text{if } i=0 \text{ and } 3\le j\le N-n,\\
\left.\begin{array}{l} Q_c(0,m)\cdot Q_c^r(0,m)\cdot Q_{nc}(0,n)\cdot Q_{nc}^r(1,n)\\ \quad +Q_c(0,m)\cdot Q_c^r(0,m)\cdot Q_{nc}(1,n)\cdot Q_{nc}^r(1,n)\\ \quad +Q_c(1,m)\cdot Q_c^r(0,m)\cdot Q_{nc}(0,n)\cdot Q_{nc}^r(1,n), \end{array}\right\} & \text{if } i=0 \text{ and } j=-1,\\
Q_c(0,m)\cdot Q_c^r(0,m)\cdot Q_{nc}(0,n)\cdot Q_{nc}^r(2,n), & \text{if } i=0 \text{ and } j=-2,\\
\left.\begin{array}{l} Q_c(0,m)\cdot Q_c^r(1,m)\cdot Q_{nc}(0,n)\cdot Q_{nc}^r(0,n)\\ \quad +Q_c(1,m)\cdot Q_c^r(1,m)\cdot Q_{nc}(0,n)\cdot Q_{nc}^r(0,n)\\ \quad +Q_c(0,m)\cdot Q_c^r(1,m)\cdot Q_{nc}(1,n)\cdot Q_{nc}^r(0,n), \end{array}\right\} & \text{if } i=-1 \text{ and } j=0,\\
Q_c(0,m)\cdot Q_c^r(1,m)\cdot Q_{nc}(0,n)\cdot Q_{nc}^r(1,n), & \text{if } i=-1 \text{ and } j=-1,\\
Q_c(0,m)\cdot Q_c^r(2,m)\cdot Q_{nc}(0,n)\cdot Q_{nc}^r(0,n), & \text{if } i=-2 \text{ and } j=0,\\
0, & \text{otherwise.}
\end{cases}
\tag{3.15}
$$

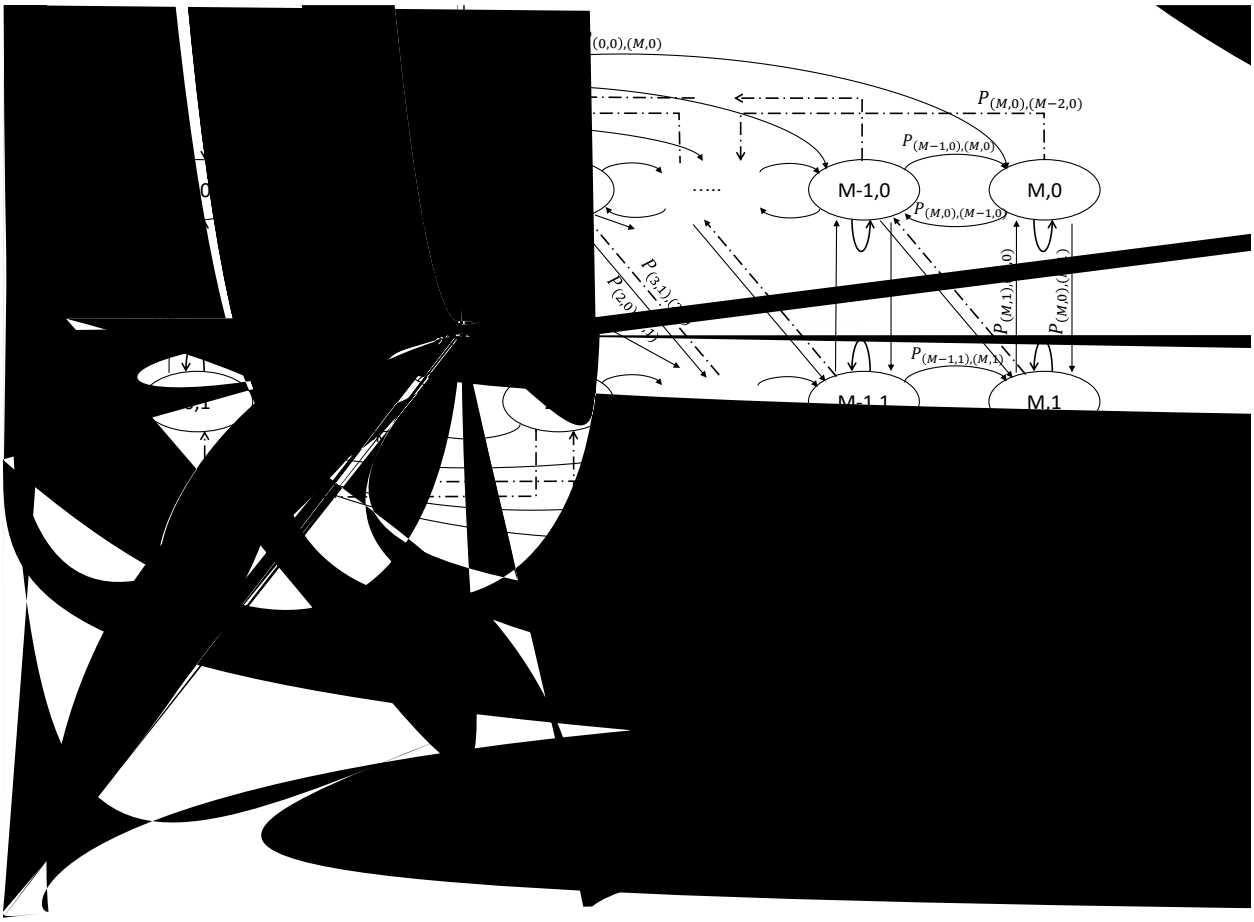

Figure 3.2: Transition diagram of the Markov chain. The straight line corresponds to either a successful transmission or an increase in backlogged packets, whereas the dashed line represents a successful transmission with ZigZag.

Note that the only absorbing state with no arrivals and no departures (i.e., deadlock state) is the state (M, N). Thus, from now on we consider $q_c \neq 0$ and $q_{nc} \neq 0$, and we chose $\varepsilon = 10^{-4}$ such that $(q_c, q_{nc}) \in [\varepsilon, 1]^2$. $\square$

3.3.3 Performance evaluation

Proposition 3.3.2 *The average throughput of cooperative and non-cooperative users is given, respectively, as follows*

$$TH_c = \frac{p_c}{T_s} \sum_{m=0}^{M} \left[(M-m) \sum_{n=0}^{N} \Pi_{m,n} \right], \tag{3.16}$$

$$TH_{nc} = \frac{p_{nc}}{T_s} \sum_{n=0}^{N} \left[(N-n) \sum_{m=0}^{M} \Pi_{m,n} \right]. \tag{3.17}$$

Proof To derive the throughput expression, we need to define the packet's transmission time T_s.

The slots' lengths in SA are of the same size. However, in SAZD, the slot duration depends on the stations' transmission activities. In the case of ZigZag, the transmission duration takes two slots. Otherwise, the transmission takes one slot duration. Therefore, T_s can be defined as follows

$$T_s = 1 \cdot (1 - P_{ZigZag}) + 2 \cdot P_{ZigZag}, \tag{3.18}$$

$$= 1 + P_{ZigZag}, \tag{3.19}$$

where P_{ZigZag} is the probability that two packets are sent using ZD, and it is given by

$$P_{ZigZag} = \sum_{m=0}^{M} \sum_{n=0}^{N} \sum_{i,j,k,l \in \mathbb{N}} \left[Q_c(i,m) \cdot Q_{nc}(j,m) \cdot Q_c^r(k,m) \cdot Q_{nc}^r(l,m) \right] \cdot \Pi_{m,n} \cdot \mathbb{1}_{\{i+j+k+l=2\}}. \tag{3.20}$$

$\mathbb{1}$ is the indicator function, such that

$$\mathbb{1}_{\{i+j+k+l=2\}} := \begin{cases} 1 & \text{if} \quad i+j+k+l=2, \\ 0 & \text{otherwise.} \end{cases} \tag{3.21}$$

Now, we can find the average throughput of cooperative users.

At the steady-state, the average number of transmitted packets equals the average number of arrivals. Therefore, for a fixed value of m, the cooperative arrival rate in each state (m,n), where $n = 0, ..., N$, is $p_c(M-m)/T_s$. Then, by taking all possible cases for m, we can derive the throughput of cooperative users as equation (3.16) of the previous proposition. Similarly, the average number of arrival packets of non-cooperative users is $p_{nc}(N-n)/T_s$, which yields equation (3.17) by considering all the possible cases of n. □

Remark 3.3.3 *Equations* (3.16) *and* (3.17) *represent the average throughput entering the system. At the stationary regime, the expected number of arrivals derived from equations* (3.16), (3.17) *equals to the expected number of departures. Therefore, the throughput can be expressed as follows*

$$TH_c = \frac{1}{T_s} \sum_{m=0}^{M} \sum_{n=0}^{N} P_c^s(m,n) \cdot \Pi_{m,n}, \tag{3.22}$$

$$TH_{nc} = \frac{1}{T_s} \sum_{m=0}^{M} \sum_{n=0}^{N} P_{nc}^s(m,n) \cdot \Pi_{m,n}, \tag{3.23}$$

where $P_c^s(m,n)$ and $P_{nc}^s(m,n)$ are the average number of successfully delivered packets among

cooperative and non-cooperative users, respectively. They are given as follows

$$\begin{aligned} P_c^s(m,n) = &\sum_{i,j\in\mathbb{N}} (i+j)\big[Q_c(i,m)\cdot Q_{nc}(j,m)\cdot Q_c^r(0,m)\cdot Q_{nc}^r(0,m)\big]\Pi_{m,n}\cdot \mathbb{1}_{\{1\leq i+j\leq 2\}} \\ &+ \sum_{i,j,k,l\in\mathbb{N}} \big[Q_c(i,m)\cdot Q_{nc}(j,m)\cdot Q_c^r(k,m)\cdot Q_{nc}^r(l,m)\big]\cdot \mathbb{1}_{\{(i+j)(k+l)=1\}}, \end{aligned} \tag{3.24}$$

$$\begin{aligned} P_{nc}^s(m,n) = &\sum_{k,l\in\mathbb{N}} (k+l)\big[Q_c(0,m)\cdot Q_{nc}(0,m)\cdot Q_c^r(k,m)\cdot Q_{nc}^r(l,m)\big]\Pi_{m,n}\cdot \mathbb{1}_{\{1\leq k+l\leq 2\}} \\ &+ \sum_{i,jk,l\in\mathbb{N}} \big[Q_c(i,m)\cdot Q_{nc}(j,m)\cdot Q_c^r(k,m)\cdot Q_{nc}^r(l,m)\big]\cdot \mathbb{1}_{\{(i+j)(k+l)=1\}}. \end{aligned} \tag{3.25}$$

Proposition 3.3.4 *The average number of backlogged users is given by*

$$S_c = \sum_{m=0}^{M} m\cdot\left[\sum_{n=0}^{N}\Pi_{m,n}\right], \tag{3.26}$$

$$S_{nc} = \sum_{n=0}^{N} n\cdot\left[\sum_{m=0}^{M}\Pi_{m,n}\right]. \tag{3.27}$$

Proof The backlogged users are the ones that have a packet on hold due to a previous collision. Thus, since the state of the Markov chain corresponds to the number of backlogged packets, then the average number of backlogged cooperative users can be derived by considering the current number of backlogged users m and taking the sum over all the possible states of the non-cooperative users which is given by

$$m\cdot\left[\sum_{n=0}^{N}\Pi_{m,n}\right].$$

Then, we can sum over all the possible states of m. We can derive the average number of backlogged nodes among non-cooperative users using a similar approach. □

Corollary 3.3.4.1 *Combining equation* (3.16) *with* (3.26)*, and equation* (3.17) *with* (3.27)*, we can derive an expression for the average throughput as follows*

$$TH_c = \frac{p_c}{T_s}\left(M - S_c\right), \tag{3.28}$$

$$TH_{nc} = \frac{p_{nc}}{T_s}\left(N - S_{nc}\right). \tag{3.29}$$

Proof We can get the two results of the corollary by developing equations (3.16) and (3.17) as

follows

$$TH_c = \frac{p_c}{T_s} \sum_{m=0}^{M} \left[M \sum_{n=0}^{N} \Pi_{m,n} - m \sum_{n=0}^{N} \Pi_{m,n} \right], \tag{3.30}$$

$$= \frac{p_c}{T_s} \left[M \sum_{m=0}^{M} \sum_{n=0}^{N} \Pi_{m,n} - \sum_{m=0}^{M} m \sum_{n=0}^{N} \Pi_{m,n} \right], \tag{3.31}$$

$$= \frac{p_c}{T_s} \left(M - S_C \right), \tag{3.32}$$

and

$$TH_{nc} = \frac{p_{nc}}{T_s} \sum_{n=0}^{N} \left[N \sum_{m=0}^{M} \Pi_{m,n} - n \sum_{m=0}^{M} \Pi_{m,n} \right], \tag{3.33}$$

$$= \frac{p_{nc}}{T_s} \left[N \sum_{n=0}^{N} \sum_{m=0}^{M} \Pi_{m,n} - \sum_{n=0}^{N} n \sum_{m=0}^{M} \Pi_{m,n} \right], \tag{3.34}$$

$$= \frac{p_{nc}}{T_s} \left(N - S_{nc} \right). \tag{3.35}$$

□

Proposition 3.3.5 *The access delays of the transmitted packets of cooperative and non-cooperative users are given by*

$$D_c = 1 + \frac{S_c}{TH_c}, \tag{3.36}$$

$$D_{nc} = 1 + \frac{S_{nc}}{TH_{nc}}. \tag{3.37}$$

Proof According to Little's result [53], the average number of packets in a stationary system is equal to the average effective throughput multiplied by the average time that a packet spends in the system. Note that the actual number of packets in the system includes the backlogged packets and transmitted packets. Thus, the packet delays for both users are:

$$D_c = \frac{TH_c + S_c}{TH_c} = 1 + \frac{S_c}{TH_c}, \tag{3.38}$$

$$D_{nc} = \frac{TH_{nc} + S_{nc}}{TH_{nc}} = 1 + \frac{S_{nc}}{TH_{nc}}. \tag{3.39}$$

□

In order to accurately evaluate the system implementation, we should explore the performance of the backlogged packets. The next proposition gives the average throughput of backlogged users.

Proposition 3.3.6 *Consider the transition matrix P, where $P_{(i,j)(i',j')}$ is the transition probability from state (i,j) to state (i',j'). The average throughput of the backlogged packets transmitted by cooperative and non-cooperative users is given, respectively, as follows:*

$$BTH_c = \frac{1}{T_s} \sum_{m=0}^{M} \sum_{k=1}^{M-m} \sum_{n_2=0}^{N} \sum_{n_1=0}^{N} k \cdot P_{(m,n_1)(m+k,n_2)} \Pi_{m,n_1}, \tag{3.40}$$

$$BTH_{nc} = \frac{1}{T_s} \sum_{n=0}^{N} \sum_{k=1}^{N-n} \sum_{m_2=0}^{M} \sum_{m_1=0}^{M} k \cdot P_{(m_1,n)(m_2,n+k)} \Pi_{m_1,n}. \tag{3.41}$$

Proof In the stationary regime, the average number of backlogged packets that enter the system in a time slot T_s corresponds to the average number of packets that leave the system in the same time slot, thus the backlogged throughput. Furthermore, for a given system state (m, n_1), the probability that k backlogged packets corresponding to cooperative users enter the system, or equivalently, the probability that cooperative-users packets get backlogged is given by $P_{(m,n_1)(m+k,n_2)}$. Thus, the number of backlogged packets that enter the system at a given state (m, n_1) is $k \cdot P_{(m,n_1)(m+k,n_2)}$, where $k = 1, ..., M - m$.

Thus, by considering all possible states $n_1 \in \{0, ..., N\}$, $n_2 \in \{0, ..., N\}$, and $m \in \{0, ..., M\}$, we can obtain the expression (3.40). A similar approach can be used to derive the second equation of Proposition 3.3.6. □

Corollary 3.3.6.1 *Equations (3.40) and (3.41) can be expressed in terms of the average throughput leaving the system at the stationary regime. Thus, we can reformulate the two equations of Proposition 3.3.6 as follows:*

$$BTH_c = \frac{1}{T_s} \sum_{m=0}^{M} \sum_{n=0}^{N} P_c^b(m,n) \cdot \Pi_{m,n}, \tag{3.42}$$

$$BTH_{nc} = \frac{1}{T_s} \sum_{m=0}^{M} \sum_{n=0}^{N} P_{nc}^b(m,n) \cdot \Pi_{m,n}. \tag{3.43}$$

where

$$\begin{aligned} P_c^b(m,n) = & \sum_{i,k,l \in \mathbb{N}} Q_c(i,m) \cdot Q_c^r(1,m) \cdot Q_{nc}(k,n) \cdot Q_{nc}^r(l,n) \cdot \mathbb{1}_{\{i+k+l \leq 1\}} \\ & + 2 \cdot Q_c(0,m) \cdot Q_c^r(2,m) \cdot Q_{nc}(0,n) \cdot Q_{nc}^r(0,n), \end{aligned} \tag{3.44}$$

$$\begin{aligned} P_{nc}^b(m,n) = & \sum_{i,j,k \in \mathbb{N}} Q_c(i,m) \cdot Q_c^r(j,m) \cdot Q_{nc}(k,n) \cdot Q_{nc}^r(1,n) \cdot \mathbb{1}_{\{i+j+k \leq 1\}} \\ & + 2 \cdot Q_c(0,m) \cdot Q_c^r(0,m) \cdot Q_{nc}(0,n) \cdot Q_{nc}^r(2,n). \end{aligned} \tag{3.45}$$

Proof When either a cooperative or non-cooperative user transmits a backlogged packet, he will succeed if at most one other user transmits at the same time, which is given by the first term in equations (3.44), (3.45).

On the other hand, the second term of the previous equations comes from the fact that if two users simultaneously transmit their backlogged packets, they will all be successfully delivered thanks to ZigZag decoding. Finally, we can obtain the expression of the throughput of backlogged packets by normalizing by the time slot T_s and taking all the possible cases of M and N. □

Proposition 3.3.7 *The access delays of backlogged packets of cooperative and non-cooperative users are given by*

$$BD_c = 1 + \frac{S_c}{BTH_c}, \tag{3.46}$$

$$BD_{nc} = 1 + \frac{S_{nc}}{BTH_{nc}}. \tag{3.47}$$

Proof The average number of backlogged packets includes the packets in the system and the transmitted ones. Thus, by applying Little's result [53], we get the delays of backlogged packets as follows:

$$BD_c = \frac{BTH_c + S_c}{BTH_c} = 1 + \frac{S_c}{BTH_c},$$
$$BD_{nc} = \frac{BTH_{nc} + S_{nc}}{BTH_{nc}} = 1 + \frac{S_{nc}}{BTH_{nc}}.$$

□

3.4 Stochastic Game Formulation

To model the interaction between cooperative and selfish users, we define a finite stochastic game between a group of cooperative users $S_M := \{1, ..., M\}$ and a group of non-cooperative users $S_N := \{1, ..., N\}$. All users access a shared wireless channel using the SAZD mechanism. Furthermore, we consider that the group S_M plays a cooperative game with all users, and therefore they attempt to optimize the overall system's performance. Whereas each user in the group $S_N := \{1, ..., N\}$ attempts to optimize his own performance. We consider a game with incomplete information. Thus, even though all players know their total number in the game, they have no idea about each other's strategy.

We summarize the components of the game as follows:

- **Players:** The sets of cooperative and non-cooperative players are defined, respectively, as S_M and S_N. In what follows, we refer to the players as users.

- **Strategy space:** The set of strategies is the set of users' actions. For each user i, we define the set of pure strategies as $A_i = \{T, W\}$, where T represents the action "Transmit", and W is the action "Wait". Thus, at a given time slot, a user holding a packet can choose one action in A_i. Furthermore, we define the mixed strategies as the set of all the distributions over A_i, which is $\phi_i = \{q_c^i, 1 - q_c^i\}$ for a cooperative user i, and $\psi_j = \{q_{nc}^j, 1 - q_{nc}^j\}$ for a non-cooperative user j.

- **Utility:** The utility function corresponds to the user's level of satisfaction, which can be, in the case of our study, the average throughput, the access delay, or any other performance metric of interest. Let $u_i : \psi_i \times \psi_{-i} \rightarrow \mathbb{R}$ denote the utility function of user i in S_N. u_i depends on q_r^i the transmission probability of user i and the vector $q_r^{-i} = [q_r^1, q_r^2, ..., q_r^{i-1}, q_r^{i+1}, ...]$ of others' transmission probabilities. Thus, each non-cooperative user possesses his own utility function. On the other hand, let U_g be the common utility function of all cooperative users among the set S_M, which corresponds to the overall system performance.

- **Game information:** We assume that all players share a common knowledge, which is: the total number of players in the game, their own strategy space, and the strategy space of others, their utility, and the utility of others. On the other hand, we assume that cooperative players do not have the knowledge of the existence of selfish players among them. As a result, they behave cooperatively assuming that others will behave similarly. However, selfish users assume that everyone in the game is selfish, and therefore they behave selfishly.

In the mixed game defined in this chapter, cooperative users are interested in maximizing the overall utility function (e.g., the system throughput), whereas selfish users maximize their own utility functions.

3.4.1 Basic Assumptions

Assumption 1. *We assume that each player considers a symmetric strategy profile. Thus, he chooses his actions expecting that others will behave similarly.*

Assumption 2. *Cooperative players assume that everyone in the game is cooperating, whereas non-cooperative players assume that everyone is selfish. Therefore, we assume that cooperative players decide their actions based on the information they have about the game. Thus, since they assume that everyone in the game is cooperating (which is not always true since there may be some selfish players among them), they choose to cooperate expecting that others will do the same thing. Similarly, non-cooperative players decide to not cooperate due the information they have. Thus, they choose to act selfishly expecting that others will behave in a similar way.*

Cooperative players choose a strategy that optimizes the expected utility of the system, which is the joint utility of all players. As a result, the equilibrium profile of cooperative players is defined by the social optimally concept. On the other hand, non-cooperative players attempt to optimize their own utility function which leads them to the Nash equilibrium.

3.4.2 Characterization of the game equilibrium

The game equilibrium is a situation where all users are satisfied with their action choices, and no one is interested in deviating. In game theory, an equilibrium is usually characterized by a strategy profile where different users (players) choose different actions [76]. However, for simplicity purposes, we focus on the symmetric strategy profile (Ψ_c^*, Ψ_{nc}^*). Where Ψ_c^* is the strategy chosen by all cooperative users, and Ψ_{nc}^* is the strategy chosen by all non-cooperative users. Furthermore, we consider Markovian strategies that do not depend on past actions but only on the system state.

The equilibrium of the game can be obtained as a pair (Ψ_c^*, Ψ_{nc}^*), where Ψ_c^* is the social optimal for cooperative users and Ψ_{nc}^* is Nash equilibrium for non-cooperative game. The following theorem provides the conditions for the existence of the equilibrium.

Theorem 3.4.1 *The pair (Ψ_c^*, Ψ_{nc}^*) is an equilibrium of the game if it satisfies:*

$$i) \Psi_c^* \text{ maximizes the global utility } U_g(\Psi). \tag{3.48}$$

$$ii) \Psi_{nc}^* \in \underset{\Psi^i \in [\varepsilon,1]^2}{\operatorname{argmax}} \{u_i([\Psi_{nc}^*]^{-i}, \Psi^i)\}, \quad \forall i \in S_N, \quad \forall \varepsilon > 0. \tag{3.49}$$

Proof To prove the existence of an equilibrium profile, we should investigate the two games. First, let us consider the cooperative game where users of the set S_M attempt to maximize the overall system performance U_g. We emphasize that cooperative users are aware of the total number of users $M + N$. Besides, they assume that all users cooperate. Thus, the game from the point of view of users in S_M is a cooperative game of $M + N$ users.

Therefore, the equilibrium is given by the social optimality concept, which is defined by the following optimization problem:

$$\max_{\Psi \in [\varepsilon,1]^2} U_g(\Psi) \text{ subject to:}$$
$$\begin{cases} \Pi(\Psi) = \Pi(\Psi) \cdot P(\Psi), \\ \Pi_{m,n}(\Psi) \geq 0, \quad m = 0, ..., M, \quad n = 0, ..., N \\ \sum_{m=0}^{M} \sum_{n=0}^{N} \Pi_{m,n}(\Psi) = 1, \end{cases} \tag{3.50}$$

where $\Psi = [\psi, ..., \psi]$. and $\psi = (q_r, 1 - q_r)$

For any value $q_r \in [0, 1]$, the steady-state probabilities are continuous functions in $]0, 1]$. Therefore, a solution to the optimization problem (3.50) might not exist if we consider the non-closed interval $]0, 1]$. However, since we optimize on the closed interval $[\varepsilon, 1]$, an optimal solution exists.

Let us now consider the game from the point of view of a selfish user. Each user in the set S_N plays a non-cooperative game with all other users on the system, including users that choose to cooperate. Thus, selfish users assume that everyone is rational and attempt to optimize their own utility functions. Therefore, from the point of view of the set S_N, the game is a non-cooperative game of $M + N$ users. As a result, the equilibrium is obtained using the Nash concept, which satisfies for every user i in S_N the following condition:

$$u_i(\Psi^*) \geq u_i([\Psi^*]^{-i}, \Psi^i) \qquad \forall \psi^i \neq \psi^*, \tag{3.51}$$

where $\Psi_{nc} = \{\psi^*_{nc}, ..., \psi_i, ..., \psi^*_{nc}\}$, $\psi_i = (q^i_r, 1 - q^i_r)$ and $\psi^*_{nc} = (q^*_{nc}, 1 - q^*_{nc})$.

According to Nash theorem, a mixed-strategy Nash equilibrium exists since the game includes a finite number of users and actions.

Let us now consider the set $\mathcal{R}_i$ of the best response strategies of a user i in S_N.

$$\mathcal{R}_i = \underset{\Psi^i \in [\varepsilon,1]^2}{\text{argmax}}\{u_i(\Psi^{-i}, \Psi^i)\}, \tag{3.52}$$

$$= \{\Psi^i \in [\varepsilon, 1]^2 \quad / \quad u_i(\Psi) \leq u_i(\Psi^i), \quad \forall \Psi \in [\varepsilon, 1]^2\}. \tag{3.53}$$

We are interested in a symmetric equilibrium where all selfish users use the same strategy. Thus, we have

$$\Psi^*_{nc} \in \underset{\Psi^i \in [\varepsilon,1]^2}{\text{argmax}}\{u_i([\Psi^*_{nc}]^{-i}, \Psi^i)\}, \quad \forall i \in S_N, \quad \forall \varepsilon > 0. \tag{3.54}$$

□

Condition (3.49) means that Ψ^*_{nc} is the best strategy for user i given that others will play the same strategy.

Remark 3.4.2 *The proposed stochastic game model is a generalization of some models that have been proposed in the literature [57, 58, 59, 60, 61, 2]. In the special case of $N = 0$, the game corresponds to the pure cooperative game, and the case $M = 0$ is equivalent to a non-cooperative game model.*

3.5 Numerical Results

In this section, we present the numerical results and discuss the main findings of this study. The overall system throughput is taken as the utility function of cooperative users $U_g := TH_c$. Whereas the utility function of a single selfish user is the individual throughput.

We investigate and compare two game scenarios. First, we consider a network where the number of cooperative users exceeds the number of selfish users, $M = 3$ and $N = 2$. Then, in the second game scenario, we consider the opposite case where the number of selfish is $N = 3$ and the number of cooperative users is $M = 2$. In each scenario, we compare the performance of cooperative users and selfish users. Furthermore, we provide the performance of the overall system in each case. To maintain a fair channel condition, we set for all users the same arrival rate, i.e., $p_a = p_c = p_{nc}$. Finally, we take $\varepsilon = 10^{-4}$.

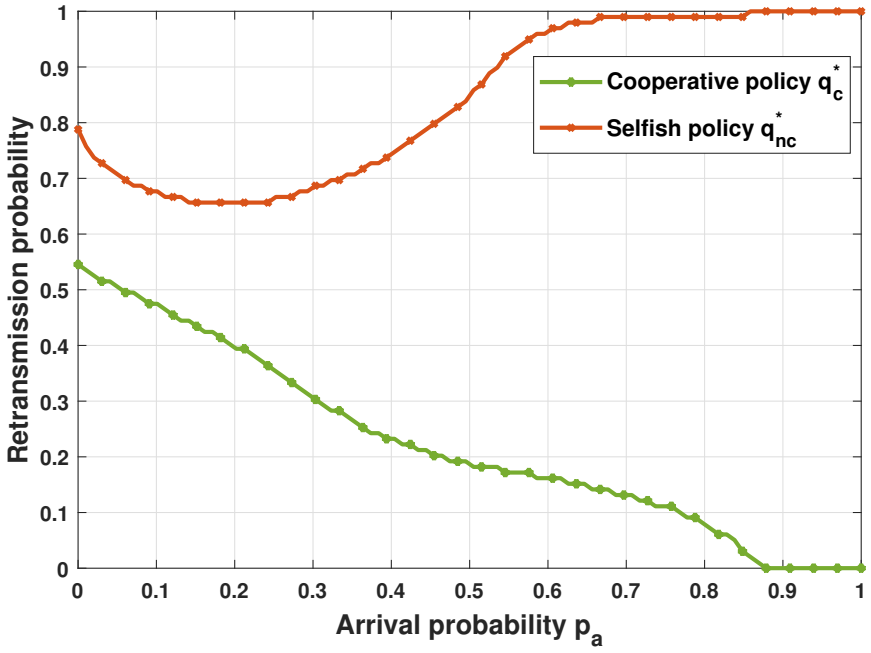

Figure 3.3: Retransmission policy for cooperative users and selfish users.

Figure 3.3 shows the game equilibrium $(\Psi_c^*, \Psi nc^*)$ as a function of the arrival rate p_a, where $\Psi_c^* = (q_c^*, 1 - q_c^*)$ and $\Psi nc^* = (q_{nc}^*, 1 - q_{nc}^*)$. The retransmission probabilities q_c^* and q_{nc}^* represent the optimal retransmission probability of cooperative and selfish users, respectively. The results show that selfish users access the wireless channel more aggressively than cooperative users.

Since the collision rate is meager, cooperative users use a high retransmission probability in light load conditions. However, as the arrival rate increases, they lower their retransmission rate to reduce network congestion. In contrast, selfish users transmit with high probability than cooperative users. Moreover, they increase the transmission rate even in the case of high load conditions. Even though this aggressive behavior is not suitable for any user, selfish users cannot unilaterally deviate from their retransmission strategy due to the rationality concept.

Assuming that all others will cooperate, a selfish user could improve his utility function by choosing to cooperate. However, if he cooperates while the others defect, he will be heavily penalized. Thus, in such a situation, selfish users prefer to defect since they do not know the strategy of others. This conflict situation is known in game theory as the prisoner dilemma. On the other hand, cooperative users assume that everyone is cooperating. Thus, they do not have any information about the existence of selfish users. Therefore, they play a cooperative game, assuming that everyone behaves similarly.

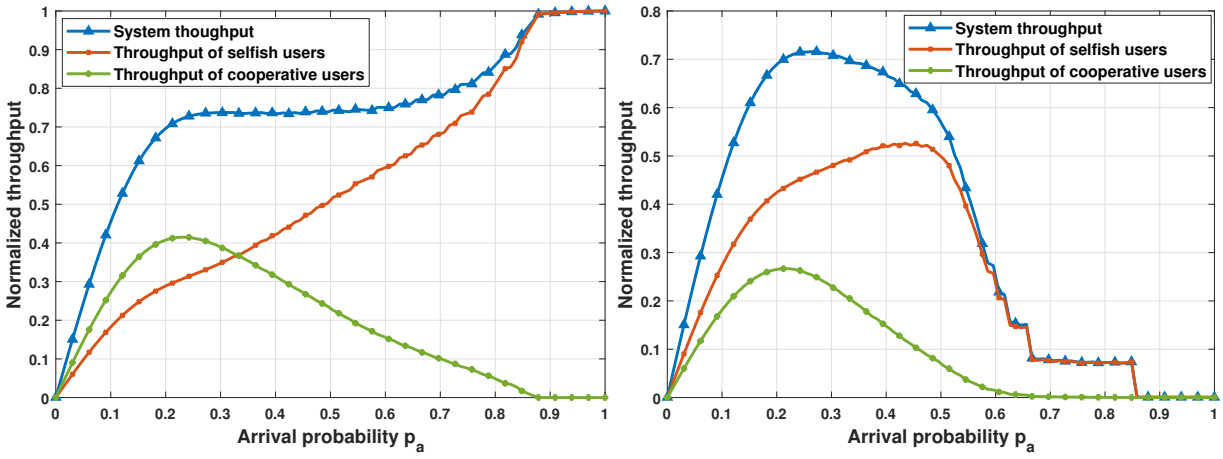

(a) $M = 3$, $N = 2$ (b) $M = 2$, $N = 3$

Figure 3.4: Normalized throughput for different retansmission policies. (a) cooperative users are more than selfish users, and (b) is the opposite case where selfish users are more than cooperative users.

In the following results, we present the performance metrics at the equilibrium, i.e., when the cooperative and selfish users use the retransmission probability q_c^* and q_{nc}^*, respectively. Figure 3.4 shows the throughput of cooperative and selfish users and also the global system throughput. Furthermore, we compare two scenarios: a) when the number of cooperative users exceeds the number of selfish users and b) when the number of selfish users is greater than the number of cooperative users.

Figure 3.4a shows that in light load conditions, cooperative users get higher throughput than selfish users. This is because both users use a high retransmission probability. Even though the retransmission probability of selfish users is slightly higher, its impact is not significant in light load conditions. Thus, due to the dominant number of cooperative users, their throughput is slightly higher than selfish users'. However, in high load conditions, selfish users get significantly better throughput since they transmit with higher probability and also because cooperative users lower their transmission probability, as seen from Figure 3.3. In very high load conditions $p_a \geq 0.88$, cooperative users stop the retransmission of backlogged packets while selfish users transmit at the highest probability. This aggressive behavior allows selfish users to dominate the overall system throughput.

From the above results, it seems that the aggressive behavior of selfish users is beneficial for the system, even if it is done at the expense of the performance of cooperative users. However, it is not always the case, as shown in Figure 3.4b where the number of selfish users dominates over the number of cooperative users. Figure 3.4b shows that selfish users always get better throughput, not only because of their dominant number but also because of their aggressive behavior. However, when $p_a \geq 0.5$, the system throughput drops considerably due to the collisions caused by the selfish

users.

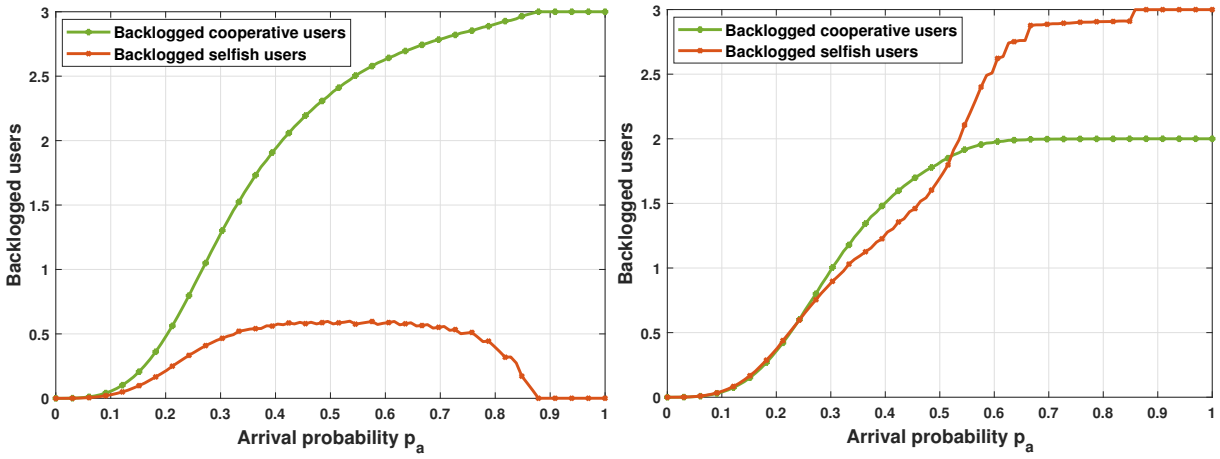

(a) $M = 3$, $N = 2$ (b) $M = 2$, $N = 3$

Figure 3.5: Number of backlogged users for different retansmission policies. (a) cooperative users are more than selfish users, and (b) is the opposite case where selfish users are more than cooperative users.

Figure 3.5 shows the number of backlogged users as a function of the arrival rate. In the first game scenario Figure 3.5a, the cooperative users get heavily penalized by the aggressive behavior of selfish users since the number of their backlogged packets grows more rapidly as the traffic load increases.

As for the selfish users, $\approx 30\%$ of them get backlogged when $p_a = 0.53$. Note that when $p_a \geq 0.88$, cooperative users refrain from transmitting their backlogged packets, refer to Figure 3.3, as a result they all get backlogged, see Figure 3.5a. Indeed, due to the high arrival rate, cooperative users stay silent to allow the newly arrived packets to access the channel without any disturbance. On the other hand, selfish users take advantage of the situation and access the channel with the highest probability, i.e., $q^*_{nc} = 1$, refer to Figure 3.3. Even in the presence of two selfish users, they get the maximum throughput thanks to the ZigZag decoding technique that decodes all their collided packets.

In the second game scenario Figure 3.5b, selfish users get penalized by their aggressive behavior more than cooperative users because they collide very often, especially in high load conditions.

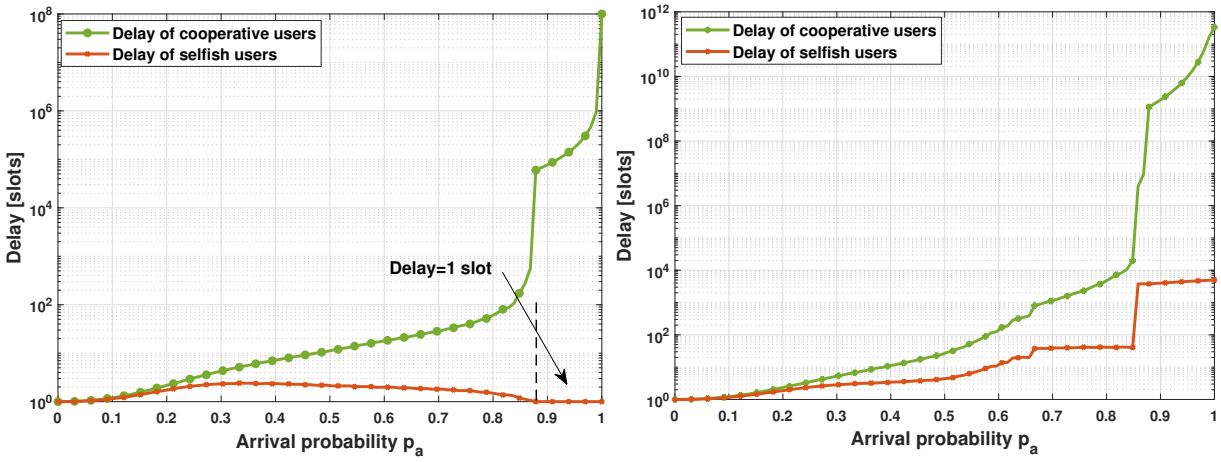

(a) $M = 3$, $N = 2$ (b) $M = 2$, $N = 3$

Figure 3.6: Delay of transmitted packets for different retansmission policies. (a) cooperative users are more than selfish users, and (b) is the opposite case where selfish users are more than cooperative users.

Figure 3.6 shows the access delay as a function of the arrival rate. The access delay represents the time in slots elapsed from the packet generating time and its successful transmission. The results show that the delay increases with the arrival rate. Furthermore, cooperative users exhibit the worst delay due to their low retransmission policy. For instance, under heavy load conditions, the delay reaches $9.99 \cdot 10^7$ and 10^8 slots in the first and second game scenarios, respectively. However, in the first game scenario, the delay of selfish users under the same load conditions is limited to 1 slot. That is to say, the selfish users are able to successfully transmit all their packets at the first attempt. On the other hand, selfish users get a considerably high delay of $5 \cdot 10^5$ slots in the second game scenario due to the increasing number of selfish users.

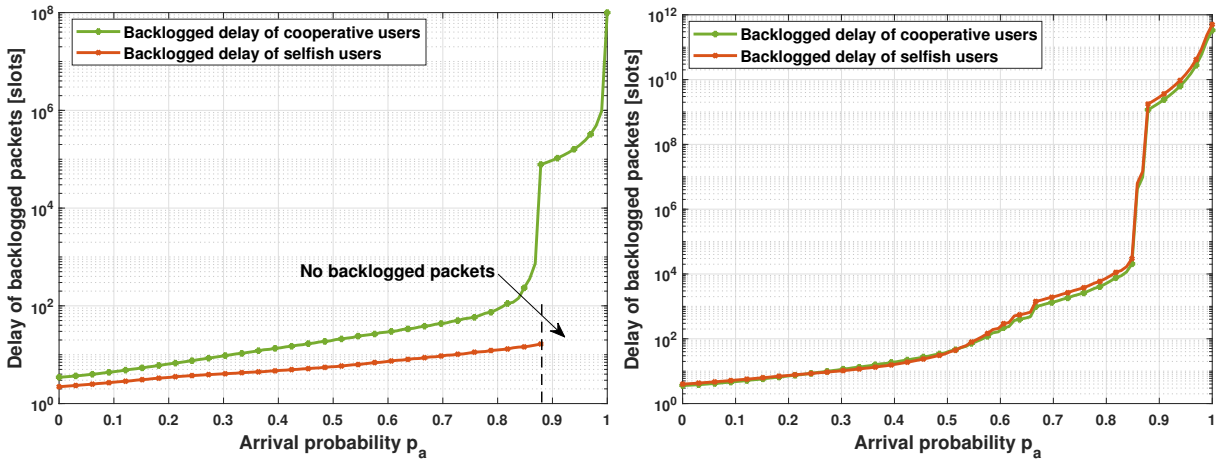

(a) $M = 3$, $N = 2$ (b) $M = 2$, $N = 3$

Figure 3.7: Delay of backlogged packets for different retansmission policies. (a) cooperative users are more than selfish users, and (b) is the opposite case where selfish users are more than cooperative users.

Figure 3.7 shows the delay of backlogged packets as a function of the arrival rate. Backlogged packets are the pending packets that went through a collision, and the ability to deliver backlogged packets is crucial for real-time traffics. Similar to the previous results, cooperative users have the worst delay. The first game scenario shows that backlogged packets get delayed more as the traffic load increases. However, as the arrival rate gets closer to 1, the backlogged packets of cooperative users become very large. In contrast, selfish users do not report any delay when $p_a \geq 0.88$ since they do not possess any backlogged packet, as shown in Figure 3.5a. On the other hand, both cooperative and selfish users suffer a longer delay when the load increases in the second game scenario (see Figure 3.7b). However, selfish users get slightly higher backlogged delay than cooperative users due to their number and exaggerated aggressive behavior.

The mathematical and numerical models in this study provide the basis for the performance analysis and protocol design of future generation wireless networks and protocols. With the ever increasing number of interconnected wireless devices, there is an increasing need of developing more robust protocols capable of limiting the impact of interference on the network performance. Furthermore, the lack of cooperation of even a single user may result in the malfunctioning of the overall network.

In order to illustrate the potential use of our models in the context of the research and development efforts of future telecommunications systems, let us consider a network of $M = 10$ and $N = 2$ users. Table 3.1 shows the results as a function of the arrival probability p_a. In the table, TH_c^i and TH_{nc}^i indicate the throughput of a cooperative user and a non-cooperative user, respectively. As seen from the table, as the arrival probability increases, selfish users get more aggressive and attempt accessing the shared wireless channel using the highest probability $q_{nc}^* = 0.9999$. In

contrast, the cooperative users lower their retransmission probability to avoid collisions and allow everyone to use the network resources. Under very heavy load conditions (i.e., $p_a \geq 0.9$), the cooperative users reduce drastically their retransmission probability q_c^* while the two selfish users can successfully transmit all their packets thanks to the use of the ZigZag scheme. In fact, the impact of the ZigZag scheme can be particularly seen on all the performance metrics under very high load conditions. The last two rows of the table show that the delay experienced by the traffic of the cooperative users experience increases by several orders of magnitude as all the cooperative users get their packets backlogged, $S_c = 10$.

On the contrary, the non-cooperative users benefit from the use of the ZigZag scheme by equally sharing the channel $TH_{nc}^j = 0.49$ and are able to transmit practically all their packets at their first attempt, $S_{nc} = 1.99 \times 10^{-3}$. The results also show that the collision probability resulting on packet losses reduces drastically to $P_{col} = 9.99 \times 10^{-4}$ as the packets of the two non-cooperative rarely collide with the packets of the cooperative users. Remember that by implementing the ZigZag code, the receiver may properly recover the information of up to two colliding packets. Even though the use of the ZigZag proves effective in improving the network's performance, it also raises some concerns on the dangers of the misuse of such features. As seen from our results, non-cooperative may take advantage of such decoding scheme. Therefore, further studies are required to explore the use of such scheme even in the presence of non-cooperative users. One possible line of research will be a dynamic implementation of such code by enabling and disabling its operation as a means to discourage non-cooperative users.

Table 3.1: Performance evaluation in the case of $M = 10$ and $N = 2$. P_{col} is the system collision probability, TH_c^i and TH_{nc}^j are the individual throughputs of a cooperative user i and a selfish user j, respectively.

		Cooperative user				**Non-cooperative user**			
$\mathbf{p_a}$	$\mathbf{P_{col}}$	$\mathbf{q_c^*}$	$\mathbf{TH_c^i}$	$\mathbf{D_c}$	$\mathbf{S_c}$	$\mathbf{q_{nc}^*}$	$\mathbf{TH_{nc}^j}$	$\mathbf{D_{nc}}$	$\mathbf{S_{nc}}$
0.0001	2.53×10^{-10}	4.14×10^{-1}	1.00×10^{-4}	1.00	1.50×10^{-9}	0.8787	1.00×10^{-4}	1.00	1.55×10^{-10}
0.1	2.14×10^{-1}	1.61×10^{-1}	5.29×10^{-2}	7.38	3.38	0.9999	7.21×10^{-2}	2.37	1.98×10^{-1}
0.2	2.64×10^{-1}	8.08×10^{-2}	4.21×10^{-2}	18.28	7.29	0.9999	1.30×10^{-1}	2.21	3.17×10^{-1}
0.3	3.05×10^{-1}	7.07×10^{-2}	3.26×10^{-2}	27.24	8.57	0.9999	1.70×10^{-1}	2.21	4.36×10^{-1}
0.4	3.11×10^{-1}	6.06×10^{-2}	2.52×10^{-2}	37.30	9.15	0.9999	2.20×10^{-1}	2.10	4.95×10^{-1}
0.5	3.47×10^{-1}	6.06×10^{-2}	1.88×10^{-2}	51.19	9.48	0.9999	2.50×10^{-1}	2.15	5.93×10^{-1}
0.6	3.25×10^{-1}	5.05×10^{-2}	1.37×10^{-2}	71.58	9.67	0.9999	3.00×10^{-1}	1.97	5.88×10^{-1}
0.7	2.92×10^{-1}	4.04×10^{-2}	9.02×10^{-3}	109.65	9.81	0.9999	3.40×10^{-1}	1.79	5.50×10^{-1}
0.8	2.44×10^{-1}	3.03×10^{-2}	4.85×10^{-3}	205.01	9.90	0.9999	3.90×10^{-1}	1.60	4.76×10^{-1}
0.9	9.99×10^{-4}	1.00×10^{-4}	1.14×10^{-5}	8.70×10^4	9.99	0.9999	4.97×10^{-1}	1.00	1.99×10^{-3}
0.9999	9.99×10^{-4}	1.00×10^{-4}	9.99×10^{-9}	1.00×10^8	10.00	0.9999	4.99×10^{-1}	1.00	1.99×10^{-3}

3.6 Conclusion

In this chapter, we have presented a novel stochastic game analysis that considers the existence of cooperative and selfish users in the same game and studies the interaction between them. First, the system state evolution is modeled using a bi-dimensional Markov chain in which we derived different performance metrics. Then, we constructed the proposed stochastic game using cooperative and non-cooperative game theories. Finally, we showed that the game ends at an equilibrium that combines the social optimality and the Nash concept. The chapter provided a comparative study between two game scenarios: 1) the case where the game consists mostly of cooperative users and 2) the opposite case where the game contains more selfish users. In each case, we highlighted the impact of the selfish behavior on the other users and on the overall system. Our results showed that the number of selfish users and the arrival rate significantly impact the system's performance. The proposed model provides a general framework that can be implemented in a wide range of application areas, such as resource management, network architecture, and protocol design.

Part II

Probabilistic Approach towards the Design of a Multicast MAC Mechanism for Video Communications over IEEE 802.11 Networks

Chapter 4

Performance Evaluation and Tuning of an IEEE 802.11 Audio Video Multicast Collision Prevention Mechanism: Saturated Conditions

Contents

4.1 Introduction

IEEE 802.11 Wireless Local Area Networks (WLANs) are the most widely implemented technology in the field of wireless access networks. The worldwide deployment IEEE 802.11-based hotspots, together with the increasing demand for audiovisual services, have spurred the need for enhancing the performance of the underlying channel access mechanisms while keeping downward compatibility with the basic principles of operation [77] [78].

Mobile audiovisual (A/V) traffic is forecast to grow by around 50 percent annually through 2022 to account for 75% of all mobile data traffic. Due to the stringent requirements of A/V services, namely, short delays, high throughput, and highly sensitive to losses [79], numerous enhancements to the original IEEE 802.11 Medium Access Control (MAC) mechanisms have been introduced. First, the IEEE 802.11e standard defined a multiple priority hierarchy whose highest priorities have been assigned to A/V services [80]. Thereafter, the IEEE 802.11aa amendment looked into the definition of multicast medium access mechanisms with an aim to respond to the stringent requirements of the A/V services and improve the channel utilization rate [81]. This latter amendment was motivated by the fact that numerous A/V applications will require the delivery to more than a single recipient at the time. Recently, the need for implementing broadcast services at hotspots has given birth to the ongoing work focusing on the definition of reliable and secured wireless multicast services [82, 34].

With the increasing demand for A/V multicast services, numerous schemes have been proposed in the literature to ensure the Quality-of-Service (QoS), and Quality-of-Experience (QoE) guarantees required by A/V applications [31, 83, 84]. However, the success of any new multicast MAC mechanism to be deployed will mainly depend on two operational requirements: 1) it should interwork with the legacy (unicast) Distributed Coordination Function (DCF) MAC mechanism; and 2) it should prove to enhance the key performance indicators of both, the network performance and the QoS delivered to the end-users [77].

In this chapter, we undertake the study of the Multicast Collision Prevention (MCP) mechanism, whose performance has been previously evaluated via simulation in [32]. The main goal of this work is to provide a framework allowing us to configure the MCP to guarantee the QoS requirements of A/V wireless multicast services. Towards this end, we develop a Markov Chain model to evaluate the mechanism operation under saturation conditions. This should allow us to determine the guaranteed capacity available for the multicast service as well as to evaluate the main performance metrics of both services, i.e., the multicast and unicast traffic. As shown in [85], a network operating below saturation traffic conditions will be able to deliver all the traffic while keeping the delay within reasonable limits. That is to say, obtaining the throughput under saturation load conditions allows us to determine the upper bounds of the available capacity allocated to the multicast service and the delay. Since our study considers the presence of unicast traffic, our results also provide us with the upper bounds of the allocated capacity and delay of the unicast service. Furthermore, we also undertake the tuning of the MCP mechanism taking into account the stringent requirement of the A/V multicast services.

The rest of this chapter is organized as follows. Section 4.2 highlights the relevance of the work undertaken within the framework of wireless communications. It first provides a general overview of the main activities in the area of wireless A/V services carried out by the IEEE working groups. It then describes the principles of operation of the MCP mechanism. In Section 4.3, we outline some recent works regarding the mathematical modeling of the DCF access mechanism for IEEE 802.11 WLANs. In section 4.4, we present the bi-dimensional Markov models of the MCP and DCF mechanisms. Section 4.5 defines the performance metrics of interest. Section 4.6

reports our numerical results and validates our model by simulations. In Section 4.7, we undertake the optimization of the main system parameter of the MCP mechanism and highlight the main implementation issues of our proposal. Section 4.8 summarizes and positions our main findings within the context of the latest efforts carried out by the IEEE 802.11 standards. Finally, Section 4.9 concludes the chapter.

4.2 Rationale

The main access mechanism in the IEEE 802.11 is the DCF mechanism, which is a random access mechanism based on Carrier Sense Multiple Access with Collision Avoidance (CSMA/CA) protocol. Another alternative method for accessing the channel is called Point Coordination Function (PCF), which has been developed to support applications requiring synchronous access to the medium and time-bounded delay. However, current commercial IEEE 802.11 interfaces do not implement the PCF protocol mechanism. Most efforts have therefore focused on developing QoS mechanisms around the basic principles of operation of the DCF protocol [77].

According to the DCF mechanism specifications, when a station becomes ready to transmit a frame, it has to first check the status of the channel before attempting to access the channel, i.e., whenever a station has a frame to transmit, it must sense the medium for a period of time equal to a Distributed Inter-Frame Space (DIFS). If the medium is sensed idle, it transmits. Otherwise, if the medium is found busy, the station must wait for the medium to be idle. Then, the station selects a random backoff value with uniform distribution in the range $[0, W_i - 1]$, $i \in \{1, ..., m\}$, where W_i is the contention window at the backoff stage i. Starting from $W_1 = CW_{\min}$, the contention window is doubled after each unsuccessfully transmission (up to $W_m = CW_{max}$). However, if the retransmission fails at the last backoff stage, the frame is discarded. In each backoff stage, the station transmits when its backoff counter expires. After each successful transmission, an Acknowledgment (ACK) is immediately transmitted by the destination station after a Short Inter-Frame Space (SIFS). Since SIFS is shorter than DIFS, no other station is able to detect the medium idle for DIFS. Therefore, all other stations have to wait for DIFS after the ACK to decrease backoff counters.

In the case when a station gets ready to transmit a unicast frame, it starts running the DCF mechanism previously described. Under this mechanism, immediately after sending a unicast frame, the sender waits for an acknowledgment. If no ACK is received, the station activates the backoff process to retransmit the unicast frame once again. Thus, the reliability of unicast transmission is guaranteed by the frame confirmation mechanism. However, in the case of a multicast frame, not such a mechanism has been included in the standard. Therefore, the reliability of the multicast traffic is considerably lower than the one provided to the unicast traffic. Indeed, the multicast mechanism only defines the equivalent of a single backoff stage of the unicast service. Unlike the unicast stations, a multicast station does not get a second chance to retransmit the data. The rationale behind the simplicity of the multicast access mechanism has mainly been based on avoiding the ACK implosion problem. However, the Quality of Service requirements of audio/video

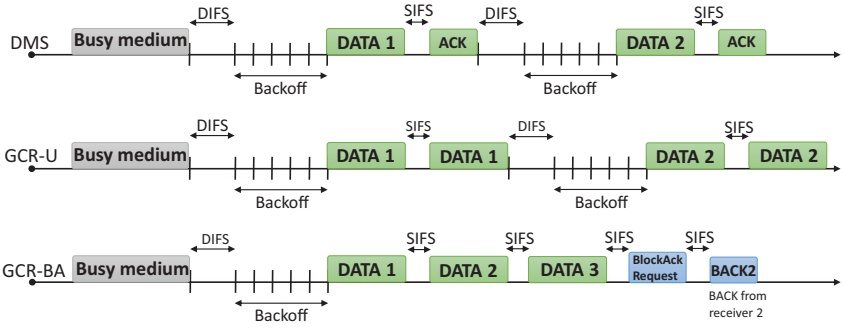

Figure 4.1: The IEEE 802.11aa amendment mechanisms

applications have spurred the interest in enhancing the reliability of the multicast MAC protocols.

4.2.1 The IEEE 802.11aa amendment

In 2012, the IEEE 802.11aa amendment introduced a set of multicast mechanisms for robust audio/video streaming while ensuring the coexistence with other types of traffic [81]. The IEEE 802.11aa amendment includes three different mechanisms: Directed Multicast Service (DMS), Groupcast with Unsolicited Retries (GCR-U), and Groupcast with Block ACK (GCR-BA).

Figure 4.1 depicts the operation mode of all three methods. As seen from the figure, all three proposed schemes follow the DCF mechanism, i.e., the multicast and unicast traffic follow the same principles. Under the DMS mechanism, the multicast sender transmits each and every frame to each one of the multicast receivers. Each receiver responds in turn by issuing an ACK frame. While DMS exhibits higher reliability than the legacy multicast mechanism, the amount of overhead and delay is highly dependent on the multicast group size. In fact, the DMS implements multicast services using the unicast service principles of operation. Under the GCR-U mechanism, a frame is transmitted U times, where U is an implementation-dependent parameter. The third mechanism, GCR-BA makes use of the Block ACK mechanism defined in the original IEEE 802.11 Standard. In this latter scheme, the sender sends several multicast frames and then polls one or several receivers for a confirmation, ACK. The number of frames transmitted before requesting a Block ACK is an implementation parameter. Despite numerous research studies, the benefits and effectiveness of the proposed multicast mechanisms for providing the QoS/QoE required by A/V are still an open issue [26].

Among the various research effort reported in the literature, the MCP mechanism originally introduced in [31] exhibits good QoS guarantees [32] and integrates into the IEEE 802.11 MAC operation principles. In this work, we develop a performance model and optimization study to properly tune-up the MCP system parameters. In the following, we first describe the MCP operation.

4.2.2 MCP overview

In this section, we outline the operation principles of the MCP mechanism developed in [31]. We consider the scenario given in Figure 4.2 in which a group of unicast senders (USs) is connected to a single Access Point (AP). Since the AP transmits unicast and multicast frames, two mechanisms have been implemented. The first one is used to serve unicast frames, and it operates as defined by the IEEE 802.11 Standard. The second is the MCP mechanism, which is implemented only at the AP. Both schemes follow the main principles of the DCF mechanism.

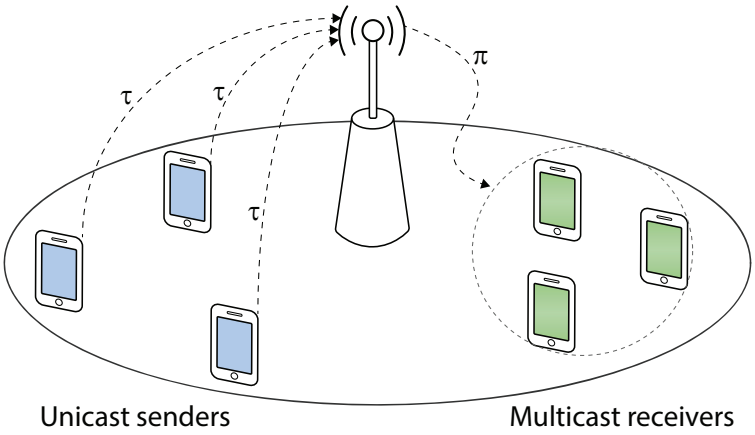

Figure 4.2: Scenario of the model, USs transmit with a probability τ using DCF mechanism and the AP transmit with a probability π using MCP mechanism

The operation of the MCP can be simply described as follows, see Figure 4.3. When the AP holds a multicast frame, it first selects a random backoff value with uniform distribution in the range $[0, W_1 - 1]$, i.e., similar to the first stage of DCF. However, the AP does not immediately transmit the multicast frame when the backoff expires. Instead, and in order to reduce the collision probability of the multicast frame with one or more unicast frames, the AP initializes a timer called *temp*, whose length is denoted by L. Then, it starts sensing the channel with the timer *temp* running. In this case, three events may arise:

1. **The AP receives a valid unicast frame.** When a US successfully transmits a unicast frame, the AP responds with an ACK after a period of SIFS. Then it starts the transmission of the multicast frame after a shorter waiting time denoted by Reduced Inter-Frame Space (RIFS [1]). Since RIFS is shorter than DIFS, no other station is able to transmit by detecting an idle period of DIFS. Thus, the multicast frame is transmitted successfully. In this case, the collision probability of the multicast frame is 0.

[1] In the original MCP proposal [31], the authors propose the use of a Point Inter- Frame Space (PIFS) period. However, in this work, we have preferred the use of the Reduced Inter-frame Space (RIFS) period, which was introduced in IEEE 802.11n.

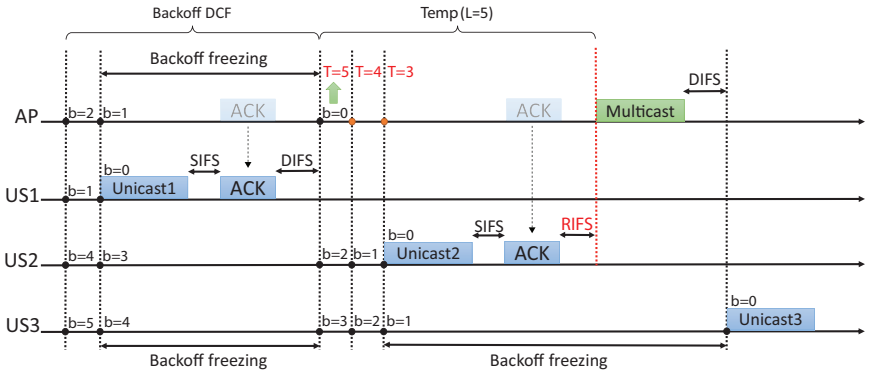

Figure 4.3: The multicast collision prevention mechanism

2. **The AP senses the medium busy.** When a collision occurs between two or more USs, the AP detects the medium busy. In this case, the AP behaves in the same way as in the previous event (1), i.e., once the medium becomes idle, it transmits the multicast frame after a period of RIFS.

3. **Channel idle** i.e., no unicast station transmits before *temp* expires. When no station attempts to transmit before the timer *temp* expires, i.e., the medium remains idle for L consecutive slots, the AP immediately starts the transmission of the multicast frame. In this case, the multicast frame may collide with other unicast frames transmitted exactly at the same time. The value of L should be set taking into account the delay and frame loss probability that the end-user application may tolerate.

4.3 Related Work

Since the introduction of the DCF mechanism, various amendments to the IEEE 802.11 Standard have been approved with an aim to provide the QoS guarantees required by numerous and diverse applications [79]. The approval of the various amendments has been spurred by the urgent need of provisioning the network protocol architecture with simple and efficient QoS mechanisms.

In 2012, the IEEE 802.11aa was released introducing various multicast mechanisms particularly, but not exclusively to support A/V applications [81]. Numerous analyses and experimental evaluations of the various mechanisms have since then been reported in the literature [86]. Despite the efforts conducted up to date, there is no consensus among the community on the benefits of implementing the various IEEE 802.11aa multicast mechanisms [26]. In fact, the debate is still open within the standards community actively seeking simple multicast mechanisms developed on top of the legacy DCF mechanism [34]. In order to validate the effectiveness of the amendments and numerous proposals, researchers have focused their efforts on developing probabilistic models.

Most previous research efforts on modeling the IEEE 802.11 DCF access mechanisms have been based on Discrete-Time Markov Chain (DTMC) models. Among them is the pioneering work of Bianchi [25], in which a bi-dimensional Markov chain was proposed with an infinite number of retransmission attempts. By computing the stationary distribution, the author provided the saturated throughput of the basic and Request-to-Send/Clear-to-Send (RTS/CTS) access mechanisms. This model has been reviewed and improved to better capture the performance of the access mechanisms.

Besides the works reported on the evaluation of IEEE 802.11 models [26][27], most works focus on the performance provided by IEEE 802.11 DCF networks to the unicast service. A few number of works considered the presence of unicast and multicast traffics. Indeed, the overall benefits of a multicast mechanism have to be evaluated taking into account the impact that this one may have on the unicast service. In [28], Oliveira et al. proposed an analytical model of the IEEE 802.11 legacy multicast mechanism in the presence of both unicast and multicast traffic under saturated conditions. They further extended their analysis to the unsaturated traffic condition [29, 30]. The authors assumed a single-hop network in which each station is able to transmit unicast and multicast traffic. This setup differs from the scenario considered herein, where the AP is the only station in charge of delivering multicast traffic.

In [31], Santos et al. introduced a simple multicast collision prevention mechanism. The authors showed that their proposal could properly coexist with the legacy DCF mechanism. The authors have further conducted a simulation-based performance study [32]. Despite confirming that their proposal is able to properly interoperate with legacy IEEE 802.11 mechanisms, they have not provided the configuration guidelines for guaranteeing the QoS requirements of A/V services.

Based on the results reported in the literature, including the IEEE 802.11aa amendment and the promising results of the MCP mechanism [32], we further explore its performance and potential integration into the IEEE 802.11 protocol architecture.

First, we start by developing a Markov Chain model of the MCP multicast mechanism. This novel model is used throughout our study to evaluate the performance of an AP implementing the unicast and multicast services. While the unicast service makes use of the IEEE 802.11 DCF mechanism, the multicast service is implemented using the MCP mechanism, see Figure 4.4. We also adapt the Markov model of the DCF introduced by Bianchi [25] to model a group of USs. While Bianchi's model does not consider a finite number of transmission attempts, our model follows the DCF mechanism specifications, i.e., a frame having exhausted the maximum number of transmission attempts is dropped.

Second, we make use of the developed models to evaluate the performance of a wireless network consisting of an AP supporting unicast and multicast services and a varying number of unicast stations. Our results verify the correct interoperation of the DCF and MCP mechanisms. We also include a comparison between the performance results reported by the legacy multicast MAC and MCP.

Third, we define an algorithm to optimize the operation of the MCP mechanism as a function of the number of active unicast stations, see Figure 4.4. Besides being able to guarantee a frame

loss rate meeting the requirements of the video services, our study aims to show that the MCP can be easily fine-tuned. This latter goal is of high relevance; the optimization of most multicast mechanisms introduced in the literature, including the IEEE 802.11aa amendments, is still an open issue [27].

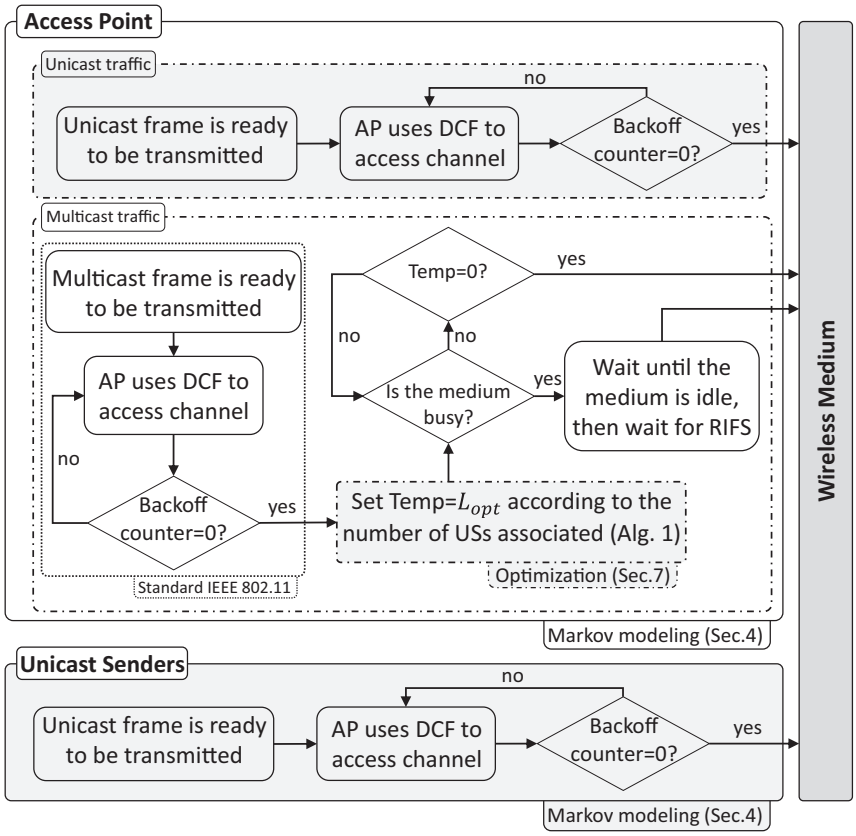

Figure 4.4: System architecture, workflow and main chapter contributions

4.4 Markov Model of the MCP Mechanism

4.4.1 Model assumptions

In this work, we consider the wireless network scenario shown in Figure 4.2 which consists of N USs and a group of Multicast Receivers (MRs) connected to a single AP. Each US transmits only unicast frames using the DCF mechanism. However, the AP is transmitting unicast and multicast frames using DCF and MCP mechanisms, respectively. The wireless channel is assumed ideal, i.e., all erroneously delivered frames are due to collisions. Furthermore, we assume that all stations operate in saturated conditions.

The system time is slotted into virtual time slots in which each slot is the time interval between two consecutive countdowns of backoff timers by non-transmitting stations. Hence, the length of the time slot is a random variable that depends on the transmission activities of all stations. For simplicity, we assume a constant frame payload size for unicast and multicast traffic. Although the time slot does not have the same length, the system time is synchronized between all nodes since they are in the coverage area of each other. This is why we shall consider the use of a discrete-time Markov chain in our analysis.

In order to predict the behavior of the AP, we propose a bi-dimensional Markov model incorporating unicast and multicast traffics. Then, we model the behavior of each US using a similar model to [25] where the collided frame in the last backoff stage is considered lost.

We assume that the AP can either transmit a unicast or a multicast frame at a given time slot. Let P_u and P_m be the probability that the AP starts the unicast and multicast frame backoff counter, respectively. For both types of frames, the value of the backoff process is initially set in the range $[0, CW_{\min} - 1]$ following a uniform random distribution. In the case of the unicast frame, the backoff counter is doubled upon an unsuccessful transmission up to a maximum value CW_{max}.

Following the MCP specifications, the AP does not transmit the multicast frame when its corresponding backoff counter expires. Instead, it sets a timer *temp* whose length is denoted by L and starts sensing the channel. Let W_0, W_1, and W_m denote $L+1$, $CW_{\min}$ and CW_{max}, respectively. The overall MCP backoff process of the multicast traffic can be simply stated as follows:

$$W_i = \begin{cases} W_1, & i = -1, \\ L + 1, & i = 0, \\ 2^{i-1} \cdot W_1, & i \in \{1, 2, ..., m\}. \end{cases} \tag{4.1}$$

4.4.2 Model description

We start by modeling the operation of the AP. The following theorem provides the description of the stochastic process of the backoff procedure of the AP.

Theorem 4.4.1 *For $P_m \in (0, 1)$, the stochastic process $\{(s(t), b(t)), t \in \mathbb{N}\}$ is a Markov process with a unique stationary distribution.*

Proof Let consider the stochastic process $(b(t))_{t\in\mathbb{N}}$ representing the backoff time counter of the AP at time slot t. According to the MCP specifications, the evolution of the system state follows discrete time. Thus, t and $t + 1$ refer to the beginning of two consecutive time slots. In our model, the backoff counter decrements at the beginning of the time slot.

Since the AP generates multicast and unicast traffics, the length of the backoff period depends on the transmission history of the unicast frame, i.e., the number of retransmission attempts the unicast frame has suffered. Moreover, it depends on the packet type held by the AP, i.e., unicast or multicast. As a result, the stochastic process $(b(t))_{t\in\mathbb{N}}$ is non-Markovian.

We define $s(t)$ as the stochastic process representing the backoff stages of the multicast and unicast frames.

$$s(t) = \begin{cases} -1 & \text{DCF stage for multicast frame,} \\ 0 & \textit{temp} \text{ stage for multicast frame,} \\ 1 & \text{first stage for unicast frame,} \\ \vdots & \\ m & \text{last stage for unicast frame.} \end{cases} \tag{4.2}$$

We can then model the bi-dimensional process $\{(s(t), b(t)),\ t \in \mathbb{N}\}$ as a discrete-time Markov chain depicted in Figure 4.5. The non-null one-step transition probabilities of the Markov chain are then expressed as follows:

$$\begin{cases} P\left((i,j+1),(i,j)\right) = 1, & i \in \{-1,1,...,m\},\ j \in \{0,...,W_i-2\}, \\ P((-1,0),(0,L)) = 1, & \\ P((i-1,0),(i,j)) = \frac{p_c}{W_i}, & i \in \{2,...,m\},\ j \in \{0,...,W_i-1\}, \\ P((i,0),(1,j)) = \frac{P_u(1-p_c)}{W_1}, & i \in \{1,...,m-1\},\ j \in \{0,...,W_1-1\}, \\ P((i,0),(-1,j)) = \frac{P_m(1-p_c)}{W_1}, & i \in \{1,...,m-1\},\ j \in \{0,...,W_1-1\}, \\ P((m,0),(1,j)) = \frac{P_u}{W_1}, & j \in \{0,...,W_1-1\}, \\ P((m,0),(-1,j)) = \frac{P_m}{W_1}, & j \in \{0,...,W_1-1\}, \\ P((0,l),(1,j)) = \frac{P_u(1-P_{idle})}{W_1}, & l \in \{1,...,L\},\ j \in \{0,...,W_1-1\}, \\ P((0,l),(-1,j)) = \frac{P_m(1-P_{idle})}{W_1}, & l \in \{1,...,L\},\ j \in \{0,...,W_1-1\}, \\ P((0,0),(-1,j)) = \frac{P_m}{W_1}, & j \in \{0,...,W_1-1\}, \\ P((0,0),(1,j)) = \frac{P_u}{W_1}, & j \in \{0,...,W_1-1\}. \end{cases} \tag{4.3}$$

By assuming $P_m = 0$ or $P_m = 1$, the Markov chain will result an absorbing sub-chain. Thus, we shall consider exclude the case of $P_m = 0$ or $P_m = 1$.

For $P_m \in (0,1)$, all states communicate with each other and the state space is finite. Therefore, the Markov chain is ergodic [53]. Thus, the steady-state probability exists, and it is unique. We denote by $\pi_{i,j}$ the probability that the packet held by the AP is in stage i, and in the backoff state j. We have

$$\pi_{i,j} = \lim_{t \to +\infty} P(s(t) = i, b(t) = j). \tag{4.4}$$

We can derive the expression of $\pi_{i,j}$ from the balance equations as follows

$$\begin{cases} \pi_{i,j} = \frac{W_i - j}{W_i} p_c^{i-1} \pi_{1,0}, & i = 1,...,m, \text{ and } j = 0,...,W_i - 1 \\ \pi_{0,j} = P_{idle}^{L-j} \frac{P_m}{P_u} \pi_{1,0}, & j = 0,...,L \\ \pi_{-1,j} = \frac{W_1 - j}{W_1} \cdot \frac{P_m}{P_u} \pi_{1,0}, & j = 0,...,W_1 - 1, \end{cases} \tag{4.5}$$

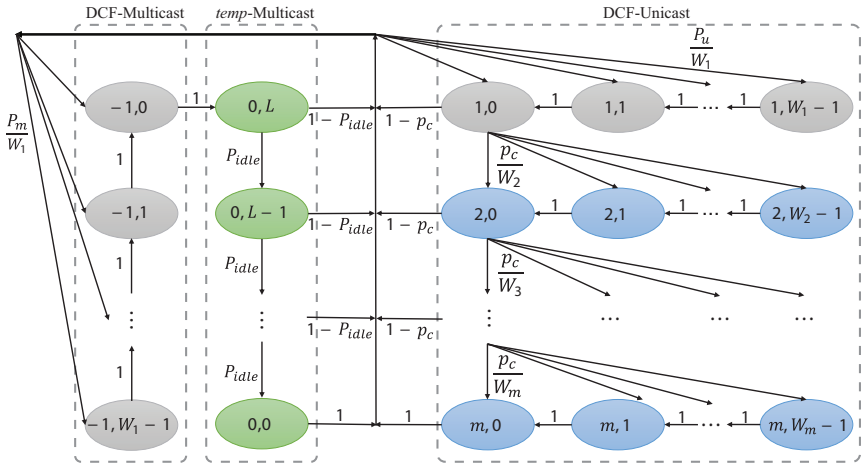

Figure 4.5: Markov chain model of the AP

where $\pi_{1,0}$ can be obtained from the normalization condition:

$$\sum_{i=-1}^{m} \sum_{j=0}^{W_i-1} \pi_{i,j} = 1. \tag{4.6}$$

□

Remark 4.4.2 *Since the Markov chain of the AP has an absorbing sub-chain for $P_m = 0$ and $P_m = 1$, we consider from now on that $P_m \in [\varepsilon, 1-\varepsilon]$, where $\varepsilon = 10^{-4}$.*

Let us now model the backoff process of a single US. The backoff process of a US is similar to the backoff process of the unicast frames of the AP. Hence, let $b'(t)$ be a random process representing the backoff counter in the time slot t, and let $s'(t)$ be the backoff stage. The Markov model of the US adopted here is similar to Bianchi's model [25]. However, unlike [25], we assume that the unicast frame is discarded when it collides at the last backoff stage. We adopt the same notation for the contention window and maximum backoff stage $W_1 = CW_{\min}$, $W_i = 2^{i-1}W_1$, $W_m = CW_{max}$. The process $\{s'(t), b'(t)\}$ can be then modeled using a DTMC, where the non-null one-step transition probabilities are given by

$$\begin{cases} P\left((i,j+1),(i,j)\right) = 1, & i \in \{1,...,m\},\ j \in \{0,...,W_i-2\}, \\ P\left((i,0),(1,j)\right) = \frac{1-q_c}{W_1}, & i \in \{1,...,m-1\},\ j \in \{0,...,W_1-1\}, \\ P\left((i-1,0),(i,j)\right) = \frac{q_c}{W_i}, & i \in \{2,...,m\},\ j \in \{0,...,W_i-1\}, \\ P\left((m,0),(1,j)\right) = \frac{1}{W_1}, & j \in \{0,...,W_1-1\}. \end{cases} \tag{4.7}$$

The Markov chain admits a unique steady-state distribution. Let $\tau_{i,j}$ denotes the probability that a packet held by a US is in stage i, and in the backoff state j. We have

$$\tau_{i,j} = \lim_{t\to\infty} P(s'(t) = i, b'(t) = j). \tag{4.8}$$

After computing the balance equation equations of the Markov chain, we can get the expression of $\tau_{i,j}$ as follows

$$\tau_{i,j} = \frac{W_i - j}{W_i} q_c^{i-1} \tau_{1,0}, \qquad i = 1, ..., m, \text{ and } j = 0, 1, ..., W_i - 1, \tag{4.9}$$

where $\tau_{1,0}$ can be derived from the normalization condition:

$$\sum_{i=1}^{m} \sum_{j=0}^{W_i-1} \tau_{i,j} = 1. \tag{4.10}$$

Remark 4.4.3 *Note that the transition probabilities are expressed in the short notation, such that*

$$P\left((i,j),\left(i',j'\right)\right) = P\left(s\left(t+1\right) = i', b\left(t+1\right) = j' \mid s\left(t\right) = i, b\left(t\right) = j\right). \tag{4.11}$$

4.4.3 Model probabilities

Let p_c be the probability that a unicast frame transmitted by the AP collides, and let q_c be the collision probability of unicast frame transmitted by the US. We define P_{idle} to be the probability that the AP meets an idle slot when sensing the channel. Obviously, we have $P_{idle} = 1 - p_c$. We define the probability that the AP transmits in a given time slot by

$$\pi = \pi^u + \pi^m, \tag{4.12}$$

where π^u (resp. π^m) is the probability that the AP transmits unicast (resp. multicast) frame. We have

$$\pi^u = \sum_{i=1}^{m} \pi_{i,0} = \frac{1 - p_c^m}{1 - p_c} \pi_{1,0}, \tag{4.13}$$

$$\pi^m = (1 - P_{idle}) \sum_{j=1}^{L} \pi_{0,j} + \pi_{0,0} = \frac{P_m}{P_u} \pi_{1,0}. \tag{4.14}$$

The transmission probability of a US is given by

$$\tau = \sum_{i=1}^{m} \tau_{i,0} = \frac{1 - q_c^m}{1 - q_c} \tau_{1,0}. \tag{4.15}$$

The probabilities p_c and q_c is then given by

$$p_c = 1 - (1-\tau)^N, \tag{4.16}$$

$$q_c = 1 - (1-\tau)^{N-1}\left(1 - \pi_{0,0} - \pi^u\right). \tag{4.17}$$

$\pi_{1,0}$ and $\tau_{1,0}$ are obtained using the normalization condition.

$$\pi_{1,0} = \left(\frac{P_m}{P_u}\left[\sum_{j=0}^{W_1-1}\frac{W_1-j}{W_1} + \sum_{j=0}^{L} P_{idle}^{L-j}\right] + \sum_{i=1}^{m}\sum_{j=0}^{W_i-1}\frac{W_i-j}{W_i}p_c^{i-1}\right)^{-1}, \tag{4.18}$$

$$\tau_{1,0} = \left(\sum_{i=1}^{m}\frac{W_i+1}{2}q_c^{i-1}\right)^{-1}. \tag{4.19}$$

Equations (4.12), (4.15), (4.16), (4.17), (4.18) and (4.19) form a non-linear system with six unknowns π, τ, p_c, q_c, $\pi_{1,0}$ and $\tau_{1,0}$. This non-linear system has a unique solution and can be numerically solved using MATLAB.

4.5 Performance Metrics

Based on the model introduced in the previous section, we define the three main performance metrics of interest for both: the multicast and the unicast traffics. We define the throughput of each station as the number of successful transmission attempts per the total number of transmission attempts, i.e., the ratio of successful transmissions.

Proposition 4.5.1 *The unicast and multicast throughput of the AP, and the unicast throughput of a US are given as follows*

$$S_{AP}^u = (1-\tau)^N, \tag{4.20}$$

$$S_{AP}^m = \frac{(1-P_{idle})\sum_{j=1}^{L}\pi_{0,j} + (1-\tau)^N\pi_{0,0}}{\pi^m}, \tag{4.21}$$

$$S_{US} = (1-\tau)^{N-1}(1-\pi_{0,0}-\pi^u). \tag{4.22}$$

Proof The AP can transmit a unicast frame when its backoff counter expires, i.e., in state $(i,0)$, where $i = 1, ..., m$. Thus, the total number of transmissions attempts can be derived as follows

$$\sum_{i=1}^{m}\pi_{i,0} = \frac{1-p_c^m}{1-p_c}\cdot\pi_{1,0} = \pi^u. \tag{4.23}$$

On the other hand, a unicast frame transmitted by the AP succeeds if none of the N USs transmits at the same time slot. Therefore, the number of successful transmissions is

$$\pi^u(1-\tau)^N.$$

Thus, the throughput can be derived as the number of successful transmissions over the total number of transmission attempts.

$$S_{AP}^{u} = \frac{\pi^{u}(1-\tau)^{N}}{\pi^{u}} = (1-\tau)^{N}. \tag{4.24}$$

Let us now consider the multicast traffic. The AP can successfully transmit a multicast frame when the timer *temp* is activated, and at least one US transmit before it expires. Otherwise, if the timer expires, the multicast frame will be successfully transmitted if no US transmit. Thus, the number of successful transmissions is

$$(1-P_{idle})\sum_{j=1}^{L}\pi_{0,j} + (1-\tau)^{N}\pi_{0,0}.$$

The total number of multicast transmission attempts can be derived in a similar way as follows

$$(1-P_{idle})\sum_{j=1}^{L}\pi_{0,j} + \pi_{0,0} = \pi^{m}. \tag{4.25}$$

Thus, the multicast throughput can be derived as the number of successful transmission attempts over the total number of transmissions.

$$S_{AP}^{m} = \frac{(1-P_{idle})\sum_{j=1}^{L}\pi_{0,j} + (1-\tau)^{N}\pi_{0,0}}{\pi^{m}}. \tag{4.26}$$

The unicast and multicast frames within the AP cannot collide since they are sent separately by the same station. However, unicast frames of a US can collide with multicast and unicast frames transmitted by the AP when they are sent at the same time slot. Besides, USs can collide with each other. Therefore, a given US can successfully transmit its packet if no one in the remaining $N-1$ USs transmit, and the AP does not transmit. Thus, the number of successful transmissions can be derived as follows

$$\tau(1-\tau)^{N-1}(1-\pi_{0,0}-\pi^{u}).$$

The total number of transmissions can be derived in similar way as for the AP.

$$\tau = \sum_{i=1}^{m}\tau_{i,0}. \tag{4.27}$$

The throughput can then be derived as follows:

$$S_{US} = \frac{\tau(1-\tau)^{N-1}(1-\pi_{0,0}-\pi^{u})}{\tau}, \tag{4.28}$$

$$= (1-\tau)^{N-1}(1-\pi_{0,0}-\pi^{u}). \tag{4.29}$$

□

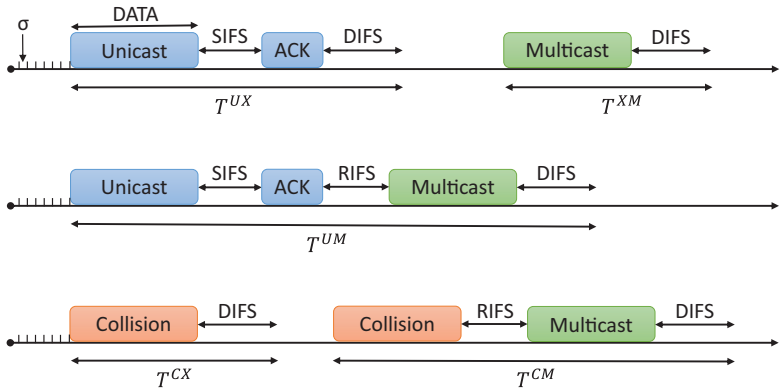

Figure 4.6: Slot time for MCP access mechanism, σ is the duration of an empty slot

4.5.1 Medium access delay

The medium access delay is computed from the instant when the frame arrives at the head of the line until it is successfully transmitted. To compute this delay, let's analyze the system timeline. The following events summarise what can happen in a randomly chosen time slot.

- Idle: no station attempts to transmit,
- UX: successful transmitted unicast frame followed by non-multicast frame,
- UM: successful transmitted unicast frame followed by a multicast frame,
- CX: a collision followed by a non-multicast frame,
- CM: a collision followed by multicast frame,
- XM: an idle slot followed by a multicast frame.

The length of a given time slot is then a random value that depends on the stations' transmission activities. As illustrated in Figure 4.6, we define the time slot length of the events above as follows:

$$\begin{aligned} T^{UX} &= \text{DATA+SIFS+ACK+DIFS+}2\delta, \\ T^{UM} &= 2\cdot\text{DATA+SIFS+ACK+RIFS+DIFS+}3\delta, \\ T^{CX} &= \text{DATA+DIFS+}\delta, \\ T^{CM} &= \text{DATA+RIFS+DATA+DIFS+}2\delta, \\ T^{XM} &= \text{DATA+DIFS+}\delta, \end{aligned} \tag{4.30}$$

where δ denotes the propagation delay.

Let's first compute the delay of unicast frames transmitted by the AP. When the AP is holding a frame, either unicast or multicast, the transition time to the next backoff state depends on the activities of the N USs. Thus, three events may happen, either idle slot, successful transmission

of one US, or collision between two or more USs. The probabilities of these three events are given respectively by P_{idle}, P_s^{us}, P_c^{us}. The average transition time to the next backoff state is then

$$E[slot_{AP}] = P_{idle}\sigma + P_s^{us}T^{UX} + P_c^{us}T^{CX}, \tag{4.31}$$

where σ is the duration of a idle slot and

$$P_s^{us} = N\tau(1-\tau)^{N-1}, \tag{4.32}$$
$$P_c^{us} = 1 - P_s^{us} - P_{idle}. \tag{4.33}$$

Let T_k be the average delay in a given backoff stage k.

$$T_k = E[X_k] \cdot E[slot_{AP}] + T^{UX}, \tag{4.34}$$

where $E[X_k]$ is the average number of backoff slots at the backoff stage k and it is given by

$$E[X_k] = \frac{W_k - 1}{2}. \tag{4.35}$$

$E[slot_{AP}]$ as already defined is the average transition time to the next backoff state from the AP point of view. Note that the time experienced by the unicast frame at each backoff stage (either collided or not) includes the ACK.

Let Y be the random variable representing the number of unicast transmission attempts of the AP. Y follows a geometric distribution with success probability $(1-p_c)$. Therefore, the probability that the frame is transmitted successfully at the i^{th} stage is:

$$P(Y = i) = p_c^{i-1}(1 - p_c). \tag{4.36}$$

Hence, the total delay reported for the unicast frame is the sum of the delay from the first stage to the stage i, given that the frame is transmitted successfully at i^{th} stage. Thus we have

$$D_u^{AP} = \sum_{i=1}^{m} \frac{P(Y=i)}{1-p_c^m} \cdot \sum_{k=1}^{i} \left(\frac{W_k - 1}{2} \cdot E[slot_{AP}] + T^{UX} \right). \tag{4.37}$$

In order to estimate the multicast traffic delay, we should first get the average delay in the states $(-1, j),\ j \in \{0, ..., W_1 - 1\}$ corresponding to the DCF process of the multicast frame.

$$T_{DCF} = \frac{W_1 - 1}{2} \cdot E[slot_{AP}]. \tag{4.38}$$

Similarly, the number of idle slots the multicast frame has to wait in the stage *temp* follows a geometric distribution with success probability $(1 - P_{idle})$. Thus, the average delay in the *temp* stage is

$$T_{temp} = \sum_{k=0}^{L-1} P_{idle}^k \cdot \left[(1 - P_{idle})k\sigma + P_s^{us}T^{UM} + P_c^{us}T^{CM} \right] + P_{idle}^L \left(L\sigma + T^{XM} \right). \tag{4.39}$$

Finally, the average delay of a multicast frame is obtained as the total time elapsed in the DCF process and the *temp* stage.

$$D_m^{AP} = T_{DCF} + T_{temp}. \tag{4.40}$$

Now, let's find the delay of unicast frames transmitted by the USs. Unlike the AP, the average transition time to the next backoff state from the point of view of a unicast sender depends on the activity of the AP and $(N-1)$ remaining USs. Therefore, one of the six events {idle, UX, UM, CX, CM, XM} discussed above may happen. We define the probabilities of these events respectively as follows

$$P_{us}^{idle} = (1-\tau)^{N-1}(1-\pi_{0,0}-\pi^u), \tag{4.41}$$

$$P_{us}^{UX} = \pi^u(1-\tau)^{N-1} + (N-1)\tau(1-\tau)^{N-2}\left(1-\pi^u-\sum_{j=0}^{L}\pi_{0,j}\right), \tag{4.42}$$

$$P_{us}^{UM} = (N-1)\tau(1-\tau)^{N-2}\sum_{j=1}^{L}\pi_{0,j}, \tag{4.43}$$

$$P_{us}^{CX} = (N-1)\tau(1-\tau)^{N-2}(\pi_{0,0}+\pi^u) + \sum_{i=2}^{N-1}\binom{N-1}{i}\tau^i(1-\tau)^{N-1-i}\left(1-\sum_{j=1}^{L}\pi_{0,j}\right), \tag{4.44}$$

$$P_{us}^{CM} = \sum_{i=2}^{N-1}\binom{N-1}{i}\tau^i(1-\tau)^{N-1-i}\cdot\sum_{j=1}^{L}\pi_{0,j}, \tag{4.45}$$

$$P_{us}^{XM} = (1-\tau)^{N-1}\pi_{0,0}. \tag{4.46}$$

Since one of these events may happen in a given time slot, we have

$$P_{us}^{\sigma} + P_{us}^{UX} + P_{us}^{UM} + P_{us}^{CX} + P_{us}^{CM} + P_{us}^{XM} = 1. \tag{4.47}$$

The average transition time to the next backoff state is then given by

$$E[slot_{US}] = P_{us}^{\sigma}\sigma + P_{us}^{UX}T^{UX} + P_{us}^{UM}T^{UM} + P_{us}^{CX}T^{CX} + P_{us}^{CM}T^{CM} + P_{us}^{XM}T^{XM}. \tag{4.48}$$

Similarly, the number of transmission attempts for a single US follows a geometric distribution with success probability $(1-q_c)$, given the collision probability q_c. The delay of the frames transmitted by USs is then given by

$$D^{us} = \sum_{i=1}^{m}\frac{q_c^{i-1}(1-q_c)}{1-q_c^m}\cdot\left[\sum_{k=1}^{i}\left(\frac{W_k-1}{2}\cdot E[slot_{US}] + T^{UX}\right)\right]. \tag{4.49}$$

Thus, we have proved the following proposition

Proposition 4.5.2 *The unicast and multicast delay of the AP, and the unicast delay of a US are given as follows*

$$D_u^{AP} = \sum_{i=1}^{m} \frac{P(Y=i)}{1-p_c^m} \cdot \left[\sum_{k=1}^{i} \left(\frac{W_k - 1}{2} \cdot E[slot_{AP}] + T^{UX} \right) \right], \tag{4.50}$$

$$D_m^{AP} = T_{DCF} + T_{temp}, \tag{4.51}$$

$$D^{us} = \sum_{i=1}^{m} \frac{q_c^{i-1}(1-q_c)}{1-q_c^m} \cdot \left[\sum_{k=1}^{i} \left(\frac{W_k - 1}{2} \cdot E[slot_{US}] + T^{UX} \right) \right]. \tag{4.52}$$

Proposition 4.5.3 *The unicast and multicast loss probability of the AP, and the unicast loss probability of a US are given as follows*

$$P_{lossU}^{AP} = \frac{\pi_{m,0}\,(1-P_{idle})}{\pi^u}, \tag{4.53}$$

$$P_{lossM} = \frac{\pi_{0,0}(1-P_{idle})}{\pi^m}, \tag{4.54}$$

$$P_{lossU}^{US} = \frac{\tau_{m,0} \cdot \left(1-(1-\tau)^{N-1}\,(1-\pi_{0,0}-\pi^u)\right)}{\tau}. \tag{4.55}$$

Proof The frame loss probability is given as the number of failed transmissions over the total number of transmission attempts. The AP can lose a unicast frame when it reaches the last backoff stage $(m, 0)$ and collides with other frames transmitted at the same time slot. Thus, we have

$$P_{lossU}^{AP} = \frac{\pi_{m,0}\,(1-P_{idle})}{\pi^u}, \tag{4.56}$$

where π^u is the total number of unicast transmissions attempts by the AP. P_{idle} is the probability that the AP senses an idle slot, or equivalently, the probability that no US transmit, which is given by

$$P_{idle} = 1 - p_c = (1-\tau)^N. \tag{4.57}$$

However, the AP can lose a multicast frame when the timer temp expires and at least one of the N USs transmits at the same time slot. We have then

$$P_{lossM} = \frac{\pi_{0,0}(1-P_{idle})}{\pi^m}. \tag{4.58}$$

On the other hand, a given US can lose a packet when it reaches the last backoff stage $(m, 0)$ and at least one of the other stations (i.e., AP and $N-1$ USs) transmits at the same time slot. Then, we have

$$P_{lossU}^{US} = \frac{\tau_{m,0} \cdot \left(1-(1-\tau)^{N-1}\,(1-\pi_{0,0}-\pi^u)\right)}{\tau}. \tag{4.59}$$

□

4.6 Numerical Results

Table 4.1: MCP and DCF parameters used in simulations and numerical analysis

Parameter	Value	Parameter	Value
DATA	8192 bits	Propagation delay δ	$2\,\mu s$
SIFS	$10\,\mu s$	Slot time σ	$20\,\mu s$
DIFS	$50\,\mu s$	W_1	32
RIFS	$30\,\mu s$	Backoff stages m	5
ACK	304 bits	Probability of multicast P_m	$1-\varepsilon$
Data rate	1 Mbps	L length of "temp" in slots	0, 8, 16, 32

In this section, we present the analytical and simulation results of the proposed mechanism in different scenarios. The simulation study was carried out using a custom-made Matlab simulator. Table 4.1 lists the numerical parameters used in our evaluations. In order to accurately capture the performance of the system, we set the simulation time to $10^9\,\mu s$, and we run our simulation 100 times.

To validate our model accuracy, we compare the analytical results with the ones obtained from our simulations. Our analysis also includes a comparative evaluation of the results reported by the legacy IEEE 802.11 multicast mechanism and MCP. The comparison should allow us to quantify the expected performance improvements in terms of all the performance metrics of interest.

Another main goal of our study is to properly configure the MCP system parameter L, taking into account the QoS requirements of audiovisual applications. Furthermore, we should evaluate the impact that L may have on the performance of the unicast traffic. In this way, we should be able to show that MCP can operate side to side with IEEE 802.11-compliant stations, i.e., making use of the legacy unicast DCF mechanism.

In our analysis, three metrics are examined: throughput, delay, and frame loss probability. We start by presenting the normalized throughput of unicast and multicast traffics. Then, we show the delay and the frame loss probability of both traffics. We assume that the AP generates only multicast frames (i.e., $P_m = 1-\varepsilon$), and all the USs transmit unicast frames. Thus, collisions may occur either between two or more unicast frames or between multicast and unicast frames. The frame size and parameter values used in the analysis are shown in Table 4.1. In order to get a better insight into the impact of the parameter L, we propose to compare the MCP mechanism using different values of L with the standard IEEE 802.11.

Figure 4.7a shows the normalized throughput of multicast traffic obtained as the ratio of successful transmissions over the total number of transmissions. For the standard IEEE 802.11 (i.e., MCP with $L = 0$), we observe that the multicast throughput decreases as the number of USs increases. This is mainly due to the growing number of collisions involving multicast and unicast frames. However, as we increase the parameter L, we can significantly improve the multicast throughput. In fact, $L = k$ means that the multicast frames could benefit from one of k opportunities to be transmitted without colliding with unicast frames, providing that at least one US attempts to

transmit before the timer *temp* expires. In this case (i.e., when *temp* expires), the multicast frame may collide with other unicast frames transmitted exactly at the same time. Moreover, we observe for $L < 10$ that the multicast throughput first decreases and then increases with the number of USs increases. Indeed, since the length L of the timer *temp* is small, the probability of losing the multicast frame becomes larger as we increase the number of USs. However, when the number of USs increases, there is a high probability of transmitting the multicast frame before the timer *temp* expires, which explains the increase in the multicast throughput.

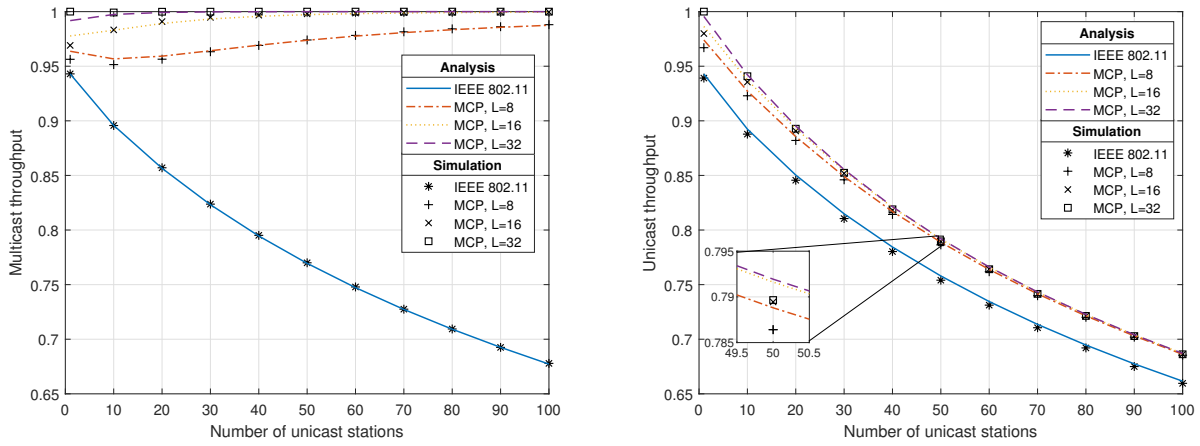

(a) Throughput of multicast frames transmitted by the AP using MCP mechanism, for different values of $L \in \{0, 8, 16, 32\}$.

(b) Throughput of unicast frames transmitted by the USs.

Figure 4.7: Throughput of unicast and multicast.

In Figure 4.7b, we show the impact of the parameter L on the unicast throughput. We can see a slight increase in the unicast throughput as the L increases. This result clearly shows the benefits of reducing the collision involving multicast frames. However, as expected, the unicast throughput decreases as the number of USs increases.

Figure 4.8a shows the delay of multicast frames for different values of L. The results show that the delay increases when L increases, which is expected since the multicast frame will wait for an extra period of time after the backoff process, defined by the timer *temp*. However, the multicast delay is influenced more by the number of USs. This is mainly due to the backoff freezing experienced by the multicast frame in the backoff process. In fact, the backoff counter is stopped whenever the medium is sensed as busy.

Similarly, as shown in Figure 4.8b, the delay of unicast frames is also increasing as the number of USs increases due to the backoff freezing. However, since unicast frames pass through more backoff stages, the unicast delay is shown to be greater than the multicast delay. On the other hand, we observe that the unicast delay is increased as L increases. In fact, as L gets larger, multicast frames

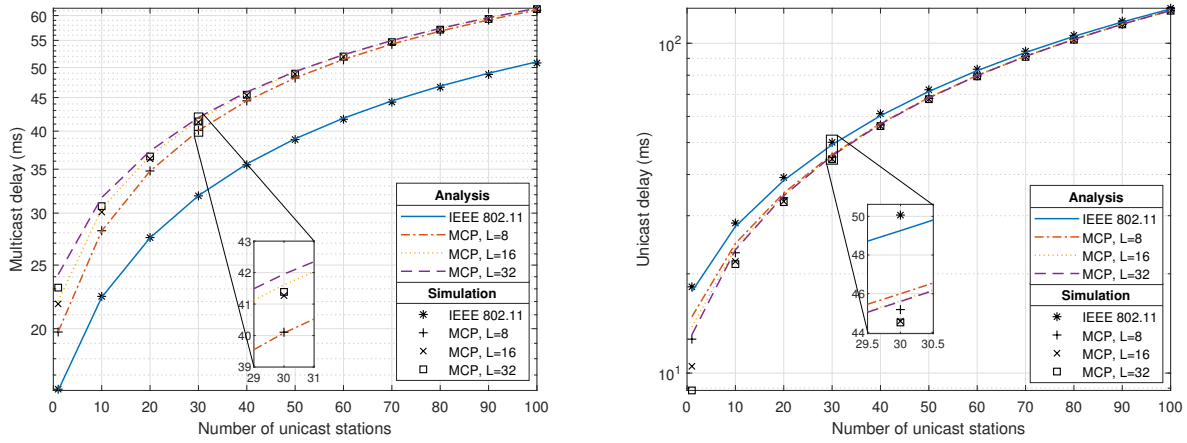

(a) Delay of multicast frames for different values of $L \in \{0, 8, 16, 32\}$.

(b) Delay of unicast frames for different values of $L \in \{0, 8, 16, 32\}$.

Figure 4.8: Delay of unicast and multicast.

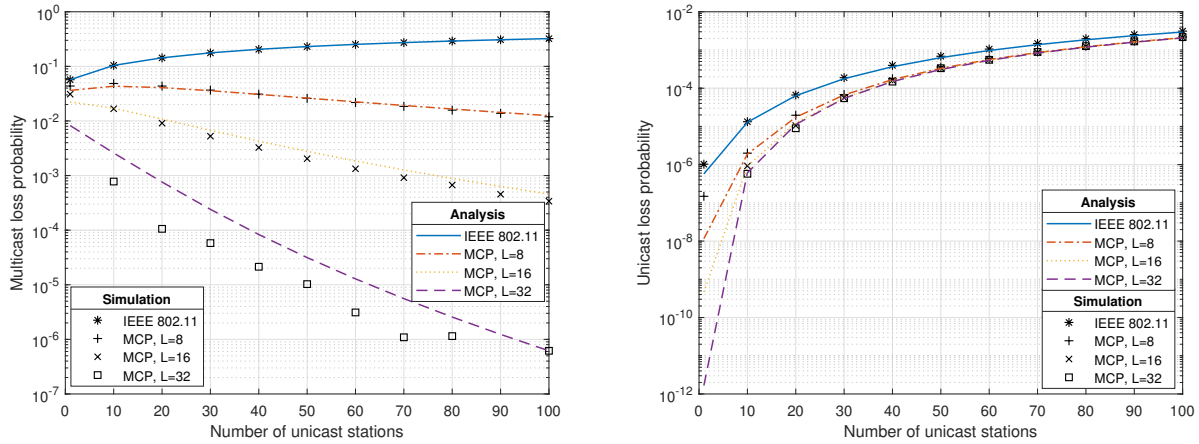

(a) Multicast frame loss probability for different values of $L \in \{0, 8, 16, 32\}$.

(b) Unicast frame loss probability for different values of $L \in \{0, 8, 16, 32\}$.

Figure 4.9: Frame loss probability of unicast and multicast.

are more likely to be successfully transmitted, which adds more waiting time to the delay of unicast frames that are in the backoff stage.

Figures 4.9a and 4.9b show the frame loss probability for different values of L, respectively for multicast and unicast traffics. The results depicted in Figure 4.9a highlight the impact of the parameter L on the reliability of multicast transmissions. It is clearly shown that the MCP

mechanism proves very effective compared to the standard, especially for a large value of L. From Figure 4.9a, we can also explain why the multicast throughput first increases then decreases when the number of USs increases. The results in Figure 4.9b show a slight improvement in the reliability provided to the unicast transmission when L increases. This is due to the fact that by increasing L, we reduce the probability of collisions involving unicast and multicast frames. Unlike multicast traffic, the reliability provided by the standard to unicast traffic is guaranteed by the retransmission mechanism. Consequently, the loss probability of multicast frames is greater compared with unicast. However, by increasing L we ensure more reliability to multicast frames but at the expense of a slight increase in the delay.

4.7 QoS-aware Audio-Video Communications

Table 4.2: Multicast Performance Metrics - frame size = 8192 bits

			Results for L_{opt}			Results for L		
N	L_{opt}	L	Loss probability	Temp (ms)	Delay (ms)	Loss probability	Temp (ms)	Delay (ms)
5	41	64	$9.0941 \cdot 10^{-6}$	8.5831	45.897	$3.1752 \cdot 10^{-8}$	8.5834	45.897
10	27	32	$8.6632 \cdot 10^{-6}$	8.5312	59.555	$1.2335 \cdot 10^{-6}$	8.5314	59.555
15	22	32	$7.3807 \cdot 10^{-6}$	8.5055	68.275	$5.2636 \cdot 10^{-8}$	8.5057	68.275
25	17	32	$7.0441 \cdot 10^{-6}$	8.4742	79.953	$3.8257 \cdot 10^{-10}$	8.4743	79.954
35	14	16	$9.1878 \cdot 10^{-6}$	8.4530	88.102	$1.9119 \cdot 10^{-6}$	8.4531	88.102
50	12	16	$6.5966 \cdot 10^{-6}$	8.4292	97.145	$1.4551 \cdot 10^{-7}$	8.4293	97.145

Table 4.3: Multicast Performance Metrics - frame size = 1000 bits

			Results for L_{opt}			Results for L		
N	L_{opt}	L	Loss probability	Temp (ms)	Delay (ms)	Loss probability	Temp (ms)	Delay (ms)
5	41	64	$9.0941 \cdot 10^{-6}$	1.3914	7.2050	$3.1752 \cdot 10^{-8}$	1.3914	7.2051
10	27	32	$8.6632 \cdot 10^{-6}$	1.3394	9.1821	$1.2335 \cdot 10^{-6}$	1.3394	9.1821
15	22	32	$7.3807 \cdot 10^{-6}$	1.3136	10.4138	$5.2636 \cdot 10^{-8}$	1.3137	10.4138
25	17	32	$7.0441 \cdot 10^{-6}$	1.2823	12.0152	$3.8257 \cdot 10^{-10}$	1.2823	12.0152
35	14	16	$9.1878 \cdot 10^{-6}$	1.2612	13.0938	$1.9119 \cdot 10^{-6}$	1.2612	13.0938
50	12	16	$6.5966 \cdot 10^{-6}$	1.2373	14.2458	$1.4551 \cdot 10^{-7}$	1.2373	14.2458

The previous section shows that the MCP outperforms the legacy multicast IEEE 802.11 services in all three performance metrics, namely, throughput delay and frame loss probabilities.

In this section, we should tune up the MCP mechanism in order to meet the A/V QoS requirements. Numerous studies have been reported in the literature on the analysis of the QoS of A/V requirements [87]. Due to the wide variety of encoding and compression, the impact of a loss frame

will highly depend on the piece of information being conveyed in the frame. Taking as a reference the recommendations published in [88], we should set the MCP's L parameter that guarantees a loss probability of less than 10^{-5}. Therefore, we propose the following optimization:

$$\begin{cases} \min L, \\ \text{s.t. } P_{lossM} < 10^{-5}, \quad \forall N \geq 0, \end{cases} \tag{4.60}$$

where the optimization is solved numerically using Algorithm 1. It should be noticed that by setting L to the minimum value to guarantee an acceptable loss probability, we are also implicitly limiting the frame delay.

Algorithm 1: Find L_{opt}

Input: Multicast loss probability threshold (i.e., 10^{-5}) and number of unicast stations N
Output: L_{opt}
$L \leftarrow 0$
$L_{opt} \leftarrow 0$
repeat
  $L \leftarrow L + 1$
  get $P_{lossM}(L)$; `// Eqn. (4.54) is used`
until $P_{loss}(L) < 10^{-5}$;
$L_{opt} \leftarrow L$
return L_{opt};

Following the same evolution of the contention window, we propose a practical value L in the set $S = \{0, 8, 16, 32, 64, ...\}$ which can be used by the AP and can be adjusted according to the number of USs associated with the AP. The proposed value L is based on the optimal value L_{opt}. That is to say, for any number N of USs we obtain the corresponding $L_{opt}(N)$, then the value L is chosen as the smallest value of S such that $L_{opt}(N) \leq L$.

Table 4.2 and 4.3 show the performance obtained using a frame size of 8192 bits and 1000 bits, respectively. We focus through these results on the multicast frame loss probability, the extra delay introduced by the MCP mechanism (i.e., "Temp", see Figure 4.3), and the access delay. Our analysis shows that our proposal is able to guarantee a frame loss probability lower than 10^{-5} when using L_{opt}.

The results show a significant improvement in terms of loss probability at the expense of a slight increase in the frame delay with respect to the one reported by the legacy IEEE 802.11 multicast mechanism. As seen from the tables, the extra delay depends on the frame size of the unicast frame. This is due to the fact that the multicast frame is transmitted following the transmission of a unicast frame. However, the extra delay introduced does not have a negative impact on the QoS provided to the A/V services since the reported values are well below the delays tolerated by most A/V applications [88].

4.8 Results Analysis

In this section, we summarize our results and main contributions to the goal of showing that the MCP multicast can be streamlined and integrated into the IEEE 802.11 protocol architecture.

Performance model. We have successfully developed a Markov model of the MCP protocol. The developed model considered a wireless IEEE 802.11 LAN supporting multicast and unicast services. We derived the expressions for the three main metrics of interest, namely, throughput, delay, and frame loss probabilities. All metrics were defined for both communications services: unicast and multicast services. Our model results were compared and validated with the ones obtained using a discrete-event simulator. We also included numerical results for the IEEE 802.11 legacy multicast mechanisms.

MCP inter-operability. As for the inter-operability of the MCP protocol, our results showed that the MCP protocol could properly interoperate with IEEE 802.11-compliant stations. In fact, as seen from the results reported in Section 4.5, the MCP protocol mechanism outperforms the legacy multicast mechanism for both communications services. In terms of the throughput metric, this latter result is of great relevance taking into account that the multicast mechanisms introduced by the IEEE 802.11aa have reported lower throughput rates in a similar setup, see Figure 6 in [27]. Furthermore, contrary to all other multicast mechanisms, the MCP mechanism's multicast throughput and frame loss probability improve as the overall network load increases, see Figures 4.7a and 4.9a.

Protocol configuration algorithm. Another major result of our work focused on the configuration algorithm taking into account the QoS of audiovisual applications. Due to its simplicity, the configuration protocol consisted of setting the MCP control parameter L given a target loss probability. Based on the QoS recommended for video services [88], we fixed the frame loss probability to 10^{-5}. The main core of the proposed algorithm was then built around the Markov model developed in the first part of our work. Compared to the configuration approaches reported for the IEEE 802.11aa multicast mechanisms where a frame loss of 10% has been set as a target, the MCP configuration algorithm is much simpler and can guarantee a much lower frame loss probabilities than any of the other open-loop multicast protocols.

4.9 Conclusion

In this chapter, we have studied the performance and implementation feasibility of MCP: a multicast collision prevention mechanism designed following the interoperability principles of the IEEE 802.11 protocol architecture. The main goal of our study has focused on developing a discrete-time Markov model to numerically evaluate the performance of the MCP under various scenarios. Our study has shown the great benefits and improvements offered by MCP over the legacy IEEE 802.11 multicast mechanism. Furthermore, our evaluation scenarios allowed us to show the feasibility of integrating MCP by considering scenarios integrating unicast and multicast services. In all scenarios, the unicast service made use of the standard DCF mechanism, while the multicast service made use of

the MCP mechanism.

In the second part of our study, we made use of our model to develop a simple configuration algorithm for the MCP mechanism. We have then shown that the MCP is capable of meeting the QoS requirements of audiovisual applications. Our results not only show that the MCP mechanism outperforms the IEEE 802.11 legacy multicast protocols, but more importantly, it can be easily configured to provide better results than the open-loop multicast mechanism introduced in the IEEE 802.11aa amendments.

Based on the results reported in this work and recent trends in the literature, our immediate work plans include the performance evaluation of the MCP mechanism under unsaturated conditions. Another main research task will focus on exploring the transmission of multiple frames and the interoperability with Enhanced Distributed Channel Access (EDCA). For instance, we may consider the transmission of multiple multicast frames separated by RIFS periods. In the case of multiple priority services (EDCA), we should evaluate the impact of the MCP over unicast audiovisual, video, and voice services. We also considered extending our model to scenarios comprising multiple access points.

Chapter 5

Opportunistic Multicast Access Mechanism for Video Communications over IEEE 802.11 with QoS/QoE Guarantees: Unsaturated Conditions

Contents

5.1 Introduction

The design and performance evaluation of diverse IEEE 802.11 MAC protocols capable of offering converged communications services have been the subject of many research and development efforts over the past few years [89] [90]. Despite the great benefits that a multicast MAC mechanism may provide to numerous end-user applications, the definition and integration into the protocol suite of a robust multicast mechanism is still a matter of research and standardization efforts [91]. Moreover, the efficient deployment of novel network architectures, such as the Named Data Networking (NDN)

WLANs, will rely on the efficiency of the underlying multicast MAC services. In [92], the authors have concluded that the deployment of NDN WLANs will require the use of efficient multicast MAC protocols. According to their studies, the multicast data ratio of NDN WLANs can reach up to 40%, while most data will consist of audiovisual material.

The specification and wide adoption of a multicast MAC mechanism aimed to be integrated into the IEEE 802.11 protocol suite will heavily depend on: 1) its ability to provide the reliability and provisioning of QoS/QoE guarantees required by numerous current and emerging applications, e.g., NDN, audiovisual services; and 2) its integration into the converged IEEE 802.11 protocol suite, e.g., coexistence with the unicast MAC mechanisms [91]. Different mechanisms have been proposed in the literature to ensure the Quality-of-Service (QoS) guarantees. The QoS of most of the proposed multicast mechanisms have been evaluated in terms of frame loss probability, or delay [32, 93]. However, audiovisual services are also highly sensitive to jitter. Furthermore, a comprehensive evaluation of the multicast MAC mechanism should jointly consider the QoS and QoE metrics. Moreover, any potential multicast MAC mechanism to be integrated into the IEEE 802.11 protocol architecture should be evaluated in scenarios where unicast and multicast share the wireless medium.

In this chapter, we undertake the modeling, evaluation, and tuning of an opportunistic multicast MAC mechanism under various load conditions and by considering the requirements and characteristics of digital video coding schemes. For our study, we consider the Multicast Collision Prevention (MCP) protocol recently introduced in the literature [32]. Our solution is motivated due to its great flexibility, and excellent results recently reported [94]. In fact, the MCP can be simply seen as an opportunistic MAC protocol; MCP does not require the use of extra signaling mechanisms to operate. In other words, MCP is a suitable alternative to the multicast mechanisms introduced in the IEEE 802.11aa amendment [95].

The multicast service is known to be less reliable than the unicast service. Due to the point-to-multipoint communications of the multicast service, several acknowledgments (ACKs) would be required in order to ensure reception at all receivers. This will result in the ACK implosion problem. This issue has been the subject of many studies attempting to improve the reliability of the MAC multicast service while limiting the signaling traffic. Since there are no ACKs for multicast traffic, the Access Point (AP) is unable to know whether or not the multicast receiver successfully receives a packet. Therefore, it is of great interest to design reliable multicast mechanisms. Although multicasting in wired links suffers from the same problem, the wireless network is much more sensitive to the presence of background traffic. Common packet loss rates of 5% or more have been reported by numerous multicast mechanisms in the literature, such loss rates are clearly unfeasible for video streaming and other services where high data rates and high reliability are required [27].

Multimedia streaming applications have become a common service for many IP (Internet Protocol) service providers, especially live and Video-on-Demand (VOD) streams. Video streaming service and IP traffics are present in a wide variety of applications. Globally, IP video traffic will be estimated at 82% of all consumers' Internet traffic by 2021. Therefore, live Internet video will be accounted for 13% of Internet video traffic by 2021 based on the visual Networking Index of Cisco

and forecasting of mobile data [96]. On the one hand, the development of ultra-high definition equipment such as cameras, displays, and playback systems has facilitated viewing the resolutions of 2K, 4K, and 8K videos. On the other hand, video frame rates have also considerably increased. As a result, the increase in High Definition (HD) video quality playback, 4K and 8K at rates of 60 fps, for both live and video-on-demand streaming services requires implementing more effective control mechanisms in terms of delay, jitter, and losses.

The Ultra-High Definition (UHD) video quality has an important role due to the smart devices capable of capturing and processing high-quality video content. Since delivery of the high-quality video stream over the wireless networks adds challenges to the end-users, the network behaviors factors such as delay of arriving packets, delay variation between packets, and packet loss impact the Quality of Experience (QoE).

Due to the fact that the legacy IEEE 802.11 multicast MAC is a simple broadcast mechanism, no ARQ mechanism was included in its specifications. Numerous proposals have been reported in the literature. For instance, the LBP-based (Leader Based Protocol) Automatic Repeat Request (ARQ) scheme, where the AP selects a user as the leader of a given group of multicast receivers, introduces the use of selective ACK frames. When a frame is successfully received, the leader sends an ACK on behalf of the multicast reivers. Meanwhile, all the other multicast receivers remain silent. However, when a frame is not well received, the non-leader users send a Negative ACK (NACK). Consequently, the AP receives the leader's ACK when a frame is successfully delivered, and it gets a NACK otherwise. The main inconvenience of this scheme is the feedback overhead introduced for leader management [97, 98]. Other schemes propose to adapt the data rate for multicast packets according to the channel quality of the user experiencing the worst channel conditions [99, 97, 100]. In this way, the mechanism aims to improve the probability that all users in the multicast group will successfully receive the multicast frame. Even though this approach provides improved multicast reliability, it limits the network throughput due to the data rate adaptation with the weakest user.

In this study, we employ a Markov chain model to analyze and obtain the stationary probability of transmission at each station in an arbitrary time slot. When first introduced, the MCP protocol was designed to reduce packet loss probability even in high load conditions [31]. However, the impact of frame loss over the multicast video service is considerably higher due to the decoding dependency between video frames, especially in non-scalable videos (i.e., MPEG-4 or H.264) [98]. Indeed, the video sequence consists of different types of frames. Therefore, losing a frame implies the loss of all related frames, which leads to a dramatic decrease in the quality of the video. For this reason, we are interested in this chapter to keep the loss probability as minimum as possible (below 10^{-6}). However, audiovisual services are also characterized by their stringent requirements for the delay and jitter and QoE metrics. Applications, such as real-time conferencing or broadcasting of diverse events, are highly sensitive to delays and jitter. Therefore, we should consider all relevant metrics and the tuning configuration of the MCP to meet the QoS/QoE requirements of audiovisual services.

The main contributions of this chapter are summarized as follows:

1. We develop an accurate Markov model of the multicast MAC protocol under unsaturated

conditions and taking into account the backoff freezing mechanism.

2. We derive the throughput, delay, and loss probability for the three different traffic sources: unicast traffic generated by the Unicast Senders (USs), unicast traffic generated by the AP, and the multicast traffic generated by the AP.

3. We define the jitter of the multicast traffic as the standard deviation of the inter-arrival time of the received multicast frames.

4. We extend the model in [94] by considering the AP unicast and multicast services. Furthermore, we take advantage of the multicast MAC mechanism operation to resolve internal collisions between unicast and multicast traffics within the AP.

5. Our model considers the interoperability between the multicast and unicast mechanisms. Our results show that the MCP mechanism can be properly integrated into the IEEE 802.11 protocol stack.

6. We include an optimization study of the multicast MAC mechanism in terms of the QoS metrics taking into account the needs of three popular video encoders.

7. We undertake a QoE-aware study of the optimal configuration of the multicast MAC mechanism in terms of the Mean Opinion Score (MOS) and Video Quality Metric (VQM) using the H.265, VP9, and Xvid video codecs.

8. Finally, we validate our analytical results with a custom-made MATLAB simulator.

5.2 The Multicast Collision Prevention MAC protocol

We illustrate the operation principles of the Multicast Collision Prevention mechanism developed in [31, 32]. We consider the scenario shown in Figure 5.1 in which an Access Point (AP) and a group of unicast senders are contending for channel access. Upon the arrival of a multicast packet, the AP starts the contention stage using the Distributed Coordination Function (DCF) mechanism. Unlike the standard IEEE 802.11 [82], the multicast packet is not transmitted when its backoff expires. Instead, and in order to avoid potential collisions with other unicast packets, the AP starts a timer denoted as *temp* (whose length is given by L, measured in slots) and monitors the channel for transmission activities. During the stage *temp*, one of these events may arise:

1. **The AP receives a valid unicast frame**. If one unicast frame is transmitted successfully (either by a US or by the AP), the AP responds with an ACK. Then, it starts the transmission of the multicast frame after a shorter waiting time denoted by Reduced Inter-frame Space (RIFS). According to the standard [82], all the other stations will remain silent for a longer period denoted by DIFS. Thus, the multicast frame will be successfully transmitted.

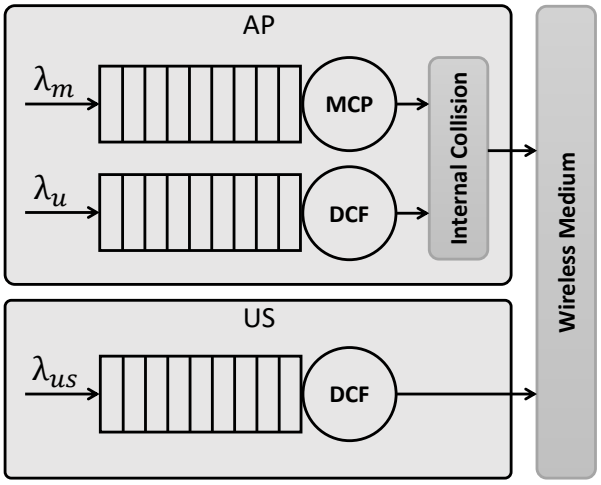

Figure 5.1: Scenario of the model. In the AP we have one queue for each traffic, and in the US we have only unicast queue.

2. **The AP senses the medium busy**. When a collision is detected in the channel, the AP transmits the multicast frame after sensing the medium idle for the RIFS period.

3. **No transmission activity is detected**. When the medium remains idle during L consecutive slots, the AP immediately transmits the multicast frame. In this case, it may collide with other USs transmitting at the same time. However, if the unicast frame of the AP is transmitted exactly at the same time as *temp* expires, an internal collision arises. Our approach to resolving the internal collision is to allow the priority to the unicast frame and transmit the multicast after a period of RIFS as in the event (1). This way, even if the unicast frame of the AP collides with other USs, the multicast frame will still be successfully transmitted.

5.3 Related Work

The mathematical modeling and performance evaluation of the IEEE 802.11 standard and its amendments have been widely explored in the literature over the past few years. In [25], the author presents an analytical model to evaluate the performance of the IEEE 802.11 distributed coordination function using Markov chains. The proposed model assumes an infinite retransmission retry limit and ideal channel conditions. Furthermore, the model is investigated under the assumption of saturated conditions. The model was later used in [101] to evaluate the performance of the IEEE 802.11a amendment and the IEEE 802.11b standard operating at data rates of 6 Mbps and 1 Mbps, respectively. The authors in [27] propose an analytical model of the 802.11aa standard using Markov chain processes. They also introduce an algorithm to select the multicast mechanism best meeting the needs of different WLAN operation scenarios.

The authors in [102] introduce a Markov model-based approach for modeling the IEEE 802.11 DCF network with fragmentation under a lightly disturbed channel and saturated conditions. However, the chapter investigates the performance only in terms of the throughput and lacks significant performance metrics such as delay, jitter, and loss probability. Furthermore, the unsaturated conditions are not considered, and the analytical results are not validated with simulation.

The non-saturated models are an extension of saturated models and differ in terms of network load. In [103], the authors develop a theoretical model using two 3D Markov models for the WiFi and LAA (Licensed Assisted Access) coexistence system using the IEEE 802.11e EDCA mechanism and the LAA category-4 LBT (Listen Before Talk) procedure under unsaturated conditions. They take into consideration the transmission priority. The LAA Cat.4 LBT procedure is a channel access mechanism for downlink data transmission. It uses a frame structure in which a subframe is of a fixed length, and the number of subframes is variable.

The authors in [104] study the IEEE 802.11 standard taking into account the interference from the IEEE 802.11 and non-IEEE 802.11 sources. They employ a Markov model to predict latency and throughput in saturated and unsaturated conditions.

The authors in [105] propose a three-level renewal process model for the slotted non-persistent CSMA with a binary exponential backoff mechanism for the IEEE 802.15.4 standard. They consider saturated and unsaturated traffic conditions and validate their model with simulation.

The authors in [98] propose a flexible wireless multicast solution for efficient video streaming over WLANs named FlexVi . By considering the frame aggregation mechanism, they allow the AP to dynamically adjust the data rate according to several criteria. In addition, they propose an approach allowing multiple clients to deliver their ACKs to an AP simultaneously without collision.

In the literature, most studies of the QoE evaluation focus on QoS/QoE mapping models. These studies are objective-based approaches, and they address the QoE evaluation problem by finding the appropriate mapping function between the QoS metrics and QoE estimation. These approaches are not as reliable as the subjective ones, where people/subjects give their opinion about the video quality. However, they remain practical and realistic for collecting and measuring user opinion, especially in real-time applications. One of the most popular objective approaches is the IQX hypothesis [106]. It provides an exponential relationship between the QoS and the QoE in terms of Mean Opinion Scores (MOS). Several other mapping functions have been proposed in the literature to estimate the QoE based on the QoS metrics [107]. Among these mapping functions, there is the linear mapping function [108], the cubic polynomial function [109], the logistic functions [110], the exponential function [108], the power function [108], the logarithmic function [111] and Five Parameter Logistics function (5PL) [112].

In [113], the authors provide mapping functions between QoS and QoE metrics for the H.265/HEVC and VP9 codecs. They conducted several experimental evaluations using the Evalvid framework, and the network simulator toolkit ns-2 was tested using various video sequences. Furthermore, they perform a subjective evaluation using 59 participants of different ages. The main QoS metrics used are packet loss, jitter, throughput, and resolution scaling.

Unlike the previous study, our study develops an analytical model by considering the following

QoS and QoE metrics of the multicast traffic: throughput, delay, loss rate, and jitter. In order to guarantee the audio/video requirements, we perform an optimization analysis by setting upper bounds to the delay, loss, and jitter of the multicast traffic. Since the multicast MAC mechanism has to be integrated into the IEEE 802.11 protocol architecture, we also consider the interoperability of the multicast mechanism with DCF unicast stations. Indeed, the design specifications of the multicast mechanism allow multicast frames to be transmitted collision-free only after obtaining the channel access following the operation rules of the DCF mechanism. We show that the proposed setting does not have a negative impact on the unicast service.

Table 5.1: Notation and terminology

Parameter	Description
N	Number of unicast stations
L	Length of the timer *temp* in slots
Λ	Average system slot time
λ	Arrival rate of unicast traffic (AP's and USs' traffic) in [packet/slot]
λ_u	Arrival rate of unicast traffic of the AP in [packet/slot]
λ_{us}	Arrival rate of unicast traffic of US in [packet/slot]
λ_m	Arrival rate of multicast traffic in [packet/slot]
p_c	Conditional collision probability for unicast frames of the AP
q_c	Conditional collision probability for unicast frames of the US
P_u	Probability of a packet availability at the unicast queue of the AP
P_{us}	Probability of a packet availability at the unicast queue of the US
P_m	Probability of a packet availability at the multicast queue
P_{idle}	Probability that the AP detects an idle slot
$CW_{\min}$	Minimum contention window

5.4 System Model

We consider the wireless network scenario presented in Figure 5.1 with N unicast senders and a group of multicast receivers connected to a single AP. The data packets arrive at each US queue following a Poisson distribution with rate λ_{us}. We assume that the AP contains two independent queues, one for unicast and another for multicast. The packet arrival rate to each queue follows a Poisson distribution with the rate λ_u and λ_m, respectively. The probability of a packet availability at each queue is then given by:

$$\begin{cases} P_{us} = 1 - \exp\left(-\lambda_{us}\Lambda\right), \\ P_u = 1 - \exp\left(-\lambda_u\Lambda\right), \\ P_m = 1 - \exp\left(-\lambda_m\Lambda\right), \end{cases} \tag{5.1}$$

where Λ is the average system slot time. The value of Λ can be derived in a similar way as $E[T_{slotUS}]$ in the equation (5.30) by considering $N+1$ unicast stations. Table 5.1 shows the description of the

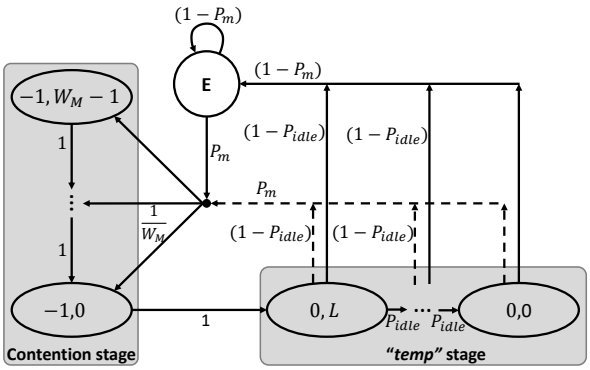

Figure 5.2: Markov chain of the MCP mechanism. The state "E" refers to the idle state.

notations adopted in the chapter.

We start by modeling the backoff procedure of unicast frames. We denote by W_i the contention window size in the *i-th* backoff stage of unicast packet, where $i \in \{1, ..., m\}$ and m is the maximum backoff stage. Starting from its initial value $CW_{\min}$, the contention window is doubled after each unsuccessful transmission until it reaches the maximum value CW_{max}. Thus, we have:

$$W_i = 2^{i-1} CW_{\min}, \quad i \in \{1, ..., m\}. \tag{5.2}$$

We assume that the colliding packet at the last backoff stage is dropped, and no transmission retry is considered. Furthermore, we consider an ideal wireless channel. Thus, all packet losses are due to collisions.

In order to evaluate the performance of unicast traffic, we adopt an extension of the Markov model reported in [25] by taking into account the backoff freezing and unsaturated stations. We denote by $\tau_{i,j}^k$ the corresponding steady-state distribution, where $k = 1$ in the case of unicast frames of the US and $k = 2$ in the case of unicast frames of the AP. Thus, for $i \in \{1, ..., m\}$, and $j \in \{1, ..., W_i - 1\}$ we have:

$$\begin{cases} \tau_{i,j}^k &= \frac{W_i - j}{W_i} \cdot \frac{\left(1-p_s^k\right)^{i-1}}{p_e^k} \cdot \tau_{1,0}^k, \\ \tau_{i,0}^k &= \left(1-p_s^k\right)^{i-1} \cdot \tau_{1,0}^k, \\ \tau_E^k &= \frac{1-P_u^k}{P_u^k} \tau_{1,0}^k, \end{cases} \tag{5.3}$$

where

$$P_u^k = \begin{cases} P_{us}, & \text{if } k = 1, \\ P_u, & \text{if } k = 2. \end{cases} \tag{5.4}$$

The conditional success probability is usually the probability of meeting an idle slot while sensing the channel, which is the case of unicast traffic generated by the USs i.e., $p_s^1 = p_e^1 = (1-\tau^{us})^{N-1}(1-\tau^u)(1-\pi_{0,0})$. However, this is not the case with unicast traffic generated by the AP since they goes through the internal collision. Therefore, $p_s^2 = (1-\tau^{us})^N$ and $p_e^2 =$

$(1-\tau^{us})^N(1-\pi_{0,0})$. We denote by τ_E^k the stationary distribution of being in state "E" i.e., empty queue state.

Let $W_{-1}=W_M$ and $W_0=L+1$, where W_M is the multicast's contention window size and L is the length of the timer *temp*. Since multicast frames are transmitted using the MCP mechanism, we shall use a different Markov chain. Let $s(t)$ be the stochastic process representing the stage of a multicast frame, either contention stage or *temp* stage. And let $b(t)$ be the stochastic process representing the state of each stage. We model the bi-dimensional process $\{s(t),b(t)\}$ using the discrete Markov chain presented in Figure 5.2. Let $P\left((i,j),(i',j')\right)$ denote one-step transition probability, we adopt the short following notation:

$$P\left((i,j),(i',j')\right)=P\left(s(t+1)=i',b(t+1)=j'|s(t)=i,b(t)=j\right). \tag{5.5}$$

We denote by $\pi_{i,j}=\lim_{t\to\infty}(s(t)=i,b(t)=j)$ the steady state distribution of the Markov chain. By computing the balance equations, we obtain:

$$\pi_{0,j}=P_{idle}^{L-j}\pi_{0,L},\quad j\in\{0,...,L\}, \tag{5.6}$$

$$\pi_{-1,j}=\frac{W_M-j}{W_M}\cdot\frac{1}{P_{idle}}\pi_{0,L},\quad j\in\{1,...,W_M-1\}, \tag{5.7}$$

$$\pi_{-1,0}=\pi_{0,L}, \tag{5.8}$$

$$\pi_E=\frac{1-P_m}{P_m}\pi_{0,L}. \tag{5.9}$$

where P_{idle} is the probability that the AP meets an idle slot. It is given by

$$P_{idle}=(1-\tau^{us})^N(1-\tau^u). \tag{5.10}$$

Using the normalization condition, we compute the remaining unknown parameters:

$$\tau_{1,0}^k=\left(\sum_{i=1}^{m}\sum_{j=0}^{W_i-1}\tau_{i,j}^k+\tau_E^k-\tau_{1,0}^k\right)^{-1}, \tag{5.11}$$

$$\pi_{0,L}=\left(\sum_{j=0}^{L-1}\pi_{0,j}+\sum_{j=0}^{W_M-1}\pi_{-1,j}+\pi_E\right)^{-1}. \tag{5.12}$$

The transmission probabilities of US's frames, AP's unicast, and multicast frames are given by:

$$\tau^{us}=\frac{1-\left(1-p_s^1\right)}{p_s^1}\tau_{1,0}^1, \tag{5.13}$$

$$\tau^{u}=\frac{1-\left(1-p_s^2\right)}{p_s^2}\tau_{1,0}^2, \tag{5.14}$$

$$\pi^m=(1-P_{idle})\sum_{j=1}^{L}\pi_{0,j}+\pi_{0,0}. \tag{5.15}$$

5.4.1 Unsaturated Throughput

The throughput is given by the number of successful transmissions over the total number of transmissions, i.e.,

$$S^{us} = \frac{\tau^{us}(1-\tau^{us})^{N-1}(1-\tau^{u})(1-\pi_{0,0})}{\tau^{us}}, \tag{5.16}$$

$$S^{u} = \frac{\tau^{u}(1-\tau^{us})^{N}}{\tau^{u}}, \tag{5.17}$$

$$S^{m} = \frac{(1-P_{idle})\sum_{j=1}^{L}\pi_{0,j} + \pi_{0,0}\left[\tau^{u} + (1-\tau^{u})(1-\tau^{us})^{N}\right]}{\pi^{m}}. \tag{5.18}$$

The frame loss probability is another important performance measure for data transmission. We consider that losses are due only to collisions. Thus, we have:

$$P^{us}_{loss} = \frac{\tau^{1}_{m,0}\left[1-(1-\tau^{us})^{N-1}(1-\tau^{u})(1-\pi_{0,0})\right]}{\tau^{us}}, \tag{5.19}$$

$$P^{u}_{loss} = \frac{\tau^{2}_{m,0}\left[1-(1-\tau^{us})^{N}\right]}{\tau^{u}}, \tag{5.20}$$

$$P^{m}_{loss} = \frac{\pi_{0,0}\left[1-(1-\tau^{us})^{N}\right](1-\tau^{u})}{\pi^{m}}. \tag{5.21}$$

5.4.2 Unicast Access Delay

The medium access delay is calculated as the time elapsed from the moment the packet is at the head of the line to the moment of its successful transmission. To compute this delay, let's analyze the timeline of the system. The following items summarize all potential events in the system.

- Idle: no station attempts to transmit,
- UX: successful transmitted unicast frame followed by non-multicast frame,
- UM: successful transmitted unicast frame followed by a multicast frame,
- CX: a collision followed by a non-multicast frame,
- CM: a collision followed by multicast frame,
- XM: an idle slot followed by a multicast frame.

The length of a given time slot is then a random value that depends on the stations' transmission activities. We define the time slot length of the events above as follows:

$$\begin{aligned} T^{UX} &= \text{DATA+SIFS+ACK+DIFS+}2\delta, \\ T^{UM} &= 2\cdot\text{DATA+SIFS+ACK+RIFS+DIFS+}3\delta, \\ T^{CX} &= \text{DATA+DIFS+}\delta, \\ T^{CM} &= \text{DATA+RIFS+DATA+DIFS+}2\delta, \\ T^{XM} &= \text{DATA+DIFS+}\delta. \end{aligned} \tag{5.22}$$

where δ denotes the propagation delay, and the duration of the event "Idle" is σ.

The average transition time to the next backoff state, from the point of view of a unicast sender, depends on the activity of the AP and $(N-1)$ remaining USs. Therefore, one of the six events discussed above may happen. We define the probabilities of these events respectively as follows:

$$P_{us}^{idle} = (1-\tau)^{N-1}(1-\tau^u)(1-\pi_{0,0}), \tag{5.23}$$

$$P_{us}^{UX} = \tau^u(1-\tau)^{N-1}\left(1-\sum_{j=0}^{L}\pi_{0,j}\right) + (N-1)\tau(1-\tau)^{N-2}(1-\tau^u)\left(1-\sum_{j=0}^{L}\pi_{0,j}\right), \tag{5.24}$$

$$P_{us}^{UM} = (N-1)\tau(1-\tau)^{N-2}\sum_{j=1}^{L}\pi_{0,j}\left(1-\tau^u\right) + \tau^u\left(1-\tau\right)^{N-1}\sum_{j=0}^{L}\pi_{0,j}, \tag{5.25}$$

$$\begin{aligned} P_{us}^{CX} = &\sum_{i=2}^{N-1}\binom{N-1}{i}\tau^i(1-\tau)^{N-1-i}\left(1-\sum_{j=1}^{L}\pi_{0,j}\right)(1-\tau^u) \\ &+ \sum_{i=1}^{N-1}\binom{N-1}{i}\tau^i(1-\tau)^{N-1-i}\left(1-\sum_{j=0}^{L}\pi_{0,j}\right)\tau^u + (N-1)\tau(1-\tau)^{N-2}\pi_{0,0}(1-\tau^u), \end{aligned} \tag{5.26}$$

$$\begin{aligned} P_{us}^{CM} = &\sum_{i=2}^{N-1}\binom{N-1}{i}\tau^i(1-\tau)^{N-1-i}\cdot\sum_{j=1}^{L}\pi_{0,j}(1-\tau^u) \\ &+ \sum_{i=1}^{N-1}\binom{N-1}{i}\tau^i(1-\tau)^{N-1-i}\cdot\sum_{j=0}^{L}\pi_{0,j}\tau^u, \end{aligned} \tag{5.27}$$

$$P_{us}^{XM} = \pi_{0,0}(1-\tau)^{N-1}(1-\tau^u). \tag{5.28}$$

By summing the equations above, we obtain:

$$P_{us}^{idle} + P_{us}^{UX} + P_{us}^{UM} + P_{us}^{CX} + P_{us}^{CM} + P_{us}^{XM} = 1. \tag{5.29}$$

The average slot time from the point of view of an US is then given by:

$$E[T_{slotUS}] = P_{us}^{idle}\sigma + P_{us}^{UX}T^{UX} + P_{us}^{UM}T^{UM} + P_{us}^{CX}T^{CX} + P_{us}^{CM}T^{CM} + P_{us}^{XM}T^{XM}. \tag{5.30}$$

The number of transmission attempts for a single US follows a geometric distribution with success probability $(1-q_c)$, where q_c is the conditional collision probability, and it is defined as $q_c = 1 - p_s^1$. The delay of the frames transmitted by USs is then given by:

$$D_{us} = \sum_{i=1}^{m}\frac{q_c^{i-1}(1-q_c)}{1-q_c^m}\cdot\left[\sum_{k=1}^{i}\left(\frac{W_k-1}{2}\cdot E[T_{slotUS}] + T^{UX}\right)\right]. \tag{5.31}$$

Now, let us compute the delay of the unicast frames transmitted by the AP. The transition time to the next backoff state depends on the activity of multicast traffic and the N USs. Therefore, one of the six events {Idle, UX, UM, CX, CM, XM} discussed above is considered in a given slot. The probabilities of these events are respectively

$$P_u^{idle} = (1-\tau)^N(1-\pi_{0,0}), \tag{5.32}$$

$$P_u^{UX} = N\tau(1-\tau)^{N-1}\left(1-\sum_{j=0}^{L}\pi_{0,j}\right), \tag{5.33}$$

$$P_u^{UM} = N\tau(1-\tau)^{N-1}\sum_{j=1}^{L}\pi_{0,j}, \tag{5.34}$$

$$P_u^{CX} = \sum_{i=2}^{N-1}\binom{N}{i}\tau^i(1-\tau)^{N-i}\left(1-\sum_{j=1}^{L}\pi_{0,j}\right) + N\tau(1-\tau)^{N-1}\pi_{0,0}, \tag{5.35}$$

$$P_u^{CM} = \sum_{i=2}^{N}\binom{N}{i}\tau^i(1-\tau)^{N-i}\cdot\sum_{j=1}^{L}\pi_{0,j}, \tag{5.36}$$

$$P_u^{XM} = \pi_{0,0}(1-\tau)^N. \tag{5.37}$$

Note that the sum of the probabilities above is equal to one. The delay of unicast traffic generated by the AP is then:

$$D_u = \sum_{i=1}^{m}\frac{p_c^{i-1}(1-p_c)}{1-p_c^m}\cdot\left[\sum_{k=1}^{i}\left(\frac{W_k-1}{2}\cdot E[T_{slotU}] + T^{UX}\right)\right], \tag{5.38}$$

where $E[T_{slotU}]$ is the average slot time from the point of view of unicast traffic of the AP. It is given by

$$E[T_{slotU}] = P_u^{idle}\sigma + P_u^{UX}T^{UX} + P_u^{UM}T^{UM} + P_u^{CX}T^{CX} + P_u^{CM}T^{CM} + P_u^{XM}T^{XM}, \tag{5.39}$$

and p_c is the conditional collision probability of unicast frames of the AP. It is defined as $p_c = 1-p_s^2$.

5.4.3 Multicast Delay

Finally, let us find the delay of multicast traffic. We should first get the delay in the DCF stage, which is similar to the first stage of unicast traffic. Then, we obtain the delay in the stage *temp*.

When the multicast frame is at the DCF stage, the average slot length depends not only on the activities of the N USs, but also on the unicast traffic generated by the AP. Therefore, the three following events: Idle, Unicast success, and Collision, are considered in the slot length. The

probabilities of these events are given, respectively, as follows:

$$P_{idle} = (1-\tau)^N(1-\pi_u), \tag{5.40}$$
$$P_s^m = N\tau(1-\tau)^{N-1}(1-\pi_u) + \pi_u(1-\tau)^N, \tag{5.41}$$
$$P_c^m = 1 - P_s^u - P_{idle}. \tag{5.42}$$

Then, the average slot time is:

$$E[T_{slotM}] = P_{idle}\sigma + P_s^m T^{UX} + P_c^m T^{CX}. \tag{5.43}$$

The average delay in the DCF stage is then:

$$T_{DCF} = \frac{W_M - 1}{2} E[T_{slotM}]. \tag{5.44}$$

When the multicast frame is at the *temp* stage, the number of idle slots it has to wait before a free-collision transmission opportunity follows a geometric distribution with a success probability $(1 - P_{idle})$. Thus, the average delay in the *temp* stage is:

$$\begin{aligned} T_{temp} = &\sum_{k=0}^{L-1} P_{idle}^k \left(P_s^m(k\sigma + T^{UM}) + P_c^m(k\sigma + T^{CM})\right) \\ &+ P_{idle}^L \left((1-\tau^u)\left(L\sigma + T^{XM}\right) + \tau^u\left(L\sigma + T^{UM}\right)\right). \end{aligned} \tag{5.45}$$

The average delay of a multicast frame is obtained as the total time elapsed in the DCF process and the *temp* stage.

$$D_m = T_{DCF} + T_{temp}. \tag{5.46}$$

Proposition 5.4.1 *The mean and the variance of multicast delay are given by:*

$$E[D_m] = E[d_1] + E[d_2] \tag{5.47}$$
$$Var(D_m) = Var(d_1) + Var(d_2). \tag{5.48}$$

where d_1 is the time spend in the DCF stage, and d_2 is the time spend in the temp stage.

Proof The access delay of a multicast frame contains the time spend in the DCF stage and also the time spend in the *temp* stage, which we denote respectively as d_1 and d_2. Let Nb be the random variable (r.v.) representing the chosen number in the contention window $[0, W_M - 1]$ which follows a uniform distribution. Thus, we can define d_1 as

$$d_1 = \sum_{k=1}^{Nb} T_{slotM}, \tag{5.49}$$

where T_{slotM} is the time slot length as seen by the multicast traffic of the AP. Then, the mean of d_1 is obtained as follows:

$$\begin{aligned} E[d_1] &= E\left[E\left[d_1/Nb\right]\right], \\ &= \sum_{k=0}^{W_m-1} E[d_1/Nb=k]P\left(Nb=k\right), \\ &= E[T_{slotM}] \sum_{k=0}^{W_m-1} \frac{1}{Wm-1}k, \\ &= E[T_{slotM}]E[Nb]. \end{aligned} \tag{5.50}$$

According to the law of total variance, we have:

$$\begin{aligned} Var(d_1) &= E\left[Var(d_1/Nb)\right] + Var\left(E\left[d_1/Nb\right]\right), \\ &= E\left[Var(\sum_{k=1}^{Nb} T_{slotM}/Nb)\right], \\ &+ Var\left(E\left[\sum_{k=1}^{Nb} T_{slotM}/Nb\right]\right), \\ &= E\left[Nb \cdot Var\left(T_{slotM}\right)\right] + Var\left(Nb \cdot E\left[T_{slotM}\right]\right), \\ &= E\left[Nb\right] Var\left(T_{slotM}\right) + E[T_{slotM}]^2 Var(Nb). \end{aligned} \tag{5.51}$$

Let us now find the probability distribution of the r.v. d_2.

$$\begin{aligned} P(d_2 = k\sigma + T^{UM}) &= P_{idle}^k P_s^m, \\ P(d_2 = k\sigma + T^{CM}) &= P_{idle}^k P_c^m, \\ P(d_2 = L\sigma + T^{UM}) &= (1/Ps_{00}) P_{idle}^L \tau^u (1-\tau)^N, \\ P(d_2 = L\sigma + T^{CM}) &= (1/Ps_{00}) P_{idle}^L \tau^u (1-(1-\tau)^N), \\ P(d_2 = L\sigma + T^{XM}) &= (1/Ps_{00}) P_{idle}^L (1-\tau^u)(1-\tau)^N. \end{aligned} \tag{5.52}$$

where Ps_{00} is the probability that a multicast frame succeed when it reaches the state $(0,0)$ (see Figure 5.2), it is defined as follows:

$$Ps_{00} = \tau^u + \left(1-\tau^u\right)\left(1-\tau\right)^N. \tag{5.53}$$

The first two moments of d_2 can be derived from the probability distribution above. We have:

$$\begin{aligned} E[d_2] = &\sum_{k=0}^{L-1} \left(k\sigma + T^{UM}\right) P(d_2 = k\sigma + T^{UM}), \\ &+ \left(k\sigma + T^{CM}\right) P(d_2 = k\sigma + T^{CM}), \\ &+ \left(L\sigma + T^{UM}\right) P(d_2 = L\sigma + T^{UM}), \\ &+ \left(L\sigma + T^{CM}\right) P(d_2 = L\sigma + T^{CM}), \\ &+ \left(L\sigma + T^{XM}\right) P(d_2 = L\sigma + T^{XM}). \end{aligned} \tag{5.54}$$

$$\begin{aligned} E[(d_2)^2] = &\sum_{k=0}^{L-1} \left(k\sigma + T^{UM}\right)^2 P(d_2 = k\sigma + T^{UM}), \\ &+ \left(k\sigma + T^{CM}\right)^2 P(d_2 = k\sigma + T^{CM}), \\ &+ \left(L\sigma + T^{UM}\right)^2 P(d_2 = L\sigma + T^{UM}), \\ &+ \left(L\sigma + T^{CM}\right)^2 P(d_2 = L\sigma + T^{CM}), \\ &+ \left(L\sigma + T^{XM}\right)^2 P(d_2 = L\sigma + T^{XM}). \end{aligned} \tag{5.55}$$

Then, we can obtain the variance using the classic method:

$$Var(d_2) = E[(d_2)^2] - E[d_2]^2. \tag{5.56}$$

Since the two r.vs. d_1 and d_2 are independent, we finally obtain the mean and the variance of the multicast delay.

$$E[D_m] = E[d_1] + E[d_2], \tag{5.57}$$

$$Var(D_m) = Var(d_1) + Var(d_2). \tag{5.58}$$

□

5.4.4 Multicast Jitter

The jitter is defined as the standard deviation of the inter-arrival time of received frames at the destination. To find the analytical form of the jitter, we need to define some variables.

Proposition 5.4.2 *The mean and the variance of inter-success time of multicast frames are defined as:*

$$E[Z] = E[Nb_{loss}]E[Y_1] + E[Y_2], \tag{5.59}$$

$$Var(Z) = E[Nb_{loss}]Var(Y_1) + E[Y_1]^2 Var(Nb_{loss}) + Var(Y_2). \tag{5.60}$$

Proof Let X_1 be the r.v. representing the elapsed time while the multicast queue is empty. Let N_e be the number of slots during which the multicast queue stays empty. N_e is a r.v. following a geometric distribution with parameter P_m. The mean and the variance of N_e are then given by:

$$E[N_e] = \frac{(1 - P_m)}{P_m}, \tag{5.61}$$

$$Var(N_e) = \frac{(1 - P_m)}{P_m^2}. \tag{5.62}$$

Now, we can define the r.v. X_1 as the sum of N_e time slots.

$$X_1 = \sum_{k=0}^{N_e} T_{slotM}, \tag{5.63}$$

where T_{slotM} is the slot duration as seen by the multicast traffic of the AP. We get the mean and the variance from the distribution of T_{slotM}.

$$E[T_{slotM}] = P_{idle}\sigma + P_s^m T^{UX} + P_c^m T^{CX}, \tag{5.64}$$

$$Var(T_{slotM}) = E[T_{slotM}^2] - E[T_{slotM}]^2, \tag{5.65}$$

where $E[T_{slotM}^2]$ is the second moment of the r.v. T_{slotM} and it is defined by:

$$E[T_{slotM}^2] = P_{idle}\sigma^2 + P_s^m (T^{UX})^2 + P_c^m (T^{CX})^2. \tag{5.66}$$

Using the two laws of total expectation and total variance, respectively, we can get the mean and the variance of X_1 as follows:

$$\begin{aligned}
E[X_1] &= E\left[E\left[X_1/N_e\right]\right], \qquad (5.67)\\
&= \sum_{k=1}^{\infty} E\left[X_1/N_e = k\right] \cdot P(N_e = k),\\
&= \sum_{k=0}^{\infty} k \cdot E[T_{slotM}] \cdot (1 - P_m)^k P_m,\\
&= P_m E[T_{slotM}] \sum_{k=0}^{\infty} k \left(1 - P_m\right)^k,\\
&= P_m E[T_{slotM}] \frac{1 - P_m}{P_m^2},\\
&= \frac{1 - P_m}{P_m} E[T_{slotM}],\\
&= E[N_e] E[T_{slotM}].
\end{aligned}$$

$$\begin{aligned} Var(X_1) &= E[Var(X_1/N_e)] + Var(E[X_1/N_e]), \\ &= E[N_e Var(T_{slotM})] + Var(N_e E[X_1]), \\ &= E[N_e] Var(T_{slotM}) + Var(N_e) E[X_1]^2. \end{aligned} \tag{5.68}$$

Let us now define X_2 the r.v. representing the dropping time of a multicast frame. The dropping time consists of the elapsed time in DCF stage denoted by X_2^1 and also the time in *temp* stage denoted by X_2^2. Therefore

$$X_2 = X_2^1 + X_2^2. \tag{5.69}$$

The r.v. X_2^1 is defined as the sum of a random number N_b of time slots. Therefore, we can use the law of total expectation and the law of total variance to get the mean and the variance of X_2^1.

$$E[X_2^1] = E[N_b] E[T_{slotM}], \tag{5.70}$$

$$Var(X_2^1) = E[N_b] Var(T_{slotM}) + E[T_{slotM}]^2 Var(N_b). \tag{5.71}$$

A multicast dropped frame experience L idle slots in *temp* stage before being dropped. Thus:

$$E[X_2^2] = L\sigma + T^{CX}, \tag{5.72}$$

$$Var(X_2^2) = 0. \tag{5.73}$$

The mean and the variance of X_2 can now be obtained by

$$E[X_2] = E[X_2^1] + E[X_2^2], \tag{5.74}$$

$$Var(X_2) = Var(X_2^1). \tag{5.75}$$

Let Y_1 be the r.v. defined as

$$Y_1 = X_1 + X_2, \tag{5.76}$$

which represents the time elapsed from the last transmission attempt to the moment of the first failed transmission. The mean and the variance of Y_1 can be obtained using the ones of the r.v. X_1 and X_2. Since this latter random variables are independent, we have:

$$E[Y_1] = E[X_1] + E[X_2], \tag{5.77}$$

$$Var(Y_1) = Var(X_1) + Var(X_2). \tag{5.78}$$

Let us define the r.v. Y_2 as the time elapsed from the last transmission attempt to the moment of the first successful transmission. We have

$$Y_2 = X_1 + X_2', \tag{5.79}$$

where X_2' is the access delay of non dropped frame. Its mean is refereed as D_m in 5.4.3. X_1 and X_2' are independent, thus

$$E[Y_2] = E[X_1] + E[X_2'], \tag{5.80}$$
$$Var(Y_2) = Var(X_1) + Var(X_2'). \tag{5.81}$$

Finally, we can define the time between two successful consecutive multicast transmissions, denoted by the r.v. Z. This time contains a random number of failed transmissions plus the time of the successful transmission. Let us denote by Nb_{loss} the number of failed transmissions before the first successful one. Nb_{loss} follows a geometric distribution with a parameter P_{loss}^m. Thus

$$E[Nb_{loss}] = \frac{P_{loss}^m}{(1 - P_{loss}^m)}, \tag{5.82}$$
$$Var(Nb_{loss}) = \frac{P_{loss}^m}{(1 - P_{loss}^m)^2}. \tag{5.83}$$

Using the law of total expectation again, the law of total variance, and the independence of the three random variables Nb_{loss}, Y_1 and Y_2, we obtain

$$E[Z] = E[Nb_{loss}]E[Y_1] + E[Y_2], \tag{5.84}$$
$$Var(Z) = E[Nb_{loss}]Var(Y_1) + E[Y_1]^2 Var(Nb_{loss}) + Var(Y_2). \tag{5.85}$$

□

Corollary 5.4.2.1 *The jitter of multicast frames is defined as the standard deviation of the inter-success time.*

$$Jitter = \sqrt{Var(Z)}. \tag{5.86}$$

5.5 Numerical results

Table 5.2: MCP and DCF System Parameters

Parameter	Value	Parameter	Value
DATA	1000 bits	Propagation delay δ	$2\,\mu s$
SIFS	$10\,\mu s$	Slot time σ	$20\,\mu s$
DIFS	$50\,\mu s$	W_1, W_M	32
RIFS	$30\,\mu s$	Maximum backoff stage m	5
ACK	304 bits	Data rate	1 Mbps

In this section, we present the analytical and simulation results. The simulation study has been carried out using a custom-made MATLAB simulator in which the unicast normalized offered load $\lambda = \lambda_{us} = \lambda_u$ is varied from starvation to saturation. The simulations are conducted 100 times with a duration of $10^9 \mu s$ each.

The accuracy of our analytical model is validated by comparing it with simulation results. Our analysis also includes a comparative evaluation of the results reported by the standard IEEE 802.11 multicast mechanism. The comparison should allow us to quantify the expected performance improvements in terms of all the performance metrics of interest.

Our analytical and simulation models are valid for any number N of unicast senders. We first consider in this section $N = 10$, and later, we will investigate the case of different values of N and λ. Notice that the AP generates unicast and multicast frames. As a result, we have in total 11 unicast stations along with one single multicast station (see Figure 5.1 for further details).

The multicast offered load λ_m is fixed to one packet per time slot. However, the unicast offered load is varied from 0 to 1 packet per time slot. Further parameters used in the analysis are listed in Table 5.2.

Figure 5.3 and 5.4 show the normalized throughput of unicast frames transmitted by the AP and by the USs, respectively. We vary the offered load of unicast traffic λ, considering different values for L. For both IEEE 802.11 and MCP, the unicast throughput decreases as the offered load increases. This is due to the collision arising from multiple transmissions. However, we notice that the MCP mechanism shows a slight improvement compared to the standard IEEE 802.11. This is because of the ability of the MCP to mitigate internal collisions between unicast and multicast frames within the AP.

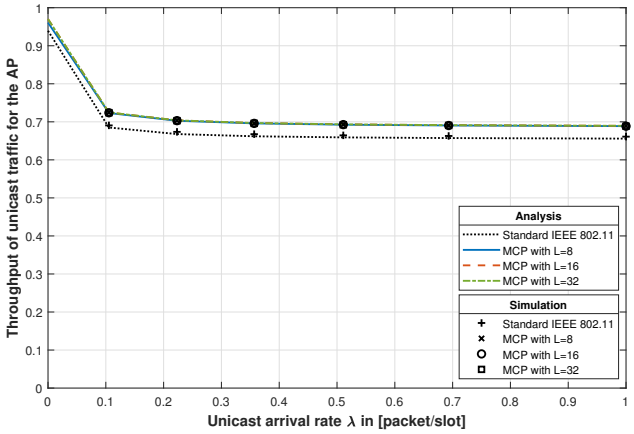

Figure 5.3: Normalized throughput of unicast frames transmitted by the AP. MCP for $L = 8$, 16, 32 compared with the standard IEEE 802.11.

Figure 5.5 shows the normalized multicast throughput as a function of the unicast arrival rate. The multicast throughput of the standard IEEE 802.11 shows a similar value compared with the unicast service. Unlike the unicast service, multicast frames' delivery is not guaranteed due to the lack of an acknowledgment mechanism. As a result, all the collided multicast frames are lost, and no retransmission is considered, which results in a data loss in the video flow and degradation in the QoS/QoE metric. On the other hand, the MCP mechanism provides the best multicast throughput regardless of the unicast offered load.

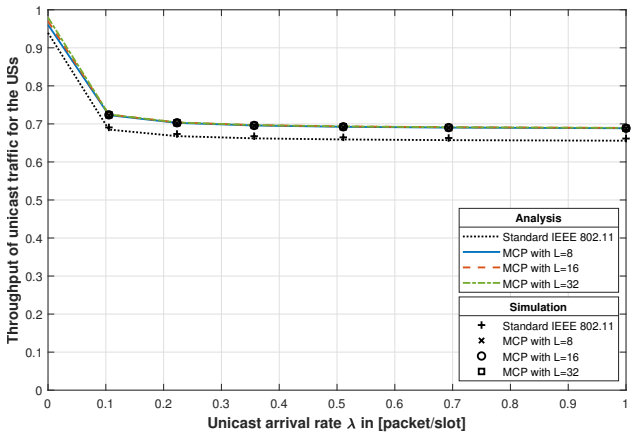

Figure 5.4: Normalized throughput of unicast frames transmitted by the USs. MCP for $L = 8, 16, 32$ compared with the standard IEEE 802.11.

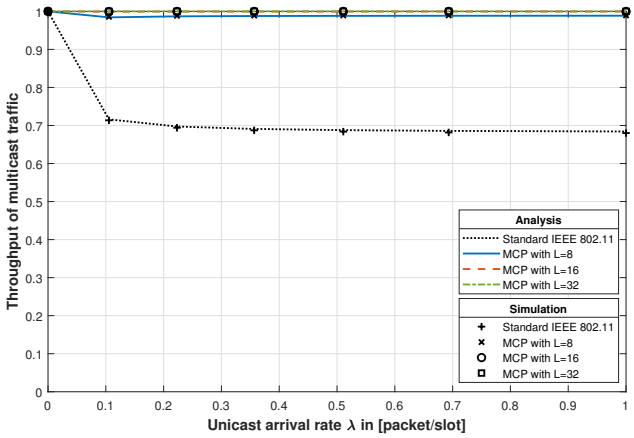

Figure 5.5: Normalized throughput of multicast frames. MCP for $L = 8, 16, 32$ compared with the standard IEEE 802.11.

Figure 5.6 and 5.7 show the loss probability of unicast frames transmitted by the AP and by USs as a function of the unicast arrival rate. The unicast frames transmitted by the AP or USs show a very similar loss rate. However, the unicast loss for the MCP mechanism is 38% lower compared with the standard IEEE 802.11.

In Figure 5.8, we show the loss probability of the multicast frames as a function of the unicast arrival rate. When transmitting a multicast frame, the MCP mechanism utilizes the ongoing unicast transmissions to guarantee a free-collision transmission of the multicast frames. Therefore, as the number of unicast transmission attempts increases, multicast traffic gets more opportunities to be transmitted without collision. This is the reason behind the slight decreases in multicast losses in Figure 5.8. On the other hand, the multicast loss reported by the MCP mechanism is very low

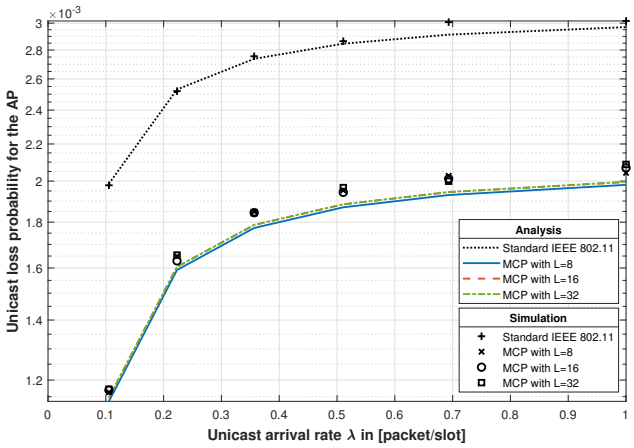

Figure 5.6: Loss probability of unicast frames transmitted by the AP. MCP for $L = 8, 16, 32$ compared with the standard IEEE 802.11.

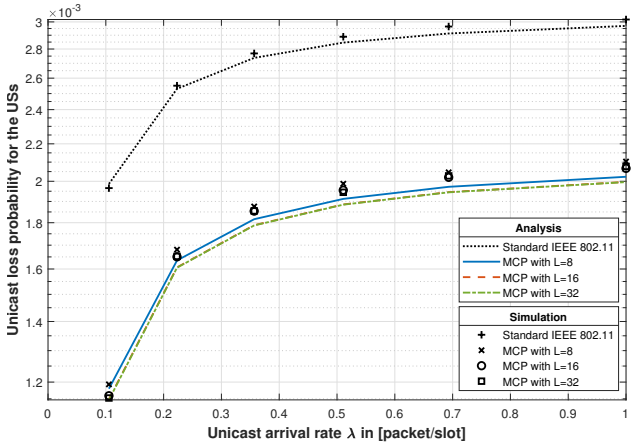

Figure 5.7: Loss probability of unicast frames transmitted by the USs. MCP for $L = 8, 16, 32$ compared with the standard IEEE 802.11.

compared with the standard IEEE 802.11. Besides, when the value of L increases, the multicast service in the MCP mechanism shows to be more reliable than the unicast service.

We show in Figure 5.9 and 5.10 the delay of unicast frames transmitted by the AP and by the USs as a function of the unicast arrival rate. The access delay is given in ms and represents the required time to transmit a packet from its source to the destination. This delay includes the time elapsed in the contention stage and transmission time as well as the propagation delay in the wireless medium. The results presented in Figure 5.9 show that the delay increases with the unicast arrival rate. In standard IEEE 802.11, the unicast traffic generated by the AP can cause internal collisions with multicast traffic and can also collide with unicast frames transmitted by other USs.

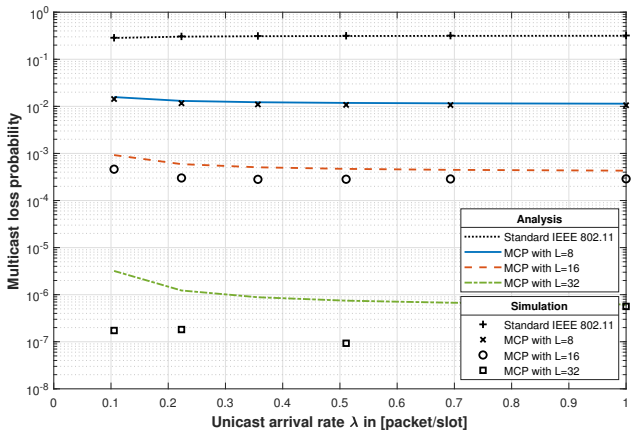

Figure 5.8: Loss probability of multicast frames. MCP for $L = 8, 16, 32$ compared with the standard IEEE 802.11.

However, in the MCP mechanism, multicast frames cannot collide with unicast traffic generated by the AP. Unlike the standard IEEE 802.11, the multicast traffic in the MCP is more likely to be successfully transmitted in the presence of the unicast traffic generated by the AP. Therefore, the delay of unicast traffic in MCP is slightly lower compared to the standard IEEE 802.11.

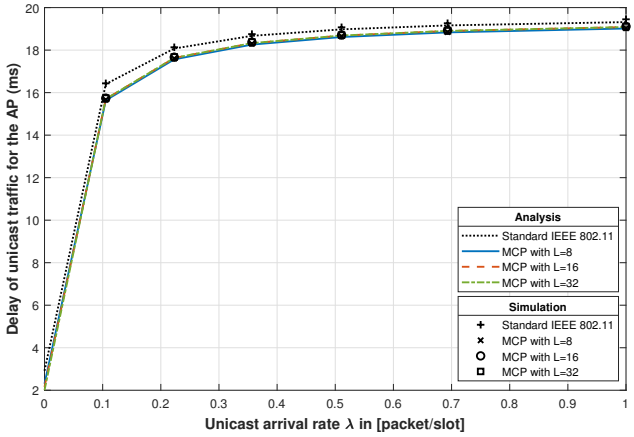

Figure 5.9: Access delay of unicast frames transmitted by the AP in ms. MCP for $L = 8, 16, 32$ compared with the standard IEEE 802.11.

On the other hand, the multicast delay presented in Figure 5.11 shows that the standard IEEE 802.11 outperforms the MCP mechanism with a difference of less than 1.62 ms. This delay difference is due to the *temp* stage introduced by the MCP mechanism to allow multicast frames to be transmitted without collision and therefore increase their reliability.

Finally, we show in Figure 5.12 the multicast jitter as a function of the unicast arrival rate. The

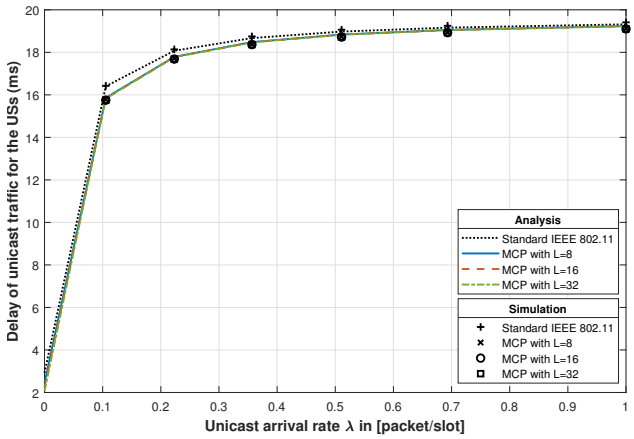

Figure 5.10: Access delay of unicast frames transmitted by the USs in ms. MCP for $L = 8, 16, 32$ compared with the standard IEEE 802.11.

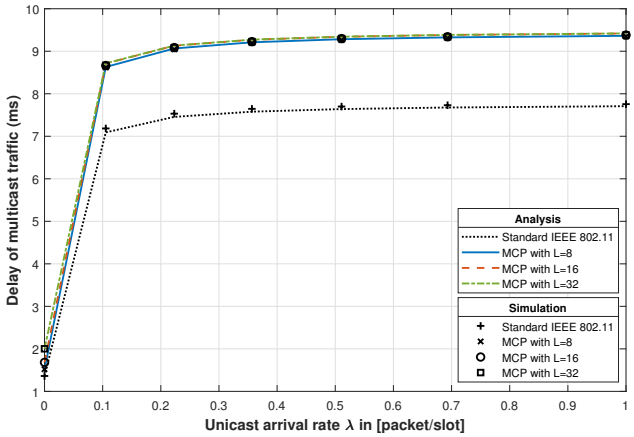

Figure 5.11: Access delay of multicast frames in ms. MCP for $L = 8, 16, 32$ compared with the standard IEEE 802.11.

jitter is defined as the standard deviation of the difference between the arrival times of multicast frames at the multicast receivers side. Unlike the delay, the jitter reported for the MCP mechanism is very low compared with the standard IEEE 802.11. On the other hand, the difference between the inter-arrival time of multicast frames is very high in the standard IEEE 802.11 because between two successive successful transmissions, it could be one or more lost frames which increase the jitter.

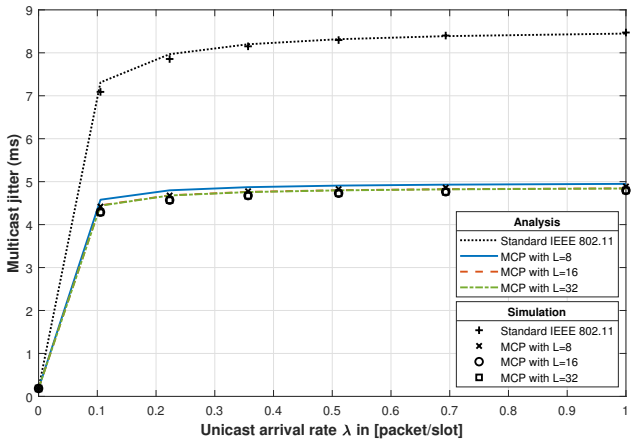

Figure 5.12: Jitter of multicast frames in ms. MCP for $L = 8, 16, 32$ compared with the standard IEEE 802.11

5.6 MAC Mechanism Optimization and QoE Evaluation

In this section, we first set the basis for optimizing the multicast MAC mechanism in terms of the previously defined QoS. Our study then follows a holistic approach by relating the QoS metrics to the QoE metrics reported in the literature [114].

The main goal of this section is to provide a powerful approach allowing us to evaluate and optimize the operation of the multicast MAC mechanism. We consider all the three relevant QoS performance metrics: loss probability, delay, and jitter. As stated by (5.87), for different values of $\lambda \in [0, 1]$, our task consists of tuning the main multicast system parameters in order to ensure a frame loss probability lower than 10^{-6}, a frame delay no greater than 200 ms and a jitter less than 50 ms under all load conditions, i.e., in the presence of unicast traffic.

In [94], we have shown that the multicast mechanism is very effective in terms of all performance metrics of interest. However, the study was exclusively performed under the assumption of saturated unicast traffic. However, it is worth considering the protocol operation over all workload conditions. This is mainly motivated since collisions may involve the multicast and unicast traffic of the AP, and the unicast traffic of all the other nodes may arise much more likely under light traffic conditions.

We emphasize that we could get the best performance by optimizing both MAC mechanisms, i.e., the multicast and DCF mechanisms. However, our goal is to show the feasibility of integrating the MCP mechanism into the IEEE 802.11 protocol architecture, i.e., it is very important to guarantee the inter-operation of MCP and the legacy (unicast) DCF MAC mechanism. Toward this end, we optimize according to the main MCP parameter L under the three thresholds below.

The optimization problem can be simply stated as follows:

$$\text{Minimize } L, \text{ such that:} \quad \begin{cases} P_{loss}^{m} < 10^{-6}, & \forall\, \lambda \in [0,1], \\ D_m < 200\, ms, & \forall\, \lambda \in [0,1], \\ Jitter < 50\, ms, & \forall\, \lambda \in [0,1]. \end{cases} \tag{5.87}$$

Remark 5.6.1 *Note that the multicast loss probability is a decreasing function of L.*

$$P_{loss}^{m} \underset{L\to\infty}{\longrightarrow} 0. \tag{5.88}$$

On the other hand, the multicast delay is an increasing function of L, which leads to a tread-off between the delay and the loss probability. This is the reason for optimizing according to the three thresholds introduced above. The choice we adopted for the thresholds follows the recommendations for the best video/audio quality [114].

We emphasize that the case of saturated unicast traffic [94] is the most beneficial scenario for multicast frames in the MCP mechanism since there are more opportunities for the multicast frame to be transmitted without collision. However, this does not mean that the multicast frame will always meet an ongoing unicast transmission when it reaches the temp stage since unicast frames should go through the backoff process due to previous collision or the retransmission time out.

QoE evaluation is performed to describe the quality level interpreted by the end-user, and it is usually used in multimedia services. QoE can be evaluated objectively (by mathematical models) or subjectively (by asking users for their ratings). Also, the quality of a system can be determined offline (i.e., in a laboratory setting for developing new codecs or services), or in-service (to monitor and ensure a certain level of quality).

We assume that the unicast is transmitted at the highest rate, which results in a bit rate of 54 Mbps. On the other hand, multicast is always sent at the lower rate, which is 1 Mbps [115].

Hereafter, we evaluate the QoE of the optimized MCP in terms of Mean Opinion Score (MOS) and Video Quality Metric (VQM). The QoE is obtained from different QoE/QoS correlation models for multimedia services and for the codecs H.265, VP9, and Xvid. Table 5.3 summarizes the results obtained from the optimization and the corresponding QoE.

For the MOS evaluation, we adopt the exponential mapping functions reported in [113]:

- Mapping function for the H.265:

$$QoE(X) = 4.51 \cdot e^{-0.37 \cdot X} - 2 \cdot 10^{-16} e^{6.73 \cdot X}, \tag{5.89}$$

$$QoE(Y) = 3.66 \cdot e^{-1.56 \cdot Y} + 0.57 \cdot e^{-0.06 \cdot Y}. \tag{5.90}$$

- Mapping function for VP9:

$$QoE(X) = 11.62 \cdot e^{-3.39 \cdot X} + 4.4 \cdot e^{-0.35 \cdot X}, \tag{5.91}$$

$$QoE(Y) = 2.96 \cdot e^{-1.38 \cdot Y} + 1.13 \cdot e^{-0.05 \cdot Y}. \tag{5.92}$$

For the VQM evaluation, we adopt the mapping function reported in [116] for Xvid:

$$VQM(X,Y) = \frac{P_1 + P_2X + P_3X^2 + P_4Y + P_5Y^2}{1 + P_6X + P_7X^2 + P_8Y + P_9Y^2}, \tag{5.93}$$

where $X = Jitter$ and $Y = P_{loss}^m$. The parameters P_i, for $i = 1, ..., 9$ are given below:

$$\begin{aligned} P_1 &= 0.00421683208981546, \\ P_2 &= -0.00173344507412777, \\ P_3 &= 0.0935525137413507, \\ P_4 &= 0.788253736441116, \\ P_5 &= -0.113184563779598, \\ P_6 &= 0.140708756966682, \\ P_7 &= 0.064602569193934, \\ P_8 &= 0.814736390397921, \\ P_9 &= -0.147553823779441. \end{aligned} \tag{5.94}$$

Table 5.3: Multicast mechanism optimization and QoE evaluation

λ	L^*	Loss probability	Delay (ms)	Jitter (ms)	H.265 codec		VP9 codec		Xvid codec
					MOS(Jitter) Eqn. (5.89)	MOS(Loss) Eqn. (5.90)	MOS(Jitter) Eqn. (5.91)	MOS(Loss) Eqn. (5.92)	VQM(Jitter,Loss) Eqn. (5.93)
0	0	0	1.362	0.18466	Good	Good	Good	Excellent	Excellent
0.1	36	$8.618 \cdot 10^{-7}$	1.7754	0.38663	Good	Fair	Good	Excellent	Excellent
0.2	33	$9.2626 \cdot 10^{-7}$	1.7918	0.39854	Good	Fair	Good	Excellent	Excellent
0.3	32	$9.791 \cdot 10^{-7}$	1.7974	0.40254	Good	Fair	Good	Excellent	Excellent
0.4	32	$8.3035 \cdot 10^{-7}$	1.8002	0.40453	Good	Fair	Good	Excellent	Excellent
0.5	32	$7.5225 \cdot 10^{-7}$	1.8018	0.40572	Good	Fair	Good	Excellent	Excellent
0.6	32	$7.0454 \cdot 10^{-7}$	1.803	0.4065	Good	Fair	Good	Excellent	Excellent
0.7	32	$6.7256 \cdot 10^{-7}$	1.8037	0.40705	Good	Fair	Good	Excellent	Excellent
0.8	31	$9.7653 \cdot 10^{-7}$	1.8043	0.40747	Good	Fair	Good	Excellent	Excellent
0.9	31	$9.5182 \cdot 10^{-7}$	1.8048	0.40778	Good	Fair	Good	Excellent	Excellent
1	31	$9.3277 \cdot 10^{-7}$	1.8051	0.40803	Good	Fair	Good	Excellent	Excellent

To show the impact of the number of unicast stations N over the optimal value L^*, we perform an optimization analysis with different values of N and λ. The analysis is based on the problem (5.87) and the results are presented in Table 5.4. The results show that N has a similar impact as λ over the L^*. This is because the total offered load for unicast traffic increases with N. The selection of L^* should be performed following the evolution of the number of unicast stations and the unicast offered load, which can be done using a simple algorithm based on the proposed optimization problem (5.87). Our proposed approach is able to achieve the most robust QoS and QoE configurations for audio/video applications by tuning the main multicast parameter L according to Table 5.4.

Table 5.4: Optimal values of L as a function of the number of unicast stations and the offered unicast load

N	Unicast offered load									
	10%	20%	30%	40%	50%	60%	70%	80%	90%	100%
15	28	27	26	26	26	26	26	26	26	26
20	24	23	23	23	23	22	22	22	22	22
25	21	21	20	20	20	20	20	20	20	20
30	19	19	19	19	19	18	18	18	18	18
35	18	17	17	17	17	17	17	17	17	17
40	17	16	16	16	16	16	16	16	16	16
45	16	15	15	15	15	15	15	15	15	15
50	15	15	14	14	14	14	14	14	14	14

5.7 Conclusion

In this chapter, we have evaluated the performance of an opportunistic multicast access mechanism for IEEE 802.11. We considered the coexistence of unicast and multicat traffic on the same WLAN operating under saturated and unsaturated conditions. The network scenario considered in this chapter consists of an AP generating unicast and multicast traffic and a set of unicast senders and multicast receivers. We used three Markov chains to model, respectively, the backoff operation of unicast and multicast traffic generated by the AP and the unicast frames generated by each US. To show the MCP's effectiveness, we have explored different values of the MCP's main parameter L. In both saturated and unsaturated conditions, our results showed that, compared with the standard IEEE 802.11, the MCP is very reliable in delivering multicast frames. Due to the *temp* stage introduced in the MCP mechanism, the multicast frames exhibit a slight delay which is acceptable since we gained in return a low loss rate. We also showed that there is no difference between saturation and unsaturation, as may be expected. This is because multicast frames will always be transmitted after a short time which is defined by the value of L. To achieve the best QoS and QoE estimation for video applications, we tuned the MCP's main parameter L, taking into account the arrival rate of unicast frames, the loss rate, the average delay, and the average jitter. Furthermore, we have tested our approach using different QoE mapping functions and with different video codecs. Our results showed that the QoS/QoE aware MCP mechanism provides high QoS and QoE levels for all scenarios.

Chapter 6

Energy Analysis of a Multicast Access Mechanism for Video Communications over IEEE 802.11

Contents

6.1 Introduction

In IEEE 802.11 WLANs, the channel access strategy is defined by the CSMA/CA medium access control (Carrier-Sense Multiple Access with Collision Avoidance). CSMA/CA is based on the Distributed Coordination Function (DCF), which exploits the Binary Exponential Backoff scheme (BEB). Thus, when a station is ready to transmit a data packet, it should first sense the channel for a DIFS period as specified in the IEEE 802.11 standard [81]. If the channel stays idle during a DIFS interval, the station can transmit. Otherwise, it should initiate the backoff procedure. However, this backoff scheme does not entirely mitigate the collision problem. Unfortunately, the standards do not provide any retransmission mechanism for multicast and broadcast frames. This is mainly due to avoiding the ACK implosion problem resulting from the simultaneous reception of multiple ACKs [94]. This issue poses a major reliability problem for the multimedia traffic making use of the multicast service. Moreover, it makes the multicast mechanism energy-inefficient due to the losses incurred.

The Multicast Collision Prevention (MCP) mechanism [32] was introduced to improve multicast reliability by reducing multicast losses. MCP exploits a shorter period than the DIFS used by DCF. This period is defined as the Reduced Inter-frame Space (RIFS). In order to ensure the same fairness level for other unicast stations, the multicast station is allowed to use the RIFS only after getting access to the channel following the DCF procedure as any other station.

The energy model developed in this chapter aims to estimate the energy consumption of the mechanism under study between two successfully delivered multicast frames. Therefore, it could be used to estimate the expected energy required for successfully delivering a flow of frames belonging, for instance, to a video streaming session. Furthermore, the model takes into consideration the presence of legacy DCF unicast traffic.

The MCP may be particularly useful for deploying multicast services in power-constrained devices, such as battery-operated portable 4G/WLAN routers or the use of a smartphone as a WLAN router. The mobile router should serve all multicast users with maximal reliability and minimal latency while guaranteeing a fair Quality-of-Service (QoS) for unicast stations. Indeed, this is a major challenge taking into consideration the energy constraints of battery-powered mobile routers.

The main contributions of this chapter are summarized as follows:

1. We develop a model for estimating the energy consumption of the multicast access mechanism (MCP).
2. We undertake a comparative energy study between the IEEE 802.11 legacy multicast mechanism and the proposed multicast access mechanism (MCP), taking into consideration different system configurations and network load.
3. We estimate the energy-gain level of the proposed multicast access mechanism.
4. We highlight the trade-off between energy consumption and access delay.
5. We show that the proposed mechanism fulfills the QoS requirements for video communication services.
6. Finally, to validate our results, we conduct extensive simulations using a custom-made MATLAB simulator.

The remainder of this chapter is organized as follows. In Section 6.3, we present a brief overview of the MCP mechanism. Section 6.4 describes our energy model. In Section 6.5, we discuss the numerical results, and finally, Section 6.6 concludes the chapter.

6.2 Related Work

In order to respond to the increasing need for multicast services, the IEEE 802.11aa Task Group TGaa defined three different multicast mechanisms to efficiently support audiovisual applications [81]. However, none of the performance studies reported in the literature have been able to provide a definite answer on the QoS capabilities of the proposed mechanisms under different scenarios [79].

In [32], the authors have shown that the MCP is a promising multicast MAC solution. Their simulation results have shown that MCP is capable of reducing the frame collision probability to the QoS levels required by audiovisual applications. In one of our previous works [94], we have

investigated the performance of the multicast medium access mechanism MCP under saturated conditions. We showed that the multicast mechanism provides high reliability for multicast traffic, and at the same time, it does not penalize the performance of the unicast stations. This feature allows the multicast mechanism to be properly integrated with the legacy DCF mechanism.

In [92], the authors proposed a multicast rate-adaptation scheme for NDN WLANs with multi-transmission stages. According to their studies, the energy improvement of the proposed scheme under the scenario of 60 stations is 14.1% and 14.5% compared with Basic-Rate and Min-Rate schemes, respectively. However, under the same scenario, the proposed scheme reaches a considerably high loss rate of more than 14%.

A novel energy-efficient MAC protocol named Parallel Gated Poll (PGP) was introduced in [117] for WLANs based on IEEE 802.11 PCF. According to their study, PGP is efficient in terms of the energy up to 700% as the network payload increases, compared with the PCF. However, the analysis lacks the evaluation of multicast energy consumption. The authors in [118] provide a detailed survey of the energy consumption issues in the IEEE 802.11 WLANs. They considered different MAC access protocols, namely DCF, PCF, PSM (Power Saving Mode), EDCA, and HCCA (Controlled Channel Access). Furthermore, they highlighted the existence of a trade-off between the energy consumed and the throughput. A similar trade-off is investigated in this chapter between energy consumption and delay.

6.3 The Multicast Collision Prevention MAC protocol

We illustrate in Figure 6.1 the operation of the Multicast Collision Prevention mechanism (MCP) [32]. When the Access Point (AP) holds a multicast frame, it starts the contention stage using the Distributed Coordination Function (DCF) mechanism exactly as specified in the IEEE 802.11 standard [81]. However, when the backoff expires, it starts a timer *temp* with a length of L slots. During this timer, the AP monitors the channel for transmission activities, as illustrated in Figure 6.1. Thus, one of these events may arise when *temp* is active:

1. **The AP senses a busy channel**. If the channel is busy (either with successful transmission or collision), the AP waits until it is idle, then starts the transmission of the multicast frame after a shorter waiting time denoted by Reduced Inter-frame Space (RIFS).

2. **The channel stays idle for L slots**. In this case, the AP immediately transmits the multicast frame, which may collide with a potential simultaneous unicast transmission. This is the case illustrated in Figure 6.1.

6.4 Energy Formulation Model

We consider a wireless scenario consisting of an AP and a set of N unicast stations. We assume that the AP is the only entity transmitting multicast frames. Furthermore, the channel access for multicast traffic is defined by the multicast access mechanism MCP. In contrast, the channel

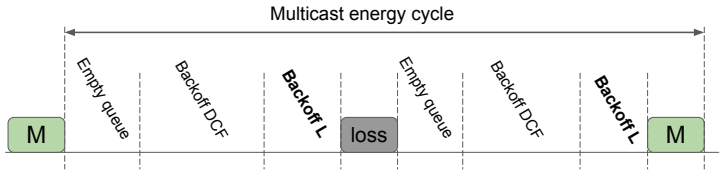

Figure 6.1: Multicast energy cycle defined as the interval between two successful multicast transmissions.

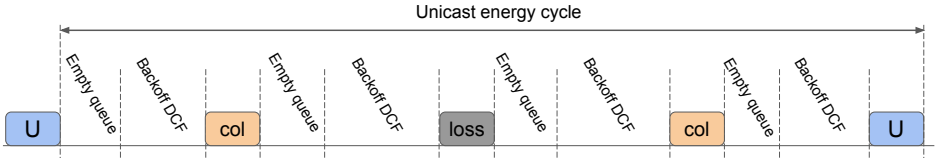

Figure 6.2: Unicast energy cycle defined as the interval between two successful unicast transmissions.

access for unicast traffic follows the DCF mechanism, which makes use of the Binary Exponential Backoff (BEB) algorithm predefined in the CSMA mechanism. We focus through this study on the energy consumed for accessing the channel, which includes the energy for sensing the channel and transmitting data frames. The main goal of this study is to estimate the energy consumed by the new multicast mechanism and compare it with the IEEE 802.11 standard. Since we have shown that the multicast MCP mechanism guarantees a reliable multicast service for video communication, it is of great interest to evaluate its energy consumption and highlight the potential relevant issues. Another objective of the study is to show the impact of energy consumption on the delay. In the following, we adopt the analytical model presented in Chapter 5 to derive all the probabilities involved in the energy model. The power consumption parameters used in this chapter are taken from [119]. In case a station has no packet to transmit, its stays in an idle state. However, when the multicast frame is in the temp stage introduced by the MCP mechanism, it senses the channel for σ period of time, where σ is defined by the standard as the duration of an empty slot. Finally, when a station transmits, it consumes power in the transmission regardless of its outcome (i.e., success, collision, loss). The power consumption, as well as DCF and MCP parameters, are shown in Table 6.1.

The station's energy consumption depends on its activity, i.e., transmitting (t), listening (s), receiving (r), or idling (e), and also depends on the duration of this activity. Thus, we denote by $En_i[\Delta t]$ the energy consumed by the activity i in the interval Δt.

$$En_i[\Delta t] = Pw_i[Watt] \cdot \Delta t[second], \quad i \in \{t, r, s, e\}. \tag{6.1}$$

Proposition 6.4.1 *The energy consumed in each contention period within one cycle period is*

defined as

$$En_e = En_e^{succ} + En_e^{idle} + En_e^{col}, \tag{6.2}$$
$$En_{DCF} = En_{DCF}^{succ} + En_{DCF}^{idle} + En_{DCF}^{col}, \tag{6.3}$$
$$En_L = L \cdot E[\sigma] \cdot Nb_{loss} + E_L, \tag{6.4}$$
$$En_{loss} = Nb_{loss} \cdot E_t[DATA], \tag{6.5}$$
$$En_{succ} = E_t[DATA]. \tag{6.6}$$

Proof After each successful transmission or loss, the multicast queue can be empty for Ne slots before a new frame arrives. Ne is a random variable (r.v.) following a geometric distribution with parameter P_m, where P_m is the arrival probability of multicast frames, and it is defined by

$$P_m = 1 - \exp\left(-\lambda_m \Lambda\right). \tag{6.7}$$

λ_m is the multicast arrival rate, and Λ is the system slot time. Thus, the mean value of Ne can be obtained as

$$E[Ne] = \frac{1 - Pm}{Pm}. \tag{6.8}$$

The number Ne includes different slot states: idle slots, slots with successful transmission from other stations, and slots with a collision. The probabilities of these events are given respectively as $P_s = N\tau(1-\tau)^{(N-1)}(1-\tau^u) + \tau^u(1-\tau)^N$, $P_i = (1-\tau)^N(1-\tau^u)$, and $P_c = 1 - P_s - P_i$. Since $Ne = P_s Ne + P_i Ne + P_c Ne$, we can derive the average number of empty-queue slots in each state as follows

$$E[Ne_i] = P_s \cdot E[Ne], \tag{6.9}$$
$$E[Ne_s] = P_i \cdot E[Ne], \tag{6.10}$$
$$E[Ne_c] = P_c \cdot E[Ne]. \tag{6.11}$$

We denote by Nl the number of encountered losses between two successful transmissions. Nl is a r.v. following a geometric distribution with parameter Pm_{loss}, where Pm_{loss} is the multicast loss probability that can be computed similarly to equation (42) in [94] considering unsaturated conditions. Thus, the mean can be obtained using the geometric distribution as follows

$$E[Nl] = \frac{Pm_{loss}}{1 - Pm_{loss}}. \tag{6.12}$$

A multicast frame encounters Nl losses before a successful transmission. Each lost frame is preceded by an empty queue duration. Thus, the total number of empty queue slots between two successful transmissions is given below for the three medium states: idle, success, and collision.

$$E[Ne_{ti}] = E[Ne_i] \cdot (E[Nl] + 1), \tag{6.13}$$
$$E[Ne_{ts}] = E[Ne_s] \cdot (E[Nl] + 1), \tag{6.14}$$
$$E[Ne_{tc}] = E[Ne_c] \cdot (E[Nl] + 1). \tag{6.15}$$

Note that the duration of the last empty interval before the successful transmission is not included in the r.v. Nl. This is why we added 1 to the previous equations.

Using equation (6.1) and (6.13), we can now compute the total energy consumed when the multicast queue is empty as follows

$$E[E_e] = E[Ne_{ti}] \cdot En_e[T_i] + E[Ne_{ts}] \cdot En_e[T_s] + E[Ne_{tc}] \cdot En_e[T_c], \tag{6.16}$$

where $T_i = \sigma$, $T_s = DATA + SIFS + ACK + DIFS$, $T_c = DATA + DIFS$.

Let us now define Nb as the r.v. representing the number of backoff slots during the DCF process. Nb follows a uniform distribution over $[0, Wm-1]$, where Wm is the multicast contention window. The mean can be obtained as follows

$$E[Nb] = \sum_{k=0}^{Wm-1} \frac{k}{Wm} = \frac{Wm-1}{2}. \tag{6.17}$$

During the DCF process of a multicast frame, the channel can be in one of the three states discussed above. Therefore, the number of backoff slots during each state can be derived as follows

$$E[Nb_i] = P_s \cdot E[Nb], \tag{6.18}$$
$$E[Nb_s] = P_i \cdot E[Nb], \tag{6.19}$$
$$E[Nb_c] = P_c \cdot E[Nb], \tag{6.20}$$

and the total number of backoff slots between two successful transmissions can be obtained in a similar way as we did with Ne.

$$E[Nb_{ti}] = E[Nb_i] \cdot (E[Nl] + 1), \tag{6.21}$$
$$E[Nb_{ts}] = E[Nb_s] \cdot (E[Nl] + 1), \tag{6.22}$$
$$E[Nb_{tc}] = E[Nb_c] \cdot (E[Nl] + 1). \tag{6.23}$$

Using the energy consumed during each one of the three medium states, we can get the total energy consumed in the backoff process as follows

$$E[E_b] = E[Nb_{ti}] \cdot En_s[T_i] + E[Nb_{ts}] \cdot En_s[T_s] + E[Nb_{tc}] \cdot En_s[T_c]. \tag{6.24}$$

Let us now get the energy consumed in the Backoff L period. Between two successful transmissions, a multicast frame encounters Nl losses. Before each loss, the multicast frame stays in the Backoff period L until it expires. Thus, the energy consumed by lost frames during the backoff period L is

$$E[E_L^{loss}] = L \cdot Nl \cdot En_s[T_i]. \tag{6.25}$$

We still need to find the energy consumed by a successful multicast transmission during the L period. This energy depends on many factors like the value of L, the channel state, and other

stations' activities during this period. Thus we have

$$\begin{aligned} E[E_L^{succ}] = \sum_{k=0}^{L-1} P_{idle}^{k} \big[& P_s(kEn_s[T_i] + En_s[T^{UM}]) \\ & + P_c\left(kEn_s[T_i] + En_s[T^{CM}]\right) \big] \\ & + \frac{P_{idle}^{L}}{Ps_{00}} \big[\tau^u (1-\tau)^N \left(L \cdot En_s[T_i] + En_s[T^{UM}]\right) \\ & + \tau^u (1-(1-\tau)^N) \left(L \cdot En_s[T_i] + En_s[T^{CM}]\right) \\ & + (1-\tau^u)(1-\tau)^N L \cdot En_s[T_i] \big], \end{aligned} \tag{6.26}$$

where $T^{UM} = DATA + SIFS + ACK + RIFS$ and $T^{CM} = DATA + RIFS$. The last sum of equation (6.26) is conditioned on the probability that the AP transmits a unicast frame or no one transmit, which is given by

$$Ps_{00} = \tau^u + (1-\tau^u)(1-\tau)^N. \tag{6.27}$$

The total energy consumed by the backoff period L between two successful transmissions is then the sum of the energy consumed by all the lost frames in that period L plus the energy consumed by the successful transmission, which can be summarized as follows

$$E[E_L] = E[E_L^{loss}] + E[E_L^{succ}]. \tag{6.28}$$

Finally, the energy consumed by lost transmissions and the energy consumed by a successful transmission can be obtained respectively as follows

$$E[E_{loss}] = E[Nl]En_t[DATA], \tag{6.29}$$

$$E[E_s] = En_t[DATA]. \tag{6.30}$$

□

Remark 6.4.2 *Note that the energy consumed for successful transmission is constant since we only have one successful event in each cycle period. We can use a similar approach to compute the energy consumed by a single unicast station between two successfully transmitted unicast frames, see Figure 6.2.*

Corollary 6.4.2.1 *The total energy consumed by the multicast access mechanism in one cycle period is defined as the sum of the energy wasted in each contention period.*

$$En_{Total} = En_e + En_{DCF} + En_L + En_{loss} + En_{succ}. \tag{6.31}$$

Table 6.1: MCP and DCF System Parameters

Parameter	Value	Parameter	Value
DATA	1000 bits	Propagation delay δ	2 μs
SIFS	10 μs	Slot time σ	20 μs
DIFS	50 μs	W_1, W_M	32
RIFS	30 μs	Maximum backoff stage m	5
ACK	304 bits	Data rate	1 Mbps
Pw_t	1316 mW	Pw_r	958.8 mW
Pw_s	836.6 mW	Pw_e	836.6 mW

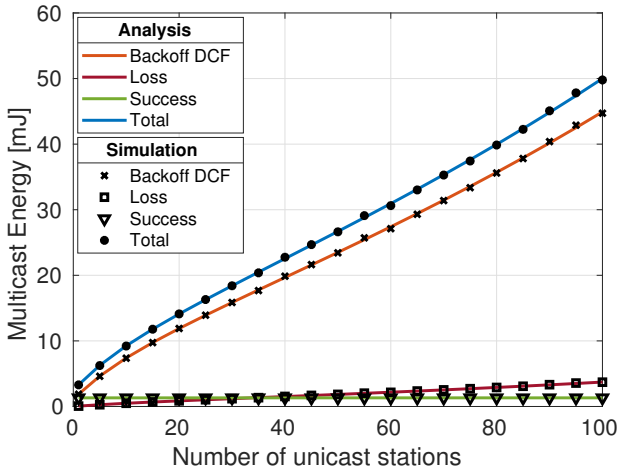

Figure 6.3: IEEE 802.11 Standard.

6.5 Numerical and Simulation Results

In this section, we present the numerical and simulation results of the proposed model. The network scenario consists of a portable router acting as an AP supporting unicast and multicast services and a set of N unicast stations. We set the unicast offered load to 20%, and we consider saturated multicast traffic. In addition, we set $CW_{\min} = 32$ as the initial contention window for both unicast and multicast traffic. Finally, we assume ideal channel conditions. Thus, losses are due only to collisions.

To validate our results, we conducted 100 simulations of 1000 seconds each using a custom-made MATLAB simulator. Table 6.1 shows all the DCF and MCP parameters.

The results show that the total multicast energy consumption in the MCP mechanism is significantly less than the energy reported for the standard IEEE 802.11. Figure 6.3 shows the multicast energy consumption for the standard, which shows that multicast energy increases linearly with the number of unicast stations. This figure also shows that the backoff procedure is the most energy-demanding period due to the carrier sensing process implemented by the DCF mechanism.

Figures 6.4, 6.5 show that the MCP is much more energy-efficient than the standard multicast

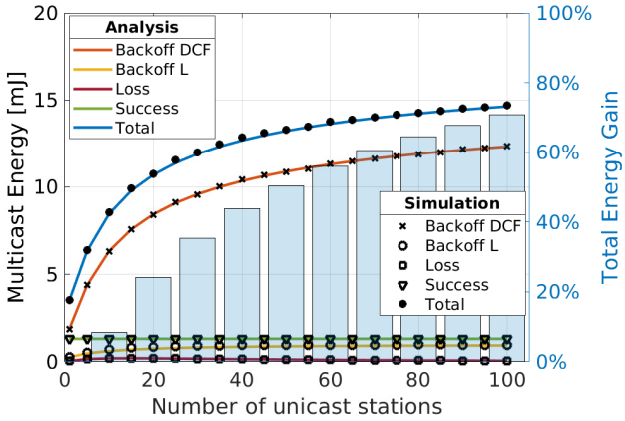

Figure 6.4: MCP with L=2.

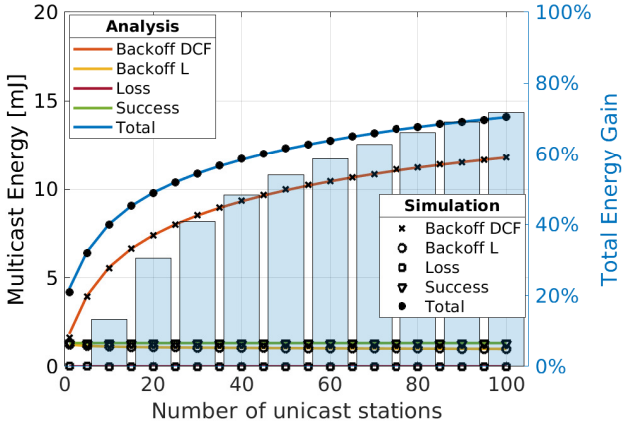

Figure 6.5: MCP with L=32.

mechanism. The figures also show the ratio of the energy gained compared with the standard IEEE 802.11. In high load conditions, the MCP multicast mechanism can reach an energy gain of up to 70%. In contrast, the legacy multicast mechanism consumes a huge amount of energy in high load conditions due to the number of incurred collisions. On the other hand, the energy consumption decreases with the value of L. For $L = 32$, Figure 6.5 shows a significant improvement in the energy consumed in the DCF backoff. Our choice of $L = 32$ follows the optimal settings of the QoS requirements reported in our previous work [94].

Figures 6.6, 6.7, and 6.8 show the multicast QoS Evaluation of the MCP mechanism for L=1, L=2, L=32, and $\lambda_u = 0.2$ compared with standard IEEE 802.11. Figure 6.6 shows that L does not have a significant impact on the delay. For instance, the extra delay introduced for $L = 32$ in high and light traffic load is only 1.19 ms and 1.3 ms, respectively. However, the benefit of this extra delay is considerably huge. In terms of loss rate Figure 6.7, it decreases from 73% to almost 0%

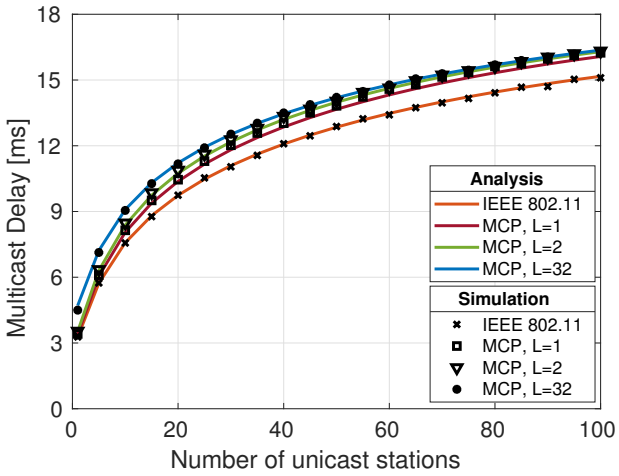

Figure 6.6: Multicast Delay in (ms)

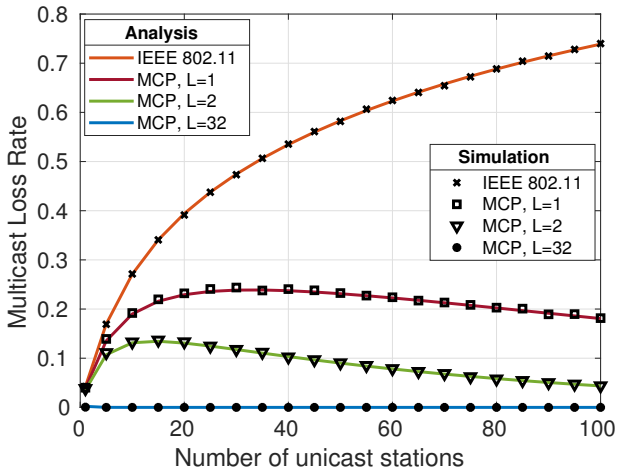

Figure 6.7: Multicast Loss rate

($\approx 1,42 \cdot 10^{-19}\%$) in heavy traffic conditions. Furthermore, L provides much low jitter, as seen from Figure 6.8.

6.6 Conclusion

This chapter investigates the energy consumption of a multicast medium access mechanism MCP for IEEE 802.11 networks. We also included an estimation of the access delay, loss rate, and jitter for different MCP configurations. Our results showed that the MCP mechanism is energy efficient, very reliable, compatible with DCF-compliant unicast stations, and can guarantee the

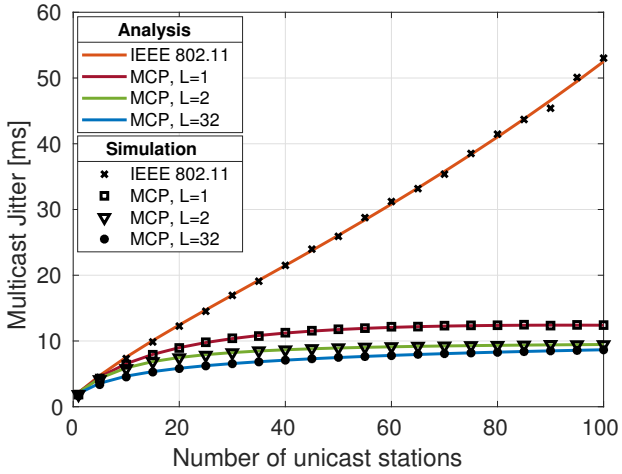

Figure 6.8: Multicast Jitter in (ms)

QoS requirements of most video communication services. Furthermore, we have highlighted the existing trade-off between multicast energy and the access delay. Finally, all our analytical results have been validated with extensive simulations. In our future work, we plan to optimize the main system parameter L according to the energy/delay constraints.

Conclusions and Perspectives

The development and design of accurate analytical models is the fundamental process that leads to a better understanding of wireless networks. The analysis is based on the abstraction of the real-life system to get a simplified mathematical description. The goal is to design improved mechanisms that efficiently exploit the available network resources. In this dissertation, we studied some random access mechanisms, namely: Slotted ALOHA, Slotted ALOHA enhanced by ZigZag Decoding (SAZD), Distributed Coordination Function (DCF), and Multicast Collision Prevention mechanism (MCP). We also provide strategies that mitigate contentions in a shared network.

In the first part of this dissertation, we addressed the selfishness problem in the ALOHA network. We investigated the case of a variant of the ALOHA mechanism named SAZD. To tackle the problem, we started by studying the ideal case of cooperation. In this scenario, we assumed that users are cooperating with each other to achieve a common goal. Therefore, we treated the system as one coalition that aims to optimize the objective function of the entire system. We considered various cooperative games with different objective functions. First, we proposed to maximize the system throughput. Through an optimization approach, we derived the optimal transmission policy that yields the best system throughput. While this allowed for the most efficient use of resources, it also raised the problem of fairness as some users experienced a significant delay. To overcome this issue, we proposed a second game scenario in which we minimized the delay of affected users. However, this led to a slight degradation in the system throughput. In order to optimize this inherent trade-off, we have proposed a third game in which we take into account maximizing the system throughput and minimizing the delay of backlogged users. Next, we introduced a pricing strategy using two different approaches. Through a numerical investigation, we have shown that we can further optimize the existing trade-off and achieve better performance by using the right pricing configuration. On the other hand, we considered the case of non-cooperation, where all users act selfishly by optimizing their own objective functions. As discussed in the results, this selfish behavior is not desired since it results in the worst performance. However, it is unavoidable since users are not interested in deviating from their strategies. This situation is known in game theory as the prisoner's dilemma. Our solution to address this problem is to charge users a cost for each transmission attempt. This way, the aggressive behavior of users is significantly decreased as a function of the cost. This motivated us to optimize the transmission cost with the aim of achieving the same performance as if users were actually cooperating. However, the cooperative game's trade-off has arisen again. To overcome this issue, we proposed an optimal adjustable cost that allows us to choose the required system performance. To generalize cooperative and non-cooperative game models, we proposed a novel stochastic game model of a scenario consisting of a mix of M cooperative and N non-cooperative users. The model provides a general game-theoretic framework in such a way that for $N = 0$, we get the model proposed in Chapter 1; and for $M = 0$, we get the model proposed in Chapter 2. The model also generalizes other ALOHA-based models with an appropriate transition matrix.

In the second part of this dissertation, we addressed the reliability issue of multicast communication over IEEE 802.11 networks. The mechanism studied in this part belongs to the same family of random access mechanisms studied in the first part of this manuscript. The general network scenario is similar to the one discussed in the first part, where several users share the same wireless channel to transmit data. However, we have considered two kinds of traffic in this case: unicast and multicast, which coexist in the same network. Unicast traffic is transmitted using the CSMA mechanism, whereas multicast traffic makes use of the MCP mechanism. We started with the case where stations always have a packet ready for transmission. Although this is a restricted case, it is worth investigating since it appears to be the most beneficial case of MCP. We then modeled the system using a Markov chain, in which we take into account the deep specifications of the mechanism as well as time constraints such as the backoff freezing and various inter-frame spaces. We conducted an optimization study that allowed us to achieve multicast reliability of more than 99.999%. As for unicast traffic, it already benefits from a very high level of reliability thanks to the CSMA retransmission policy. Next, we investigated the case of non-saturated traffic conditions, in which we extended the original MCP proposal. We also extended the saturated scenario such that the unicast and multicast traffic are separated within the AP. Since we are dealing with different traffic kinds (i.e., unicast traffic of the unicast stations and unicast and multicast traffic of the AP), we considered three Markov chains to model the system. Then, we optimized the main system parameter in order to achieve much higher reliability of more than $99,9999\%$. To show the effectiveness of our proposal, we conducted various Quality-of-Service (QoS) and Quality-of-Experience (QoE) evaluations. The last but not least study undertaken in this thesis is the energy consumption evaluation. Our intention was to investigate whether this very high reliability came at the cost of energy. Surprisingly, we found that MCP yields an energy gain of 70% compared with the legacy multicast service introduced by the IEEE 802.11 standard.

Future Research

This thesis opens up a substantial amount of research lines regarding mathematical modeling. Game theory is one of the most theories implemented in this work, along with Markov chain theory. However, the development of accurate mathematical models is still a challenging task, especially the modeling of complex systems. Our future works in this context include the development of a more complex game theory model where each player can choose between several levels of cooperation and selfishness. Indeed, this would allow significant degrees of freedom since players or users will behave independently and heterogeneously, which reflects the nature of many real-life network systems. On the other hand, we plan to study the system from the evolutionary game perspective. We also plan to develop some approaches that help mitigate the non-desired selfish behavior.

An important question that has been raised in this thesis is about the future implementation of the multicast mechanism. Thanks to its high reliability and ability to interoperate with legacy unicast services, we believe that the multicast mechanism studied in this thesis will be a good candidate for future amendments to the IEEE standard.

Conclusions et Perspectives

Le développement et la conception de modèles analytiques précis constituent le processus fondamental qui permet de mieux comprendre les systèmes de réseau sans fil. L'analyse est basée sur l'abstraction du système réel pour obtenir une description mathématique simplifiée. L'objectif est de concevoir des mécanismes améliorés qui exploitent efficacement les ressources disponibles du réseau. Dans cette thèse, nous avons étudié quelques mécanismes d'accès aléatoire, à savoir: Slotted ALOHA, Slotted ALOHA amélioré par ZigZag Decoding (SAZD), Distributed Coordination Function (DCF), et le mécanisme Multicast Collision Prevention (MCP). Nous fournissons également des stratégies qui atténuent les contentions dans un réseau partagé.

Dans la première partie de cette thèse, nous avons abordé le problème de l'égoïsme dans un réseau sans fil opérant le mécanisme ALOHA. Nous avons étudié le cas d'une variante du mécanisme ALOHA appelée SAZD. Pour aborder le problème, nous avons commencé par étudier le cas idéal de coopération. Dans un tel scénario, nous avons supposé que les utilisateurs coopèrent les uns avec les autres pour atteindre un objectif commun. Par conséquent, nous avons traité le système comme une coalition qui vise à optimiser la fonction objective du système tout entier. Nous avons considéré plusieurs jeux coopératifs avec différentes fonctions objectives. Tout d'abord, nous avons proposé de maximiser le débit du système. Grâce à une approche d'optimisation, nous avons dérivé la politique de transmission optimale qui permet d'obtenir le meilleur débit du système. Bien que cette politique permette l'utilisation la plus efficace des ressources, elle soulève également le problème de l'équité, car certains utilisateurs subissent un délai important. Pour surmonter ce problème, nous avons proposé un deuxième scénario de jeu dans lequel nous avons minimisé le délai des utilisateurs concernés. Cependant, cela a entraîné une légère dégradation du débit du système. Afin d'optimiser ce compromis inhérent, nous avons proposé un troisième jeu dans lequel nous prenons en compte la maximisation du débit du système et la minimisation du delai des utilisateurs en attente. Ensuite, nous avons présenté une stratégie de tarification utilisant deux approches différentes. Grâce à une étude numérique, nous avons montré que nous pouvons optimiser davantage le compromis existant et obtenir de meilleures performances en utilisant la bonne configuration de tarification. D'autre part, nous avons considéré le cas de non-coopération, où tous les utilisateurs agissent de manière égoïste en optimisant leurs propres fonctions objectives. Comme nous l'avons vu dans les résultats, ce comportement égoïste n'est pas souhaité car il entraîne les pires performances. Cependant, il est inévitable puisque les utilisateurs ne sont pas intéressés à dévier de leurs stratégies. Cette situation est connue dans la théorie des jeux comme le dilemme du prisonnier. Notre solution pour résoudre ce problème est de faire payer aux utilisateurs un coût pour chaque tentative de transmission. De cette façon, le comportement agressif des utilisateurs est considérablement réduit en fonction du coût. Cela nous a motivés à optimiser le coût de transmission dans le but d'obtenir les mêmes performances que si les utilisateurs coopéraient réellement. Cependant, le compromis du jeu coopératif s'est à nouveau présenté. Pour surmonter ce problème, nous avons proposé un coût optimal ajustable qui nous permet de choisir la performance requise du système. Pour généraliser

les modèles de jeux coopératifs et non coopératifs, nous avons proposé un nouveau modèle de jeu stochastique d'un scénario constitué d'un mélange de M d'utilisateurs coopératifs et de N d'utilisateurs non coopératifs. Le modèle fournit un cadre général de théorie des jeux de telle sorte que pour $N = 0$, nous obtenons le modèle proposé au chapitre 1 ; et pour $M = 0$, nous obtenons le modèle proposé au chapitre 2. Le modèle généralise également d'autres modèles basés sur ALOHA avec une matrice de transition appropriée.

Dans la deuxième partie de cette thèse, nous avons abordé le problème de la fiabilité des communications multicast sur les réseaux IEEE 802.11. Le mécanisme étudié dans cette partie appartient à la même famille de mécanismes d'accès aléatoire étudiés dans la première partie de ce manuscrit. Le scénario général du réseau est similaire à celui discuté dans la première partie, où plusieurs utilisateurs partagent le même canal sans fil pour transmettre des données. Cependant, nous avons considéré deux types de trafic dans ce cas : unicast et multicast, qui coexistent dans le même réseau. Le trafic unicast est transmis à l'aide du mécanisme CSMA, tandis que le trafic multicast fait appel au mécanisme MCP. Nous avons commencé par le cas où les stations ont toujours un paquet prêt à être transmis. Bien qu'il s'agisse d'un cas restreint, il mérite d'être étudié car il semble être le cas le plus avantageux du MCP. Nous avons ensuite modélisé le système à l'aide d'une chaîne de Markov, dans laquelle nous prenons en compte les spécifications profondes du mécanisme ainsi que les contraintes temporelles telles que le gel du backoff et les différents espaces inter-trames. Nous avons mené une étude d'optimisation qui nous a permis d'atteindre une fiabilité multicast de plus de $99,999\%$. Quant au trafic unicast, il bénéficie déjà d'un très haut niveau de fiabilité grâce à la politique de retransmission de CSMA. Ensuite, nous avons étudié le cas de conditions de trafic non saturées, dans lequel nous avons étendu la proposition originale de MCP. Nous avons également étendu le scénario saturé de sorte que le trafic unicast et multicast soit séparé au sein du point d'accès. Puisque nous avons affaire à différents types de trafic (c'est-à-dire le trafic monodiffusion des stations monodiffusion et le trafic monodiffusion et multidiffusion du point d'accès), nous avons considéré trois chaînes de Markov pour modéliser le système. Ensuite, nous avons optimisé le principal paramètre du système afin d'obtenir une fiabilité beaucoup plus élevée, supérieure à $99,9999\%$. Pour démontrer l'efficacité de notre proposition, nous avons effectué diverses évaluations de la qualité de service (QoS) et de la qualité d'expérience (QoE). La dernière étude abordée dans cette thèse est l'évaluation de la consommation d'énergie. Notre intention était d'étudier si cette très haute fiabilité se faisait au détriment de l'énergie. De manière surprenante, nous avons constaté que le MCP permet un gain énergétique de 70% par rapport au service de multidiffusion traditionnel introduit par la norme IEEE 802.11.

Recherche future

Cette thèse ouvre une quantité substantielle de lignes de recherche concernant la modélisation mathématique. La théorie des jeux est l'une des théories les plus mises en œuvre dans ce travail, ainsi que la théorie des chaînes de Markov. Cependant, le développement de modèles mathématiques précis reste une tâche difficile, en particulier pour la modélisation de systèmes complexes. Nos

travaux futurs dans ce contexte incluent le développement d'un modèle de théorie des jeux plus complexe où chaque joueur peut choisir entre plusieurs niveaux de coopération et d'égoïsme. En effet, cela permettrait des degrés de liberté importants puisque les joueurs ou les utilisateurs se comporteront de manière indépendante et hétérogène, ce qui reflète la nature de nombreux systèmes de réseaux réels. D'autre part, nous prévoyons d'étudier le système du point de vue des jeux évolutifs. Nous prévoyons également de développer certaines approches permettant d'atténuer le comportement égoïste non désiré.

Une question importante qui a été soulevée dans cette thèse concerne l'implémentation future du mécanisme multicast. Grâce à sa grande fiabilité et à sa capacité à interopérer avec les services unicast existants, nous croyions que le mécanisme multicast étudié dans cette thèse sera un bon candidat pour les futurs amendements à la norme IEEE.

Conclusiones y Perspectivas

El desarrollo y diseño de modelos analíticos precisos es el proceso fundamental que conduce a una mejor comprensión de los sistemas de red. El análisis se basa en la abstracción del sistema real para obtener una descripción matemática simplificada. El objetivo es diseñar mecanismos mejorados que exploten eficazmente los recursos de red disponibles. En esta tesis, estudiamos algunos mecanismos de acceso aleatorio, a saber: Slotted ALOHA, Slotted ALOHA enhanced by ZigZag Decoding (SAZD), Distributed Coordination Function (DCF), y Multicast Collision Prevention mechanism (MCP). También proporcionamos estrategias que mitigan las contenciones en una red compartida.

En la primera parte de esta tesis, abordamos el problema del egoísmo en la red ALOHA. Investigamos el caso de una variante del mecanismo ALOHA denominada SAZD. Para abordar el problema, comenzamos estudiando el caso ideal de cooperación. En este escenario, asumimos que los usuarios cooperan entre sí para lograr un objetivo común. Por tanto, tratamos el sistema como una coalición que pretende optimizar la función objetivo de todo el sistema. Consideramos varios juegos cooperativos con diferentes funciones objetivo. En primer lugar, propusimos maximizar el rendimiento del sistema. Mediante un enfoque de optimización, derivamos la política de transmisión óptima que produce el mejor rendimiento del sistema. Aunque esto permitía un uso más eficiente de los recursos, también planteaba el problema de la equidad, ya que algunos usuarios experimentaban un retraso importante. Para superar este problema, propusimos un segundo escenario de juego en el que minimizamos el retraso de los usuarios afectados. Sin embargo, esto provocó una ligera degradación del rendimiento del sistema. Para optimizar esta compensación inherente, propusimos un tercer juego en el que teníamos en cuenta la maximización del rendimiento del sistema y la minimización del retraso de los usuarios afectados. A continuación, introducimos una estrategia de precios utilizando dos enfoques diferentes. Mediante una investigación numérica, hemos demostrado que podemos optimizar aún más el equilibrio existente y lograr un mejor rendimiento utilizando la configuración de precios adecuada. Por otro lado, hemos considerado el caso de no cooperación, en el que todos los usuarios actúan de forma egoísta optimizando sus propias funciones objetivo. Como se ha comentado en los resultados, este comportamiento egoísta no es deseado, ya que da lugar al peor rendimiento. Sin embargo, es inevitable ya que los usuarios no están interesados en desviarse de sus estrategias. Esta situación se conoce en la teoría de juegos como el dilema del prisionero. Nuestra solución para abordar este problema es cobrar a los usuarios un coste por cada intento de transmisión. De este modo, el comportamiento agresivo de los usuarios disminuye significativamente en función del coste. Esto nos motivó a optimizar el coste de transmisión con el objetivo de conseguir el mismo rendimiento que si los usuarios cooperaran realmente. Sin embargo, volvió a surgir la disyuntiva del juego cooperativo. Para superar este problema, propusimos un coste óptimo ajustable que permite elegir el rendimiento requerido del sistema. Para generalizar los modelos de juego cooperativo y no cooperativo, propusimos un novedoso modelo de juego estocástico de un escenario formado por una mezcla de M usuarios cooperativos y N usuarios no cooperativos. El modelo proporciona un marco teórico de juego general de forma que para $N = 0$,

obtenemos el modelo propuesto en el capítulo 1; y para $M = 0$, obtenemos el modelo propuesto en el capítulo 2. El modelo también generaliza otros modelos basados en ALOHA con una matriz de transición adecuada.

En la segunda parte de esta tesis, abordamos el problema de la fiabilidad de la comunicación multicast en redes IEEE 802.11. El mecanismo estudiado en esta parte pertenece a la misma familia de mecanismos de acceso aleatorio que SAZD. El escenario general de la red es similar al analizado en la primera parte, donde varios usuarios comparten el mismo canal inalámbrico para transmitir datos. Sin embargo, en este caso hemos considerado dos tipos de tráfico: unicast y multicast, que coexisten en la misma red. El tráfico unicast se transmite utilizando el mecanismo CSMA, mientras que el tráfico multicast hace uso del mecanismo MCP. Comenzamos con el caso en el que las estaciones siempre tienen un paquete listo para ser transmitido. Aunque se trata de un caso restringido, merece la pena investigarlo ya que parece ser el caso más beneficioso de MCP. A continuación, modelamos el sistema mediante una cadena de Markov, en la que tenemos en cuenta las especificaciones profundas del mecanismo, así como las restricciones de tiempo, como la congelación del backoff y los distintos espacios entre tramas. Realizamos un estudio de optimización que nos permitió alcanzar una fiabilidad de multidifusión superior a $99,999\%$. En cuanto al tráfico unicast, ya se beneficia de un nivel de fiabilidad muy alto gracias a la política de retransmisión CSMA. A continuación, investigamos el caso de condiciones de tráfico no saturado, en el que ampliamos la propuesta original de MCP. También ampliamos el escenario saturado de tal manera que el tráfico unicast y multicast están separados dentro del AP. Dado que estamos tratando con diferentes tipos de tráfico (es decir, el tráfico unicast de las estaciones unicast y el tráfico unicast y multicast del AP), consideramos tres cadenas de Markov para modelar el sistema. A continuación, optimizamos el parámetro principal del sistema para conseguir una fiabilidad mucho mayor, superior a $99,9999\%$. Para demostrar la eficacia de nuestra propuesta, realizamos varias evaluaciones de la calidad del servicio (QoS) y la calidad de la experiencia (QoE). El último pero no menos importante estudio realizado en esta tesis es la evaluación del consumo de energía. Nuestra intención era investigar si esta altísima fiabilidad se producía a costa de la energía. Sorprendentemente, descubrimos que MCP produce una ganancia de energía del 70% en comparación con el servicio de multidifusión heredado introducido por el estándar IEEE 802.11.

Investigación futura

Investigación futura Esta tesis abre una cantidad sustancial de líneas de investigación en cuanto a la modelización matemática. La teoría de juegos es una de las teorías más implementadas en este trabajo, junto con la teoría de cadenas de Markov. Sin embargo, el desarrollo de modelos matemáticos precisos sigue siendo una tarea difícil, especialmente el modelado de sistemas complejos. Nuestros trabajos futuros en este contexto incluyen el desarrollo de un modelo de teoría de juegos más complejo en el que cada jugador pueda elegir entre varios niveles de cooperación y egoísmo. De hecho, esto permitiría importantes grados de libertad, ya que los jugadores o usuarios se comportarán de forma independiente y heterogénea, lo que refleja la naturaleza de muchos

sistemas de red de la vida real. Por otra parte, tenemos previsto estudiar el sistema desde la perspectiva de los juegos evolutivos. También planeamos desarrollar algunos enfoques que ayuden a mitigar el comportamiento egoísta no deseado.

Una cuestión importante que se ha planteado en esta tesis es la de la futura implementación del mecanismo de multidifusión. Gracias a su alta fiabilidad y a su capacidad para interoperar con los servicios unicast heredados, creemos que el mecanismo de multidifusión estudiado en esta tesis será un buen candidato para futuras modificaciones del estándar IEEE.

Bibliography

[1] Bo Zhao, Guangliang Ren, and Huining Zhang. Slotted ALOHA game for medium access control in satellite networks. In *2019 IEEE/CIC International Conference on Communications in China (ICCC)*, pages 518–522. IEEE, 2019.

[2] Imane Cheikh, Essaid Sabir, Rachid Aouami, Mohamed Sadik, and Sébastien Roy. Throughput-delay tradeoffs for slotted-ALOHA-based lorawan networks. In *2021 International Wireless Communications and Mobile Computing (IWCMC)*, pages 2020–2025. IEEE, 2021.

[3] Luca Beltramelli, Aamir Mahmood, Patrik Österberg, and Mikael Gidlund. Lora beyond ALOHA: An investigation of alternative random access protocols. *IEEE Transactions on Industrial Informatics*, 17(5):3544–3554, 2020.

[4] Christos Milarokostas, Dimitris Tsolkas, Nikos Passas, and Lazaros Merakos. A comprehensive study on lpwans with a focus on the potential of lora/lorawan systems. 2021.

[5] Takafumi Oku, Tomotaka Kimura, and Jun Cheng. Performance evaluation of hierarchical slotted ALOHA for iot applications. In *2020 IEEE International Conference on Consumer Electronics-Taiwan (ICCE-Taiwan)*, pages 1–2. IEEE, 2020.

[6] Yitong Li, Wen Zhan, and Lin Dai. Rate-constrained delay optimization for slotted ALOHA. *IEEE Transactions on Communications*, 69(8), 2021.

[7] Sotiris A Tegos, Panagiotis D Diamantoulakis, Athanasios S Lioumpas, Panagiotis G Sarigiannidis, and George K Karagiannidis. Slotted aloha with noma for the next generation iot. *IEEE Transactions on Communications*, 68(10):6289–6301, 2020.

[8] Hai Wang and Abraham O Fapojuwo. Design and performance evaluation of successive interference cancellation-based pure ALOHA for internet-of-things networks. *IEEE Internet of Things Journal*, 6(4):6578–6592, 2019.

[9] Dmitry Bankov, Evgeny Khorov, and Andrey Lyakhov. Mathematical model of lorawan channel access with capture effect. In *2017 IEEE 28th Annual International Symposium on Personal, Indoor, and Mobile Radio Communications (PIMRC)*, pages 1–5. IEEE, 2017.

[10] Shyamnath Gollakota and Dina Katabi. Zigzag decoding: Combating hidden terminals in wireless networks. In *Proceedings of the ACM SIGCOMM 2008 conference on Data communication*, SIGCOMM '08, pages 159–170. Association for Computing Machinery, 2008.

[11] Ahmed Boujnoui, Abdellah Zaaloul, and Abdelkrim Haqiq. Enhanced pricing strategy for slotted ALOHA with zigzag decoding: A stochastic game approach. *Int. J. Comput. Inf. Syst. Ind. Manag. Appl*, 13:160–171, 2021.

[12] Mingjun Dai, Bailu Mao, Xueqing Gong, Chi Wan Sung, Weihua Zhuang, and Xiaohui Lin. Zigzag-division multiple access for wireless networks with long and heterogeneous delays. *IEEE Transactions on Aerospace and Electronic Systems*, 55(6):2822–2835, 2019.

[13] Andrea Baiocchi and Fabio Ricciato. Analysis of pure and slotted aloha with multi-packet reception and variable packet size. *IEEE Communications Letters*, 22(7):1482–1485, 2018.

[14] Abdessamad Bellouch, Ahmed Boujnoui, Abdellah Zaaloul, and Abdelkrim Haqiq. Modeling and performance evaluation of lora network based on capture effect. In *Enabling Machine Learning Applications in Data Science*, pages 249–263. Springer, 2021.

[15] Abdessamad Bellouch, Ahmed Boujnoui, Abdellah Zaaloul, and Abdelkrim Haqiq. Hybrid approach for improving slotted aloha based on capture effect and zigzag decoding techniques. In *Hassanien A.E. et al. (eds) Proceedings of the International Conference on Artificial Intelligence and Computer Vision (AICV2021). AICV 2021. Advances in Intelligent Systems and Computing*, pages 218–227. Springer, 2021.

[16] Eitan Altman, Rachid El-Azouzi, and Tania Jimenez. Slotted aloha as a stochastic game with partial information. In *WiOpt'03: Modeling and Optimization in Mobile, Ad Hoc and Wireless Networks*, page 9, 2003.

[17] Zaaloul Abdellah and Haqiq Abdelkrim. Enhanced slotted aloha mechanism by introducing zigzag decoding. *Journal of Mathematics and Computer Science*, 10(4):275–285, 2015.

[18] Chongbin Xu, Li Ping, Peng Wang, Sammy Chan, and Xiaokang Lin. Decentralized power control for random access with successive interference cancellation. *IEEE Journal on Selected Areas in Communications*, 31(11):2387–2396, 2013.

[19] Jinho Choi. Noma-based random access with multichannel aloha. *IEEE Journal on Selected Areas in Communications*, 35(12):2736–2743, 2017.

[20] Yitong Li and Lin Dai. Maximum sum rate of slotted aloha with successive interference cancellation. *IEEE Transactions on Communications*, 66(11):5385–5400, 2018.

[21] Orhan Tahir Yavascan and Elif Uysal. Analysis of slotted aloha with an age threshold. *IEEE Journal on Selected Areas in Communications*, 39(5):1456–1470, 2021.

[22] Luca de Alfaro, Molly Zhang, and JJ Garcia-Luna-Aceves. Approaching fair collision-free channel access with slotted aloha using collaborative policy-based reinforcement learning. In *2020 IFIP Networking Conference (Networking)*, pages 262–270. IEEE, 2020.

[23] Abdelillah Karouit, Essaid Sabir, Fernando Ramirez-Mireles, Luis Orozco Barbosa, and Abdelkrim Haqiq. A stochastic game analysis of the binary exponential backoff algorithm with multi-power diversity and transmission cost. *Journal of Mathematical Modelling and Algorithms in Operations Research*, 12(3):291–309, 2013.

[24] Giuseppe Bianchi, Luigi Fratta, and Matteo Oliveri. Performance evaluation and enhancement of the csma/ca mac protocol for 802.11 wireless lans. In *Proceedings of PIMRC'96-7th International Symposium on Personal, Indoor, and Mobile Communications*, volume 2, pages 392–396. IEEE, 1996.

[25] Giuseppe Bianchi. Performance analysis of the IEEE 802.11 distributed coordination function. *IEEE Journal on Selected Areas in Communications*, 18(3):535–547, 2000.

[26] Alexander Ivanov, Evgeny Khorov, Andrey Lyakhov, and Egor Kuznetsov. Mathematical study of QoS-aware multicast streaming in Wi-Fi networks. In *2018 IEEE Wireless Communications and Networking Conference (WCNC)*, pages 1–6. IEEE, 2018.

[27] Albert Banchs, Antonio De La Oliva, Lucas Eznarriaga, Dariusz R Kowalski, and Pablo Serrano. Performance analysis and algorithm selection for reliable multicast in IEEE 802.11 aa wireless LAN. *IEEE Transactions on Vehicular Technology*, 63(8):3875–3891, 2014.

[28] Rodolfo Oliveira, Luis Bernardo, and Paulo Pinto. Performance analysis of the ieee 802.11 distributed coordination function with unicast and broadcast traffic. In *2006 IEEE 17th International Symposium on Personal, Indoor and Mobile Radio Communications*, pages 1–5. IEEE, 2006.

[29] Rodolfo Oliveira, Luis Bernardo, and Paulo Pinto. Modelling delay on IEEE 802.11 MAC protocol for unicast and broadcast nonsaturated traffic. In *2007 IEEE Wireless Communications and Networking Conference*, pages 463–467. IEEE, 2007.

[30] Rodolfo Oliveira, Luis Bernardo, and Paulo Pinto. The influence of broadcast traffic on IEEE 802.11 DCF networks. *Computer Communications*, 32(2):439–452, 2009.

[31] Maria Ángeles Santos, José Villalón, Fernando Ramírez-Mireles, Luis Orozco-Barbosa, and Jesús Delicado. A Novel Multicast Collision Prevention Mechanism for IEEE 802.11. *IEEE Communications Letters*, 15(11):1190–1192, 2011.

[32] Maria Ángeles Santos, José Villalón, Luis Orozco-Barbosa, and Fernando Ramírez-Mireles. A performance study for the multicast collision prevention mechanism for IEEE 802.11. *Wireless Networks*, 24(4):1297–1311, 2018.

[33] Ieee draft standard for information technology–telecommunications and information exchange between systems local and metropolitan area networks–specific requirements - part 11: Wireless lan medium access control (mac) and physical layer (phy) specifications - amendment: Enhanced broadcast service. *IEEE P802.11bc/D3.0, March 2022*, pages 1–117, 2022.

[34] Charlie Perkins, Michael McBride, Dorothy Stanley, Warren Kumari, and Juan Carlos Zuniga. Multicast Considerations over IEEE 802 Wireless Media. *Internet Draft*, pages 1–26, 2019.

[35] Kai Lai Chung. Harald cramér, the elements of probability theory and some of its applications. *Bulletin of the American Mathematical Society*, 61(5):449–450, 1955.

[36] Ronald Howard. Dynamic probabilistic systems, volume 1 and volume 12 john f, 1971.

[37] Roger B Myerson. *Game theory: analysis of conflict*. Harvard university press, 1997.

[38] JMPGR Smith and George R Price. The logic of animal conflict. *Nature*, 246(5427):15–18, 1973.

[39] Smith J Maynard and D Harper. Animal signals: Oxford series in ecology and evolution. ny: Oxford university press. 2003.

[40] Eitan Altman, Rachid El-Azouzi, Yezekael Hayel, and Hamidou Tembine. The evolution of transport protocols: An evolutionary game perspective. *Computer Networks*, 53(10):1751–1759, 2009.

[41] Eitan Altman, Rachid ElAzouzi, Yezekeael Hayel, and Hamidou Tembine. An evolutionary game approach for the design of congestion control protocols in wireless networks. In *2008 6th International Symposium on Modeling and Optimization in Mobile, Ad Hoc, and Wireless Networks and Workshops*, pages 547–552. IEEE, 2008.

[42] Lloyd S Shapley. Stochastic games. *Proceedings of the national academy of sciences*, 39(10):1095–1100, 1953.

[43] Dean Gillette. Stochastic games with zero stop probabilities. *Contributions to the Theory of Games III*, 39:179–187, 1957.

[44] Arlington M Fink. Equilibrium in a stochastic n-person game. *Journal of science of the hiroshima university, series ai (mathematics)*, 28(1):89–93, 1964.

[45] Masayuki Takahashi. Equilibrium points of stochastic non-cooperative n-person games. *Journal of Science of the Hiroshima University, Series AI (Mathematics)*, 28(1):95–99, 1964.

[46] Philip David Rogers. *Nonzero-sum stochastic games*. University of California, Berkeley, 1969.

[47] Alan J Hoffman and Richard M Karp. On nonterminating stochastic games. *Management Science*, 12(5):359–370, 1966.

[48] Thomas M Liggett and Steven A Lippman. Stochastic games with perfect information and time average payoff. *Siam Review*, 11(4):604–607, 1969.

[49] John Nash. Non-cooperative games. *Annals of mathematics*, pages 286–295, 1951.

[50] William Poundstone. *Prisoner's Dilemma/John Von Neumann, game theory and the puzzle of the bomb*. Anchor, 1993.

[51] Norman Abramson. The ALOHA system: Another alternative for computer communications. In *Proceedings of the November 17-19, 1970, fall joint computer conference*, AFIPS '70 (Fall), pages 281–285, 1970.

[52] Dimitri Bertsekas and Robert Gallager. *Data networks*. Athena Scientific, 2021.

[53] Arnold O Allen. *Probability, statistics, and queueing theory*. Academic press, 2014.

[54] Eitan Altman, Dhiman Barman, Rachid El Azouzi, and Tania Jiménez. A game theoretic approach for delay minimization in slotted aloha. In *2004 IEEE International Conference on Communications (IEEE Cat. No. 04CH37577)*, volume 7, pages 3999–4003. IEEE, 2004.

[55] Zaaloul Abdellah and Haqiq Abdelkrim. Analysis of performance parameters in wireless networks by using game theory for the non cooperative slotted aloha enhanced by zigzag decoding mechanism. *arXiv preprint arXiv:1501.00881*, 2015.

[56] Ahmed Boujnoui, Abdellah Zaaloul, and Abdelkrim Haqiq. A stochastic game analysis of the slotted aloha mechanism combined with zigzag decoding and transmission cost. In *Abraham A., Haqiq A., Muda A., Gandhi N. (eds) Innovations in Bio-Inspired Computing and Applications. IBICA 2017. Advances in Intelligent Systems and Computing*, volume 735, pages 102–112. Springer, 2018.

[57] Eitan Altman, Rachid El Azouzi, and Tania Jiménez. Slotted ALOHA as a game with partial information. *Computer networks*, 45(6):701–713, 2004.

[58] Rachid El-Azouzi, Essaid Sabir, Tania Jiménez, and El-Houssine Bouyakhf. Modeling slotted ALOHA as a stochastic game with random discrete power selection algorithms. *Journal of Computer Systems, Networks, and Communications*, 2009, 2009.

[59] Rachid El-Azouzi, Tania Jiménez, ES Sabir, S Benarfa, and El-Houssine Bouyakhf. Cooperative and non-cooperative control for slotted ALOHA with random power level selections algorithms. In *Proceedings of the 2nd international conference on Performance evaluation methodologies and tools*, ValueTools '07, pages 1–10. ICST (Institute for Computer Sciences, Social-Informatics and Telecommunications Engineering), 2007.

[60] Abdelillah Karouit. Efficient incentive scheme forwireless random channel access with selfish users. In *International Symposium on Ubiquitous Networking*, volume 366, pages 27–38. Springer, 2015.

[61] Essaid Sabir, Rachid El-Azouzi, and Yezekael Hayel. Hierarchy sustains partial cooperation and induces a braess-like paradox in slotted ALOHA-based networks. *Computer Communications*, 35(3):273–286, 2012.

[62] Masaru Oinaga, Shun Ogata, and Koji Ishibashi. Zigzag decodable coded slotted aloha. In *2018 15th Workshop on Positioning, Navigation and Communications (WPNC)*, pages 1–6. IEEE, 2018.

[63] Mutlu Ahmetoglu, Orhan Tahir Yavascan, and Elif Uysal. Mista: Threshold-ALOHA with mini slots. In *2021 IEEE International Black Sea Conference on Communications and Networking (BlackSeaCom)*, pages 1–6. IEEE, 2021.

[64] Ahmed Boujnoui, Abdellah Zaaloul, and Abdelkrim Haqiq. Mathematical model based on game theory and markov chains for analysing the transmission cost in sa-zd mechanism. *Int. J. Comput. Inf. Syst. Ind. Manag. Appl*, 10:197–207, 2018.

[65] Youngmi Jin and George Kesidis. Equilibria of a noncooperative game for heterogeneous users of an ALOHA network. *IEEE Communications Letters*, 6(7):282–284, 2002.

[66] Sneihil Gopal, Sanjit K Kaul, Rakesh Chaturvedi, and Sumit Roy. A non-cooperative multiple access game for timely updates. In *IEEE INFOCOM 2020-IEEE Conference on Computer Communications Workshops (INFOCOM WKSHPS)*, pages 924–929. IEEE, 2020.

[67] Bo Zhao, Guangliang Ren, and Huining Zhang. Cooperative contention resolution diversity slotted ALOHA with transmit power diversity for multi-satellite networks. In *2019 IEEE 90th Vehicular Technology Conference (VTC2019-Fall)*, pages 1–5. IEEE, 2019.

[68] Kaveh Vaezi and Farid Ashtiani. Delay-optimal cooperation policy in a slotted ALOHA full-duplex wireless network: Static approach. *IEEE Systems Journal*, 14(2):2257–2268, 2019.

[69] Kaveh Vaezi, Nail Akar, and Ezhan Karasan. Age of information in a cooperative slotted ALOHA network: Marginal and joint distributions. 2021.

[70] Rui Liu, Tao Hong, Xiaojin Ding, Yunfeng Wang, and Gengxin Zhang. Multi-satellite cooperative beamforming ALOHA for leo satellite iot networks. *Frontiers in Space Technologies*, 2:9, 2021.

[71] Ahmed Boujnoui, Abdellah Zaaloul, and Abdelkrim Haqiq. Cooperative slotted aloha with zigzag decoding and a pricing mechanism. In *Abraham A., Sasaki H., Rios R., Gandhi N., Singh U., Ma K. (eds) Innovations in Bio-Inspired Computing and Applications. IBICA 2020. Advances in Intelligent Systems and Computing*, volume 1372, pages 111–119. Springer, 2021.

[72] Younggeun Cho and Fouad A Tobagi. Cooperative and non-cooperative ALOHA games with channel capture. In *IEEE GLOBECOM 2008-2008 IEEE Global Telecommunications Conference*, pages 1–6. IEEE, 2008.

[73] Christian Hilbe, Štěpán Šimsa, Krishnendu Chatterjee, and Martin A Nowak. Evolution of cooperation in stochastic games. *Nature*, 559(7713):246–249, 2018.

[74] Maran Van Heesch, Pascal LJ Wissink, Ramtin Ranji, Mehdi Nobakht, and Frank Den Hartog. Combining cooperative with non-cooperative game theory to model wi-fi congestion in apartment blocks. *IEEE Access*, 8:64603–64616, 2020.

[75] Yang Yang, Yecheng Wu, Nanxi Chen, Kunlun Wang, Shanzhi Chen, and Sha Yao. Locass: Local optimal caching algorithm with social selfishness for mixed cooperative and selfish devices. *IEEE Access*, 6:30060–30072, 2018.

[76] Allen B MacKenzie and Stephen B Wicker. Selfish users in ALOHA: a game-theoretic approach. In *IEEE 54th Vehicular Technology Conference. VTC Fall 2001. Proceedings (Cat. No. 01CH37211)*, volume 3, pages 1354–1357. IEEE, 2001.

[77] Boris Bellalta, Luciano Bononi, Raffaele Bruno, and Andreas Kassler. Next generation IEEE 802.11 Wireless Local Area Networks: Current status, future directions and open challenges. *Computer Communications*, 75:1–25, 2016.

[78] Pablo Serrano, Pablo Salvador, Vincenzo Mancuso, and Yan Grunenberger. Experimenting with commodity 802.11 hardware: Overview and future directions. *IEEE Communications Surveys & Tutorials*, 17(2):671–699, 2015.

[79] Hassan Ibrahim Zawia, Rosilah Hassan, and Dahlila Putri Dahnil. A survey of medium access mechanisms for providing robust audio video streaming in IEEE 802.11aa standard. *IEEE Access*, 6:27690–27705, 2018.

[80] IEEE Standard for Information Technology–Telecommunications and Information Exchange Between Systems–Local and Metropolitan Area Networks–Specific Requirements. Part 11: Wireless LAN Medium Access Control (MAC) and Physical Layer (PHY) Specifications. Amendment 8: Medium Access Control (MAC) Quality of Service (QoS) Enhancements. *IEEE Amendment 802.11e*, 2005.

[81] IEEE 802.11aa Standard for Information technology–Telecommunications and information exchange between systems Local and metropolitan area networks–Specific requirements. Part 11: Wireless LAN Medium Access Control (MAC) and Physical Layer (PHY) Specifications Amendment 2: MAC Enhancements for Robust Audio Video Streaming. 2012.

[82] IEEE P802.11bc Standard for Information technology-Telecommunications and information exchange between systems Local and metropolitan area networks-Specific requirements. Part 11: Wireless LAN Medium Access Control (MAC) and Physical Layer (PHY) Specifications Amendment: Enhanced Broadcast Service. work in progress.

[83] Yousri Daldoul, Djamal-Eddine Meddour, Toufik Ahmed, and Raouf Boutaba. Block Negative Acknowledgement protocol for reliable multicast in IEEE 802.11. *Journal of Network and Computer Applications*, 75:32–46, 2016.

[84] Yinan Li and Ray Chen. Hierarchical agent-based secure and reliable multicast in wireless mesh networks. *Computer Communications*, 36(14):1515–1526, 2013.

[85] David Malone, Peter Clifford, and Douglas J. Leith. On buffer sizing for voice in 802.11 WLANs. *IEEE Communications Letters*, 10(10):701–703, 2006.

[86] Aqsa Malik, Junaid Qadir, Basharat Ahmad, Kok-Lim Alvin Yau, and Ubaid Ullah. Qos in IEEE 802.11-based wireless networks: A contemporary review. *J. Network and Computer Applications*, 55:24–46, 2015.

[87] Parikshit Juluri, Venkatesh Tamarapalli, and Deep Medhi. Measurement of quality of experience of video-on-demand services: A survey. *IEEE Communications Surveys and Tutorials*, 18(1):401–418, 2016.

[88] Wright S. (eds) Rahrer T, Fiandra R. Technical report tr-126 triple-play services quality of experience (qoe) requirements. 2006.

[89] Vandung Nguyen, Oanh Tran Thi Kim, Chuan Pham, Thant Zin Oo, Nguyen H Tran, Choong Seon Hong, and Eui-Nam Huh. A survey on adaptive multi-channel MAC protocols in VANETs using Markov models. *IEEE Access*, 6:16493–16514, 2018.

[90] Christina Thorpe and Liam Murphy. A survey of adaptive carrier sensing mechanisms for IEEE 802.11 wireless networks. *IEEE Commun. Surv. Tutorials*, 16(3):1266–1293, 2014.

[91] Charlie Perkins, Michael McBride, Dorothy Stanley, Warren Kumari, and Juan Carlos Zuniga. Multicast Considerations over IEEE 802 Wireless Media. *Internet Draft*, pages 1–26, 2021.

[92] Fan Wu, Wang Yang, Ju Ren, Feng Lyu, Peng Yang, Yaoxue Zhang, and Xuemin Shen. NDN-MMRA: Multi-Stage Multicast Rate Adaptation in Named Data Networking WLAN. *IEEE Transactions on Multimedia (to appear)*, pages 1–14, 2021.

[93] Linjie Zhu, Bin Wu, and Tianchun Ye. An Enhanced ARQ Scheme for A-MPDU Transmission Under Error-Prone WLANs. *IEEE Communications Letters*, 23(4):580–583, 2019.

[94] Ahmed Boujnoui, Luis Orozco Barbosa, and Abdelkrim Haqiq. Performance evaluation and tuning of an ieee 802.11 audio video multicast collision prevention mechanism. *Wireless Networks*, 26:5047–5061, 2020.

[95] Maria Ángeles Santos, José Villalón, and Luis Orozco-Barbosa. Evaluation of the IEEE 802.11aa group addressed service for robust audio-video streaming. In *Proceedings of IEEE International Conference on Communications, ICC 2012, Ottawa, ON, Canada, June 10-15, 2012*, pages 6879–6884, 2012.

[96] Cisco visual networking index: Global mobile data traffic forecast update, 2017–2022, white paper c11-738429-01, February 2019.

[97] Young Deok Park, Seokseong Jeon, Kyungjun Kim, and Young-Joo Suh. RAMCAST: Reliable and adaptive multicast over IEEE 802.11 n WLANs. *IEEE Communications Letters*, 20(7):1441–1444, 2016.

[98] Young Deok Park, Seokseong Jeon, Jae-Pil Jeong, and Young-Joo Suh. FlexVi: PHY aided flexible multicast for video streaming over IEEE 802.11 WLANs. *IEEE Transactions on Mobile Computing*, 19(10):2299–2315, 2019.

[99] Wan-Seon Lim, Dong-Wook Kim, and Young-Joo Suh. Design of efficient multicast protocol for IEEE 802.11 n WLANs and cross-layer optimization for scalable video streaming. *IEEE Transactions on Mobile Computing*, 11(5):780–792, 2011.

[100] Ranveer Chandra, Sandeep Karanth, Thomas Moscibroda, Vishnu Navda, Jitendra Padhye, Ramachandran Ramjee, and Lenin Ravindranath. DirCast: A practical and efficient Wi-Fi multicast system. In *2009 17th IEEE International Conference on Network Protocols*, pages 161–170. IEEE, 2009.

[101] Mohammad Hossein Manshaei, Jean-Pierre Hubaux, et al. Performance analysis of the IEEE 802.11 distributed coordination function: Bianchi model. *Mobile Networks: http://mobnet. epfl. ch Ni W., Romdhani L., Turletti T.(2004), A Survey of QoS Enhancements for IEEE*, 802, 2007.

[102] Mohamed Toumi and Fouzi Semchedine. Improving the throughput in lightly disturbed IEEE 802.11 DCF saturated network using the fragmentation mechanism under basic access mode. *Wireless Personal Communications*, pages 1–15, 2021.

[103] Jun Zheng, Jie Xiao, Qilei Ren, and Yuan Zhang. Performance Modeling of an LTE LAA and WiFi Coexistence System using the LAA Category-4 LBT Procedure and 802.11e EDCA Mechanism. *IEEE Transactions on Vehicular Technology*, 69(6):6603–6618, 2020.

[104] Patrick Bosch, Steven Latré, and Chris Blondia. An analytical model for IEEE 802.11 with non-IEEE 802.11 interfering source. *Computer Networks*, 172:107154, 2020.

[105] Xinhua Ling, Yu Cheng, Jon W Mark, and Xuemin Shen. A renewal theory based analytical model for the contention access period of IEEE 802.15. 4 MAC. *IEEE Transactions on Wireless Communications*, 7(6):2340–2349, 2008.

[106] Markus Fiedler, Tobias Hossfeld, and Phuoc Tran-Gia. A generic quantitative relationship between quality of experience and quality of service. *IEEE Network*, 24(2):36–41, 2010.

[107] Federica Battisti, Marco Carli, and Pradip Paudyal. QoS to QoE mapping model for wired/wireless video communication. In *2014 Euro Med Telco Conference (EMTC)*, pages 1–6. IEEE, 2014.

[108] Jari Korhonen, Nino Burini, Junyong You, and Ehsan Nadernejad. How to evaluate objective video quality metrics reliably. In *2012 Fourth International Workshop on Quality of Multimedia Experience*, pages 57–62. IEEE, 2012.

[109] Wyllian B da Silva, Keiko Vo Fonseca, and Alexandre de AP Pohl. Report on the validation of video quality models for high definition video content, version 2.0 report on the validation of video quality models for high definition video content, version 2.0, 2010. *IEICE Transactions on Information and Systems*, 96(3):708–718, 2013.

[110] J Recommendation. 149: Methods for specifying accuracy and cross-calibration of Video Quality Metrics (VQM). *ITU-T. March*, 2004.

[111] ITU-T Estimating End-to End. Performance in IP Networks for Data Applications. *ITU-T Recommandation G*, 1030, 2005.

[112] Wei Song and Dian W Tjondronegoro. Acceptability-based QoE models for mobile video. *IEEE Transactions on Multimedia*, 16(3):738–750, 2014.

[113] Debajyoti Pal and Vajirasak Vanijja. A no-reference modular video quality prediction model for H. 265/HEVC and VP9 codecs on a mobile device. *Advances in Multimedia*, 2017, 2017.

[114] Ed Reuss (Plantronics) Ganesh Venkatesan (Intel), Alex Ashley (NDS) and Todor Cooklev (Hitachi). IEEE 802 Tutorial: Video over 802.11, mar 2007.

[115] Pinar Akyazi and Touradj Ebrahimi. Comparison of compression efficiency between HEVC/H. 265, VP9 and AV1 based on subjective quality assessments. In *2018 Tenth International Conference on Quality of Multimedia Experience (QoMEX)*, pages 1–6. IEEE, 2018.

[116] Tianyi Wang, Anjum Pervez, and Hua Zou. VQM-based QoS/QoE mapping for streaming video. In *2010 3rd IEEE International Conference on Broadband Network and Multimedia Technology (IC-BNMT)*, pages 807–812. IEEE, 2010.

[117] Guan Zheng, Yang Zhi-Jun, He Min, and Qian Wen-Hua. Energy-efficient analysis of an IEEE 802.11 PCF MAC protocol based on WLAN. *Journal of Ambient Intelligence and Humanized Computing*, 10(5):1727–1737, 2019.

[118] Shiao-Li Tsao and Chung-Huei Huang. A survey of energy efficient MAC protocols for IEEE 802.11 WLAN. *Computer Communications*, 34(1):54–67, 2011.

[119] Salvatore Chiaravalloti, Filip Idzikowski, and Lukasz Budzisz. Power consumption of WLAN network elements. *Tech. Univ. Berlin, Tech. Rep. TKN-11-002*, 2011.

[120] Ken Binmore. *Game theory: a very short introduction*. OUP Oxford, 2007.

[121] Richard TB Ma, Vishal Misra, and Dan Rubenstein. An analysis of generalized slotted-aloha protocols. *IEEE/ACM Transactions on networking*, 17(3):936–949, 2008.

[122] Essaid Sabir, Sidi Ahmed Ezzahidi, and El Houssine Bouyakhf. Generalized slotted aloha revisited: A throughput and stability analysis. In *International Symposium on Ubiquitous Networking*, pages 3–15. Springer, 2015.

[123] Luis Orozco-Barbosa. Performance study of the ieee 802.15.6 slotted aloha mechanism with power control in a multiuser environment. In *Ad Hoc Networks*, pages 27–37. Springer, Cham, 2017.

[124] Liqiang Zhao, Jie Zhang, and Hailin Zhang. Using incompletely cooperative game theory in wireless mesh networks. *IEEE Network*, 22(1):39–44, 2008.

[125] Samson Lasaulce and Hamidou Tembine. *Game theory and learning for wireless networks: fundamentals and applications*. Academic Press, 2011.

[126] Peijian Ju and Wei Song. Repeated game analysis for cooperative mac with incentive design for wireless networks. *IEEE Transactions on Vehicular Technology*, 65(7):5045–5059, 2015.

[127] Abdellah Zaaloul, Mohamed Ben El Aattar, Mohamed Hanini, Abdelkrim Haqiq, and Mohammed Boulmalaf. Sharing channel in ieee 802.16 using the cooperative model of slotted aloha. *arXiv preprint arXiv:1501.00923*, 2015.

[128] Eitan Altman and Rachid El-Azouzi. Non-cooperative game theory applied to telecommunication networks. *ANNALS OF TELECOMMUNICATIONS-ANNALES DES TELECOMMUNICATIONS*, 62(7-8):827–846, 2007.

[129] Peter Marbach. Transmission costs, selfish nodes, and protocol design. *Wireless Networks*, 14(5):615–631, 2008.

[130] Randolph Nelson. *Probability, stochastic processes, and queueing theory: the mathematics of computer performance modeling*. Springer Science & Business Media, 2013.

[131] Aydano Carleial and Martin Hellman. Bistable behavior of aloha-type systems. *IEEE Transactions on Communications*, 23(4):401–410, 1975.

[132] Soukaina Ihirri, Essaid Sabir, Ahmed Errami, and Mohamed Khaldoun. A scalable slotted aloha for massive iot: A throughput analysis. In *2019 15th International Wireless Communications & Mobile Computing Conference (IWCMC)*, pages 508–513. IEEE, 2019.

[133] Bo Zhao, Guangliang Ren, and Huining Zhang. Slotted aloha game for medium access control in satellite networks. In *2019 IEEE/CIC International Conference on Communications in China (ICCC)*, pages 518–522. IEEE, 2019.

[134] Abdessamad Bellouch, Ahmed Boujnoui, Abdellah Zaaloul, and Abdelkrim Haqiq. Modelling and performance evaluation of iot network during the covid-19 pandemic. In *Abraham A., Sasaki H., Rios R., Gandhi N., Singh U., Ma K. (eds) Innovations in Bio-Inspired Computing*

and Applications. IBICA 2020. Advances in Intelligent Systems and Computing, volume 1372, pages 131–140. Springer, 2021.

[135] Yu-Chih Huang, Shin-Lin Shieh, Yu-Pin Hsu, and Hao-Ping Cheng. Iterative collision resolution for slotted aloha with noma for heterogeneous devices. *IEEE Transactions on Communications*, 69(5):2948–2961, 2021.

[136] Dejan Vukobratović and Francisco J Escribano. Adaptive multi-receiver coded slotted aloha for indoor optical wireless communications. *IEEE Communications Letters*, 24(6):1308–1312, 2020.

[137] Periklis Chatzimisios, Anthony C Boucouvalas, and Vasileios Vitsas. Ieee 802.11 packet delay-a finite retry limit analysis. In *GLOBECOM'03. IEEE Global Telecommunications Conference (IEEE Cat. No. 03CH37489)*, volume 2, pages 950–954. IEEE, 2003.

[138] Eustathia Ziouva and Theodore Antonakopoulos. Csma/ca performance under high traffic conditions: throughput and delay analysis. *Computer Communications*, 25(3):313–321, 2002.

[139] Zoran Hadzi-Velkov and Boris Spasenovski. Saturation throughput-delay analysis of ieee 802.11 dcf in fading channel. In *IEEE International Conference on Communications, 2003. ICC'03.*, volume 1, pages 121–126. IEEE, 2003.

[140] Hongyuan Chen. Revisit of the markov model of ieee 802.11 dcf for an error-prone channel. *IEEE Communications Letters*, 15(12):1278–1280, 2011.

[141] Qiang Ni, Tianji Li, Thierry Turletti, and Yang Xiao. Saturation throughput analysis of error-prone 802.11 wireless networks. *Wireless Communications and Mobile Computing*, 5(8):945–956, 2005.

[142] Dhanasekaran Senthilkumar and A Krishnan. Nonsaturation throughput enhancement of ieee 802.11 b distributed coordination function for heterogeneous traffic under noisy environment. *International Journal of Automation and Computing*, 7(1):95–104, 2010.

[143] Guosong Tian and Yu-Chu Tian. Markov modelling of the ieee 802.11 dcf for real-time applications with periodic traffic. In *2010 IEEE 12th International Conference on High Performance Computing and Communications (HPCC)*, pages 419–426. IEEE, 2010.

[144] Azfar Moid and Abraham O Fapojuwo. Three-dimensional absorbing markov chain model for video streaming over ieee 802.11 wireless networks. *IEEE Transactions on Consumer Electronics*, 54(4):1672–1680, 2008.

[145] Chuan Heng Foh and Juki Wirawan Tantra. Comments on ieee 802.11 saturation throughput analysis with freezing of backoff counters. *IEEE Communications Letters*, 9(2):130–132, 2005.

[146] Yutae Lee, Dong Hwan Han, and Chul Geun Park. Ieee 802.11 saturation throughput analysis with freezing of backoff counters. In *Proc. ICCOM*, volume 5, 2005.

[147] Boris Bellalta, Alessandro Zocca, Cristina Cano, Alessandro Checco, Jaume Barcelo, and Alexey Vinel. Throughput analysis in csma/ca networks using continuous time markov networks: a tutorial. In *Wireless Networking for Moving Objects*, pages 115–133. Springer, 2014.

[148] Suong H Nguyen, Hai L Vu, and Lachlan LH Andrew. Performance analysis of ieee 802.11 wlans with saturated and unsaturated sources. *IEEE Transactions on Vehicular Technology*, 61(1):333–345, 2011.

[149] Gabriel Martorell, Felip Riera-Palou, and Guillem Femenias. Modeling fast link adaptation-based 802.11 n distributed coordination function. *Telecommunication Systems*, 56(2):215–227, 2014.

[150] Kamesh Medepalli and Fouad A Tobagi. System centric and user centric queueing models for ieee 802.11 based wireless lans. In *2nd International Conference on Broadband Networks, 2005.*, pages 612–621. IEEE, 2005.

[151] Omesh Tickoo and Biplab Sikdar. Modeling queueing and channel access delay in unsaturated ieee 802.11 random access mac based wireless networks. *IEEE/ACM Transactions on Networking (TON)*, 16(4):878–891, 2008.

[152] Katarzyna Kosek-Szott. A comprehensive analysis of ieee 802.11 dcf heterogeneous traffic sources. *Ad Hoc Networks*, 16:165–181, 2014.

[153] Chien-Erh Weng and Hsing-Chung Chen. The performance evaluation of ieee 802.11 dcf using markov chain model for wireless lans. *Computer Standards & Interfaces*, 44:144–149, 2016.

[154] Nasreddine Hajlaoui, Issam Jabri, and Maher Ben Jemaa. An accurate two dimensional markov chain model for ieee 802.11 n dcf. *Wireless Networks*, 24(4):1019–1031, 2018.

[155] Lei Lei, Ting Zhang, Liang Zhou, Xiaoqin Song, and Shengsuo Cai. Saturation throughput analysis of ieee 802.11 dcf with heterogeneous node transmit powers and capture effect. *International Journal of Ad Hoc and Ubiquitous Computing*, 26(1):1–11, 2017.

[156] Pervez Khan, Niamat Ullah, Sana Ullah, and Kyung Sup Kwak. Analytical modeling of ieee 802.15. 6 csma/ca protocol under different access periods. In *2014 14th International Symposium on Communications and Information Technologies (ISCIT)*, pages 151–155. IEEE, 2014.

[157] Ricardo Campanha Carrano, Luiz Claudio Schara Magalhães, Débora C Muchaluat Saade, and Celio VN Albuquerque. IEEE 802.11 s multihop MAC: A tutorial. *IEEE Communications Surveys & Tutorials*, 13(1):52–67, 2010.

[158] Ken Duffy, David Malone, and Douglas J Leith. Modeling the 802.11 distributed coordination function in non-saturated conditions. *IEEE communications letters*, 9(8):715–717, 2005.

[159] Chengjun Guo, Ying Cui, and Zhi Liu. Optimal multicast of tiled 360 vr video. *IEEE Wireless Communications Letters*, 8(1):145–148, 2018.

[160] Mohammed Abo-Zahhad, Osama Amin, Mohammed Farrag, and Abdelhay Ali. Survey on energy consumption models in wireless sensor networks. *Open Trans. Wirel. Sens. Netw*, 1(1), 2014.

[161] Teuku Yuliar Arif, Dery Rinaldi, and Ramzi Adriman. Energy-aware rate adaptation algorithm for high throughput ieee 802.11 n wlans. In *2018 3rd International Seminar on Sensors, Instrumentation, Measurement and Metrology (ISSIMM)*, pages 48–53. IEEE, 2018.

[162] Emna Charfi, Lamia Chaari, and Lotfi Kamoun. Upcoming wlans mac access mechanisms: An overview. In *2012 8th International Symposium on Communication Systems, Networks & Digital Signal Processing (CSNDSP)*, pages 1–6. IEEE, 2012.